UNIVERSITY OF CALIFORNIA,
IRVINE

Contribution of C5aR1 to Neuroinflammation and Neuronal Dysfunction in Alzheimer's Disease

DISSERTATION

submitted in partial satisfaction of the requirements
for the degree of

DOCTOR OF PHILOSOPHY

in Biomedical Sciences

by

Michael Hernandez

Dissertation Committee:
Professor Andrea J. Tenner, Chair
Professor Edwin S. Monuki
Associate Professor Kim Green

2017

DEDICATION

To

My sister, Jennifer, who has been there for me the entire way, and my friends, old and new.

Thank you for your support and the many adventures we've shared.

TABLE OF CONTENTS

LIST OF FIGURES

LIST OF TABLES

ACKNOWLEDGMENTS

I would like to express the deepest appreciation to my committee chair, Dr. Andrea Tenner, who has guided and encouraged me throughout my graduate work. When things weren't going well, and I wanted to call it quits, she believed in me and encouraged me to power through the tough times and appreciate all the victories, both big and small.

Thank you to all the Tenner lab members, both current and past. They have truly made coming to lab such an enjoyable experience. Special thanks to Dr. Marisa Fonseca, Dr. Elizabeth Clarke, and Sophie Chu who were always there to offer help. Thank you to my undergraduates: Naomi, Karina, Anaïs, Pouya, and Eric – they helped make this possible.

I would like to thank my committee members, Dr. Edwin Monuki and Dr. Kim Green, their advice since advancing was instrumental to move my projects along. Thank you, Dr. Ali Mortazavi and Mandy Jiang, for the wonderful collaboration. I would also like to thank Dr. Lodoen and Dr. Nelson, and their respective lab members, for the great feedback at each joint lab meeting. I'd like to especially thank Dr. Lanny Gov for being the best colleague I could ever hope for. Our walks to coffee and lunch dates offered much needed respite.

In addition, thank you to Dr. Luis Mota-Bravo, Dr. Marlene de la Cruz; they encouraged me to get involved in research when I was an undergraduate and have been my biggest cheerleaders ever since.

Thank you to all the staff at MB&B and Pathology. Special thanks to Stefani Ching for being amazing and so very helpful. Thank you, Bessy Varela and Morgan Oldham for keeping my paychecks coming despite the chaos of being involved with three departments.

Finally, I would like to thank my friends and family. Thank you, Jennifer, for all your support. Couldn't have asked for a more caring and loving sister. Thank you, Snellings family, for so much that I can't even begin to list. Thank you, Nick and Jason, for your friendship and many adventures we have shared, and for introducing me to tons of new friends. Thank you, Brandon Bennett, for being the best gym husband at 5 A.M; I don't think I could have stayed sane without our morning workouts. Thank you, Lesly for your friendship since undergrad. Lastly, thank you to an amazing man, Jason Estep, who has made these last six months very special.

The studies presented in this dissertation were supported by NIH grants NS 35144, AG00538, TG GM055246, T32 AG000096, and The Alzheimer's Association.

CURRICULUM VITAE

Michael Hernandez

Professional Address: 2419 McGaugh Hall
Department of Molecular Biology & Biochemistry
University of California, Irvine, 92697-3900

Email: mhernan4@uci.edu
Telephone: 949-824-3266

Education:

2010-2017 Ph.D. Biomedical Sciences, Department of Pathology and Laboratory Medicine, University of California, Irvine
2005-2010: B.S. Biological Sciences, University of California, Irvine

Honors and Awards:

2011-2014: NIH Research Supplement to Promote Diversity in Health-Related Research
2014-2016: NIH Neurobiology of Aging Training Grant T32 -AG000096
2014: Travel Award from UCI School of Medicine
2015: Travel Award from UCI School of Medicine
2016: NIH UC Irvine Initiative for Maximizing Student Development (IMSD) Training Grant GM055246
2016: Travel Award from International Complement Society
2017: Invited speaker for REMIND Emerging Scientists Symposium

Teaching Experience:

Fall, 2011: Teaching Assistant: Neurobiology lab, N113L
Winter 2016: Teaching Assistant: Biochemistry, Bio Sci 98
Teaching Assistant: Immunology, M121

Publications:

Benoit M.E., **Hernandez M.X.**, Dinh M.L., Benavente F., Vasquez O., Tenner A.J. 2013 C1q induced LRP1B and GPR6 Proteins Expressed Early in Alzheimer Disease Mouse Models, Are Essential for the C1q-mediated Protection against Amyloid-beta Neurotoxicity. J Biol Chem 288:654-665

Rice R.A., Spangenberg E.E., Yamate-Morgan H., Lee R.J., Arora R.P., **Hernandez M.X.**, Tenner A.J., West B.L., Green K.N. 2015 Elimination of Microglia Improves Functional Outcomes Following Extensive Neuronal Loss in the Hippocampus. J Neurosci 35:9977-9989

Hernandez M.X., Namiranian P., Nguyen E., Fonseca M.I., and Tenner A.J. 2017 C5a Increases the Injury to Primary Neurons Elicited by Fibrillar Amyloid Beta. ASN Neuro 9:1759091416687871

Fonseca, M.I., Chu, S., **Hernandez, M.X.**, Fang, M.J., Modarresi, L., Selvan, P., MacGregor G.R. and Tenner, A.J., 2017 Cell specific deletion of *C1qa* identifies microglia as the dominant source of C1q in mouse brain. J Neuroinflammation 14:48

Hernandez M.X., Jiang S., Cole T.A., Chu S., Fonseca M.I., Wetsel R.A., Mortazavi A., and Tenner A.J. 2017 Prevention of C5aR1 Signaling on Microglia Favors Clearance Pathways, Delays Inflammatory Polarization and Suppresses Cognitive Loss. *Manuscript submitted*

Alhoshani, A., Vu, V, V., **Hernandez, M.X.,** Namiranian, P., Oakes, M., Tenner, A.J., Luptak, A., Cocco, M.J. 2017 DNA Aptamers that Bind Nogo-66 Promote Neuronal Outgrowth. *Manuscript in preparation*

Abstracts and Meeting Presentations:

Hernandez M., Ochoa-de la Paz L., Martinez-Torres A.
Electrophysiological characterization of a current in *Xenopus tropicalis* oocytes. Sigma Xi Student Research Conference, The Woodlands, TX, November 14, 2009 (poster).

Hernandez M., Ochoa-de la Paz L., Martinez-Torres A.
Functional characterization of a voltage-activated ion-current of *Xenopus tropicalis* oocytes. American Association for the Advancement of Science (AAAS), San Diego, CA, February 20, 2010 (poster).

Hernandez M.X., Tenner A.J. Expression of TREM2, CR1 and CD200R on Microglia Isolated from Aged 3xTg and Age-matched Control. Society for Neuroscience (SfN), San Diego, CA, November 10, 2013 (oral presentation-nanosymposium).

Hernandez M.X., Tenner A.J. Expression of TREM2, CR1 and CD200R on Microglia Isolated from Aged 3xTg and Age-matched Control. ReMIND 5th Annual Emerging Scientists Symposium on Neurological Disorders, UCI, Irvine, CA, February 20, 2014 (oral presentation).

Hernandez M.X., Molostova K., Marsal-Cots A., Tenner A.J. Complement in Alzheimer's Disease. Molecular Biology and Biochemistry Department Retreat, Lake Arrowhead, CA, March 22, 2014 (oral presentation).

Hernandez M.X., Fonseca M.I., Chu S., Tenner A.J. Distinguishing microglia and macrophages in an AD mouse model. Keystone Symposium: Neuroinflammation in Diseases of the Central Nervous System, Taos, Colorado, January 27, 2015 (poster).

Hernandez M.X., Fonseca M.I., Chu S., Tenner A.J. Distinguishing microglia and macrophages in an AD mouse model. ReMIND 6th Annual Emerging Scientists Symposium on Neurological Disorders, UCI, Irvine, CA, February 19, 2015 (poster).

Hernandez M.X., Namiranian P., Nguyen, E., Tenner A.J. 2015 C5a enhances the injury to primary neurons elicited by fibrillar amyloid beta. Society for Neuroscience (SfN), Chicago, IL, October 17, 2015 (poster).

Hernandez M.X., Fonseca M.I., Chu S., Tenner A.J. 2016. Role of microglia C5aR1 in the Arctic Alzheimer's disease mouse model. ReMIND 7th Annual Emerging Scientists Symposium on Neurological Disorders, UCI, Irvine, CA, February 25, 2016 (poster).

Hernandez M.X, Fonseca M.I, Chu S., Tenner A.J. 2016. Role of microglia C5aR1 in the Arctic Alzheimer's disease mouse model. UCI Translational Research Day. Institute for Clinical & Translational Science (ICTS), UCI, Irvine, CA, June 3, 2016 (poster).

Hernandez M.X., Chu S., Fonseca M.I., and Tenner A.J. Role of microglia C5aR1 in the Arctic Alzheimer's disease mouse model. International Complement Workshop (ICW), Kanazawa, Japan. September 6, 2016 (oral presentation). Immunobiology 221:1187 (2016)

Hernandez M.X., Fonseca M.I., Chu S., Tenner A.J. 2016. Role of microglia C5aR1 in the Arctic Alzheimer's disease mouse model. Society for Neuroscience (SfN), San Diego, November 13, 2016 (oral presentation)

Hernandez M.X., Jiang S., Cole T.A., Chu S.H., Fonseca M.I., Wetsel R.A., Mortazavi A., and Tenner A.J. Deletion of C5aR1 in Arctic AD mouse model decreases inflammatory gene expression and enhances protein degradation pathways. ReMIND 8th Annual Emerging Scientists Symposium, UCI, Irvine, CA, February 16, 2017 (oral presentation)

Undergraduates Mentored:

- Naomi Lomeli (2011-2012) – Graduate student (Ph.D.) in Pathology and Laboratory Medicine at UCI
- Karina Molostova (2013-2015) – Medical scribe applying to medical school
- Anaïs Marsal Cots (2014) – Research assistant at Institut de Recerca Biomedica de Lleida Fundació, Spain
- Pouya Namiranian (2014-2015) – Dental student at Tufts University
- Eric Nguyen (2015-2016) – Medical scribe applying to medical school

Masters Student Mentored

- Rutav Mehta (2014-2015**)** – UCI, MS, Biotechnology, 2015

Lab, Computer and Language Skills

- Proficiency with primary mouse cell culture (microglia, astrocytes, neurons)
- Proficiency in mouse work (breeding, transcardial perfusion, i.p. injections)

- Established an adult microglia isolation procedure in the lab to study microglia ex vivo in AD mouse models
- Proficiency with FACS analysis, 4-color flow cytometry and some sorting experience
- Proficiency with immunocytochemistry
- Proficiency with light microscopy
- Proficiency with amyloid beta fibrilization assays
- Proficiency with SDS-PAGE and western blotting
- Proficiency with real-time qualitative PCR
- Proficiency with nanostring technology and analysis using nSolver Analysis Software
- Proficiency with FlowJo, Prism, Microsoft Excel, Word, PowerPoint, Adobe Photoshop, ImageJ, IPA, Metascape and PaintOmics
- Fluent in Spanish and limited Italian

Professional Society Affiliations

2013-present	Society for Neuroscience
2014-present	American Society for Neurochemistry
2016	International Complement Society

ABSTRACT OF THE DISSERTATION

Contribution of C5aR1 to Neuroinflammation and Neuronal Dysfunction

in Alzheimer's Disease

By

Michael Hernandez

Doctor of Philosophy in Biomedical Sciences

University of California, Irvine, 2017

Professor Andrea J. Tenner, Chair

C5aR1, a receptor for the complement activation proinflammatory fragment, C5a, is primarily expressed on cells of the myeloid lineage, and to a lesser extent on endothelial cells and neurons in brain. Previous work demonstrated that a C5aR1 antagonist, PMX205, decreased amyloid pathology and suppressed cognitive deficits in Alzheimer disease (AD) mouse models. However, the cellular mechanisms of this protection have not been definitively demonstrated. Here, we show that C5a can induce neuronal cell death. Both pharmacologic and genetic data indicate that C5aR1 is required for the C5a-induced decrease of neuron MAP-2. Additionally, in the context of AD, we show that increased neuronal damage is caused by the addition of C5a to neurons treated with fAβ, and can be blocked by the C5aR1 antagonist, PMX53.To understand the role of microglial C5aR1 in an AD mouse model, CX3CR1^{GFP} and CCR2^{RFP} reporter mice were bred to C5aR1 sufficient and knockout wild type and Arctic mice. Microglia (GFP-positive, RFP-negative) and infiltrating monocytes (GFP and RFP-positive) were sorted for transcriptome analysis at 2, 5, 7 and 10 months of

age. Immunohistochemical analysis showed no $CCR2^{+}$ monocytes/macrophages near the plaques in the Arctic brain with or without C5aR1. RNA-seq analysis on microglia from these mice identified inflammation related genes as differentially expressed, with increased expression in the Arctic mice relative to wildtype and decreased expression in the Arctic/C5aR1KO relative to Arctic. In addition, phagosomal-lysosomal genes were increased in the Arctic mice and further increased in the Arctic/C5aR1KO mice. These data are consistent with a microglial polarization state in the absence of C5aR1 signaling with restricted induction of inflammatory genes and enhancement of degradation/clearance pathways and support the potential of this receptor as a novel therapeutic target for AD in humans.

CHAPTER 1

Introduction

Alzheimer's Disease

Alzheimer's disease (AD) is the most common cause of dementia in the elderly. It is characterized by the presence of plaques composed of aggregated β-amyloid (Aβ), neurofibrillary tangles (NTF) composed of phosphorylated tau, and a loss of neurons resulting in brain atrophy and cognitive loss. The disease was first described by Dr. Alois Alzheimer after studying a woman, August Deter, suffering from senile dementia at the Frankfurt Asylum from 1901-1906. After her death, her brain was examined and the first report of massive neuronal loss, amyloid plaques, and neurofibrillary tangles was presented in 1906 at a meeting of the Southwest German Psychiatrists (Cipriani et al., 2011)

Alzheimer's disease affects about 5.4 million people in the United States, most cases being sporadic also known as late-onset AD (LOAD), however, roughly 200,000 of AD patients suffer from what is termed early-onset Alzheimer's disease, driven by mutations in one of three genes (Scheuner et al., 1996). The greatest risk factor for AD is age, 5.2 million people with AD are over the age of 65 and 1 in 9 people over the age of 65 have AD. The first symptom of the disease is subjective cognitive decline, a worsening memory loss or increasing frequency of confusion (Alzheimer's, 2016). The decline in cognitive function inevitably leads to patients requiring caregivers, the majority being unpaid caregivers. An

estimated 15 million Americans provided unpaid care for patients with AD and other dementias, a contribution valued at $221.3 billion, this does not include the estimated $236 billion spent for healthcare, long-term care and hospice.

Currently, a definitive diagnosis of Alzheimer's disease is not made until post mortem, when a pathologist can look for amyloid senile plaques and neurofibrillary tangles. Validated biomarkers that detect the disease early do not exist. What initiates the disease is still unclear and there is no disease-modifying drug available to patients. Currently, drugs target the consequence of neuronal loss by increasing the amount of the neurotransmitter acetylcholine by slowing down the breakdown through acetylcholinesterase inhibitors, or by enhancing the glutamatergic signal, all of which have been shown to slow the progression of cognitive symptoms (Farlow et al., 2008). However, these drugs do not alter the pathology and are only targeting the symptoms of the disease. The pathological hallmarks of the disease and the accompanying inflammatory response, primarily driven by myeloid cells in the brain, that increases with age and disease progression have led to several hypotheses put forward to explain the causative factors of this disease such as the Aβ hypothesis, the tau hypothesis, and more recently, inflammation as a contributor to the progression of the disease.

Amyloid-beta

The amyloid cascade hypothesis posits that the deposition of Aβ in the brain is a crucial initial step that leads to the formation of the senile plaques, neurofibrillary tangles, neuroinflamation, neuronal cell death, and ultimately results the dementia seen in AD (Hardy and Selkoe, 2002) . The discovery of familial AD caused by mutations in either

amyloid precursor protein (APP), presenilin 1 (PSEN1) or presenilin 2 (PSEN2) further supported the hypothesis. The APP protein, normally cleaved by α-secretase, is aberrantly processed by β and γ-secretases, resulting in the pathological Aβ peptide ($A\beta_{42}$). Presenilins are postulated to regulate APP via γ-secretase. The APP gene is found on chromosome 21, and initial support of the amyloid hypothesis was based on the finding that people with Down's syndrome develop typical AD pathology. Even more convincing is microduplications of regions of chromosome 21. When individuals have only the APP gene micro-duplicated, leaving the rest of chromosome 21 intact, they do not have Down's syndrome but get AD pathology (Rovelet-Lecrux et al., 2006). Further support of the amyloid hypothesis is the identification of a missense mutation (A673T) at the Aβ region in APP that results in a lifelong decrease in production of Aβ due to a decrease in APP cleavage by β-secretase. The effect of the mutation may be compounded since other studies have shown that the Aβ formed has altered aggregation properties (reviewed in (Selkoe and Hardy, 2016)). The hypothesis has been modified over the years and the current hypothesis suggests species of Aβ, such as oligomers, cause cellular stress and ultimately neurotoxicity and loss of synapses in the diseased brain.

Tau

The tau hypothesis postulates that tau hyperphosphorylation leads to the final common pathway of AD pathogenesis that precedes the detrimental neuronal degeneration and loss of cognitive function. Evidence strengthening this hypothesis include clinical observations of AD patients that are closer in line with tau pathology. For example, the severity of cognitive deficits in patients correlates better with increasing amounts of NTF in

the brain upon autopsy (Giannakopoulos et al., 2003). There is also a high correlation between hyperphosphorylated tau in the cerebral spinal fluid (CSF) and the cognitive impairment experienced by patients with AD (Clark et al., 2003; Maddalena et al., 2003; Toledo et al., 2014). Moreover, Tau depletion has been shown to protect against Aβ-associated neuronal death in APP/PS1 mouse model of AD (Leroy et al., 2012). Thus, tau dysfunction via hyperphosphorylation and aggregation is generally accepted to be a major player in the cause of the disease.

Neuroinflammation

Previously, neuroinflammation was thought to occur only in the late stages of the disease. Glia activation was thought to simply accompany amyloid plaque deposition but was not believed to play a major role in the disease (reviewed in (Wyss-Coray, 2006)). Recent clinical and genetic work involving genome-wide association studies (GWAS) have linked the pathology in AD with neuroinflammation, suggesting a more prominent role in the pathogenesis of the disease (Zhang et al., 2013; Karch and Goate, 2015). Neuroinflammation is described in more detail in the "cells of the CNS" subsection, below.

The Complement System

The complement system is part of the innate immune system and is crucial for protection from invading pathogens. The term complement was coined in the late nineteenth century by Ehrlich and Morgenroth as a set of heat-labile activity present in serum, complementing the activity of antibodies. However, Bordet and Gengou are noted as performing the crucial complement fixation assays demonstrating the importance of

complement as a substance rather simply an activity found in serum (Morley and Walport, 2000).

Complement consists of more than 30 proteins found in plasma and cell surfaces, which protects from infection and aids in resolution of injury (Ricklin et al., 2010). The complement system is composed of three activation pathways: the classical pathway, the mannose-binding lectin pathway, and the alternative pathway. Fibrillar amyloid beta can activate the complement cascade via the classical or the alternative pathway (**Figure 1.1**). The classical complement pathway is initiated when C1q, a component of the C1 complex, binds to immunoglobulins bound to cell surfaces or immune complexes/aggregates. In addition, C1q can recognize specific non immunoglobulin substances such as apoptotic cells, lipopolysaccharides, and fAβ. Binding of C1q to its target leads to the activation of C1r, which in turn, activates C1s. The activation of C1s leads to the cleavage of C4 generating C4b, which binds to the surface of the initiating activator of the cascade, which then recruits C2 where it is cleaved by the C1s protease into C2a and C2b. C4b and C2b form the C3 convertase (C4b2b) which can then cleave C3 into C3a and C3b. The C5 convertase is formed when C3b associates with the C4b2b on the activator to form C4b2b3b. C5 convertase can then split C5 into C5a and C5b and C5b can then initiate the formation of the pore-forming C5b-9 complex. The mannose-binding lectin (MBL) pathway is similar to the classical pathway except that the pattern recognition molecules MBL and ficolin 1, -2, -3 leads to the activation of the MBL/ficolin-associated serine proteases (MASPs) and the formation of the C3 convertase and subsequent C5 convertase. The alternative pathway is activated by spontaneous hydrolysis of C3, which functions similarly to C3b leading to the alternative C3 convertase C3bBb and alternative C5 convertase C3bBb3b (reviewed in (Merle et al., 2015)).

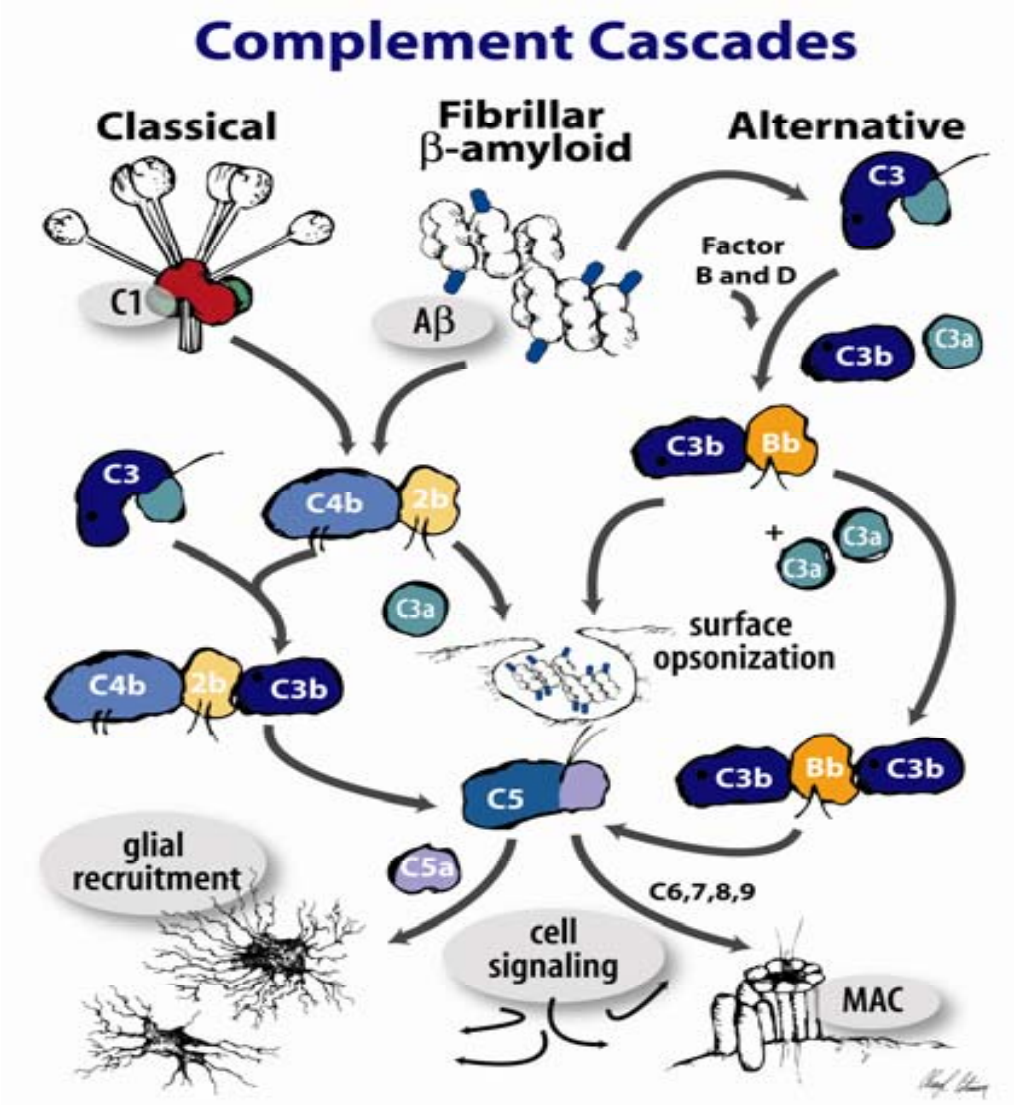

Figure 1.1: Schematic diagram of complement activation by fibrillar β-amyloid. Fibrillar Aβ can activate the classical complement pathway in the absence of antibody, or the alternative pathway. These two pathways converge at C3 cleavage with end results including opsonization (C3b deposits on fibrillar Aβ) and engulfment (of Aβ), leukocyte recruitment (by anaphylatoxins C3a and C5a) and potential bystander lysis by the membrane attack complex (MAC) (Tenner and Pisalyaput, 2008).

Synthesis of Complement Proteins in the CNS

It's been known for over 30 years that the liver is the major source of complement proteins in serum (Ramadori et al., 1984). The blood-brain barrier (BBB) limits complement proteins from crossing into the CNS so it is important that local sources of complement exist to protect the brain from possible pathogens and aid in the clearance of cellular debris. The synthesis of these proteins is now recognized to be differentially induced in multiple cell types, including myeloid cells, and importantly can be induced in CNS resident neurons, astrocytes, oligodendrocytes, and microglia with injury or aging (reviewed in (Woodruff et al., 2010)). Thus, while in many cases of AD the blood brain barrier may be transiently compromised allowing entry of blood localized complement proteins, complement components are present even with an intact blood brain barrier in both human and mouse injured/aging brain.

Complement in aging and AD brain

Over 30 years ago it was demonstrated that C1q, the initiating component of the classical complement cascade, could be synthesized in the absence of the C1 serine proteases C1r and C1s in the peripheral myeloid cells (Bensa et al., 1983). In the CNS, synthesis of C1q has also been shown to be upregulated as an early response to injury in the absence of the classical pathway serine proteases (Benoit et al., 2013) suggesting C1-independent C1q-mediated functions. Interaction of C1q but not C1, with myeloid cells, including microglia, has been shown to suppress proinflammatory cytokine production and enhance clearance of apoptotic cells and neuronal blebs (Fraser et al., 2009; Fraser et al., 2010). Recently, C1q has been found to have direct protective effects on primary cultured neurons under nutrient

stress or amyloid induced toxicity, again without the presence or activation of any downstream components of the complement cascade (Pisalyaput and Tenner, 2008a; Benoit and Tenner, 2011; Benoit et al., 2013). In a series of innovative experiments, C1q along with C3 (and presumably C1r, C1s, C4 and C2) was found to be involved in synapse pruning during retinal development and functional maturation of lateral geniculate neurons (Stevens et al., 2007), that involved phagocytosis by microglia via the complement receptor, CR3 (Schafer et al., 2012). More recently, the Stevens' lab has found that synapse loss in early AD can be attributed to complement aberrantly targeting synapses and implicated microglia in the removal of synapses via the C3 receptor (Hong et al., 2016).

Complement components are increased with aging in the CNS. An analysis of complement gene expression in human brain showed significant upregulation of complement component mRNA with aging and AD relative to that in young brain (Cribbs et al., 2012). A recent study showed C1q protein was found to be dramatically increased in the normal aging of mouse and human brain. Adult C1q knockout KO) mice exhibited enhanced synaptic plasticity compared to littermate controls, independent of C3. The aged C1q KO mice showed significantly less cognitive decline without any noticeable synapse loss (Stephan et al., 2013). Similar work investigating age-related synaptic health in C3 deficient mice showed enhanced synaptic plasticity relative to wildtype at 12 months, with dramatic synapse loss with age in WT that was absent in C3 KO mice (Shi et al., 2015). Although these last two studies found differing results in synaptic plasticity in adult mice in C3 KO relative to WT, both clearly show a decrease in synaptic plasticity and cognitive decline with aging that is rescued in the complement deficient mice.

Cells of the CNS

Neurons

Alzheimer's disease is not only characterized by pathological proteins (Aβ and Tau) but also by atrophy of the brain due to a loss of neurons and synaptic connections. The hippocampus is known to have significantly increased rates of atrophy in presymptomatic and mild cognitive impaired (MCI) patients (Scahill et al., 2002) . Many factors have been implicated in the loss of neurons in AD (Bamberger and Landreth, 2002). The generation of oligomeric and fibrillar forms of Aβ can have detrimental effects on neurons. It is widely accepted that the oligomeric form of Aβ is the toxic species for synapses on neurons, particularly considering the recent work by Hong et al. demonstrating oligomeric Aβ increases C1q and microglia phagocytic activity resulting in increased ingestion of synapses (Hong et al., 2016). Loss of synapses likely play a large role in the pathology leading to cognitive loss in AD, however, other injuries to neurons may contribute to the disease.

Recent studies have shown that C5aR1 signaling is detrimental in various neurodegenerative disease mouse models including in Huntington's disease (Singhrao et al., 1999; Woodruff et al., 2006), traumatic brain injury (Sewell et al., 2004), and ALS (Woodruff et al., 2008). The effects of C5a on neurons *in vitro* have been studied, although the results have varied greatly. Some studies have shown C5a can directly act on C5aR1 and cause apoptosis (Pavlovski et al., 2012; Hernandez et al., 2017). Others have shown that addition of C5a can protect terminally differentiated neuroblastoma cells from Aβ toxicity (O'Barr et al., 2001). Aside from direct injury to neurons from amyloid, glia in the CNS have been shown to mediate neurodegeneration by secretion of proinflammatory cytokines and reactive

oxygen species, and a loss of secretion of neuronal survival factors (reviewed in (Mosher and Wyss-Coray, 2014; Heneka et al., 2015).

Microglia

Inflammation is a fundamental response to infection and injury. In the brain, the primary immune cells are microglia. Much like resident macrophages in other tissues, microglia monitor the environment for pathogens, maintain tissue homeostasis, phagocytose dead and dying cells, and quickly respond to disturbances in the local environment (reviewed in (Ransohoff and El Khoury, 2015)). An example of a disturbance that microglia can respond to is the deposition of beta amyloid in AD to form plaques. Meyer-Luehmann et al showed that microglia are activated and recruited to newly formed plaques within 1-2 days after first appearing in the brain (Meyer-Luehmann et al., 2008). Microglia have been found to be associated with Aβ plaques in both human brains and mouse models of AD (El Khoury and Luster, 2008; Fonseca et al., 2009). As the macrophages of the brain, they play a major role in directing the immune response by the production of proinflammatory or anti-inflammatory molecules.

Microglia are a heterogenous cell type, with many functional states to accomplish the many immunomodulatory tasks required of them (reviewed in (Colton, 2009)). In vitro, microglia stimulated with fibrillar Aβ (fAβ) increase the synthesis and release of proinflammatory mediators like nitric oxide, cytokines, and reactive oxygen species. Although the release of proinflammatory mediators by fAβ is rather low, a marked increase and release is observed when microglia are additionally incubated with a costimulatory factor such as IFN-γ or LPS in addition to fAβ (Li et al., 2004). In Alzheimer's disease,

microglia can detect amyloid β via various cell-surface receptors such as CD36, CD14, and Toll-like receptors (TLR2, TLR4). The recognition of Aβ results in the activation of microglia that consequently leads to the production and release of proinflammatory mediators such as cytokines and chemokines (Jana et al., 2008; Stewart et al., 2010; Liu et al., 2012).

Microglia also express C5aR1 leading to C5a induced pro-inflammatory cytokine production as well as chemotactic functions ((Miller and Stella, 2008) and reviewed in (Woodruff et al., 2010)). In addition, microglial TLRs, have been shown to synergize with C5aR1 in the periphery in mice *in vivo*, further increasing pro-inflammatory cytokine production than when signaling alone (Zhang et al., 2007; Abe et al., 2012). In contrast, C5aR2, also expressed by neurons and microglia, is not coupled to G proteins (in both rodents and humans), and is unable to signal and elicit an intracellular Ca^{2+} response (Cain and Monk, 2002; Okinaga et al., 2003). It has been suggested that the human C5aR2 acts as a scavenger of C5a to reduce the pro-inflammatory response (Scola et al., 2009).

Microglia can also lead to neurodegeneration by inducing astrocytes, glia that normally have a support function in the CNS and blood-brain barrier, to a neurotoxic phenotype. Illuminating work just published by the Barres group and colleagues demonstrated reactive microglia (stimulated with LPS) can induce astrocytes to a neurotoxic phenotype they termed A1 by secretion of C1q, TNF-α and IL-1α. These A1 astrocytes are characterized by a loss of normal astrocytic functions (phagocytosis, promotion of synapse formation and neuron survival) and release of a soluble toxin that kills a subset of neurons and mature oligodendrocytes (Liddelow et al., 2017). This work describes yet another way microglia can lead to neurodegeneration when “classically” activated and implicates early

complement components with neurodegeneration when present with inflammatory cytokines, as is the case with AD (Cribbs et al., 2012).

Amyloid production and impaired clearance mechanisms have long been postulated to play an important role in the pathogenesis of AD. While in early-onset AD, mutations in either APP, PSEN1, or PSEN2 cause an increase in Aβ production or aggregation (that becomes pathological), in sporadic AD, clearance of Aβ may be key to the pathogenesis of the disease. Mawuenyega et al. demonstrated clearance of $A\beta_{40}$ and $A\beta_{42}$ was impaired in LOAD patients compared to cognitive normal controls, whereas production rates of either Aβ peptide was not significantly different between the LOAD patients and the controls (Mawuenyega et al., 2010). Microglia and/or infiltrating monocytes, although distinguishing the two cell types from each other has long been controversial, are thought to be crucial in the clearance of amyloid beta. It is hypothesized that downregulation of phagocytic receptors on microglia, due to the inflammatory environment in AD (TNF-α and IL-1β), is responsible for the decrease in the phagocytic potential of microglia (in part due to the decrease in Aβ-binding receptors like scavenger receptors and RAGE) and subsequent failure to degrade amyloid deposits (Hickman et al., 2008).

Here I will present, in Chapter 2, evidence that support previous results (Pavlovski et al., 2012) demonstrating C5a can induce neuronal cell death. Both pharmacologic and genetic data indicate that C5aR1 is required for the C5a-induced decrease of neuron MAP-2. Additionally, in the context of AD, increased neuronal damage is caused by the addition of C5a to neurons treated with fAβ, and can be blocked by the C5aR1 antagonist, PMX53. I will also demonstrate in Chapter 3 and 4 that genetic ablation of C5aR1 in an accelerated mouse model of AD prevented (or delayed) deficits in hippocampal dependent behavioral

performance. The gene expression profiles of microglia suggest a polarization to an inflammatory and less phagocytic state in AD with progression of plaque pathology, supporting the findings of Hickman et al, that an increase in inflammation leads to a decrease in phagocytosis and protein degradation systems (Hickman et al., 2008) . Genetic deletion of C5aR1 maintained a less inflammatory and more phagocytic program (at the transcriptome level) in the microglia. These data, consistent with the increasingly proposed role of inflammation in neurodegenerative disorders, provide additional compelling rationale to pursue inhibition of C5aR1 as a highly specifically targeted candidate therapy to slow the progression of AD in humans (**Figure 1.2**).

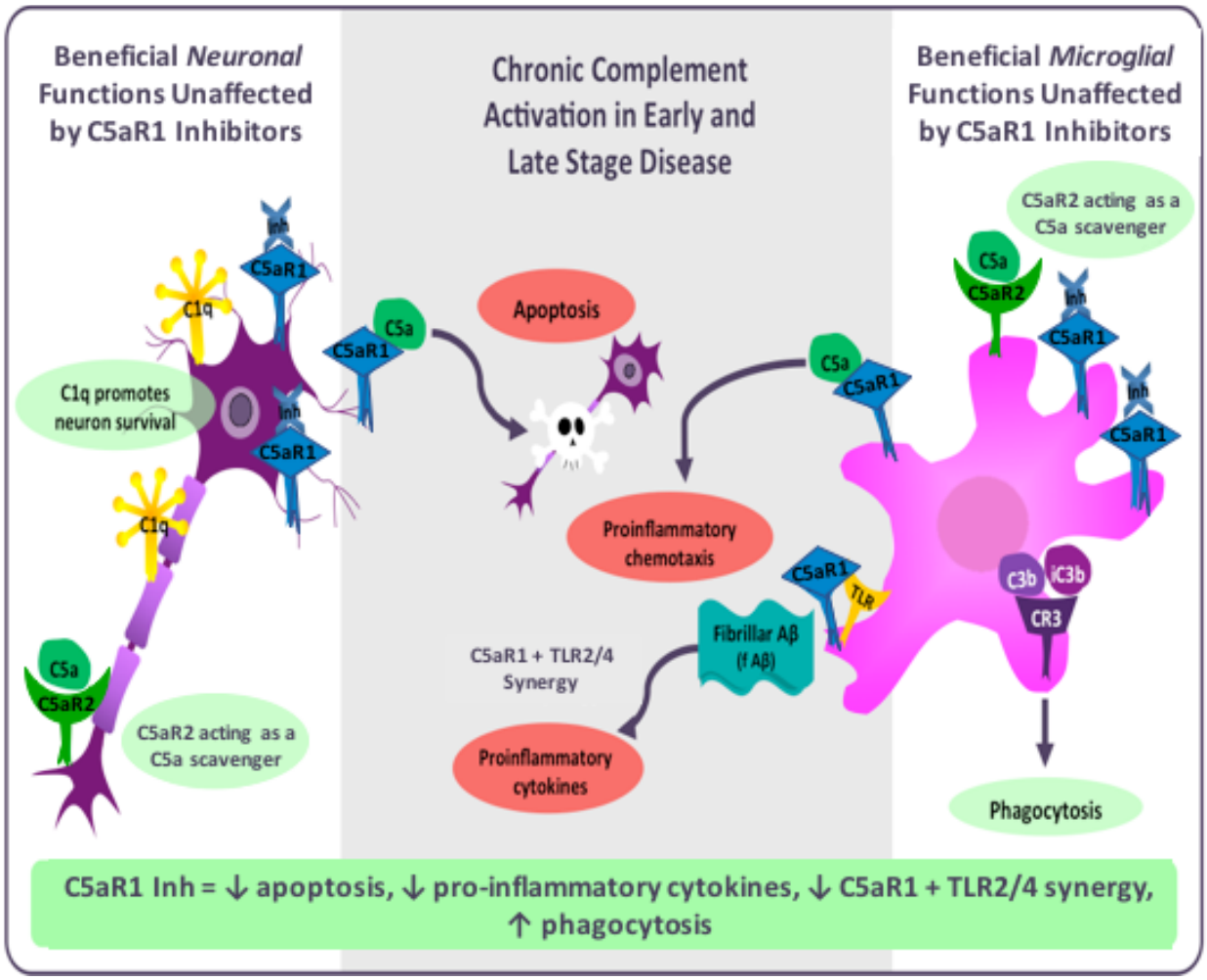

Figure 1.2. **C5aR1 inhibition maintains beneficial response of complement activation and inhibits detrimental response.** A C5aR1 specific antagonist (blue **X** Inh) is hypothesized to prevent the proinflammatory consequences of C5a interactions (in grey shadowed box) on either neurons (left panel) or microglia (right panel) or both. Adapted from (Cole, 2013).

Reference List

Abe T, Hosur KB, Hajishengallis E, Reis ES, Ricklin D, Lambris JD, Hajishengallis G (2012) Local complement-targeted intervention in periodontitis: proof-of-concept using a C5a receptor (CD88) antagonist. J Immunol 189:5442-5448.

Alzheimer's A (2016) 2016 Alzheimer's disease facts and figures. Alzheimers Dement 12:459-509.

Bamberger ME, Landreth GE (2002) Inflammation, apoptosis, and Alzheimer's disease. Neuroscientist 8:276-283.

Benoit ME, Tenner AJ (2011) Complement protein C1q-mediated neuroprotection is correlated with regulation of neuronal gene and microRNA expression. J Neurosci 31:3459-3469.

Benoit ME, Hernandez MX, Dinh ML, Benavente F, Vasquez O, Tenner AJ (2013) C1q-induced LRP1B and GPR6 Proteins Expressed Early in Alzheimer Disease Mouse Models, Are Essential for the C1q-mediated Protection against Amyloid-beta Neurotoxicity. J BiolChem 288:654-665.

Bensa JC, Reboul A, Colomb MG (1983) Biosynthesis in vitro of complement subcomponents C1q, C1s and C1 inhibitor by resting and stimulated human monocytes. The Biochemical journal 216:385-392.

Cain SA, Monk PN (2002) The orphan receptor C5L2 has high affinity binding sites for complement fragments C5a and C5a des-Arg(74). The Journal of Biological Chemistry 277:7165-7169.

Cipriani G, Dolciotti C, Picchi L, Bonuccelli U (2011) Alzheimer and his disease: a brief history. Neurol Sci 32:275-279.

Clark CM, Xie S, Chittams J, Ewbank D, Peskind E, Galasko D, Morris JC, McKeel DW, Jr., Farlow M, Weitlauf SL, Quinn J, Kaye J, Knopman D, Arai H, Doody RS, DeCarli C, Leight S, Lee VM, Trojanowski JQ (2003) Cerebrospinal fluid tau and beta-amyloid: how well do these biomarkers reflect autopsy-confirmed dementia diagnoses? Archives in Neurology 60:1696-1702.

Cole TA (2013) Complement activation in Alzheimer's disease contribution of C5a and its receptor CD88. In, p 1 online resource (189 p.). Irvine, Calif.: University of California, Irvine,.

Colton CA (2009) Heterogeneity of microglial activation in the innate immune response in the brain. J NeuroimmunePharmacol 4:399-418.

Cribbs DH, Berchtold NC, Perreau V, Coleman PD, Rogers J, Tenner AJ, Cotman CW (2012) Extensive innate immune gene activation accompanies brain aging, increasing vulnerability to cognitive decline and neurodegeneration: a microarray study. JNeuroinflammation 9:179.

El Khoury J, Luster AD (2008) Mechanisms of microglia accumulation in Alzheimer's disease: therapeutic implications. Trends in Pharmacological Sciences 29:626-632.

Farlow MR, Miller ML, Pejovic V (2008) Treatment options in Alzheimer's disease: maximizing benefit, managing expectations. Dement Geriatr Cogn Disord 25:408-422.

Fonseca MI, Ager RR, Chu SH, Yazan O, Sanderson SD, LaFerla FM, Taylor SM, Woodruff TM, Tenner AJ (2009) Treatment with a C5aR antagonist decreases pathology and

enhances behavioral performance in murine models of Alzheimer's disease. Journal of Immunology 183:1375-1383.
Fraser DA, Pisalyaput K, Tenner AJ (2010) C1q enhances microglial clearance of apoptotic neurons and neuronal blebs, and modulates subsequent inflammatory cytokine production. J Neurochem 112:733-743.
Fraser DA, Laust AK, Nelson EL, Tenner AJ (2009) C1q differentially modulates phagocytosis and cytokine responses during ingestion of apoptotic cells by human monocytes, macrophages, and dendritic cells. J Immunol 183:6175-6185.
Giannakopoulos P, Herrmann FR, Bussiere T, Bouras C, Kovari E, Perl DP, Morrison JH, Gold G, Hof PR (2003) Tangle and neuron numbers, but not amyloid load, predict cognitive status in Alzheimer's disease. Neurology 60:1495-1500.
Hardy J, Selkoe DJ (2002) The amyloid hypothesis of Alzheimer's disease: progress and problems on the road to therapeutics. Science 297:353-356.
Heneka MT et al. (2015) Neuroinflammation in Alzheimer's disease. Lancet Neurol 14:388-405.
Hernandez MX, Namiranian P, Nguyen E, Fonseca MI, Tenner AJ (2017) C5a Increases the Injury to Primary Neurons Elicited by Fibrillar Amyloid Beta. ASN Neuro 9:1759091416687871.
Hickman SE, Allison EK, El KJ (2008) Microglial dysfunction and defective beta-amyloid clearance pathways in aging Alzheimer's disease mice. JNeurosci 28:8354-8360.
Hong S, Beja-Glasser VF, Nfonoyim BM, Frouin A, Li S, Ramakrishnan S, Merry KM, Shi Q, Rosenthal A, Barres BA, Lemere CA, Selkoe DJ, Stevens B (2016) Complement and microglia mediate early synapse loss in Alzheimer mouse models. Science 352:712-716.
Jana M, Palencia CA, Pahan K (2008) Fibrillar amyloid-beta peptides activate microglia via TLR2: implications for Alzheimer's disease. J Immunol 181:7254-7262.
Karch CM, Goate AM (2015) Alzheimer's disease risk genes and mechanisms of disease pathogenesis. Biological Psychiatry 77:43-51.
Leroy K, Ando K, Laporte V, Dedecker R, Suain V, Authelet M, Heraud C, Pierrot N, Yilmaz Z, Octave JN, Brion JP (2012) Lack of tau proteins rescues neuronal cell death and decreases amyloidogenic processing of APP in APP/PS1 mice. Am J Pathol 181:1928-1940.
Li M, Pisalyaput K, Galvan M, Tenner AJ (2004) Macrophage colony stimulatory factor and interferon-gamma trigger distinct mechanisms for augmentation of beta-amyloid-induced microglia-mediated neurotoxicity. J Neurochem 91:623-633.
Liddelow SA et al. (2017) Neurotoxic reactive astrocytes are induced by activated microglia. Nature.
Liu S, Liu Y, Hao W, Wolf L, Kiliaan AJ, Penke B, Rube CE, Walter J, Heneka MT, Hartmann T, Menger MD, Fassbender K (2012) TLR2 is a primary receptor for Alzheimer's amyloid beta peptide to trigger neuroinflammatory activation. Journal of Immunology 188:1098-1107.
Maddalena A, Papassotiropoulos A, Muller-Tillmanns B, Jung HH, Hegi T, Nitsch RM, Hock C (2003) Biochemical diagnosis of Alzheimer disease by measuring the cerebrospinal fluid ratio of phosphorylated tau protein to beta-amyloid peptide42. Archives in Neurology 60:1202-1206.

Mawuenyega KG, Sigurdson W, Ovod V, Munsell L, Kasten T, Morris JC, Yarasheski KE, Bateman RJ (2010) Decreased clearance of CNS beta-amyloid in Alzheimer's disease. Science 330:1774.
Merle NS, Church SE, Fremeaux-Bacchi V, Roumenina LT (2015) Complement System Part I - Molecular Mechanisms of Activation and Regulation. Front Immunol 6:262.
Meyer-Luehmann M, Spires-Jones TL, Prada C, Garcia-Alloza M, de CA, Rozkalne A, Koenigsknecht-Talboo J, Holtzman DM, Bacskai BJ, Hyman BT (2008) Rapid appearance and local toxicity of amyloid-beta plaques in a mouse model of Alzheimer's disease. Nature 451:720-724.
Miller AM, Stella N (2008) Microglial cell migration stimulated by ATP and C5a involve distinct molecular mechanisms: Quantification of migration by a novel near-infrared method. Glia.
Morley BJ, Walport M (2000) The complement factsbook. San Diego, CA: Academic Press.
Mosher KI, Wyss-Coray T (2014) Microglial dysfunction in brain aging and Alzheimer's disease. Biochemical Pharmacology 88:594-604.
O'Barr SA, Caguioa J, Gruol D, Perkins G, Ember JA, Hugli T, Cooper NR (2001) Neuronal expression of a functional receptor for the C5a complement activation fragment. J Immunol 166:4154-4162.
Okinaga S, Slattery D, Humbles A, Zsengeller Z, Morteau O, Kinrade MB, Brodbeck RM, Krause JE, Choe HR, Gerard NP, Gerard C (2003) C5L2, a nonsignaling C5A binding protein. Biochemistry 42:9406-9415.
Pavlovski D, Thundyil J, Monk PN, Wetsel RA, Taylor SM, Woodruff TM (2012) Generation of complement component C5a by ischemic neurons promotes neuronal apoptosis. FASEB J 26:3680-3690.
Pisalyaput K, Tenner AJ (2008) Complement component C1q inhibits beta-amyloid- and serum amyloid P-induced neurotoxicity via caspase- and calpain-independent mechanisms. Journal of Neurochemistry 104:696-707.
Ramadori G, Rasokat H, Burger R, Meyer Zum Buschenfelde KH, Bitter-Suermann D (1984) Quantitative determination of complement components produced by purified hepatocytes. Clin Exp Immunol 55:189-196.
Ransohoff RM, El Khoury J (2015) Microglia in Health and Disease. Cold Spring Harb Perspect Biol 8:a020560.
Ricklin D, Hajishengallis G, Yang K, Lambris JD (2010) Complement: a key system for immune surveillance and homeostasis. Nat Immunol 11:785-797.
Rovelet-Lecrux A, Hannequin D, Raux G, Le Meur N, Laquerriere A, Vital A, Dumanchin C, Feuillette S, Brice A, Vercelletto M, Dubas F, Frebourg T, Campion D (2006) APP locus duplication causes autosomal dominant early-onset Alzheimer disease with cerebral amyloid angiopathy. Nat Genet 38:24-26.
Scahill RI, Schott JM, Stevens JM, Rossor MN, Fox NC (2002) Mapping the evolution of regional atrophy in Alzheimer's disease: Unbiased analysis of fluid-registered serial MRI. Proceedings of the National Academy of Sciences of the United States of America 99:4703-4707.
Schafer DP, Lehrman EK, Kautzman AG, Koyama R, Mardinly AR, Yamasaki R, Ransohoff RM, Greenberg ME, Barres BA, Stevens B (2012) Microglia sculpt postnatal neural circuits in an activity and complement-dependent manner. Neuron 74:691-705.

Scheuner D et al. (1996) Secreted amyloid beta-protein similar to that in the senile plaques of Alzheimer's disease is increased in vivo by the presenilin 1 and 2 and APP mutations linked to familial Alzheimer's disease. Nat Med 2:864-870.
Scola AM, Johswich KO, Morgan BP, Klos A, Monk PN (2009) The human complement fragment receptor, C5L2, is a recycling decoy receptor. MolImmunol 46:1149-1162.
Selkoe DJ, Hardy J (2016) The amyloid hypothesis of Alzheimer's disease at 25 years. EMBO MolMed.
Sewell DL, Nacewicz B, Liu F, Macvilay S, Erdei A, Lambris JD, Sandor M, Fabry Z (2004) Complement C3 and C5 play critical roles in traumatic brain cryoinjury: blocking effects on neutrophil extravasation by C5a receptor antagonist. J Neuroimmunol 155:55-63.
Shi Q, Colodner KJ, Matousek SB, Merry K, Hong S, Kenison JE, Frost JL, Le KX, Li S, Dodart JC, Caldarone BJ, Stevens B, Lemere CA (2015) Complement C3-Deficient Mice Fail to Display Age-Related Hippocampal Decline. JNeurosci 35:13029-13042.
Singhrao S, Neal JW, Morgan BP, Gasque P (1999) Increased complement biosynthesis by microglia and complement activation on neurons in Huntington's Disease. ExpNeurol 159:362-376.
Stephan AH, Madison DV, Mateos JM, Fraser DA, Lovelett EA, Coutellier L, Kim L, Tsai HH, Huang EJ, Rowitch DH, Berns DS, Tenner AJ, Shamloo M, Barres BA (2013) A Dramatic Increase of C1q Protein in the CNS during Normal Aging. J Neurosci 33:13460-13474.
Stevens B, Allen NJ, Vazquez LE, Howell GR, Christopherson KS, Nouri N, Micheva KD, Mehalow AK, Huberman AD, Stafford B, Sher A, Litke AM, Lambris JD, Smith SJ, John SW, Barres BA (2007) The classical complement cascade mediates CNS synapse elimination. Cell 131:1164-1178.
Stewart CR, Stuart LM, Wilkinson K, van Gils JM, Deng J, Halle A, Rayner KJ, Boyer L, Zhong R, Frazier WA, Lacy-Hulbert A, El Khoury J, Golenbock DT, Moore KJ (2010) CD36 ligands promote sterile inflammation through assembly of a Toll-like receptor 4 and 6 heterodimer. Nat Immunol 11:155-161.
Tenner AJ, Pisalyaput K (2008) The Complement System in the CNS: Thinking again. In: C entral Nervous System Diseases and Inflammation (Lane TE, Carson MJ, Bergmann C, Wyss-Coray T, eds), pp 153-174. New York: Springer.
Toledo JB, Weiner MW, Wolk DA, Da X, Chen K, Arnold SE, Jagust W, Jack C, Reiman EM, Davatzikos C, Shaw LM, Trojanowski JQ (2014) Neuronal injury biomarkers and prognosis in ADNI subjects with normal cognition. Acta NeuropatholCommun 2:26.
Woodruff TM, Ager RR, Tenner AJ, Noakes PG, Taylor SM (2010) The role of the complement system and the activation fragment C5a in the central nervous system. NeuromolecularMed 12:179-192.
Woodruff TM, Costantini KJ, Crane JW, Atkin JD, Monk PN, Taylor SM, Noakes PG (2008) The complement factor C5a contributes to pathology in a rat model of amyotrophic lateral sclerosis. J Immunol 181:8727-8734.
Woodruff TM, Crane JW, Proctor LM, Buller KM, Shek AB, de VK, Pollitt S, Williams HM, Shiels IA, Monk PN, Taylor SM (2006) Therapeutic activity of C5a receptor antagonists in a rat model of neurodegeneration. FASEB J 20:1407-1417.
Wyss-Coray T (2006) Inflammation in Alzheimer disease: driving force, bystander or beneficial response? NatMed 12:1005-1015.

Zhang B et al. (2013) Integrated Systems Approach Identifies Genetic Nodes and Networks in Late-Onset Alzheimer's Disease. Cell 153:707-720.
Zhang X, Kimura Y, Fang C, Zhou L, Sfyroera G, Lambris JD, Wetsel RA, Miwa T, Song WC (2007) Regulation of Toll-like receptor-mediated inflammatory response by complement in vivo. Blood 110:228-236.

CHAPTER 2

C5a Increases the Injury to Primary Neurons Elicited by Fibrillar Amyloid Beta

Abstract:

C5aR1, the proinflammatory receptor for C5a, is expressed in the CNS on microglia, endothelial cells, and neurons. Previous work demonstrated that the C5aR1 antagonist, PMX205, decreased amyloid pathology and suppressed cognitive deficits in two Alzheimer Disease (AD) mouse models. However, the cellular mechanisms of this protection have not been definitively demonstrated. Here, primary cultured mouse neurons treated with exogenous C5a show reproducible loss of MAP-2 staining in a dose-dependent manner within 24 hours of treatment, indicative of injury to neurons. This injury is prevented by the C5aR1 antagonist PMX53, a close analog of PMX205. Furthermore, primary neurons derived from C5aR1 null mice exhibited no MAP-2 loss after exposure to the highest concentration of C5a tested. Primary mouse neurons treated with both 100 nM C5a and 5 μM fAβ, to model what occurs in the AD brain, showed increased MAP-2 loss relative to either C5a or fAβ alone. Blocking C5aR1 with PMX53 (100 nM) blocked the loss of MAP2 in these primary neurons to the level seen with fAβ alone. Similar experiments with primary neurons derived from C5aR1 null mice showed a loss of MAP-2 due to fAβ treatment. However, the addition of C5a to the cultures did not enhance the loss of MAP-2 and the addition of PMX53 to the cultures did not change the MAP-2 loss in response to fAβ. Thus, at least part of the beneficial effects

of C5aR1 antagonist in AD mouse models may be due to protection of neurons from the toxic effects of C5a.

Introduction

Alzheimer's disease (AD) is the most common form of dementia among the elderly. Characteristic neuropathological changes seen in AD brain include synaptic and neuronal loss, neurofibrillary tangles (NFTs), extracellular senile plaques composed of amyloid (Aβ) protein deposits and evidence of inflammatory events. The relative contributions of these pathological markers to the cognitive dysfunction in AD remains controversial, but clinical and transgenic animal studies are increasingly suggesting that Aβ alone is not sufficient for the neuronal loss and subsequent cognitive decline observed in AD ((Aizenstein et al., 2008;Blurton-Jones et al., 2009;Fonseca et al., 2009) and reviewed in (Selkoe and Hardy, 2016)). The role of neuroinflammation in neurodegenerative diseases, particularly relating to Alzheimer's disease, is an active area of research (reviewed in (Wilcock et al., 2011;Wyss-Coray and Rogers, 2012)), and immune activation in the brain has been identified by many groups as a potential therapeutic target ((Bachstetter et al., 2012) and reviewed in (Heneka et al., 2015)).

The complement system is a well-known part of the innate immune system that consists of more than 30 proteins found in plasma and cell surfaces, which protects from infection and aids in resolution of injury (Ricklin et al., 2010). Complement activation leads to the enhancement of phagocytosis of pathogens, apoptotic cells and cellular debris as well as the generation of the anaphylatoxin C5a. This powerful anaphylatoxin can recruit phagocytes, such as microglia, to sites of infection and/or injury via its G-protein-coupled

receptor C5aR1 (Yao et al., 1990;Nolte et al., 1996), as reviewed in (Klos et al., 2009). In the CNS, the C5aR1 receptor has been reported to be expressed by many cell types including microglia, astrocytes, and neurons (reviewed in (Woodruff et al., 2010)). While issues with antibody specificity and sensitivity have led to inconsistent reports, our lab has demonstrated specific C5aR1 staining on microglia that increases in AD mouse models (Ager et al., 2010).

Evidence is accumulating that most complement factors are synthesized in the brain upon insult and are upregulated in the brain in both humans and mouse models in aging and AD, (Fonseca et al., 2011;Cribbs et al., 2012;Benoit et al., 2013) and reviewed in (Harvey and Durant, 2014). Moreover, the beta-sheet conformation of fAβ has been shown to initiate the activation of the complement cascade by the classical and alternative pathways (reviewed in (Alexander et al., 2008)). Since the 1980's, complement factors have been known to be associated with fibrillar (thioflavine-staining) amyloid plaques found in AD patient brains (McGeer et al., 1989;Rogers et al., 1992;Afagh et al., 1996). In addition, plaques from mouse models of AD have also demonstrated extensive deposition of factors of complement (Akiyama et al., 2000;Matsuoka et al., 2001;Zhou et al., 2008;Loeffler et al., 2008).

Recent studies have shown that C5aR1 signaling is detrimental in various neurodegenerative disease mouse models (Woodruff et al., 2006;Woodruff et al., 2008;Fonseca et al., 2009;Brennan et al., 2015). Indeed, our previous study in two mouse models of Alzheimer's disease showed a dramatic (50-70%) decrease in amyloid plaque deposition, glial activation markers, and phosphorylated tau after 12 weeks of treatment with the C5aR1 antagonist PMX205. However, whether this protective effect was the result of an effect of the antagonist on microglia, where receptors have clearly been documented,

or a direct effect on neurons or both could not be addressed in those models (Fonseca et al., 2009). The effects of C5a on neurons *in vitro* have been studied, although the results have varied greatly. Some studies have shown C5a can directly act on C5aR1 and cause apoptosis (Farkas et al., 1998;Pavlovski et al., 2012). Others have shown that addition of C5a can protect terminally differentiated neuroblastoma cells from Aβ toxicity (O'Barr et al., 2001). Given that cell lines do not always recapitulate findings in primary cells, we tested if C5a can enhance the injury to mouse primary neurons treated with fAβ *in vitro.*

Our new findings support previous results demonstrating that C5a can induce neuronal cell death. Both pharmacologic and genetic data indicate that C5aR1 is required for the C5a-induced decrease of neuron MAP-2. Additionally, in the context of AD, we show that increased neuronal damage is caused by the addition of C5a to neurons treated with fAβ, and can be blocked by the C5aR1 antagonist, PMX53. These findings suggest that at least part of the therapeutic benefit of C5aR1 antagonist seen earlier in mouse models of AD (Fonseca et al., 2009) may result from a direct protection of neurons and support further investigation of the use of such antagonists as part of a therapeutic strategy to slow the progression of Alzheimer's disease and other neurological disorders in which complement activation may occur generating C5a in a neuronal environment in humans.

Materials and Methods

Reagents

Hanks' balanced salt solution (HBSS), serum-free neurobasal media (NB), B27 supplement (50x), L-glutamine, Prolong Gold anti-fade reagent with 4',6-diamidino-2-phenylindole (DAPI), SuperScript III reverse transcriptase, SYBR/Green Master mix, and

Alexa 405-, 488-, or 555-conjugated secondary antibodies were obtained from ThermoFisher. Poly-L-lysine hydrobromide, cytosine β-D-arabinofuranoside hydrochloride (Ara-C), and anti-actin antibody were from Sigma. Microtubule-associated protein 2 (MAP-2) antibody was obtained from Abcam. C5aR1 antibody (10/92) was obtained from SeroTec (Ager et al., 2010). Anti VGLUT1 and anti GAD67 antibodies were obtained from Millipore. HRP-conjugated $F(ab')_2$ antibodies were from Jackson ImmunoResearch Laboratories. Human C5a peptide was obtained from CompTech. PMX53 was obtained from Cephalon. All buffers are made with Millipore-purified water with additional filters to eliminate LPS and are periodically tested for endotoxin using the *Limulus* amebocyte lysate clot assay (all solutions added to cells were < 0.1 EU/mL; 1 EU is equivalent to 0.1 ng/mL LPS).

β-amyloid synthesis, purification, and conformation characterization

Human β-amyloid (1–42) ($A\beta_{1-42}$), provided by Dr. Charles Glabe (University of California at Irvine), was synthesized by fluoren-9-ylmethoxy carbonyl chemistry using a continuous flow semiautomatic instrument as described previously (Burdick et al., 1992). The peptide was reconstituted in filter-sterilized water at a concentration of 1mM after which, equal volume of 2X TBS (0.033M Tris, 0.267 M NaCl) was added (final concentration 500 μM Aβ). After 20-24 hr at 4˚C to allow fibril formation, aliquots were frozen for future use. The peptide conformation was analyzed by circular dichroism (CD) to confirm β-sheet conformation. Briefly, after using 1x TBS as a blank, 200 μl of the peptide at 50 μM was run on a Jasco J-720 CD spectrometer and read from 200 nm to 250 nm with a step resolution of 0.5 nm and a scan speed of 20 nm/min. Four scans were acquired and averaged to generate the CD spectra of the peptide (**Figure 2.1**) (Li et al., 2004).

Animals, neuron isolation, and culture

All animal experimental procedures were reviewed and approved by the Institutional Animal Care and Use Committee of University of California, Irvine. C57BL/6J were purchased from Jackson Laboratory and C5aR1 knock out mice were originally a gift provided by Dr. Rick Wetsel (Hollmann et al., 2008). Pregnant mice were sacrificed by exposure to CO2 followed by cervical dislocation as a secondary method of euthanasia, after which the E15-E16 embryos were quickly removed and the whole brains kept in Hank's balanced salt solution free of calcium and magnesium (CMF) and cleaned of meninges. Cerebral cortices were dissected out and exposed to 0.125% of trypsin in CMF for 7 min at 37°C. Cortical tissues were then resuspended in Dulbecco's modified eagle medium (DMEM) supplemented with fetal bovine serum (DMEM/FBS10%; endotoxin concentration ≤ 0.06 EU/mL), and dissociated by trituration using flame polished siliconized Pasteur pipettes. Viable cells, quantified by trypan blue exclusion, were plated at 1-2 × 10^5 cells per well in 0.5 mL of DMEM/FBS10% on poly l-lysine (100 μg/mL) coated glass coverslips (Neuvitro) in 24-well plates (Costar, Cambridge, MA, USA). After 2 hours the media was replaced with 0.5 mL serum-free neurobasal medium supplemented with B27 (NB/B27). On day 3, the media was supplemented with Ara-C at 10 nM to reduce glia

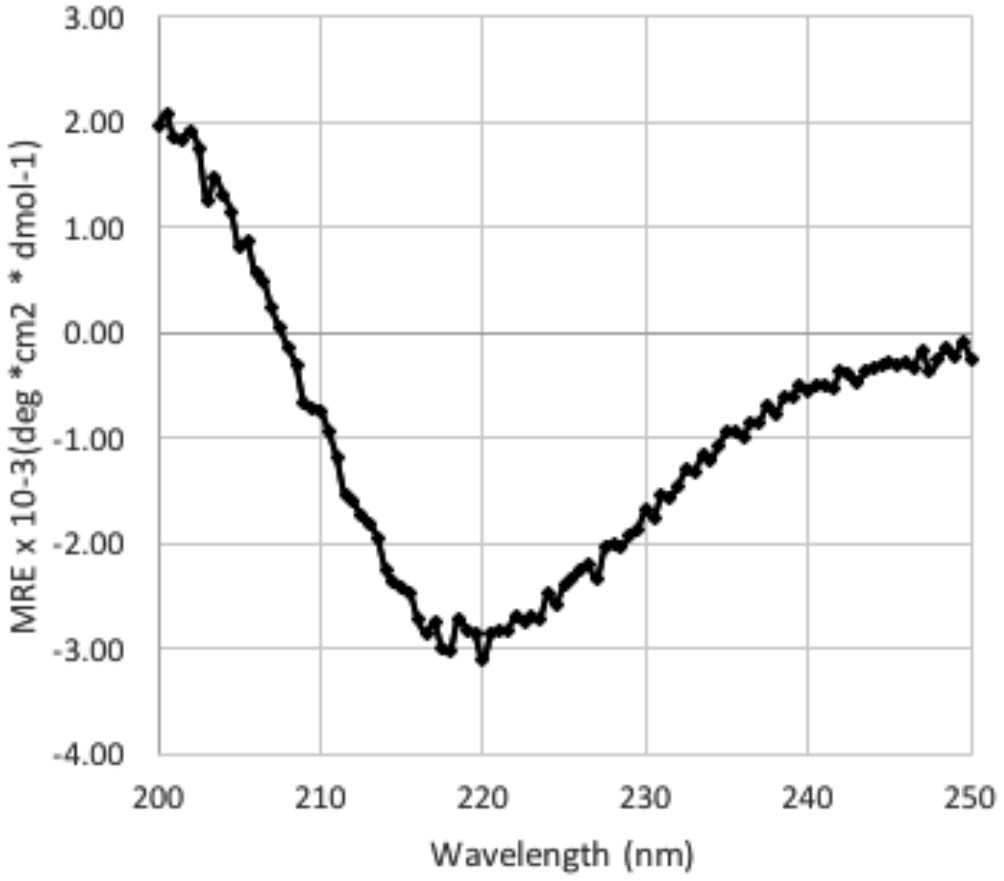

Figure 2.1. Circular dichroism of amyloid beta preparation confirms beta sheet structure. Amyloid beta peptide incubated for 20-24 hours shows minima at 218nm, indicative of β- sheet structure.

proliferation, and cultures were grown for 7–10 days *in vitro* before stimulation with 5 μM fAβ, human C5a (1, 10 and 100 nM) (Benoit and Tenner, 2011) and/or PMX53 (100 nM). The concentration of fAβ chosen was previously shown to confer partial damage to primary rat neurons (Li et al., 2004) and confirmed with mouse neurons (Benoit et al., 2013). The dose of 100 nM C5a was selected for further interaction studies with fAβ after preliminary studies demonstrated 100 nM of C5a caused the biggest decrease in MAP-2 (**Figure 2.2**). In some experiments, TNF-alpha was added on day 7 at 0, 10, and 100 ng/mL for 24 hours, followed by lysis of neurons for RNA isolation for C5aR1 qRT-PCR.

Immunocytochemistry

Neurons were fixed with 3.7% paraformaldehyde and permeabilized with 0.1% Triton X-100. Immunocytochemistry was performed as described previously (Benoit and Tenner, 2011). Briefly, after blocking with 10% FBS in PBS, neurons were incubated with chicken anti-MAP-2 antibody (dilution: 1:10000) for 24 hrs at 4˚C. After three washes, coverslips were incubated with Alexa fluor 488-conjugated anti-chicken IgG antibody (dilution: 1:1000) at room temperature for 1 hr. For colocalization experiments after blocking, cells were incubated with chicken anti MAP-2 antibody (9 ug/ml) and mouse anti GAD67 (1.5 ug/ml, clone 1G10.2, Millipore) or mouse anti VGLUT1 (1 ug/ml, Millipore) for 1h at RT. Cells were then incubated with the corresponding secondary antibodies, Alexa fluor 488-conjugated anti chicken IgG (dilution: 1:1000) and Alexa 555 conjugated anti mouse IgG (dilution: 1:300) respectively for 1 hr at RT. The slides were mounted with 5 μl of Prolong Gold anti-fade reagent with DAPI. Cells were examined using the Axiovert 200 inverted microscope with AxioCam digital camera controlled by Axiovision program (Zeiss)

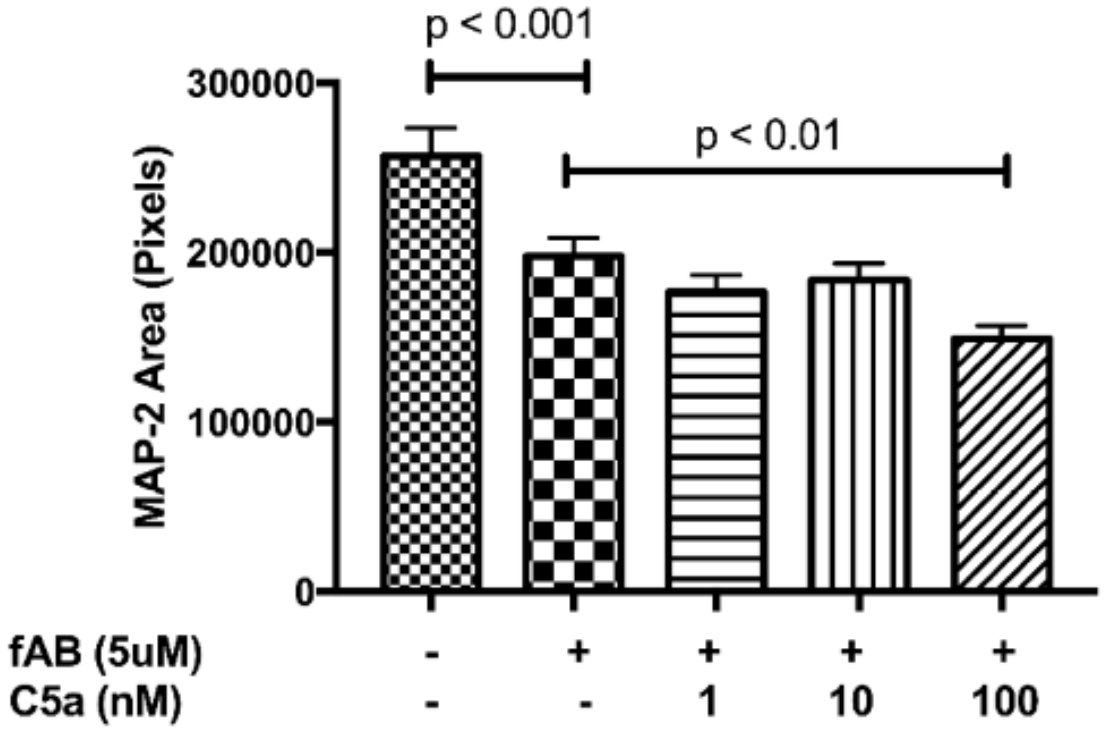

Figure 2.2. **C5a at a concentration of 100 nM increases MAP-2 loss in the presence of fAβ.** Primary neurons from WT mice were generated using E15-E16 pups and cultured for 7-10 days. The cells were then stimulated with 5 μM fAβ and 1, 10 or 100 nM hC5a for 24 hours. MAP-2 was visualized by immunocytochemistry (20x magnification) and quantified using ImageJ software as described in Materials and Methods. Data are presented as mean +/- SEM. n = 3 independent experiments, each with 3 coverslips per treatment, 3 images per coverslip. p values are calculated using One-way ANOVA, uncorrected Fisher's LSD test. Values of $p < 0.05$ were considered statistically significant.

or the Nikon Eclipse Ti-E fluorescent microscope and the NIS-Element AR 3.00 software. For each coverslip (3 per condition, per experiment), 3-5 micrographs were taken to represent the entirety of the coverslip. The MAP-2 area was quantified using ImageJ software (Benoit et al., 2013). Briefly, the images were converted to grayscale, using the adjust "threshold" function under default conditions, the MAP-2 stained neurons were highlighted as regions of interest, and the area (as measured in pixels) was quantified using the "measure" function. The loss of MAP2 immunoreactivity has been demonstrated to be directly proportional to neuronal death (Brooke et al., 1999).

For colocalization of MAP-2 and GAD67 or VGLUT-1 images were analyzed using Zeiss Axiovision 4.6 software and percent of immunopositive area (% Field Area) (immunopositive area / total image area x 100) was determined. The mean % Field Area of each condition was obtained by averaging 5-7 images per coverslip (3 per condition).

Western blot

Neurons plated in 12-well plates at 2.5 x 10^5 cells per well, were washed with 1 mL Hank's Balanced Salt Solution (HBSS) and lysed with 200 µL of SDS reducing sample buffer. Samples were boiled for 5 min and equal amount of volume was loaded and separated by a 10% sodium dodecyl sulfate polyacrylamide gel electrophoresis (SDS-PAGE), transferred to nitrocellulose membrane (GE Healthcare), and then incubated with blocking buffer (5% powdered milk in Tris buffered saline (TBS)/Tween 0.1%) for 1 hr at RT. After washing, membranes were incubated overnight at 4˚C with rat anti-C5aR1 antibody (dilution: 1:1000). After three washes, the membranes were incubated with HRP-conjugated anti-rat antibody (dilution: 1:5000) for 1 hr at RT. The blots were developed using enhanced

chemiluminescence plus (ECL+, GE Healthcare) and analyzed using the Nikon D700 digital SLR camera (Khoury et al., 2010) and ImageJ software. Equal protein loading for each lane per gel was confirmed by subsequent actin probing with mouse anti-actin antibody (dilution: 1:2000) followed by HRP-conjugated anti-mouse antibody (dilution 1:5000).

RNA extraction and qRT-PCR

Total RNA from cortical neuronal cultures was extracted using the Illustra RNAspin mini isolation kit (GE Healthcare). cDNA synthesis was performed using Superscript III reverse transcriptase following manufacturer's instructions. Quantitative RT-PCR was performed using the iCycler iQ and the iQ5 software (Bio-Rad) using SYBR/Green Master Mix. Mouse C5aR1 and HPRT primers were designed using primer-blast (ncbi.nlm.nih.gov) and obtained from Eurofins (Louisville, KY): C5aR1: Forward 5'-3': GGGATGTTGCAGCCCTTATCA; Reverse 5'-3': CGCCAGATTCAGAAACCAGATG. HPRT: Forward 5'-3': AGCCTAAGATGAGCGCAAGT; Reverse 5'-3': ATCAAAAGTCTGGGGACGCA. Quantitative RT-PCR data was only accepted if detected below 40 cycles of amplification.

Statistical analysis

All of the data are presented as mean +/- SEM. Using Prism GraphPad, two-group comparisons were analyzed by the unpaired 2-tailed Student's t test, and multiple-group comparisons were performed by One-way ANOVA uncorrected Fisher's LSD test as noted in Figure Legends. Values of $p < 0.05$ were considered statistically significant. Each independent experiment consisted of a neuronal culture derived from its own unique litter of pups to attain biological replicates.

Results

Mouse primary neurons express C5aR1

C5aR1 has previously been observed on a subset of neurons from both human and murine samples (O'Barr et al., 2001;Woodruff et al., 2010). To investigate whether the C5aR antagonist benefit seen in our previous in vivo AD mouse models could be in part due to a direct protective effect on neurons, primary mouse neuron cultures from E15.5 cortical neurons were cultured for 7 days and qRT-PCR was performed to determine C5aR1 expression in those primary mouse cultures. Unstimulated primary neurons showed C5aR1 mRNA in wild type primary neuron cultures but not neurons derived from C5aR1KO pups (**Figure 2.3A**). The expression of C5aR1 was upregulated by TNF-α in a dose-dependent manner (**Figure 2.3B**) within 24 hrs of treatment in wild type but not C5aR1KO primary neurons. Protein expression in these neuronal cultures was below the level of detection with the proven specific anti C5aR1 antibody (10/92) by immunohistochemistry and by western blot analysis. Anti-C5aR1 antibody reactivity was confirmed in primary neonatal microglia culture lysates derived from C5aR1-sufficient pups and which was absent in microglia from C5aR1KO pups. (data not shown and (Ager et al., 2010)).

C5a is toxic to primary neurons via C5aR1

Given that neuronal C5aR1 has been implicated in neurodegeneration and has been shown to lead to apoptosis of cultured neurons (Pavlovski et al., 2012), we tested whether purified

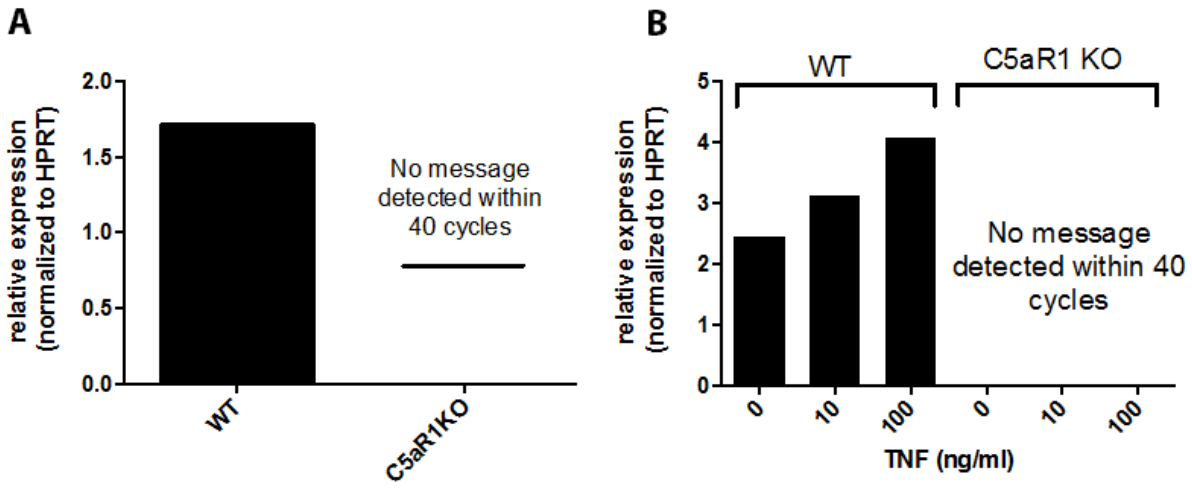

Figure 2.3. C5aR1 expression on primary neurons.

Primary neurons from WT mice and C5aR1KO mice were generated using E15-E16 pups, cultured for 7-10 days, and RNA was collected from either (A) unstimulated cultures (WT n=4; KO n=2) or from (B) cultures treated with 0, 10 or 100 ng/ml of TNF-α for 24 hrs (n=2 for WT cells and n= 1 for C5aR1 knock out cells). Quantitative RT-PCR for C5aR1 expression relative to HPRT was performed with technical triplicates in each experiment. P values are calculated using unpaired 2-tailed t-test. Values of $p < 0.05$ were considered statistically significant.

human C5a was neurotoxic to our primary mouse cortical neurons. After 24 hours of exposure to C5a, the 10 nM and 100 nM concentrations of C5a tested were found to be damaging to neurons, as assayed by MAP-2 staining (a surrogate marker of neuronal health more sensitive than other assays (Brooke et al., 1999)). The maximal concentration of 100 nM C5a led to the greatest MAP-2 loss (**Figure 2.4A-D, F**). Pretreating the neurons with equal molar concentrations of the specific insurmountable C5aR1 antagonist, PMX53, completely prevented the MAP-2 loss induced by C5a (**Figure 2.4E-F**). To further confirm that C5a was acting through C5aR1 on neurons, primary neuron cultures were isolated from C5aR1KO pups, cultured and tested as with wild type neurons. Addition of C5a at 100 nM did not decrease MAP-2 compared to untreated C5aR1KO neurons (**Figure 2.4G-I**).

C5a enhances the toxicity of fibrillar amyloid beta

Complement components have been found to be upregulated in the AD brain, with many studies suggesting a detrimental role for complement in AD (Fonseca et al., 2009;Veerhuis, 2011) . To determine whether C5a can further damage neurons treated with fAβ, 7-10 day primary neuronal cultures were exposed to fAβ that was verified to have beta-sheet structure by circular dichroism (**Figure 2.1**). While 5 uM fAβ alone reduced MAP-2 by 18.5% within 24 hrs (**Figure 2.5A-B**), addition of 100 nM C5a to fAβ-treated neurons further decreased MAP-2 by 20.8% relative to fAβ alone (**Figure 2.5D, K**). The additional decrease of MAP-2 observed after addition of C5a was blocked by pre-treatment with PMX53 (**Figure 2.5E, K**). Neuron cultures derived from C5aR1KO mice did not show a decrease in MAP-2 relative to fAβ-treated neurons after C5a was added to the cultures

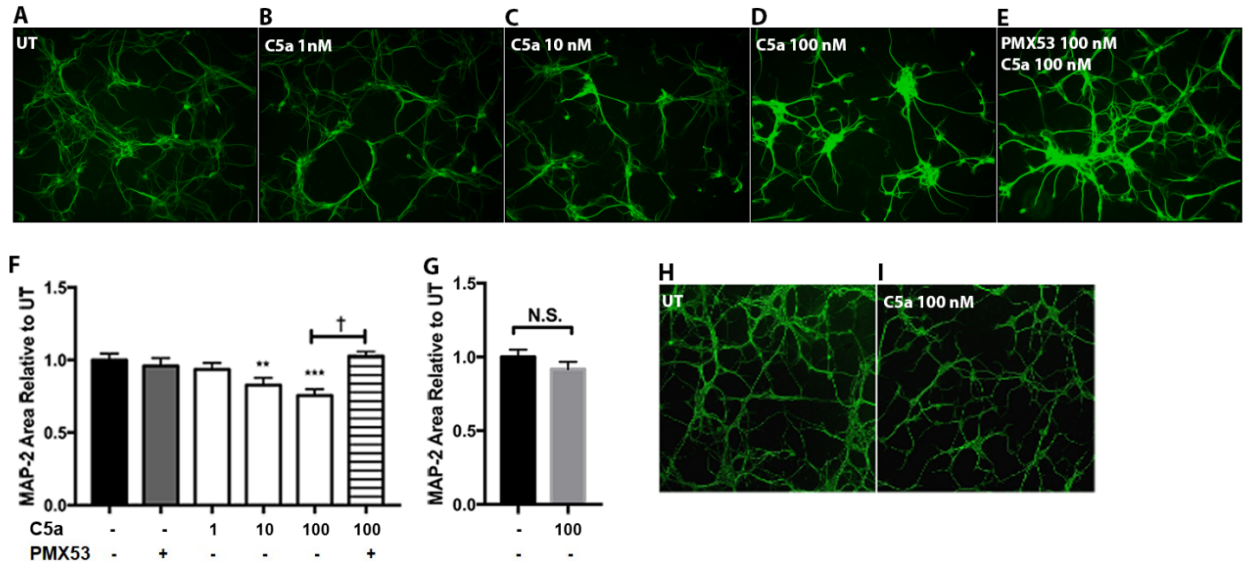

Figure 2.4. C5a causes MAP-2 loss in a dose-dependent manner. Primary neurons from WT mice (A-E and F) or C5aR1KO mice (H-I and G) were generated using E15-E16 pups and cultured for 7-10 days. The cells were then stimulated with the indicated concentrations of hC5a, and/or 100nM PMX53 for 24 hours. MAP-2 was visualized by immunocytochemistry (10x magnification) and quantified (F-G) using ImageJ software as described in M & M. Data are presented as percentage of MAP-2 area relative to untreated (UT) +/- SEM. n = 4 independent experiments (F) and n = 3 independent experiments (G), each experiment having 3 coverslips per treatment, 3-5 images per coverslip. $p<0.05$ *, $p< 0.01$ ** relative to untreated cultures using One-way ANOVA, uncorrected Fisher's LSD test (F), and $p < 0.02$ † unpaired 2-tailed t-test (F,G).

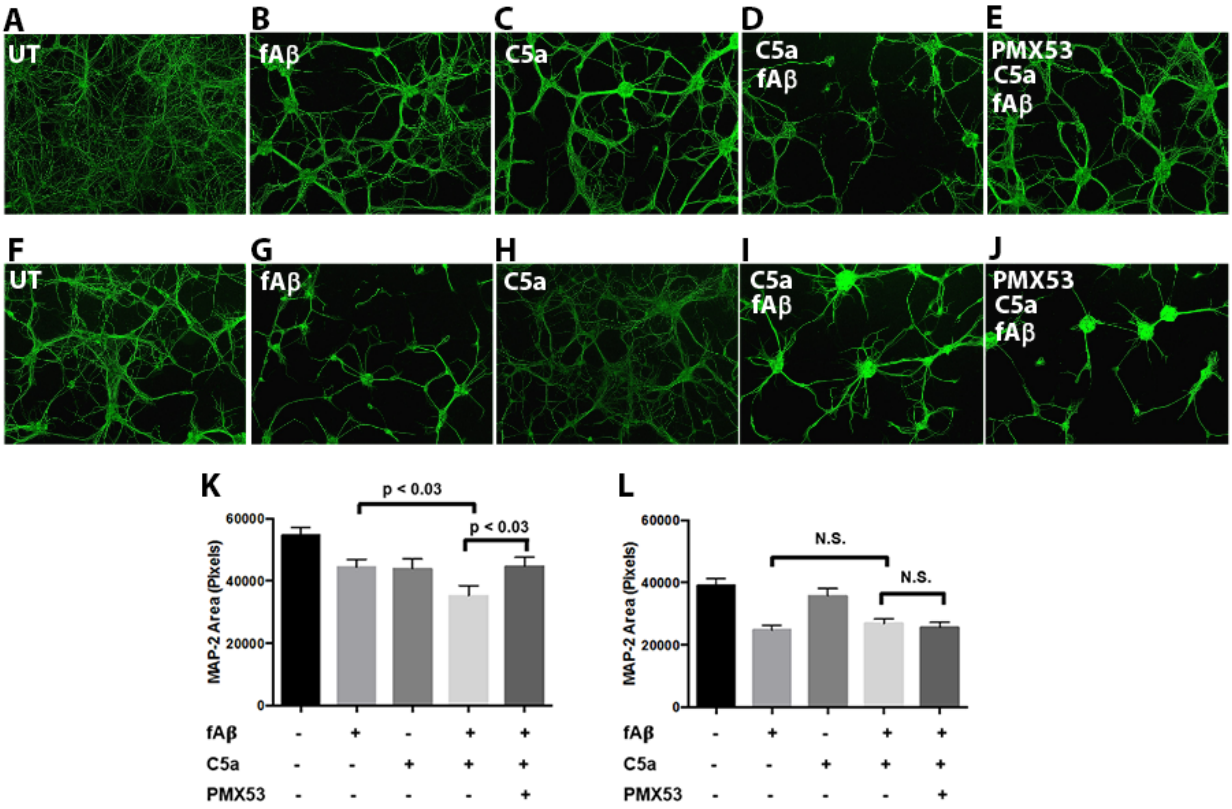

Figure 2.5. C5a increases toxicity in fAβ-treated neurons. Primary neurons from WT mice (A-E and K) or C5aR1KO mice (F-J and L) were generated using E15-E16 pups and cultured for 7-10 days. The cells were then stimulated or not with 5 μM fAβ, 100 nM hC5a, and/or 100nM PMX53 for 24 hours. MAP-2 was visualized by immunocytochemistry (20x magnification) and quantified using ImageJ software (K,L). Data are presented as mean MAP-2 area +/- SEM. n = 3 independent experiments, each with 3 coverslips per treatment, 5 images per coverslip. P values are calculated using unpaired 2-tailed t-test. Values of $p < 0.05$ were considered statistically significant.

(**Figure 2.5G-I, L**). As expected, pre-treatment with PMX53 did not protect C5aR1KO neurons from the fAβ-mediated toxicity (**Figure 2.5I, J, and L**).

VGLUT1 and GAD67 staining in mouse neuron cultures

To characterize the neuronal populations present in the 7-10 day mouse cultures and determine if either neuronal population was selectively affected by treatments, staining for GABAergic (GAD67+) and glutamatergic (VGLUT1+) markers was performed. The neuronal cultures were positive for both markers (**Figure 2.6**) and when treated with Aβ or C5a, no decrease in a selective population of neurons (glutamatergic or GABAergic) was seen (**Figure 2.7**).

Discussion

Our previous work demonstrated that blocking C5aR1 in two mouse models of Alzheimer's disease resulted in a reduction of activated glia and amyloid deposits (Fonseca et al., 2009). Given the dominant expression of C5aR1 on microglia (Ager et al., 2010), it was hypothesized that the basis for the protective role of the C5aR1 antagonist *in vivo* was by inhibiting C5aR1-dependent proinflammatory responses of microglia. However, here we show that C5a leads to a decrease in MAP-2 staining when added to primary neuron cultures alone, and increases neuronal damage resulting from Aβ treatment. PMX53, a C5aR1 specific antagonist (Otto et al., 2004), blocked the C5a-induced loss of MAP-2.

Although C5aR1 protein in these neurons was not detectable using anti C5aR1 antibody (10/92), others have evidence of C5aR1 neuronal protein expression using a polyclonal chicken antibody (Pavlovski et al., 2012). Since primary neurons derived from C5aR1KO

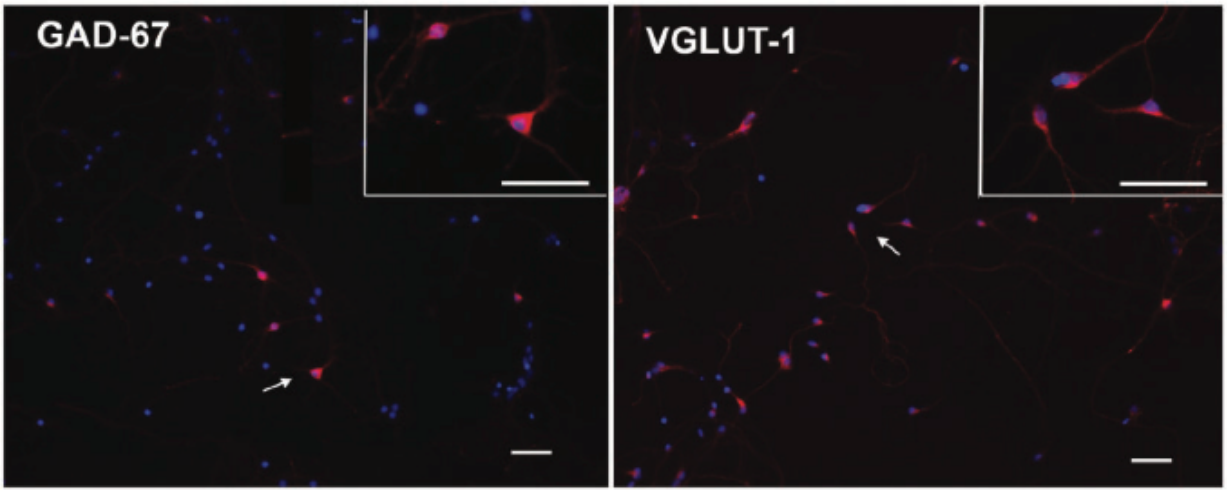

Figure 2.6. Primary neuronal cultures include GABAergic and glutamatergic neurons. Immunofluorescent staining of GAD67 (red, GABAergic neurons) (left panel) or VGLUT1 (red, Glutamatergic neurons) (right panel) in 7-day mouse neuron cultures. Nuclei are labeled with DAPI (blue) (10x magnification). Top right Inset in each panel is 20x magnification of region denoted by the arrow. Scale Bar: 50 μm

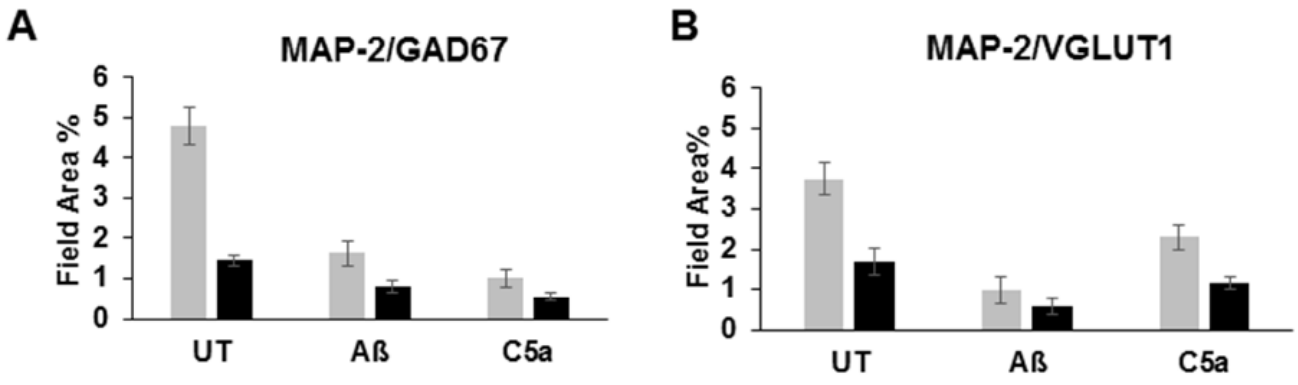

Figure 2.7. fAβ and C5a kill both GABAergic and glutamatergic neurons in culture. Quantification of the immunostaining of MAP-2 (grey bars) (A,B) and GAD67 (black bars) (A) or VGLUT1 (black bars) (B) in 7days cultures untreated or treated with 5 uM fAβ or C5a (100 uM). Bars represent the average of 5-7 images per coverslip (n=3) per condition +/- SEM.

mice showed no C5a-induced loss of MAP-2, taken together these data provide evidence that neuronal C5aR1 is the receptor mediating the C5a induced neuronal damage, and suggests that another beneficial consequence of C5aR1 antagonists in the context of AD is suppressing detrimental neuronal C5a-C5aR1 signaling.

The complement cascade is a powerful effector mechanism of the innate immune system that can be directly activated by fibrillar Aβ and has been implicated as a potential player in the inflammatory response in AD (reviewed in (Wyss-Coray and Rogers, 2012)). In brain, synthesis of most of the complement components increase during aging with a further increase in AD patients and animal models of AD consistent with a role for complement in the progression of the disease (Reichwald et al., 2009;Cribbs et al., 2012). Thus, as fibrillar plaques appear and complement component expression increase with age, complement will be activated generating C5a which will then diffuse and bind to C5aR1 expressing neurons and microglia.

Toll-like receptors (TLRs) are recognition components of the innate immune response that trigger protective inflammatory responses to the pathogens they recognize. TLR have been found to synergize with C5a-induced activation of phagocytes in the periphery (reviewed in (Song, 2012;Hajishengallis et al., 2013)) exacerbating a proinflammatory response thereby producing detrimental levels of proinflammatory cytokines (e.g. TNF-α, IL-1β). While neurons are also known to have TLR4 (Leow-Dyke et al., 2012), *in vitro*, we noted additive but not synergistic neuronal loss when C5a was added with fAβ to cultured neurons. While no preferential loss of GABAergic or glutamatergic neurons were seen in our cultures, it is possible that *in vivo* some subsets of neurons may be more susceptible to C5a mediated

damage than others. Whether proinflammatory functions of C5a and TLR triggered in microglia may synergize to enhance neuronal dysfunction *in vivo* remains to be seen.

It is worth noting that addition of recombinant C5a has been shown to decrease cell viability in undifferentiated SH-SY5Y cells while retinoic acid (RA)-differentiated SH-SY5Y cells showed no change in viability to C5a and were protected against aggregated Aβ injury (O'Barr et al., 2001). These findings can be explained by the difference in biology when comparing cell lines used in that report to primary cultures used here or to the effect of RA-differentiation. More recent work using primary mouse neurons demonstrated recombinant C5a had a negative impact on neuronal viability (Pavlovski et al., 2012), which our study corroborates.

Primary neurons, although a better alternative to transformed and dividing cell lines, do not always recapitulate what happens *in vivo*. However, in our previous work with the 3xTg AD mouse model, PMX205, a close analog of PMX53, significantly and substantially reduced hyperphosphorylated tau by 69%. Thus, *in vivo* neurons were protected directly or indirectly when C5aR1 was inhibited. The *in vitro* data here thus suggest that the use of a C5aR1 antagonist could be beneficial in neurological diseases in which complement activation generating C5a occurs. PMX53 and PMX205 are cyclic hexapeptides based on the C-terminal end of C5a that differ only in substitution of hydrocinnamate for acetylated phenylalanine, (reviewed in (Kohl, 2006)), are orally active, with PMX205 showing more favorable bioavailability (Woodruff et al., 2005). The C5aR1 specific antagonists PMX53 and/or PMX205 have been shown to reduce disease activity in several animal models, including models of CNS disease such as brain trauma (Sewell et al., 2004), amyotrophic lateral sclerosis (ALS) (Woodruff et al., 2008) and Huntington-like neurodegeneration

(Woodruff et al., 2006). In addition, the genetic deficiency of C5 has been shown to be one of a limited number of genetic differences associated with decreased amyloid deposition in DBA/2J mice vs. C57Bl6 mice transgenic for the human APP gene (Ryman et al., 2008;Jackson et al., 2015), supporting a pathogenic role for C5a in the context of the AD brain *in vivo.*

When proposing systemic C5aR1 antagonist administration, it is important to consider the possibility that the recruitment of leukocytes into areas of infection may be dampened. However, the ability to generate bacteriolytic C5b-9 and to opsonize pathogens with C3b/iC3b (for ingestion and killing of pathogens) as well as the presence of antibody and T cell mechanisms of immune protection would remain intact. Thus, killing of C5b-9 susceptible microbes could still occur, as well as protective complement-independent and C3b/iC3b dependent antibody effector mechanisms (such as Fc receptor mediated phagocytosis, neutralization, complement opsonization and enhanced cytotoxicity). The lack of observable toxicity in multiple acute rodent models previously investigated and the extended treatment in our studies (Fonseca et al., 2009), lack of adverse effects in Phase 1 and 2 studies in humans of PMX53 (Kohl, 2006;Vergunst et al., 2007) and the current use of Eculizamab (anti C5) as a therapy in humans, suggest a promising safety profile of treatment with C5a receptor antagonists.

In summary, C5a was found to induce neuronal damage both alone and in the presence of amyloid β. This damage was prevented in the presence of PMX53 and absent for neurons genetically lacking C5aR1. These findings further implicate C5aR1 antagonists as a class of AD therapeutics that could have benefit in slowing progression of the disease while having limited negative suppressive effects on the immune system.

Reference List

Afagh A, Cummings BJ, Cribbs DH, Cotman CW, Tenner AJ (1996) Localization and cell association of C1q in Alzheimer's disease brain. Exp Neurol 138:22-32.

Ager RR, Fonseca MI, Chu SH, Sanderson SD, Taylor SM, Woodruff TM, Tenner AJ (2010) Microglial C5aR (CD88) expression correlates with amyloid-beta deposition in murine models of Alzheimer's disease. J Neurochem 113:389-401.

Aizenstein HJ, Nebes RD, Saxton JA, Price JC, Mathis CA, Tsopelas ND, Ziolko SK, James JA, Snitz BE, Houck PR, Bi W, Cohen AD, Lopresti BJ, DeKosky ST, Halligan EM, Klunk WE (2008) Frequent amyloid deposition without significant cognitive impairment among the elderly. Arch Neurol 65:1509-1517.

Akiyama H, et al. (2000) Inflammation and Alzheimer's disease. Neurobiol Aging 21:383-421.

Alexander JJ, Anderson AJ, Barnum SR, Stevens B, Tenner AJ (2008) The complement cascade: Yin-Yang in neuroinflammation--neuro-protection and -degeneration. J Neurochem 107:1169-1187.

Bachstetter AD, Norris CM, Sompol P, Wilcock DM, Goulding D, Neltner JH, St CD, Watterson DM, Van Eldik LJ (2012) Early stage drug treatment that normalizes proinflammatory cytokine production attenuates synaptic dysfunction in a mouse model that exhibits age-dependent progression of Alzheimer's disease-related pathology. J Neurosci 32:10201-10210.

Benoit ME, Hernandez MX, Dinh ML, Benavente F, Vasquez O, Tenner AJ (2013) C1q-induced LRP1B and GPR6 Proteins Expressed Early in Alzheimer Disease Mouse Models, Are Essential for the C1q-mediated Protection against Amyloid-beta Neurotoxicity. J Biol Chem 288:654-665.

Benoit ME, Tenner AJ (2011) Complement protein C1q-mediated neuroprotection is correlated with regulation of neuronal gene and microRNA expression. J Neurosci 31:3459-3469.

Blurton-Jones M, Kitazawa M, Martinez-Coria H, Castello NA, Muller FJ, Loring JF, Yamasaki TR, Poon WW, Green KN, LaFerla FM (2009) Neural stem cells improve cognition via BDNF in a transgenic model of Alzheimer disease. Proc Natl Acad Sci U S A 106:13594-13599.

Brennan FH, Gordon R, Lao HW, Biggins PJ, Taylor SM, Franklin RJ, Woodruff TM, Ruitenberg MJ (2015) The Complement Receptor C5aR Controls Acute Inflammation and Astrogliosis following Spinal Cord Injury. J Neurosci 35:6517-6531.

Brooke SM, Bliss TM, Franklin LR, Sapolsky RM (1999) Quantification of neuron survival in monolayer cultures using an enzyme-linked immunosorbent assay approach, rather than by cell counting. Neurosci Lett 267:21-24.

Burdick D, Soreghan B, Kwon M, Kosmoski J, Knauer M, Henschen A, Yates J, Cotman C, Glabe C (1992) Assembly and aggregation properties of synthetic Alzheimer's A4/beta amyloid peptide analogs. J Biol Chem 267:546-554.

Cribbs DH, Berchtold NC, Perreau V, Coleman PD, Rogers J, Tenner AJ, Cotman CW (2012) Extensive innate immune gene activation accompanies brain aging, increasing vulnerability to cognitive decline and neurodegeneration: a microarray study. J Neuroinflammation 9:179.

Farkas I, Baranyi L, Takahashi M, Fukuda A, Liposits Z, Yamamoto T, Okada H (1998) A neuronal C5a receptor and an associated apoptotic signal transduction pathway. J Physiol 507 (Pt 3):679-687.

Fonseca MI, Ager RR, Chu SH, Yazan O, Sanderson SD, LaFerla FM, Taylor SM, Woodruff TM, Tenner AJ (2009) Treatment with a C5aR antagonist decreases pathology and enhances behavioral performance in murine models of Alzheimer's disease. J Immunol 183:1375-1383.

Fonseca MI, Chu SH, Berci AM, Benoit ME, Peters DG, Kimura Y, Tenner AJ (2011) Contribution of complement activation pathways to neuropathology differs among mouse models of Alzheimer's disease. J Neuroinflammation 8:4.

Hajishengallis G, Abe T, Maekawa T, Hajishengallis E, Lambris JD (2013) Role of complement in host-microbe homeostasis of the periodontium. Semin Immunol 25:65-72.

Harvey H, Durant S (2014) The role of glial cells and the complement system in retinal diseases and Alzheimer's disease: common neural degeneration mechanisms. Exp Brain Res 232:3363-3377.

Heneka MT, et al. (2015) Neuroinflammation in Alzheimer's disease. Lancet Neurol 14:388-405.

Hollmann TJ, Mueller-Ortiz SL, Braun MC, Wetsel RA (2008) Disruption of the C5a receptor gene increases resistance to acute Gram-negative bacteremia and endotoxic shock: opposing roles of C3a and C5a. Mol Immunol 45:1907-1915.

Jackson HM, Onos KD, Pepper KW, Graham LC, Akeson EC, Byers C, Reinholdt LG, Frankel WN, Howell GR (2015) DBA/2J genetic background exacerbates spontaneous lethal seizures but lessens amyloid deposition in a mouse model of Alzheimer's disease. PLoS ONE 10:e0125897.

Khoury MK, Parker I, Aswad DW (2010) Acquisition of chemiluminescent signals from immunoblots with a digital single-lens reflex camera. Anal Biochem 397:129-131.

Klos A, Tenner AJ, Johswich KO, Ager RR, Reis ES, Kohl J (2009) The role of the anaphylatoxins in health and disease. Mol Immunol 46:2753-2766.

Kohl J (2006) Drug evaluation: the C5a receptor antagonist PMX-53. Curr Opin Mol Ther 8:529-538.

Leow-Dyke S, Allen C, Denes A, Nilsson O, Maysami S, Bowie AG, Rothwell NJ, Pinteaux E (2012) Neuronal Toll-like receptor 4 signaling induces brain endothelial activation and neutrophil transmigration in vitro. J Neuroinflammation 9:230.

Li M, Pisalyaput K, Galvan M, Tenner AJ (2004) Macrophage colony stimulatory factor and interferon-gamma trigger distinct mechanisms for augmentation of beta-amyloid-induced microglia-mediated neurotoxicity. J Neurochem 91:623-633.

Loeffler DA, Camp DM, Bennett DA (2008) Plaque complement activation and cognitive loss in Alzheimer's disease. J Neuroinflammation 5:9.

Matsuoka Y, Picciano M, Malester B, LaFrancois J, Zehr C, Daeschner JM, Olschowka JA, Fonseca MI, O'Banion MK, Tenner AJ, Lemere CA, Duff K (2001) Inflammatory responses to amyloidosis in a transgenic mouse model of Alzheimer's disease. Am J Pathol 158:1345-1354.

McGeer PL, Akiyama H, Itagaki S, McGeer EG (1989) Activation of the classical complement pathway in brain tissue of Alzheimer patients. Neurosci Lett 107:341-346.

Nolte C, Möller T, Walter T, Kettenmann H (1996) Complement 5a controls motility of murine microglial cells *in vitro* via activation of an inhibitory G-protein and the rearrangement of the actin cytoskeleton. Neuroscience 73:1091-1107.

O'Barr SA, Caguioa J, Gruol D, Perkins G, Ember JA, Hugli T, Cooper NR (2001) Neuronal expression of a functional receptor for the C5a complement activation fragment. J Immunol 166:4154-4162.

Otto M, Hawlisch H, Monk PN, Muller M, Klos A, Karp CL, Kohl J (2004) C5a mutants are potent antagonists of the C5a receptor (CD88) and of C5L2: position 69 is the locus that determines agonism or antagonism. J Biol Chem 279:142-151.

Pavlovski D, Thundyil J, Monk PN, Wetsel RA, Taylor SM, Woodruff TM (2012) Generation of complement component C5a by ischemic neurons promotes neuronal apoptosis. FASEB J 26:3680-3690.

Reichwald J, Danner S, Wiederhold KH, Staufenbiel M (2009) Expression of complement system components during aging and amyloid deposition in APP transgenic mice. J Neuroinflammation 6:35.

Ricklin D, Hajishengallis G, Yang K, Lambris JD (2010) Complement: a key system for immune surveillance and homeostasis. Nat Immunol 11:785-797.

Rogers J, Cooper NR, Webster S, Schultz J, McGeer PL, Styren SD, Civin WH, Brachova L, Bradt B, Ward P, Lieberburg I (1992) Complement activation by beta-amyloid in Alzheimer disease. Proc Natl Acad Sci 89:10016-10020.

Ryman D, Gao Y, Lamb BT (2008) Genetic loci modulating amyloid-beta levels in a mouse model of Alzheimer's disease. Neurobiol Aging 29:1190-1198.

Selkoe DJ, Hardy J (2016) The amyloid hypothesis of Alzheimer's disease at 25 years. EMBO Mol Med.

Sewell DL, Nacewicz B, Liu F, Macvilay S, Erdei A, Lambris JD, Sandor M, Fabry Z (2004) Complement C3 and C5 play critical roles in traumatic brain cryoinjury: blocking effects on neutrophil extravasation by C5a receptor antagonist. J Neuroimmunol 155:55-63.

Song WC (2012) Crosstalk between complement and toll-like receptors. Toxicol Pathol 40:174-182.

Veerhuis R (2011) Histological and Direct Evidence for the Role of Complement in the Neuroinflammation of AD. Curr Alzheimer Res 8:34-58.

Vergunst CE, Gerlag DM, Dinant H, Schulz L, Vinkenoog M, Smeets TJ, Sanders ME, Reedquist KA, Tak PP (2007) Blocking the receptor for C5a in patients with rheumatoid arthritis does not reduce synovial inflammation. Rheumatology (Oxford) 46:1773-1778.

Wilcock DM, Zhao Q, Morgan D, Gordon MN, Everhart A, Wilson JG, Lee JE, Colton CA (2011) Diverse inflammatory responses in transgenic mouse models of Alzheimer's disease and the effect of immunotherapy on these responses. ASN Neuro 3:249-258.

Woodruff TM, Ager RR, Tenner AJ, Noakes PG, Taylor SM (2010) The role of the complement system and the activation fragment C5a in the central nervous system. Neuromolecular Med 12:179-192.

Woodruff TM, Costantini KJ, Crane JW, Atkin JD, Monk PN, Taylor SM, Noakes PG (2008) The complement factor C5a contributes to pathology in a rat model of amyotrophic lateral sclerosis. J Immunol 181:8727-8734.

Woodruff TM, Crane JW, Proctor LM, Buller KM, Shek AB, de VK, Pollitt S, Williams HM, Shiels IA, Monk PN, Taylor SM (2006) Therapeutic activity of C5a receptor antagonists in a rat model of neurodegeneration. FASEB J 20:1407-1417.

Woodruff TM, Pollitt S, Proctor LM, Stocks SZ, Manthey HD, Williams HM, Mahadevan IB, Shiels IA, Taylor SM (2005) Increased Potency of a Novel Complement Factor 5a Receptor Antagonist in a Rat Model of Inflammatory Bowel Disease. J Pharmacol Exp Ther 314:811-817.

Wyss-Coray T, Rogers J (2012) Inflammation in Alzheimer disease-a brief review of the basic science and clinical literature. Cold Spring Harb Perspect Med 2:a006346.

Yao J, Harvath L, Gilbert DL, Colton CA (1990) Chemotaxis by a CNS macrophage, the microglia. J Neurosci Res 27:36-42.

Zhou J, Fonseca MI, Pisalyaput K, Tenner AJ (2008) Complement C3 and C4 expression in C1q sufficient and deficient mouse models of Alzheimer's disease. J Neurochem 106:2080-2092.

CHAPTER 3

Prevention of C5aR1 Signaling Delays Microglial Inflammatory Polarization, Favors Clearance Pathways and Suppresses Cognitive Loss

Abstract

Since pharmacologic inhibition of C5aR1, a receptor for the complement activation proinflammatory fragment, C5a, in Alzheimer disease (AD) mouse models suppressed pathology and cognitive deficits, we genetically deleted C5aR1 in the Arctic AD mouse model to validate that the antagonist effect was specifically via C5aR1 inhibition. Indeed, lack of C5aR1 prevented behavior deficits at 10 months, although amyloid plaque load was not altered. In addition, since C5aR1 is primarily expressed on cells of the myeloid lineage, and only to a lesser extent on endothelial cells and neurons in brain, to understand the role of microglial C5aR1 in an AD mouse model, CX3CR1^{GFP} and CCR2^{RFP} reporter mice were bred to C5aR1 sufficient and knockout wild type and Arctic mice. Immunohistochemical analysis showed no CCR2^{+} monocytes/macrophages near the plaques in the Arctic brain with or without C5aR1. Microglia (GFP-positive, RFP-negative) were sorted from infiltrating monocytes (GFP and RFP-positive) for transcriptome analysis at 2, 5, 7 and 10 months of age. RNA-seq analysis on microglia from these mice identified inflammation related genes as differentially expressed, with increased expression in the Arctic mice relative to wildtype and decreased expression in the Arctic/C5aR1KO relative to Arctic. In addition, phagosomal-

lysosomal gene expression was increased in the Arctic mice and further increased in the Arctic/C5aR1KO mice. These data are consistent with microglial polarization in the absence of C5aR1 signaling toward restricted induction of inflammatory genes and enhancement of degradation/clearance pathways and support the potential of this receptor as a novel therapeutic target for AD in humans.

Introduction

Alzheimer's disease is a neurodegenerative disorder associated with the loss of cognitive function and characteristic neuropathological changes that include synaptic and neuronal loss, neurofibrillary tangles and extracellular senile plaques composed of amyloid beta (Aß) protein deposits. The association of complement proteins and reactive glia with senile plaques suggests that inflammatory processes may play a role in the disease and that complement activation may contribute to the inflammatory environment (Fonseca et al., 2011; Cribbs et al., 2012; Meraz-Rios et al., 2013; Heneka et al., 2015).

Inflammation is a fundamental response to infection and injury. In the brain, the primary immune cells are microglia (reviewed in (Ransohoff and El Khoury, 2015)). In AD, activated microglia have been found to be associated with Aß plaques in both human brains and mouse models of AD (El Khoury and Luster, 2008; Fonseca et al., 2009). Microglia are of particular interest in Alzheimer's disease since microglial dysfunction has been implicated as a factor in the progression of AD. Indeed, Zhang and colleagues identified the immune modulatory functions of microglia, such as cytokines, Fc receptors, TRL's and complement to be key nodes and networks of late onset Alzheimer's disease (LOAD) (Zhang et al., 2013).

The complement system is a well-known powerful effector mechanism of the immune system that normally contributes to protection from infection and resolution of injury (Ricklin and Lambris, 2013). Complement activation generates activation fragments C3a and C5a that interact with cellular receptors to recruit and/or activate phagocytes (including microglia) (Davoust et al., 1999; Monk et al., 2007). While complement activation in the brain can be beneficial and indeed crucial at times, it can also be detrimental. Recently it has been shown that early components of the classical complement are essential for synaptic pruning during development (Stevens et al., 2007). However, when excessive, this synaptic elimination is correlated with certain age-related and neurodegenerative disorders (Shi et al., 2015; Hong et al., 2016). Fibrill*ar* Aß can activate the classical complement pathway (in the absence of antibody) or the alternative complement pathway (Jiang et al., 1994; Bradt et al., 1998) and complement components are associated with human AD and mouse models of AD (Matsuoka et al., 2001; Fonseca et al., 2011). Potential consequences of this activation include opsonization (with C3b and iC3b) of fAß for engulfment by phagocytes, leukocyte recruitment (by C3a and C5a) and potential bystander lysis on neuronal cells by the membrane attack complex (MAC) (reviewed in (Alexander et al., 2008)).

In vitro cultures of C57BL6/J cortical neurons express C5aR1 and, upon binding, C5a is reported to injure neurons (Pavlovski et al., 2012; Hernandez et al., 2017). Microglia also express C5aR1 leading to C5a-induced chemotactic functions (Yao et al., 1990). In addition, microglia express TLRs (Toll Like Receptors). TLR stimulation has been shown to synergize with C5aR1 in the periphery in mice *in vivo*, increasing the pro-inflammatory cytokine production over TLR signaling alone (Zhang et al., 2007; Abe et al., 2012). Thus, to maintain the clearance promoting properties of complement, strategic therapeutic targeting,

such as through pharmacologic treatment with C5aR1 antagonists, could retain the beneficial but inhibit some of the detrimental aspects of complement activation.

Previous studies in our lab have demonstrated that treatment of mouse models of AD with a specific C5aR1 antagonist, PMX205, decreased fibrillar plaque accumulation and microglial CD45 expression and enhanced behavioral performance (Fonseca et al., 2009). Given that CD45 was thought to be upregulated in "activated" microglia, here we investigated the effect of C5aR1 gene ablation on behavior, pathology and microglial gene expression in wild type and the Arctic AD mouse model. The Arctic Alzheimer's disease mouse model has the human APP transgene containing three mutations (Swedish, Indiana, and Arctic) that increase risk of AD in humans (Nilsberth et al., 2001; Hollmann et al., 2008). The Arctic mutation results in the increased rate of fibril formation upon generation of the cleaved Aß42 peptide, resulting in a quite aggressive rate of fibrillar amyloid plaque deposition, initiating as early as 2 months of age in the mice (Cheng et al., 2004). Since that form of Aß is known to activate complement, C5a should be generated. Therefore, we crossed Arctic mice (Cheng et al., 2004) with C5aR1KO (Hollmann et al., 2008) mice to test the hypothesis that the absence of C5aR1 would suppress microglial inflammatory responses and behavior deficits. Subsequently, both Arctic and Arctic/C5aR1KO mice were crossed to the $CCR2^{RFP}$ and $CX3CR1^{GFP}$ reporter mice (Jung et al., 2000; Saederup et al., 2010) to enable fluorescence-activated cell sorting (FACS) of adult microglia (GFP+ RFP-) from monocytes/macrophages (GFP+ RFP+) isolated from brain at different ages for microglial specific gene expression analysis.

Our findings demonstrate that deletion of C5aR1 protects from spatial cognitive deficits even in the presence of fibrillar amyloid plaques. Infiltrating CCR2-positive

monocytes were not detected around the plaques in this Arctic AD mouse model. Moreover, microglial transcriptome analysis revealed inflammatory genes, including chemokines and members of the NF-κB pathway, were increased in the Arctic mouse as early as 5 months of age and remained elevated until 10 months of age while not so upregulated in the Arctic/C5aR1KO. Additionally, degradation pathways, such as the phagosome and lysosome pathways, were increased in the Arctic/C5aR1KO relative to the Arctic mice as early as 2 months of age and persisted through 10 months. Taken together, the data suggest inhibition of C5aR1 signaling suppresses the C5a-induced polarization toward a more inflammatory, less phagocytic state, and thereby can protect from cognitive deficits. The data supports further investigation of the use of antagonists for C5aR1 as part of a novel therapeutic strategy to slow the progression of Alzheimer's disease cognitive decline.

Materials and Methods

Animals

All animal experimental procedures were reviewed and approved by the Institutional Animal Care and Use Committee of University of California at Irvine, and performed in accordance with the NIH Guide for the Care and Use of Laboratory Animals. The AD mouse model used was the Arctic48, which carry the human APP transgene with the Indiana (V717F), Swedish (K670N + M671L), and Arctic (E22G) mutations (under the control of the platelet-derived growth factor-ß promoter), that produce Aß protofibrils and fibrils as early as 2-4 months old (Cheng et al., 2004), graciously provided by Dr. Lennart Mucke (Gladstone Institute, San Francisco, CA, USA). Homozygous breeding pairs of CX3CR1-GFP and CCR2-RFP mice were obtained from Jackson Laboratories and bred to C57/B6J to produce double

homozygous reporter mice ($CX3CR1^{GFP/GFP}CCR2^{RFP/RFP}$). Double homozygous reporter mice were bred with Arctic model to generate mice heterozygous for hAPP, $APP^{+/-}$ $CX3CR1^{GFP/+}CCR2^{RFP/+}$ (Arctic) and littermates lacking hAPP that were used as controls (WT). C5aR1 knockout mice generated by target deletion of the C5a receptor gene (Hollmann et al., 2008), were bred with $CX3CR1^{GFP/GFP}CCR2^{RFP/RFP}APP^{+/-}$ mice to produce Arctic mice lacking C5aR1 (Arctic/C5aR1KO) and $APP^{-/-}$ mice lacking the C5a receptor (C5aR1KO), all heterozygotic for $CX3CR1^{GFP}$ and $CCR2^{RFP}$. None of the mice generated exhibited any gross abnormalities.

Behavior Testing

Mice were handled for two minutes each for five consecutive days prior to all behavior testing. After handling, mice were acclimated (allowed to explore) to a behavior chamber for five minutes/day, for four consecutive days. On the training day (24 hours following the last day of habituation), mice were exposed to two of the same objects (e.g. 100 mL glass beakers, blue legos, or opaque light bulbs) in fixed positions within the context chamber near one wall. Twenty-four hours later they were tested in a hippocampal independent novel object recognition task (iNOR), or in a hippocampal dependent object location memory task (OLM). The iNOR paradigm involved exchanging one of the objects for a novel object (e.g. blue lego or 100 mL beaker). Testing for spatial memory (OLM) was performed by moving one of the objects to the center of the context, thus changing the spatial relationship of that object within the context. Animals' preference for novelty was tested by determining the time spent with familiar and novel objects or locations. Objects used, sizes of objects, and dimensions of the contexts were as described (Haettig et al., 2011). To prevent

olfactory distractions, all objects were cleaned with ethanol and the bedding stirred after each trial. Testing was scored blind by two independent observers using stopwatches and results correlated. Performance of mice during habituation to the context was also video recorded on Day 4 (the day preceding training) during which speed (**Figure 3.1A**), distance traveled (**Figure 3.1B**), % time spent in an inner zone of the chamber (**Figure 3.1C**), and % time spent in an outer zone of the chamber (**Figure 3.1D**) were scored using ANY-maze video tracking system software (version 4.82, Stoelting Co.). There were no significant differences found in performance between any of the genotypes in any of the measures demonstrating that there were no motor or motivational impairments in the different genotypes. Data from behavior performance were converted with the formula (time spent with novel object minus time spent with familiar object)/time spent with both objects) x 100 to obtain a percent (%) discrimination index (Stefanko et al., 2009). Data are presented as mean +/- SEM. Results were compared with two-tailed non-parametric Mann-Whitney *U* test or unpaired t-test or ANOVA followed by Tukey's post hoc tests. Differences were considered significant when p was < 0.05. Mice were removed if they spent less than 1 second/minute with the objects during training and/or testing or if the performance of mice was +/- 2 standard deviations from the mean.

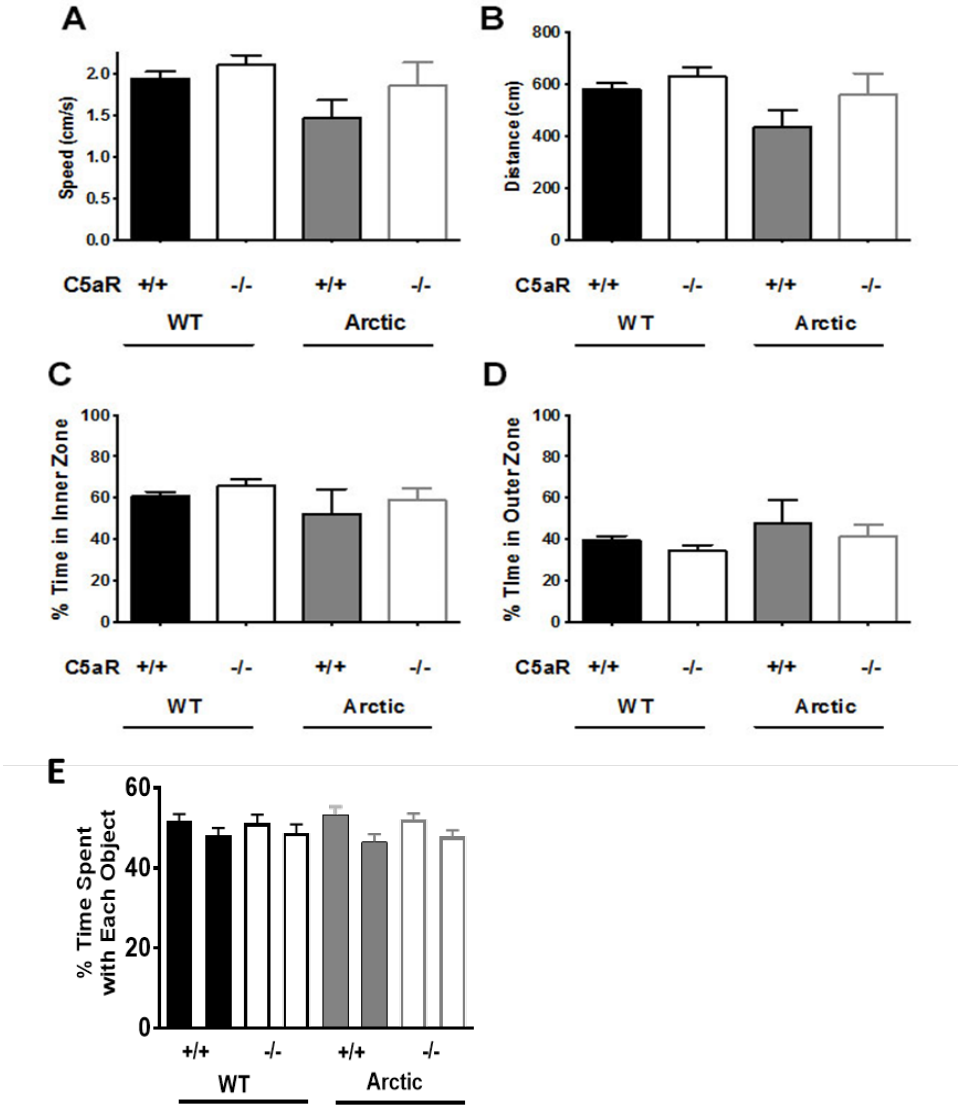

Figure 3.1. **Representative habituation performance during testing and performance during training.** Representative analysis of **(A**) Speed (**B)** distance traveled **(C)** percent of total time spent in an inner zone and **(D)** percent of total time spent in an outer zone quantified using the ANY-maze software. Data are from 10 months animals: n = 19 (WT), 16 (C5aR1KO), 7 (Arctic) and 8 (Arctic/C5aR1KO), representative of at least 2 experiments and similar assessments in 7 months animals. **(E)** During training all genotypes were assessed for time spent with each object (left and right of the context). Bars show average

percent time +/- SEM per object (left and right) for each genotype at 7 months. n = 10, 9, 9, and 10 for WT, C5aR1KO, Arctic, and Arctic/C5aR1KO respectively. No preference for left or right is detected by 1 way AVOVA.

Microglia isolation and FACS

Adapted from (Njie et al., 2012), mice from WT, C5aR1KO, Arctic and Arctic/C5aR1KO genotypes were perfused with PBS at 2, 5, 7 and 10 months, and the brains (without olfactory bulbs, cerebellum, or midbrain) collected for microglia isolation. Brains were treated with Dispase II (Roche) at 37˚C for 1 hr and passed through a 70 μM nylon cell mesh strainer (BD Biosciences) to obtain a single cell suspension. The cell suspension was washed in Hanks' balanced salt solution (HBSS; ThermoFisher) and spun at 1000 x g for 10 min at 4˚C. The cell pellet was resuspended in 70% Percoll (Sigma; diluted in HBSS), and 35% Percoll (diluted in HBSS) was carefully layered over to create a discontinuous Percoll gradient. After centrifugation at 800 x g for 45 min at 4˚C, the cells at the interphase were quickly collected, washed with HBSS + 2% heat-inactivated fetal bovine serum (FBS; Gibco) and passed through a 40 μM nylon mesh cell strainer. Using a FACS Aria II, the viable cell population was gated based on forward and side scatter properties of a propidium iodide stained control. Using these forward and side scatter parameters, the GFP^+RFP^+ and the GFP^+RFP^- cells were sorted and collected directly into RA-1 lysis buffer (Illustra RNAspin mini isolation kit, GE Healthcare).

Immunohistochemistry

Some cohorts of mice were perfused with phosphate buffered saline (PBS). The brain was dissected at 4^o C with half of the tissue immediately frozen on dry ice for biochemical analysis, and the other half drop-fixed in 4% paraformaldehyde-PBS at 4°C for immunohistochemistry. After 24 hours, the fixed tissue was placed in PBS/0.02% sodium azide at 4°C until use. Vibratome sections (coronal, 40 μm) were incubated sequentially with

3%H_2O_2/10% Methanol/Tris buffer saline (TBS) to block endoperoxidase and with 2% BSA/0.1%Triton/TBS to block nonspecific binding. Tissues were next incubated overnight at 4°C with anti mouse CD45 antibodies (rat monoclonal anti CD45, 1 µg/mL, Serotec, or goat anti CD45 0.2 µg/mL, R&D systems, Minneapolis, MN), anti Aß antibody (rabbit polyclonal 1536 (Webster et al., 2001) gift from N.R Cooper) or appropriate control IgG in blocking solution. Primary antibodies were detected with biotinylated secondary antibodies against the corresponding species, followed by ABC complex and DAB (VECTOR, Burlingame, CA). In animals lacking GFP constructs, fibrillar Aß was stained with 1% thioflavine as previously described (Fonseca et al., 1999). For immunofluorescence staining of total Aß, samples were incubated with blocking solution followed by rabbit polyclonal anti Aß (1536) and labeling detected with Alexa 405 anti rabbit secondary antibody.

Immunostaining was observed under a Zeiss Axiovert-200 inverted microscope (Carl Zeiss, Thornwood, NY) and images were acquired with a Zeiss Axiocam high-resolution digital color camera (1300x1030 pixel) and analyzed using Axiovision 4.6 software. Percent of immunopositive area (% Field Area) (immunopositive area / total image area x 100) was determined for all the markers studied by averaging 2-4 images per section for Aß and thioflavine or 6 images per section for CD45 of the hippocampal area. Digital images were obtained using the same settings, and the segmentation parameters were constant as previously reported (Fonseca et al., 2004). The mean value of the % Field Area for each marker in each animal was averaged per genotype group with the number of animals per group indicated in figure legends. Data were analyzed using one-way ANOVA statistical analysis. Staining of all genotypes that were compared by image analysis in an experiment was done simultaneously per given marker.

RNA extraction and RNA-Seq

Total RNA from $GFP^{+}RFP^{-}$ cells was extracted using the Illustra RNAspin mini isolation kit. RNA was quantified using the NanoDrop ND-1000 spectrophotometer (ThermoFisher) and the quality checked using the Agilent Bioanalyzer 2100 (Agilent Technologies). Sequencing was performed by the University of California at Irvine Genomics High Throughput Facility. The SMARTer Stranded Total RNA-Seq Kit - Pico Input Mammalian (Clontech Laboratories) was used to generate Illumina-compatible RNA-seq libraries. Briefly, total RNA was converted into cDNA and then adapters with barcodes for Illumina sequencing were added by PCR. The PCR products were then purified and the ribosomal cDNA depleted with sequence specific probes and RNaseH. The resulting cDNA fragments were further amplified (12 cycles) and the PCR products were purified once again to yield the final cDNA libraries. The barcoded cDNA libraries were multiplexed on the Illumina HiSeq 2500 platform to yield 100-bp paired-end reads.

Read alignment and expression quantification

Pair-end RNA-seq reads were aligned using STAR v.2.5.1b (Dobin et al., 2013) with parameters '--outFilterMismatchNmax 10 --outFilterMismatchNoverReadLmax 0.1 --outFilterMultimapNmax 10' to the reference genome GRCm38/mm10. We used STAR to then convert to transcriptome-based mapping with gene annotation Gencode v.M8. Gene expression was measured using RSEM v.1.2.25 (Li and Dewey, 2011) with expression values normalized into transcripts per million (TPM).

Building of gene expression matrix for time-course gene expression and pathway analysis

Libraries with uniquely mapping percentages higher than 65% were considered to be of good quality and kept for downstream analysis. Protein coding and long non-coding RNA genes, with expression TPM >=0.5 in at least one of the duplicates for each genotype, were collected and quantile normalized for subsequent time-course and pathway analysis. Fastq files and processed data matrices were deposited in GEO with the accession ID GSE93824.

Time-course gene expression analysis

Quantile normalized gene expression (TPM) profiles were analyzed with maSigPro (Nueda et al., 2014) to identify distinct gene expression profiles across time points whose expression differed in at least one other age in one other genotype with multiple cluster sizes. A cluster size of k=9 gave the best set of profiles. An alpha of 0.05 for multiple hypothesis testing and r^2 =0.7 for regression model were used to acquire significant genes for each cluster.

Gene ontology and pathway analysis

Gene clusters were analyzed for Gene ontology (GO) enrichment by Metascape (http://metascape.org) (Tripathi et al., 2015) using a hypergeometric test corrected p-value lower than 0.05. maSigPro clusters were also analyzed for KEGG pathway enrichments using PaintOmics 3 (Garcia-Alcalde et al., 2011) with significant pathways selected based on Fisher's exact test p-value lower than 0.05.

qRT-PCR

RNA was converted to cDNA using Superscript III reverse transcriptase (Life Technologies) following manufacturer's instructions and quantified using the NanoDrop ND-1000 spectrophotometer (ThermoFisher). Quantitative RT-PCR was performed using the StepOnePlus Real-Time PCR System, the StepOne software v2.3 (Applied Biosystems) with the following FAM dye and MGB quencher TaqMan probes (ThermoFisher): Mm00443111_m1 (Ccl4), Mm00436450_m1 (Cxcl2), Mm00437306_m1 (Vegfa), Mm00515586_m1 (Ctsd), Mm00487585_m1 (Man2b1, Mm00499230_m1 (Npc2). All genes were multiplexed with the VIC dye and MGB quencher probe Mm01545399_m1 (Hprt) to allow for normalization of housekeeping gene in same well. For each gene, cDNA from 3 samples (unique animals) of each genotype was tested in triplicate. Two of the samples were from the same samples as the RNA-seq dataset and one was from a sample not analyzed by RNA-seq at ages 5 and 10 months.

Results

C5aR1 Deficiency Prevents Deficits in Spatial Specific Object Location Memory

Since a C5aR1 antagonist had previously been shown to suppress AD-like pathology in mouse models of AD (Fonseca et al., 2009), we evaluated the effect of C5aR1 gene ablation on the ability to perform in both a hippocampal dependent spatial and non-spatial memory task. Spatial memory cognitive deficits are observed in AD patients and the Arctic AD mouse model has been shown to recapitulate only hippocampal dependent spatial impairments (Cheng et al., 2004). Our hypothesis was that knocking out C5aR1 would lead to less inflammation and, thus, to better performance. To confirm that the behavior deficit is only

spatial and hippocampal-dependent we used both the traditional hippocampus independent novel object recognition (iNOR) and a modification of the iNOR paradigm that assessed spatial memory and was hippocampal dependent, the object location memory (OLM) task (Mumby et al., 2002; Balderas et al., 2008). Mice of all 4 genotypes (WT, C5aR1KO, Arctic, Arctic/C5aR1KO) spent about 50% of their time with each object during the training phase demonstrating no preference for a certain side of the chamber or one of the objects within the chamber indicating that memory retrieval 24 hours later would not be confounded by inherent spatial or object preferences (**Figure 3.1E**). As expected, at 7 (data not shown) and 9 (**Figure 3.2A, B**) months of age, all genotypes performed well, and there were no differences in performance between genotypes in the hippocampal independent iNOR task demonstrating that the Arctic mice as well as C5aR1 deficient mice were not impaired.

When tested in the spatial OLM task (**Figure 3.2C**), WT and C5aR1KO mice at both 7 and 10 months of age exhibited a discrimination index greater than 30% during the first two minutes of testing, indicating that they had a strong preference for exploring the object in the new location and that genetic deletion of C5aR1 alone is not detrimental or beneficial (**Figure 3.2D, E**). The C5aR1 sufficient Arctic mice did not exhibit significant behavioral deficits at 7 months, although there were 2 animals that were noticeably performing worse than all other mice (**Figure 3.2D**, right). However, at 10 months of age, there was a significant deficit ($p < .001$) in performance of Arctic mice in comparison to wild type mice, while importantly, Arctic/C5aR1KO did not differ from wild type or C5aR1KO. A statistically significant difference in behavior ($p < .05$) was observed between the Arctic mice lacking C5aR1 compared to the C5aR1 sufficient Arctic mice indicating protection from deficit in the Arctic/C5aR1KO mice relative to the Arctic mouse **(Figure 3.2E**), consistent with the

hypothesis that blocking C5aR1-mediated events slows or prevents the progression of cognitive defects.

Microglia marker CD45, but not plaque accumulation, exhibited slight but significantly lower expression at 7 but not 10 months of age in the C5aR1 deficient AD mouse model

Arctic mice at 7 and 10 months of age have abundant fibrillar plaque pathology in the hippocampus. Genetic deletion of C5aR1 did not alter the extent of fibrillar plaque pathology at either 7 or 10 months of age (**Figure 3.3**). In contrast, in the 7 month old mice (behavior shown in **Figure 3.2D**), there was significantly less CD45 reactivity in the Arctic/C5aR1KO mice than in the C5aR1 sufficient Arctic mice, which suggests a lower microglial activation response (20%, p =.03) (**Figure 3.3B**). However, that difference was not sustained in the 10 month mice (**Figure 3.3D**). Furthermore, neither fibrillar plaque pathology nor CD45 correlated with behavioral parameters of individual animals (data not shown). These data suggest that induction of CD45 is not necessarily an indication of neurotoxic effects that impact behavior in this model.

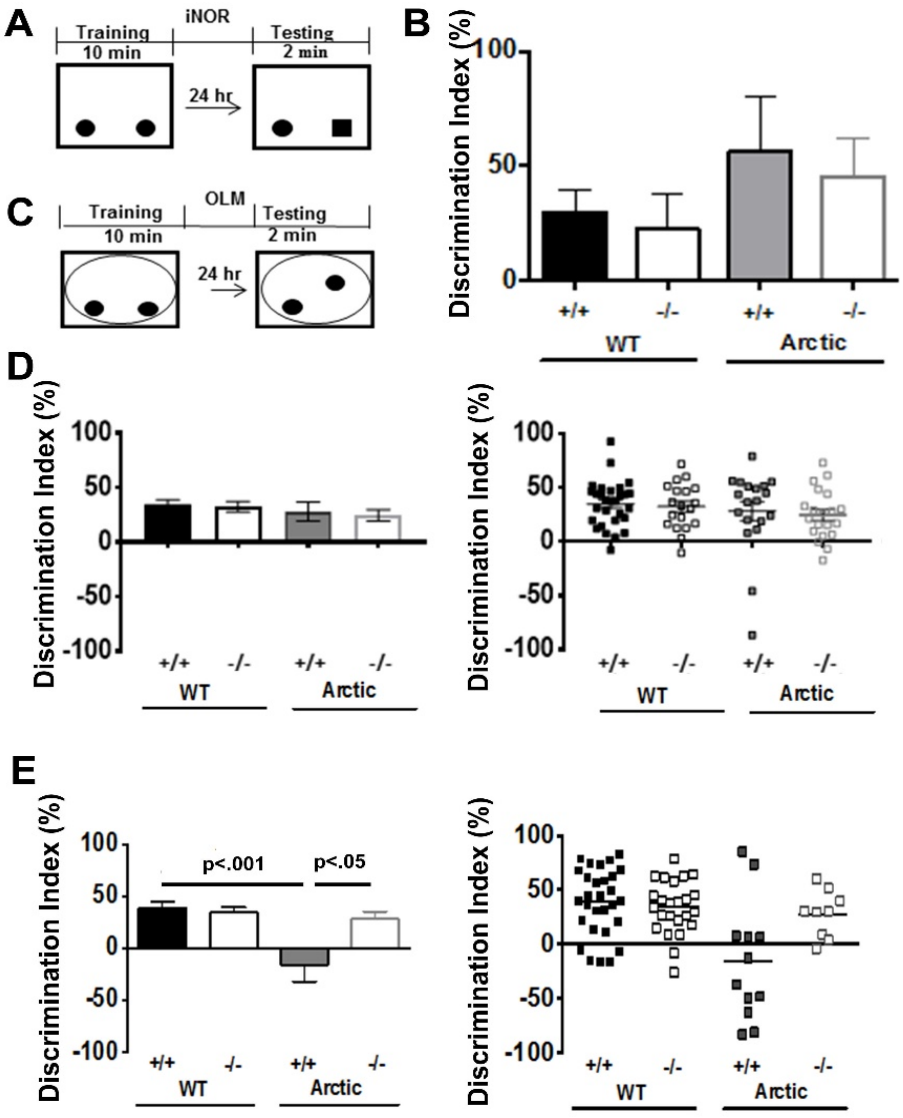

Figure 3.2. Performance in novel object and object location memory tasks. Animals were tested in novel object recognition test (**A,B**) and novel object location memory test (**C-E**). Paradigm schematics are presented for iNOR (**A**) and OLM (**C**) after 5 days of handling and 4 days of habituation to the testing chamber. Solid oblongs or circles in the boxes represent identical objects. After Day 1 training, one familiar object was replaced with a novel object (solid square) (**A**) or a familiar object was moved to the center of the context

(**C**). The novel object replacement or the object moved was counter balanced among all trials. Performance was evaluated using the first two minutes of testing at 9 months for iNOR (**B**), and either 7 months (**D**) or 10 months (**E**) for OLM. (**B**) WT n=11, C5aR1KO n=6, Arctic n=4, C5aR1KO Arctic n=5. Right plots in **D** and **E** are the scatter plots for left bar graphs, respectively. **(D)** n = 10 (WT), 9 (C5aR1KO), 9 (Arctic) and 10 (Arctic/C5aR1KO). (**E**) n = 29 (WT), 25 (C5aR1KO), 12 (Arctic) and 9 (Arctic/C5aR1KO). (**B,D,E**) Data is expressed as the average +/- SEM. P values were determined by ANOVA followed by Tukey's post hoc test (Cole, 2013).

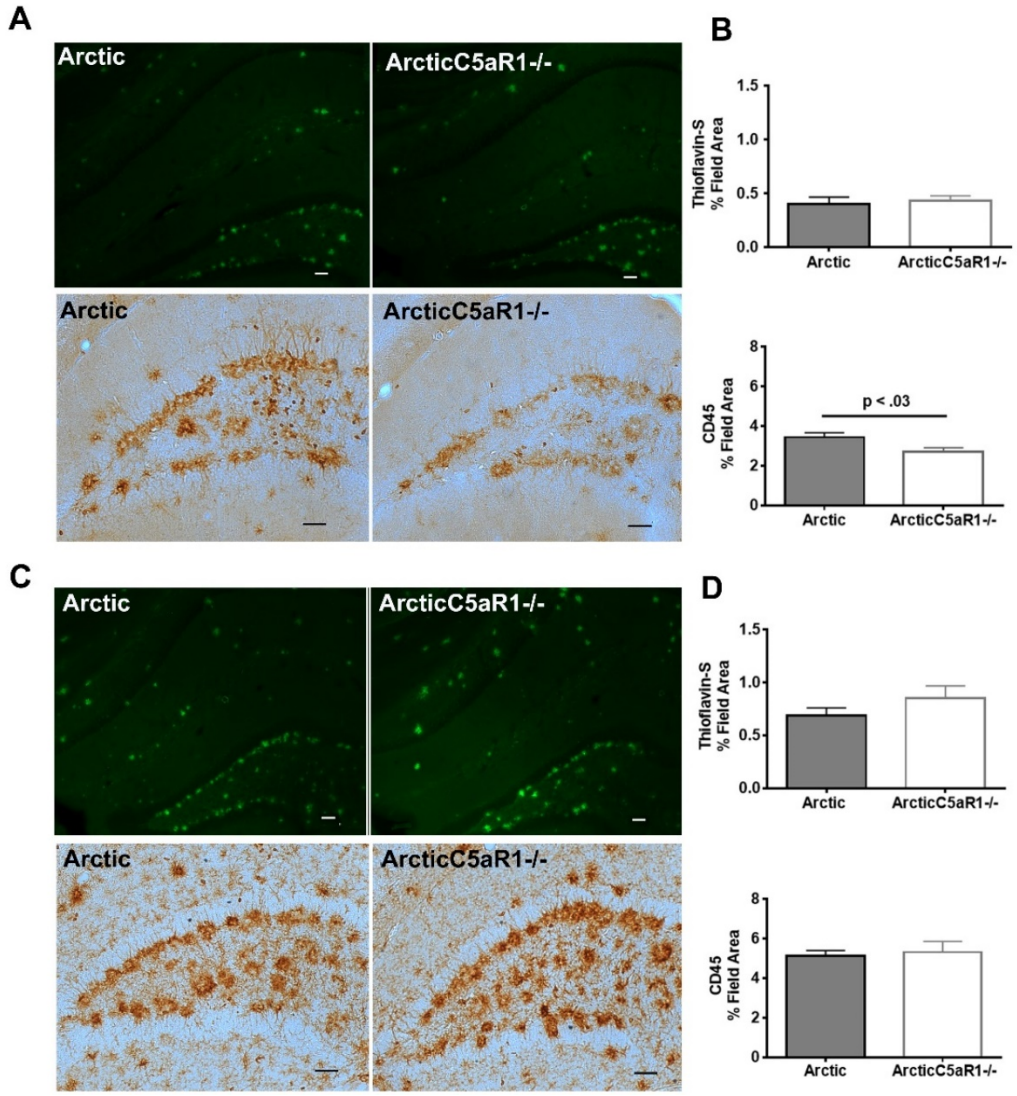

Figure 3.3. Fibrillar plaque and CD45 microglial expression in hippocampus. Representative pictures of thioflavine-S staining (fibrillar plaques) (top panels) and CD45 staining (microglia) (lower panels) at 7 (**A**) and 10 months (**C**). Scale bar: 50 um. (**B**) Image analysis of 7 month thioflavine-S (upper) and CD45 (lower) staining (Arctic n=9, Arctic/C5aR1KO n=9) (**D**) Image analysis of 10 mo thioflavine (Arctic n=12, Arctic/C5aR1KO n=9) (upper) and CD45 (Arctic n=11, Arctic/C5aR1KO n=7) lower). Bars represent group means +/- SEM of n animals per genotype. Data represent the average of 2 to 4 sections per animal. P value was calculated using one way ANOVA.

Single copy of CX3CR1 or CCR2 does not alter plaque deposition in Arctic mice

In the Arctic AD mouse model, we used the $CX3CR1^{GFP}$ and $CCR2^{RFP}$ reporter mice to differentiate microglia from infiltrating CCR2-positive monocytes (Mizutani et al., 2012). Crossing $CX3CR1^{GFP/GFP}CCR2^{RFP/RFP}$ mice with the Arctic mice generated $CX3CR1^{+/GFP}CCR2^{+/RFP}Arctic^{-/-}$ (WT) and $CX3CR1^{+/GFP}CCR2^{+/RFP}Arctic^{+/-}$ (Arctic) mice. Crossing $CX3CR1^{GFP/GFP}CCR2^{RFP/RFP}$ mice with the Arctic/C5aR1KO mice ultimately generated $CX3CR1^{+/GFP}CCR2^{+/RFP}$ $C5aR1^{-/-}$ (C5aR1KO) and $CX3CR1^{+/GFP}CCR2^{+/RFP}Arctic^{+/-}$ $C5aR1^{-/-}$ (Arctic/C5aR1KO) mice. Since some studies with Alzheimer's disease mouse models have suggested that CX3CR1 and CCR2 play a role in the progression of disease (El Khoury et al., 2007; Lee et al., 2010; Liu et al., 2010), we first determined if having only a single copy of either gene alters plaque deposition or CD45 reactivity. In this model, thioflavine staining showed no change in plaque deposition in the $CCR2^{+/RFP}$ Arctic mice and CD45 reactivity was also unchanged relative to $CCR2^{+/+}$ Arctic mice (**Figure 3.4A, C, E**). Since thioflavine staining would overlap with GFP, anti Aß staining was used to measure the plaque load in the Arctic and Arctic $CX3CR1^{+/GFP}$. Aß was unchanged in $CX3CR1^{+/GFP}$ Arctic relative to $CX3CR1^{+/+}$ Arctic and no change was seen in CD45 reactivity when compared to $CX3CR1^{+/+}$ Arctic mice (**Figure 3.4B, D, E**).

To confirm that the RFP fluorescence is localized with $CD45^{high}$ cells, we injected mice with 5mg/kg LPS i.p. to increase the number of monocytes infiltrating to the CNS. After 24 h, myeloid cells isolated using a Percoll gradient were stained with CD11b-PECy7 and CD45-APC antibodies and analyzed by flow cytometry (**Figure 3.4F**). $CD11b^{+}CD45^{low}$ cells are widely considered to be resident microglia cells (**Figure 3.4F,** left panel) and here were distinguished by their GFP and lack of RFP expression (**Figure 3.4F,** right panel,

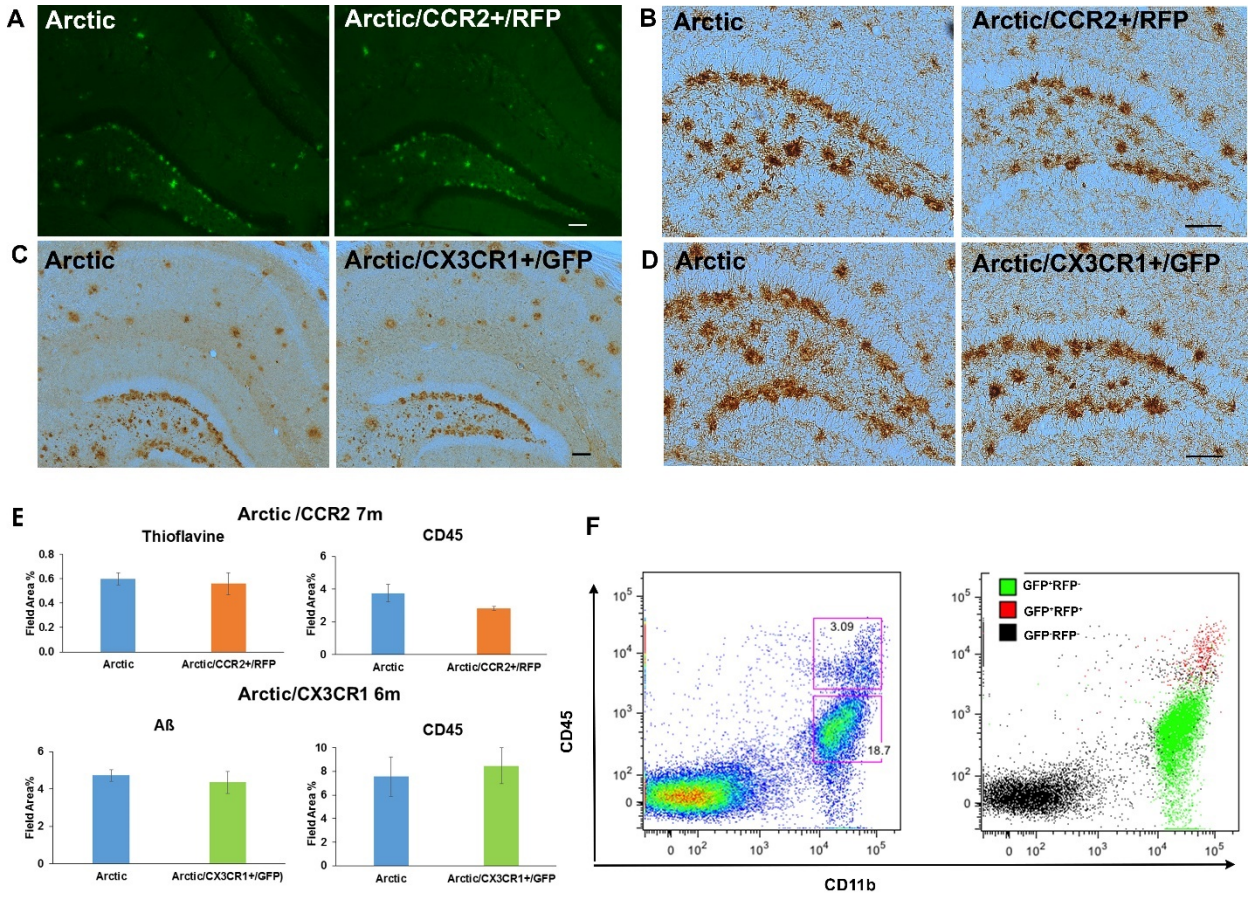

Figure 3.4. Aβ plaque load and CD45 expression in Arctic heterozygous for CX3CR1 and CCR2. Brain sections from Arctic, Arctic-CX3CR1$^{+/GFP}$ or Arctic-CCR2$^{+/RFP}$ reporter mice at 6 or 7 months were stained with either thioflavine (**A**), or an anti-Aß antibody (1536) (**C**) to assess the plaque load (**A, C**). CD45 reactivity was probed to investigate microglial activation (**B,D**). Arctic mice were compared to Arctic mice heterozygous for CCR2-RFP (**A, B**) or heterozygous for Cx3CR1-GFP (**C,D**). Scale bar is 100 µm. (**E**). Bars represent the average Field Area % of 3-4 animals per genotype (2 sections per animal). No statistically significant difference was observed in Arctic compared to Arctic-CCR2$^{+/RFP}$ in thioflavine ($p<0.75$) or CD45 ($p<0.09$) or between Arctic and Arctic-CX3CR1$^{+/GFP}$ in Aß ($p<0.67$) or CD45 ($p<0.71$) by one-way ANOVA statistical analysis. (**F**) 5 month CX3CR1$^{+/GFP}$CCR2$^{+/RFP}$

were injected with 5mg/kg LPS i.p. After 24 hours, isolated myeloid cells were stained with CD11b-PECy7 and CD45-APC antibodies and analyzed by flow cytometry to determine if infiltrating GFP+RFP+ segregate with monocytes/macrophages (CD11b+ $CD45^{high}$) and if all microglia (CD11b+ $CD45^{low}$) are GFP+RFP-. The left pseudo color dot blot shows isolated microglia/macrophages plotted as intensity of CD45 and CD11b. The right FACS plot shows GFP+RFP+ monocytes/macrophages (red) and GFP+RFP- microglia (green) gated and plotted on those same axes.

green dots). Infiltrating CCR2^{+} monocytes are described in the literature as CD11b^{+} CD45^{high} and here were distinguishable by their GFP and RFP expression (**Figure 3.4F,** right panel, red dots). Interestingly, the GFP/RFP fluorescence shows some CD45^{high} cells are RFP-negative and GFP-positive (**Figure 3.4F,** right panel, green dots), which could be microglia that have upregulated levels of CD45 (Tan et al., 2000) upon activation with LPS, or, alternatively, could be infiltrating monocytes that have downregulated CCR2.

Lack of CCR2-positive infiltrating monocytes around plaques

We next proceeded to age wildtype (WT), C5aR1KO, Arctic, and Arctic/C5aR1KO mice at 2, 5, 7, and 10-11 months. As expected, no plaque pathology nor microglia clustering was observed in wildtype mice or C5aR1KO mice (**Figure 3.5A, C**). Plaque deposition increased with age and microglia clustered around the plaques, but was similar in the Arctic and Arctic/C5aR1KO mice across the different ages (**Figure 3.5B, D**). Strikingly, no RFP-positive cells were found in areas near the plaques at any age. No RFP-positive cells were found anywhere in the parenchyma, while a few RFP-positive cells were localized around the surface of the brain, possibly meningeal macrophages (**Figure 3.5B, D** insets). Percoll gradient isolated cells, from brains of mice in the same cohort as that analyzed by IHC, when sorted by RFP and GRP identified a small population of GFP and RFP-positive cells. RFP-positive cells (which could represent the meningeal macrophages) represented 2-6% of the GFP-positive population (**Figure 3.5E**), while RFP-negative microglia made up 94-98% of the GFP-positive cells (**Figure 3.5F**). The absolute number of cells recovered varied, with means among all genotypes and ages between 700 and 2000

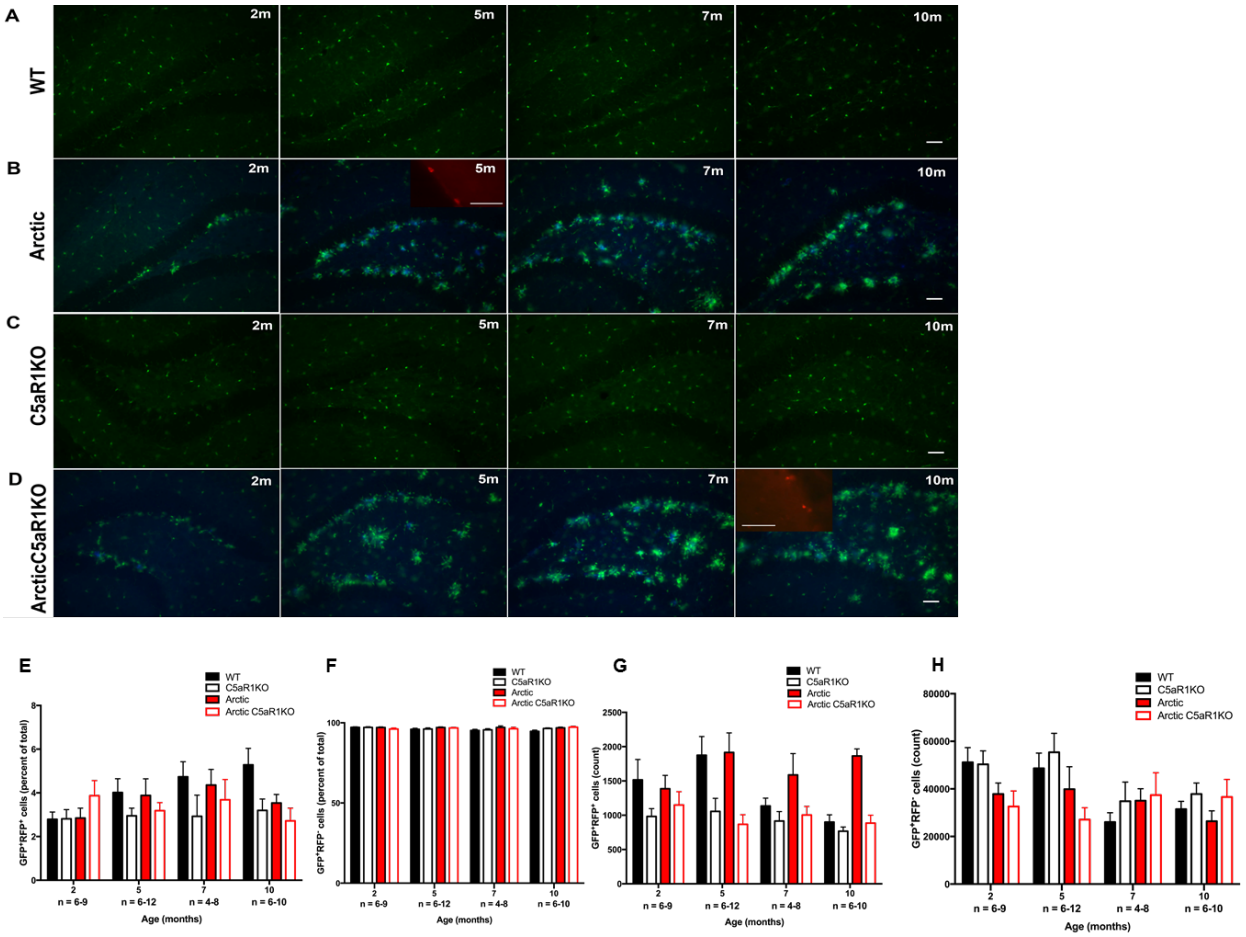

Figure 3.5. Glia clustering around plaques are CX3CR1^{+}CCR2^{-}. Brain sections of (**A**) WT, (**B**) Arctic, (**C**) C5aR1KO, and (**D**) Arctic/C5aR1KO mice (all CX3CR1$^{+/GFP}$CCR2$^{+/RFP}$) at 2, 5, 7, and 10 months were fluorescently labelled in blue with anti-Aß antibody (1536). Staining was performed at separate times for cohort one (**A, B**) and cohort 2 (**C, D**). Inset shows CCR2$^{+/RFP}$ macrophages. Scale bar: 50 µm (**E**) Percoll purified brain cells from WT, Arctic, C5aR1KO and Arctic/C5aR1KO mice (all CX3CR1$^{+/GFP}$CCR2$^{+/RFP}$; n=4-12 per genotype, per age) were FACS-sorted as GFP^{+}RFP^{+} (**E, G**) and GFP^{+}RFP^{-} cells (**F, H**) and quantified as a percentage of total GFP+ cells (**E, F**) and total cell count (**G, H**).

for RFP-positive cells (**Figure 3.5G**) and between 27,000 and 55,000 for RFP-negative GFP-positive microglia (**Figure 3.5H**).

Analysis of age dependent patterns of gene expression

To identify transcriptome changes in microglia in Arctic/C5aR1KO mice relative to Arctic mice, the FACS-sorted cells were collected and RNA extracted for RNA-seq analysis. RNA was isolated from the GFP-positive/RFP-negative cells of WT, C5aR1KO, Arctic, and Arctic/C5aR1KO mice at 2, 5, 7, and 10 or 11 months of age (**Figure 3.6A**). RNA quality and quantity was sufficient for RNA sequencing and analysis (**Table 3.1**). RNA-seq libraries that passed our quality filters were used to estimate gene expression level. By doing time-course analysis with maSigPro (Nueda et al., 2014) we identified 2156 differentially expressed genes that showed dynamic expression patterns over time with age and disease progression. The genes were partitioned into nine clusters, ranging in size from 125 genes to 445 genes, to show distinct temporal and genotype-specific profiles (**Figure 3.6B, Figure 3.7)**. To identify clusters of interest to study further, we did the following: 1) Assessed the gene expression patterns of each cluster (generated by maSigPro) to identify differences in gene expression between the Arctic and Arctic/C5aR1KO (**Figure 3.6B, Figure 3.7**). 2) Gene ontology (GO) enrichment analysis using Metascape (Tripathi et al., 2015) to aid in the identification of clusters that had genes associated with biologically relevant processes (**Table 3.2**). 3) Pathway analysis using PaintOmics 3 to identify significantly enriched KEGG pathways in each cluster (**Table 3.3**). Cluster 4 contained 125 genes (**Table 3.4**) that increased with age starting by 5 months in the Arctic relative to wildtype. Those genes did not increase in the Arctic/C5aR1KO until 10 months of age and

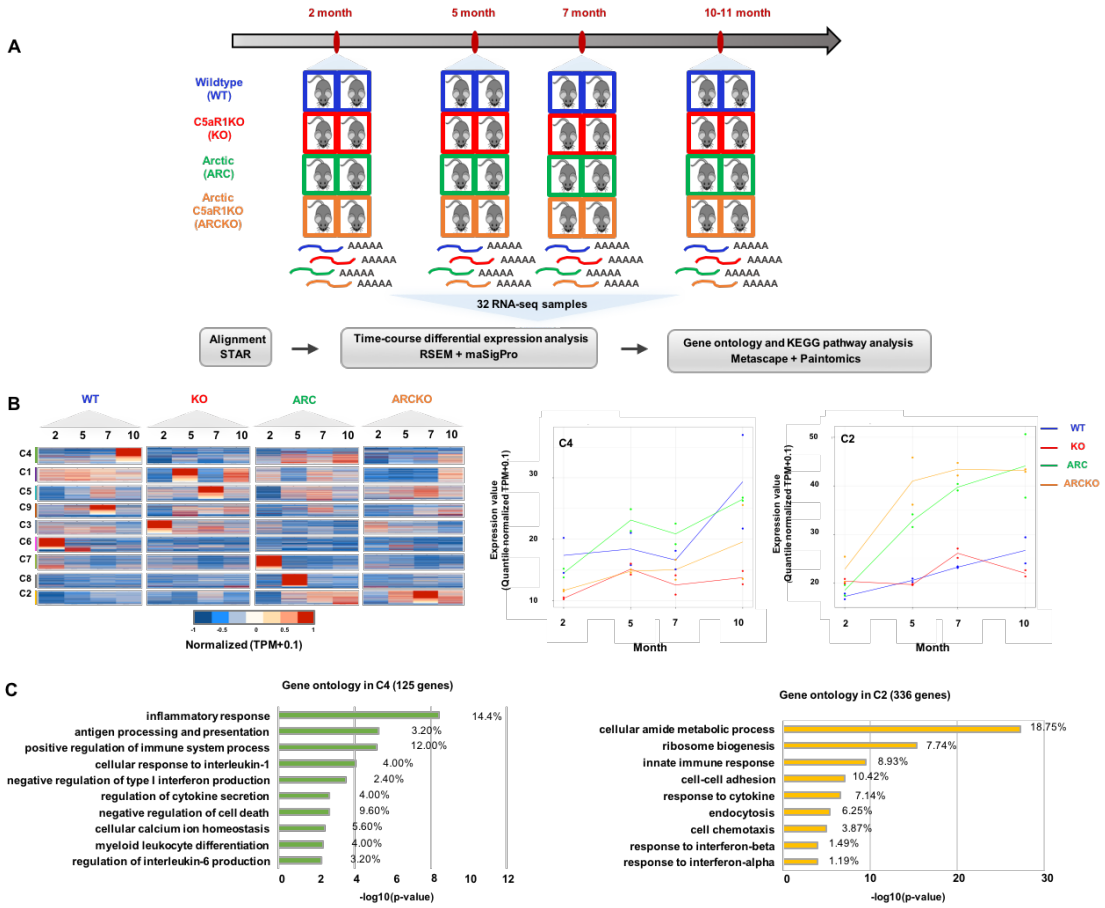

Figure 3.6. Temporal gene expression profiles across four genotypes. (**A**) RNA-seq experiments were performed using duplicate samples from WT (blue), C5aR1KO (red), Arctic (green) and Arctic/C5aR1KO (orange) mice at 2, 5, 7 and 10-11 months. A total of 32 RNA-seq libraries were sequenced and analyzed. Reads were aligned to the reference genome with STAR. Gene expression level was estimated by RSEM and analyzed with maSigPro to identify distinct gene expression profiles across time. Differentially expressed genes during the time-course were loaded into Metascape and PaintOmics 3 to acquire gene ontology (GO) and KEGG pathways enrichment. (**B,** left) Heatmap of 2156 differentially expressed genes across four genotypes and four ages. 9 gene expression clusters were derived from maSigPro and labeled with number and color on the side. Quantile normalized

TPM plus 0.1 were transformed between -1 and 1 to present high (red) and low (blue) expression level within each cluster. (**B,** right) Gene expression profiles for cluster 4 and 2. Median profile are plotted across all replicates for all the genes in the corresponding cluster. WT (blue), C5aR1KO (red), Arctic (green) and Arctic/C5aR1KO (orange). (**C**) Gene ontology enrichment was measured on genes from cluster 4 (green) and 2 (yellow). Gene ontology terms were sorted based on p-value. The percentage of genes in the cluster that are contained in the GO term is listed on the side in parentheses.

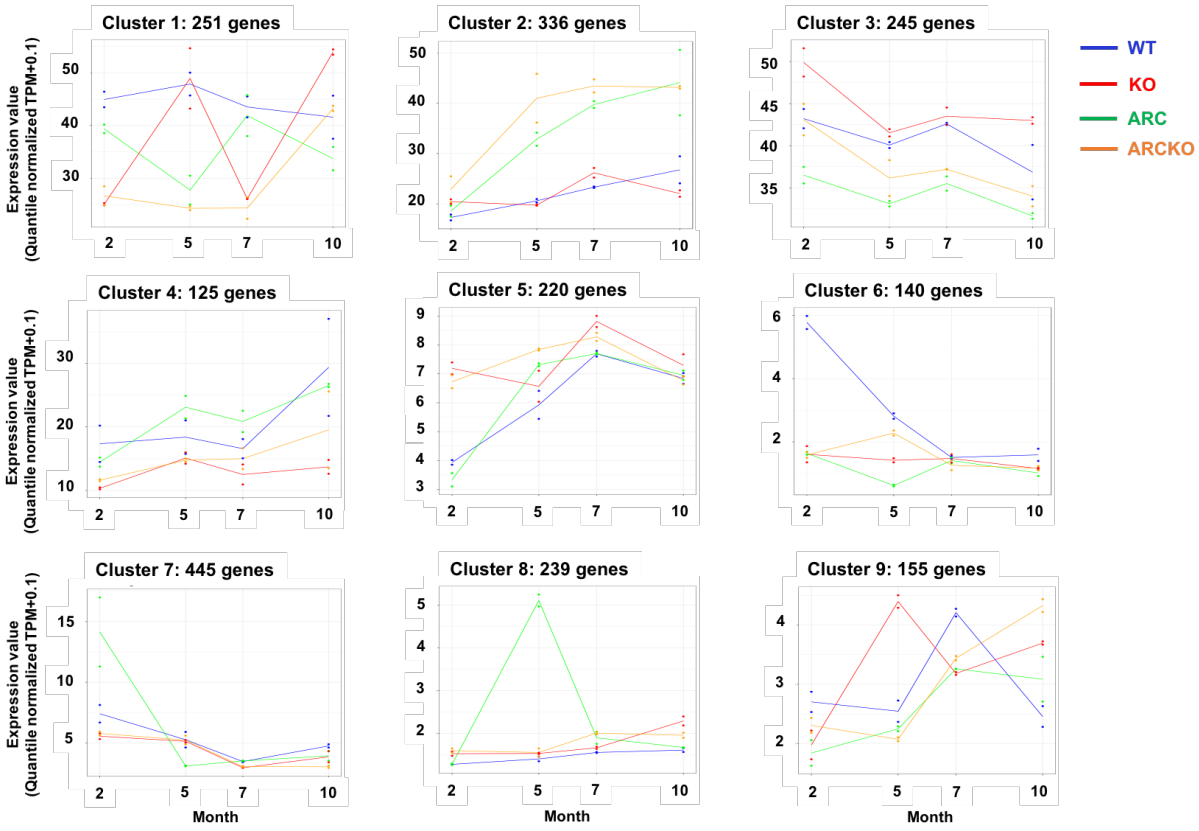

Figure 3.7. Dynamic gene expression profiles of remaining 7 clusters. Gene expression clusters were derived from maSigPro. Median profile are plotted across all replicates for all the genes in the corresponding cluster. WT (blue), C5aR1KO (red), Arctic (green) and Arctic/C5aR1KO (orange).

at that time showed levels similar to that seen in the 10 month wildtype animals and still lower than the Arctic expression at 10 months (**Figure 3.6B)**. Cluster 2 consisted of 336 genes (**Table 3.4**) that were unchanged in the C5aR1KO relative to wildtype but increased in the Arctic after 2 months relative to WT. The same genes were further increased in the Arctic/C5aR1KO (**Figure 3.6B**). Gene ontology enrichment analysis using Metascape identified the enriched GO terms for cluster 4 of which the top 3 where: inflammatory response, antigen processing and presentation, and positive regulation of immune system process (**Figure 3.6C,** left), whereas the top 3 enriched GO terms in cluster 2 were cellular amide metabolic process, ribosome biogenesis, and innate immune response (**Figure 3.6C,** right).

Pathway analysis reveals less inflammation and more protein degradation in Arctic C5aR1KO

Pathway analysis of cluster 4 identified several inflammatory diseases pointing to inflammation as well as canonical inflammation pathways. Of interest were NF-κB signaling, cytokine-cytokine receptor interaction, TLR signaling and chemokine signaling due to their statistical significance as well as their biological significance in the context of AD (**Table 3.3**). These four pathways were then investigated further and the 16 differentially expressed genes between the Arctic and Arctic/C5aR1KO (found in these 4 pathways) were plotted on a heat map (**Figure 3.8A**). These genes remained elevated in the Arctic relative to WT, C5aR1KO, and Arctic/C5aR1KO through 10 months of age (**Figure 3.8A**). Increases in those genes appeared in both WT and Arctic/C5aR1KO only beginning at 10 months (consistent with the increase in inflammatory gene expression with age (Giunta et al., 2008)) but remained significantly lower than in microglia from the

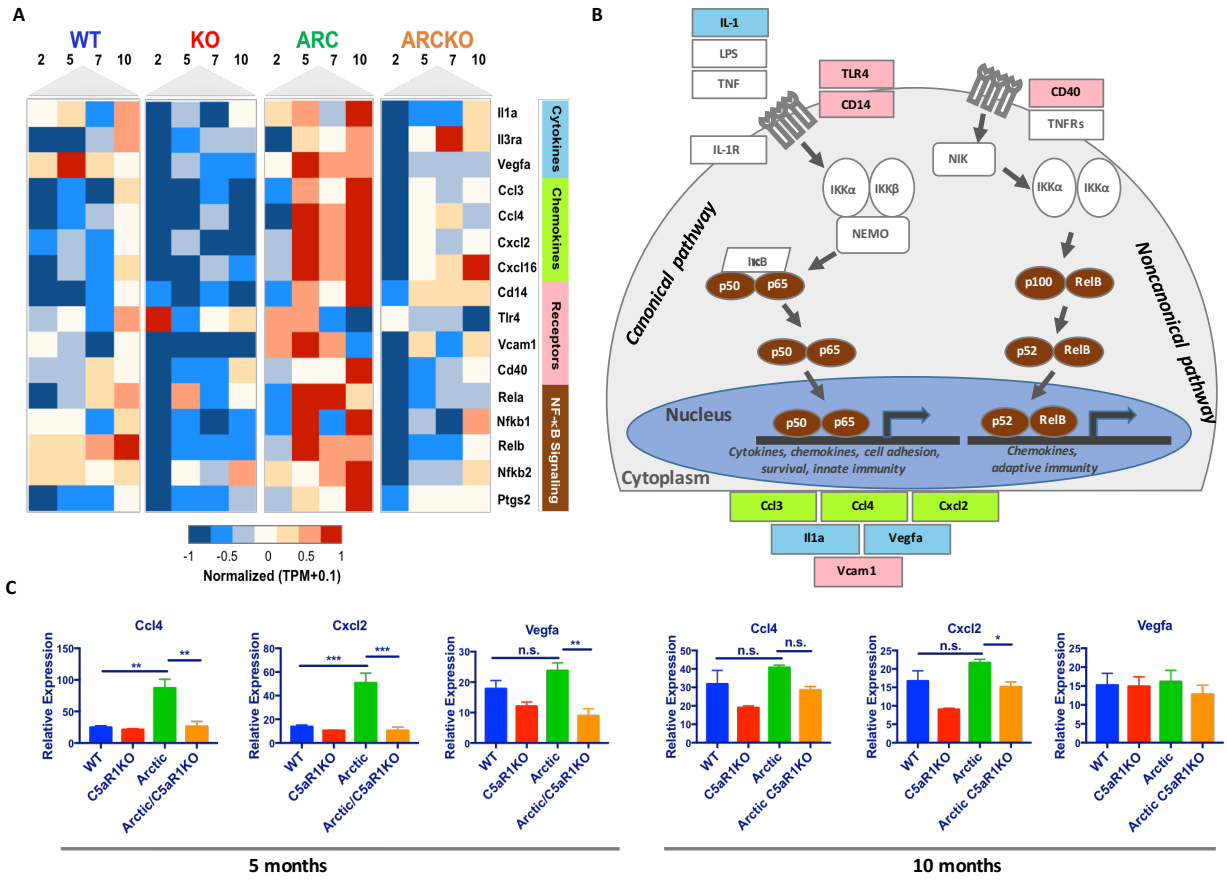

Figure 3.8. Gene expression profiles of selected genes in inflammation pathways. All genes in heat map were present in cluster 4 and found in the NF-kB signaling pathway, cytokine-cytokine receptor interaction, and/or chemokine signaling KEGG pathways. (**A**) Selected genes were clustered based on molecule functions: cytokines (skyblue), chemokines (yellow green), receptors (pink), NF-kB signaling (brown). Quantile normalized TPM plus 0.1 were transformed between -1 and 1 to present high (red) and low (blue) expression level during time-course across four genotypes for each gene. **(B**) Schematic of the NF-kB pathway with genes present in heat map colored accordingly. **(C)** RT-PCR analysis on a subset of genes to validate the RNA-seq dataset. For each gene, 3 samples, two from the RNA-seq dataset and an additional sample not analyzed by RNA-seq, were analyzed for each genotype at ages 5 (left) and 10 months (right).

Arctic mice. Most of these inflammatory genes shown in **Figure 3.8A** were either NF-κB subunits, transcriptionally regulated by NF-κB or were upstream activators of NF-κB as shown color-coded in **Figure 3.8B**. These differentially expressed genes included cytokines and growth factors or their receptors (*Il1a, Vegfa, Il3ra,*), chemokines (*Ccl3, Ccl4, Cxcl2, Cxcl16*), signaling receptors (*Tlr4, Vcam1, Cd40*), NF- κb transcription factor subunits (*Rela, Nfkb1, Relb, Nfkb2) and Ptgs2* (COX2) (**Figure 3.8A**). Representative genes were validated by RT-PCR for each genotype at ages 5 and 10 months. Ccl4 and Cxcl2 were both significantly increased in the Arctic relative to WT at 5 months (3.5x and 4.4.x respectively) and were decreased in the Arctic/C5aR1KO by 35% and 23%, respectively relative to the Arctic. Although Vegfa was not significantly increased in the Arctic relative to the WT at 5 months, it was significantly decreased by 46% in the Arctic/C5aR1KO relative to the Arctic (**Figure 3.8C**, left). At 10 months, only Cxcl2 was significantly decreased in the Arctic/C5aR1KO relative to the Arctic and all 3 genes validated by RT-PCR showed no difference in expression between the WT and Arctic (**Figure 3.8C**, right), thus following the same trend observed in the RNA-seq data where C5aR1 deficiency in the Arctic leads to reduced expression of inflammatory genes early in the progression of the disease. Aside from cluster 4, cluster 3 also included some of the same pathways as in Fig. 6, such as chemokine signaling and cytokine-cytokine receptor interaction (**Table 3.3**), however the genes in this cluster did not contain differences between the Arctic and Arctic/C5aR1KO, rather, the C5aR1KO mice were substantially upregulated relative to the other genotypes.

Like cluster 4, pathway analysis of cluster 2 genes identified pathways that were of statistical significance as well as biologically relevant for microglia. The lysosome, antigen processing and presentation, and phagosome pathways identified 22 genes that were

differentially expressed between the Arctic and Arctic/C5aR1KO. Trem2 and Tyrobp, also included in cluster 2, were added to the heat map due to known roles in microglial phagocytosis (**Figure 3.9A**). The genes in these pathways increased in the Arctic relative to WT at each age but further increased in the Arctic/C5aR1KO relative to Arctic as early as 2 months of age and remained elevated until 10 months (**Figure 3.9A**). The genes included phagocytosis-promoting receptors (*Tlr2, Fcgr4, Colec12, Trem2, Tyrobp*), lysosomal membrane proteins (*Lamp1, Cd63, Cd68, Npc2*), cathepsins (*Ctsb, Ctsd, Ctsl, Ctss, Ctsz*), glycosidases (*Gaa, Gusb, Gba, Hexa, Naglu, Man2b1*) and MHCI genes (*H2-d1, H2-m3, H2-t23, H2-q7*), all upregulated in the Arctic/C5aR1KO (**Figure 3.9B**). As with the Cluster 4 genes, representative genes were selected to validate the RNA-seq differential expression by RT-PCR. Genes Cathepsin D and Mannosidase 2b1 were strikingly decreased in the Arctic at 5 months relative to WT (21% and 28% of WT respectively), something not seen in our RNA-seq data, however, both were increased in the Arctic/C5aR1KO relative to the Arctic (6.4x and 4.4x respectively) as seen in our RNA-seq analysis. NPC intracellular cholesterol transporter 2 expression was also greater in the Arctic/C5aR1KO relative to Arctic (1.4x) although no significant difference was seen between the WT and Arctic at 5 months (**Figure 3.9C**, left). At 10 months of age, both Ctsd and Npc2 were upregulated in the Arctic relative to WT, however, only Npc2 was further increased in the Arctic/C5aR1KO (**Figure 3.9C**, right).

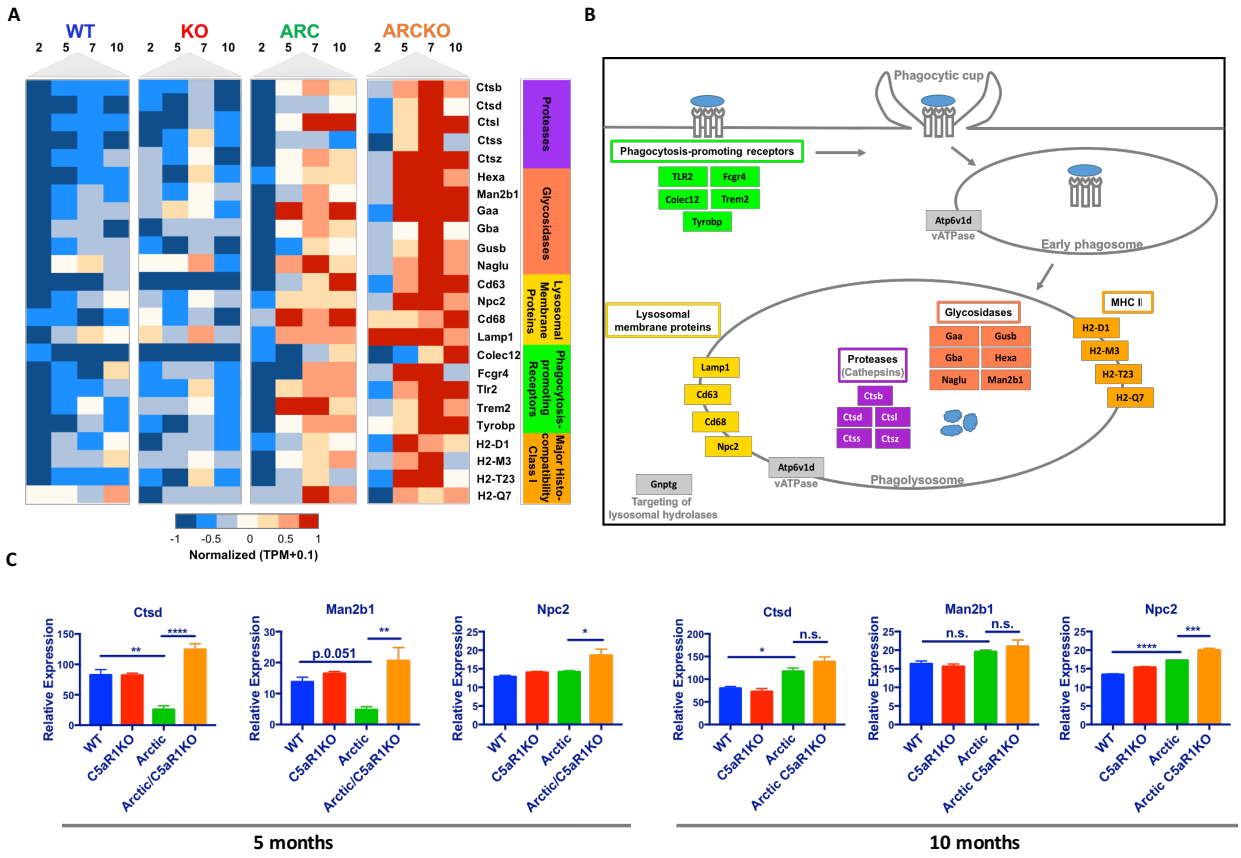

Figure 3.9. Gene expression profiles of selected genes in lysosome and phagosome pathways. All genes in heat map were present in cluster 2. All but Trem2 and Tyrobp were also found in the phagosome or lysosome KEGG pathways. Trem2 and Tyrobp were added due to known roles in microglial phagocytosis. (**A**) Selected genes were clustered based on molecule functions: protease (purple), glycosidases (coral), lysosomal membrane proteins (yellow), phagocytosis-promoting receptors (green) and major histocompatibility class I (orange). Quantile normalized TPM plus 0.1 were transformed between -1 and 1 to present high (red) and low (blue) expression level during time-course across four genotypes for each gene. (**B**) Schematic of the phagolysosome pathway with genes present in heat map colored accordingly. (**C**). RT-PCR analysis on a subset of genes to validate the RNA-seq dataset, as described in Figure 3.8 legend.

Discussion

Genetic deletion of C5aR1 in the Arctic Alzheimer's disease mouse model resulted in protection from deficits in a hippocampal dependent spatial memory task relative to the C5aR1 sufficient Arctic animals. While behavior deficits were pronounced at 10 months of age, the gene expression profile of the microglia from Arctic/C5aR1KO brain is indicative of a polarization state of the microglia with less inflammatory and greater clearance and degradation pathways than in the C5aR1 sufficient Arctic model as early as 2-5 months of age and with differences in these pathways increasing with age.

It has been previously reported that Arctic mice at 3-4 months of age have behavior deficits in the Morris water maze (Cheng et al., 2004), another spatial memory task. While the accumulation of fibrillar Aß in our cohort was somewhat slower than previously published (Cheng et al., 2004), these mice did exhibit exclusively spatial memory deficits as demonstrated by the OLM at 10 months. Our previously published studies using a pharmacological approach to block function of C5aR1 in the Tg2576 and 3xTG AD mouse models (Fonseca et al., 2009) resulted in reduced fibrillar plaques and gliosis. In contrast, the genetic approach to eliminate C5aR1 function used in this Arctic model of AD did not result in reduced fibrillar plaque accumulation, likely due to the "Arctic" mutation in the Aß peptide that leads to rapid fibril formation upon generation of Aß, such that nearly all plaques stain with thioflavine. However, the prevention of cognitive loss even in the presence of massive plaque accumulation, supports the idea that the fibrillar plaque itself is not the sole contributor to cognitive loss, but rather it is the microglial inflammatory response to the plaque that leads to neurotoxicity (Wyss-Coray and Rogers, 2012), perhaps through activation of astrocytes as recently reported (Liddelow et al., 2017).

Other innate immune system sensors of danger, such as toll-like receptors (TLRs) have been found to synergize with C5aR1 and lead to greater proinflammatory cytokine release in models of inflammatory disease in the periphery (reviewed in (Song, 2012)). Since fibrillar Aß is a ligand for TLR2 and TLR4 (Jana et al., 2008; Jin et al., 2008; Udan et al., 2008) and these receptors have been shown to contribute to the detrimental effects of Aß, C5a may synergistically enhance microglial polarization to a more inflammatory state in response to Aß interactions (or other danger associated signals) with such receptors on the C5a-stimulated plaque associated glia cells (Tahara et al., 2006). The increases in NFκB subunits may contribute to increased NF-κB signaling (**Figure 3.8**) and greater expression of inflammatory cytokines and chemokines, all of which were seen in the Arctic mice, but not so elevated in the Arctic/C5aR1KO. In the literature, C5aR1 signaling is most often shown to involve activation of PI-3K/AKT, PKC, phospholipase D, and MAP kinase (reviewed in (Sarma and Ward, 2012)). However, instances of NF-κB activation by C5a have also been demonstrated, such as in monocytes where activation of NF-κB was detected after C5a stimulation (Pan, 1998). It's also been shown in human macrophages that C5a increases the expression of plasminogen activator inhibitor-1 (PAI-1) via activation of NF-κB (Kastl et al., 2006). IL-1, Vegfa, Ccl3, Ccl4, Cxcl2 and Vcam1 are all regulated by the canonical NF-κB (p50/p65) signaling pathway, which can be activated via TLR4 (Fitzgerald et al., 2003). It seems likely that the increase in inflammatory components via NF-κB that we observed in this study is due to a synergy between TLRs and C5aR1, as mentioned above, since in the absence of C5aR1 the expression of several inflammatory genes is limited, even though amyloid plaques, a TLR ligand, is unchanged.

Also consistent with differential polarization of the microglia in Arctic vs Arctic/C5aR1KO is the increase in phagosomal and lysosomal genes (**Figure 3.9**). Phagocytosis-promoting receptors on microglia such as TREM2, FcγR's, TLR's and scavenger receptors have been associated with the clearance of amyloid beta in AD (reviewed in (Doens and Fernandez, 2014)). These genes showed higher expression in the Arctic/C5aR1KO either early in the disease (TREM2, TYROBP, Fcgr4) or later in the disease (TLR2, Colec12). Gene network analysis by Zhang and colleagues identified a microglia specific module that included Fc receptors, Major Histocompatibility Complex (MHC), TLRs and TYROBP, the signaling adaptor protein of TREM2, as key nodes of networks in late onset Alzheimer's disease (LOAD), all of which were increased in LOAD patients (Zhang et al., 2013). Recent data suggest TREM2 is important in microgliosis and containment of Aß plaques over the progression of the disease (Jay et al., 2016; Wang et al., 2016).

Cathepsins, proteases that are involved in the endosomal-lysosomal pathway, were substantially and significantly increased Arctic/C5aR1KO microglia relative to Arctic. Microglial cathepsins, particularly cysteine and aspartyl proteases, have been found to be upregulated with aging in rats (reviewed in (Stoka et al., 2016)), though we did not see an increase in expression in our wildtype mice from 2 to 10 months of age. Cathepsin B and D are Aß-degrading enzymes that have been implicated in clearance of amyloid beta *in vivo* (reviewed in ((Saido and Leissring, 2012)). Early "activation" of microglia cells has been found to be beneficial in AD models, however, as Aß plaques form, the phagocytosis and clearance of Aß is reduced ((Krabbe et al., 2013). Hickman and colleagues found that gene expression of scavenger receptors and degradation enzymes decreased with age in AD mice

(Hickman et al., 2008). C5aR1 deficiency prevents this decrease in phagocytosis and degradation enzymes seen relative to the aging AD mouse models.

It has been reported that CX3CR1 and CCR2 play a role in the pathogenesis of AD in some mouse models of the disease, either by affecting microglia or by limiting the infiltration of monocytes (El Khoury et al., 2007; Lee et al., 2010; Liu et al., 2010). In the Arctic model we found no difference in amyloid plaque load in mice that possessed a single CX3CR1 or CCR2 allele compared to mice that had both copies of CX3CR1 or CCR2. In addition, no RFP+ myeloid cells were found in the parenchyma, though they were seen around the meninges and were observed (2-6% of CX3CR1+ cells, **Figure 3.5E**) by FACS. Given that RFP is expressed in the cytosol when the CCR2 promoter is activated (as in peripheral myeloid cells), and the estimated half-life of RFP *in vivo* is ~4.6 days (Verkhusha et al., 2003), we would expect to visualize at least a fraction of them by IHC at one of the ages analyzed if indeed CCR2+ monocytes were infiltrating the CNS. The different observations may be attributed to the different animal models used, which includes oligomeric species of Aß among other differences that have been reported (Cheng et al., 2004).

Inflammation, as mentioned above, is recognized as having a complex role in the pathogenesis of AD (reviewed in (Wyss-Coray and Rogers, 2012)). The complement cascade is one aspect of the inflammatory response in AD, which results in both beneficial and detrimental outcomes and synergizes with other innate pathways (Veerhuis et al., 2011). Furthermore, epidemiologic and genetic evidence supports a role for complement in the etiology of late onset AD (Eikelenboom et al., 2012), although the GWAS CR1 protein likely has a primary role outside of the CNS on clearance of Aß (Fonseca et al., 2016). The consequences of genetic deletion of C5aR1 reported here support the contention that the

mechanism by which the previously used small molecular weight cyclic hexapeptide C5aR1 antagonist, PMX205, was mediating its beneficial effects in AD mouse models (Fonseca et al., 2009) was via the inhibition of C5aR1 cell signaling, and support the continued assessment of C5aR1 antagonists for AD therapy. Such specific antagonists have been successfully utilized in acute and chronic inflammatory disease animal models such as sepsis, asthma, ischemia/reperfusion injury (Konteatis et al., 1994; Arumugam et al., 2006; Guo and Ward, 2006; Kohl, 2006) and as reviewed in (Holland et al., 2004; Woodruff et al., 2011). In addition, blocking C5a in rodent neurodegenerative disease models has been shown to be beneficial, including in Huntington's disease (Singhrao et al., 1999; Woodruff et al., 2006), traumatic brain injury (Sewell et al., 2004), and ALS (Woodruff et al., 2008).

It is critical to note that several studies have demonstrated beneficial effects of complement in the brain (reviewed in (Lucin and Wyss-Coray, 2009)). More recently, C1q has been shown to induce gene expression critical for neuronal survival and protection against oligomeric and fibrillar Aß-induced neuronal death *in vitro* (Pisalyaput and Tenner, 2008; Benoit et al., 2013). Selective modulation of complement activation products or their receptors may therefore be an effective strategy for retaining the neuroprotective, anti-inflammatory and phagocytic functions of complement, while dampening proinflammatory induced damage.

Given the inflammatory profile seen in microglia from Arctic mice with aging and the decrease in expression of the same genes in the Arctic/C5aR1KO, along with the activation of phagocytosis and protein degradation in the Arctic/C5aR1KO, we propose a model by which C5aR1 activation contributes to AD progression (**Figure 3.10**).

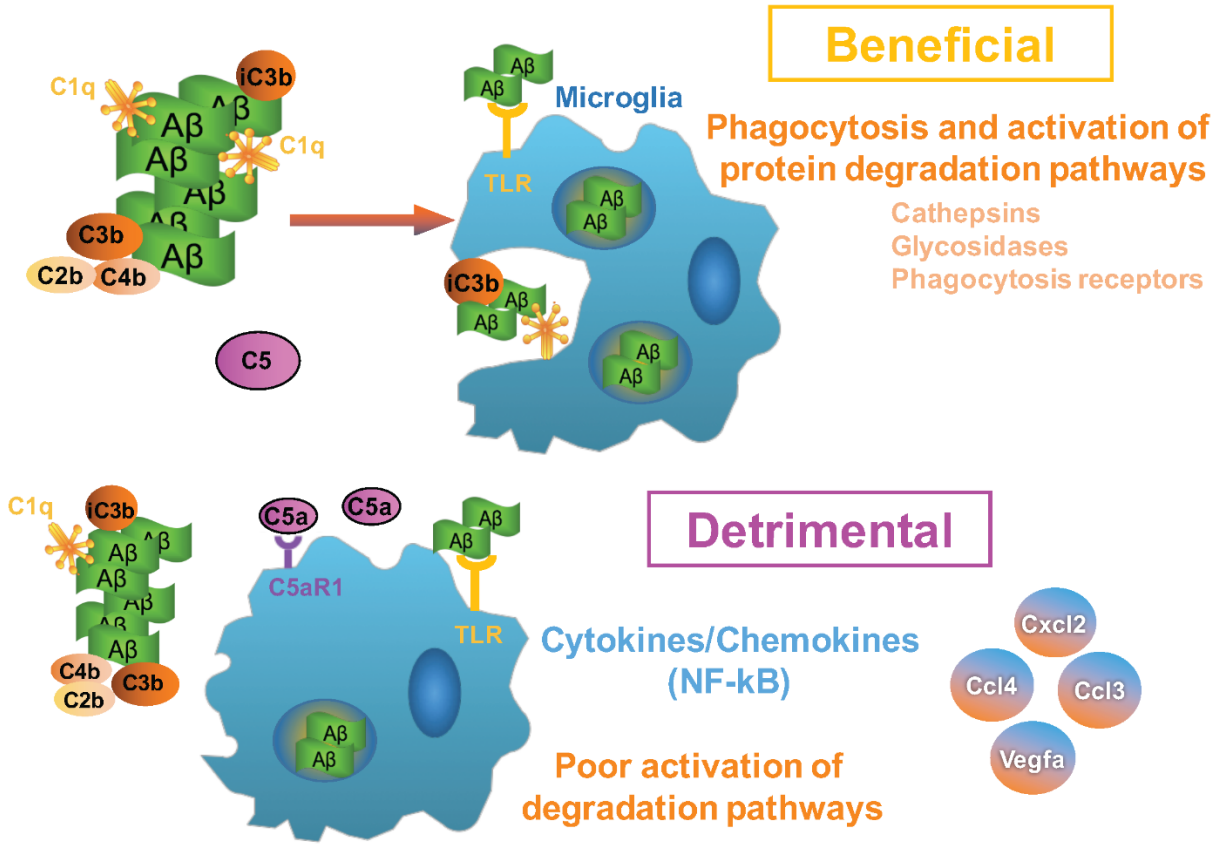

Figure 3.10. Proposed mechanism by which C5aR1 stimulation contributes to AD progression. Aβ fibrils activate complement resulting in cleavage of C3 and C5. Amyloid deposited C3b/iC3b should lead to more efficient phagocytosis by microglia/macrophages, while generated C5a recruits and alters the function of microglia. C5a induces an inflammatory polarization of the microglia, potentially synergizing with TLRs, which results in production of neurotoxic inflammatory products while suppressing beneficial phagocytosis and degradation pathways thereby contributing to neuronal damage and cognitive deficits. Targeting C5a and its receptor C5aR1 will not interfere with the beneficial effects of upstream complement components.

Complement is activated by fibrillar amyloid beta via the classical (or alternative) pathway and can have beneficial and detrimental effects. Phagocytosis-promoting components such as C1q, C4b, C3b, and iC3b (the latter 3 covalently bound via a thioester bond to plaques) could enhance clearance of Aß fibrils or protofibrils via microglial phagocytosis and/or in the periphery via the potential immune adherence mechanism (Rogers et al., 2006). Downstream consequences of the activation of the complement cascade can lead to the generation of C5a which in the CNS can bind to microglial C5aR1 and synergize with TLR's (such as TLR2 or TLR4 that recognize fibrillar Aß) when the microglia engage a plaque, polarizing the microglia to a more inflammatory state and suppressing induction of degradation pathways. The resulting inflammatory environment further damages neurons, perhaps via astrocyte activation (Liddelow et al., 2017), thereby contributing to cognitive deficits. Targeting C5a and its receptor C5aR1 will not disrupt the beneficial effects of the upstream complement activation products, but rather, it will interfere with the polarization of the microglia to an inflammatory state, allowing the phagocytosis and degradation promoting gene expression program of the cells to continue.

Significant and substantial cognitive deficits were seen in the Arctic mice at 10 months of age, with some mice showing decline as early as 7 months of age. However, interestingly, the differences between the wild type and Arctic gene expression in the noted pathways were seen as early as 5 months of age, consistent with current thought that the disease process starts considerable prior to clinical signs of the disorder, and consequently treatment to suppress those detrimental processes would best be initiated substantially prior to clinical presentation.

Recent elegant studies have shown that excessive complement-mediated synapse pruning occurs in aging, AD, and other disorders leading to cognitive or behavior changes (Hong et al., 2016; Lui et al., 2016; Sekar et al., 2016; Vasek et al., 2016). Since the activation of complement in these scenarios could also result in the generation of C5a, it remains to be seen if it is the insult of C5a-mediated effects that results in the behavioral/cognitive dysfunction, rather than only synaptic pruning, or if both mechanisms contribute to deficits. While additional studies in multiple animal models can be performed to discern this, what the balance is in human systems will require clinical trials. The data presented here supports the translational link to C5aR1-targeted treatments. The lack of detrimental toxicity of the C5aR1 antagonist PMX53 in a small human phase Ia/IIb clinical trial of refractory rheumatoid arthritis (Kohl, 2006; Vergunst et al., 2007), and the recent FDA approval of Eculizumab, an anti C5 monoclonal antibody that prevents the cleavage of C5 and thus the generation of C5a (Sahin et al., 2015), suggests that suppression of the C5a/C5aR1 axis may be not be harmful for extended clinical use in adults. An advantage of a selective C5aR1 antagonist vs Eculizumab for long term treatment of diseases such as AD is that while it blocks effects of C5a, C5b, generated by the cleavage of C5 upon activation by pathogens, is still able to initiate the assembly of the bacteriolytic C5b-9 complex. Thus, this protective bacteriolytic function of complement would not be systemically compromised by the antagonist. Finally, a small molecule has the potential for better access to the brain than antibodies to C5a (Landlinger et al., 2015) or C5aR1.

In summary, genetic ablation of C5aR1 in an accelerated mouse model of AD prevented (or delayed) deficits in hippocampal dependent behavioral performance. The data provide proof of concept that blocking C5a-C5aR1, such as through pharmacologic

treatment with C5aR1 antagonists, could prevent detrimental downstream effects of the complement cascade activation and thereby suppress damage to neurons surrounding the amyloid plaques, while preserving systemic protection from infection, which could be compromised by targeting early components in the complement cascade. The gene expression profiles using RNA-seq suggest a less inflammatory state and a greater induction of clearance pathways in microglia from the Arctic/C5aR1KO relative to Arctic that are C5aR1 sufficient. These data, consistent with the increasingly proposed role of inflammation in neurodegenerative disorders, provide additional compelling rationale to pursue inhibition of C5aR1 as a highly specifically targeted candidate therapy to slow the progression of AD in humans.

Table 3.1. RNA Quality Control. Amount of RNA extracted from FACS-sorted microglia isolated from adult mice was quantified by NanoDrop and the quality assessed by Agilent Bioanalyzer. All samples had greater than 1ng/µl of RNA and RINs greater than 4, sufficient for the SMARTer Stranded Total RNA-Seq Kit - Pico Input Mammalian by Clontech.

Genotype	Age	[RNA] ng/µL	RIN
WT	2	8 - 10	4.8 - 7.3
WT	5	5 - 6	6.0 - 7.4
WT	7	6 - 7	6.8 - 8.3
WT	10-11	7 - 10	7.6 - 8.1
C5aR1KO	2	5	7.6 - 7.8
C5aR1KO	5	8	7.9 - 8.4
C5aR1KO	7	1 - 2	8.5 - 8.8
C5aR1KO	10-11	10 - 12	8.5 - 8.9
Arctic	2	9 - 11	4.1 - 5.6
Arctic	5	10 - 16	6.7 - 7.0
Arctic	7	6 - 7	7.7 - 8.1
Arctic	10-11	9 - 10	8.2 - 9.3
Arctic/C5aR1KO	2	4 - 5	7.1 - 7.8
Arctic/C5aR1KO	5	1 - 4	7.7 - 8.0
Arctic/C5aR1KO	7	1 - 2	8.8 - 9.2
Arctic/C5aR1KO	10-11	8 - 11	9.2 - 9.5

Table 3.2. Gene ontology enrichment analysis. Clusters were analyzed with Metascape (http://metascape.org) to identify the GO terms (biological processes) enriched in each cluster. The GO terms, their descriptions, logP, log(q-value), InTerm_InList (Genes in cluster/All genes from genome in GO term), and the gene and gene symbols are listed.

	GO Term	Description	Log10 (P-value)	# of genes from cluster / total # of genes in term
Cluster 1	GO:0097011	cellular response to granulocyte macrophage colony-stimulating factor stimulus	-4.8539	3/8
	GO:0016575	histone deacetylation	-4.4219	5/59
	GO:0044802	single-organism membrane organization	-4.2787	15/710
	GO:0070932	histone H3 deacetylation	-4.2678	3/12
	GO:0070997	neuron death	-4.1137	10/344
	GO:1901698	response to nitrogen compound	-3.4382	14/756
	GO:0048168	regulation of neuronal synaptic plasticity	-3.2275	4/60
	GO:0051148	negative regulation of muscle cell differentiation	-3.2275	4/60
	GO:0045981	positive regulation of nucleotide metabolic process	-3.0769	5/114
	GO:0071559	response to transforming growth factor beta	-3.0309	6/175
	GO:0006338	chromatin remodeling	-3.0261	5/117
	GO:0001666	response to hypoxia	-2.9802	6/179
	GO:0001773	myeloid dendritic cell activation	-2.9161	3/33
	GO:0040029	regulation of gene expression, epigenetic	-2.8667	7/257
	GO:0051817	modification of morphology or physiology of other organism involved in symbiotic interaction	-2.8417	4/76
	GO:0008380	RNA splicing	-2.8395	8/335
	GO:0051260	protein homooligomerization	-2.6471	7/281
	GO:0006914	autophagy	-2.5712	9/455
	GO:0007585	respiratory gaseous exchange	-2.3009	3/54
	GO:0050954	sensory perception of mechanical stimulus	-2.2985	5/172
Cluster 2	GO:0043603	cellular amide metabolic process	-27.2911	63/908
	GO:0042254	ribosome biogenesis	-15.3660	26/251
	GO:0002181	cytoplasmic translation	-11.4767	12/53

	GO:0045087	innate immune response	-9.4646	30/596
	GO:1901135	carbohydrate derivative metabolic process	-7.8650	36/956
	GO:0042273	ribosomal large subunit biogenesis	-7.8554	10/66
	GO:0098609	cell-cell adhesion	-7.0610	35/983
	GO:0034097	response to cytokine	-6.5889	24/545
	GO:0044712	single-organism catabolic process	-5.6802	25/657
	GO:0006897	endocytosis	-5.3761	21/510
	GO:0009117	nucleotide metabolic process	-5.0221	21/538
	GO:0060326	cell chemotaxis	-4.9374	13/230
	GO:0030203	glycosaminoglycan metabolic process	-4.7672	8/86
	GO:0051270	regulation of cellular component movement	-4.6537	26/802
	GO:0009894	regulation of catabolic process	-4.6496	18/440
	GO:2000377	regulation of reactive oxygen species metabolic process	-4.2921	10/160
	GO:0044724	single-organism carbohydrate catabolic process	-4.2293	8/102
	GO:0009611	response to wounding	-3.9568	16/410
	GO:0035456	response to interferon-beta	-3.9418	5/37
	GO:0035455	response to interferon-alpha	-3.9295	4/20
Cluster 3	GO:0001775	cell activation	-9.7523	30/889
	GO:0006935	chemotaxis	-7.1593	19/496
	GO:0002684	positive regulation of immune system process	-6.9063	23/740
	GO:0051258	protein polymerization	-6.2905	12/220
	GO:0030155	regulation of cell adhesion	-5.7042	19/619
	GO:0019827	stem cell population maintenance	-5.0271	9/157
	GO:0071887	leukocyte apoptotic process	-5.0047	8/120
	GO:0030168	platelet activation	-4.9132	7/89
	GO:0002274	myeloid leukocyte activation	-4.8747	9/164
	GO:0030220	platelet formation	-4.7240	4/19
	GO:0006325	chromatin organization	-4.5637	18/680
	GO:0001568	blood vessel development	-4.4934	17/624
	GO:0009607	response to biotic stimulus	-4.4718	21/894
	GO:0033688	regulation of osteoblast proliferation	-4.3769	4/23
	GO:0000904	cell morphogenesis involved in differentiation	-4.3521	19/773
	GO:0000122	negative regulation of transcription from RNA polymerase II promoter	-4.1588	18/731
	GO:0001816	cytokine production	-4.1331	16/602
	GO:0042063	gliogenesis	-3.9630	10/265

	GO:0002683	negative regulation of immune system process	-3.8968	12/381
	GO:0035588	G-protein coupled purinergic receptor signaling pathway	-3.6674	3/14
Cluster 4	GO:0006954	inflammatory response	-10.5227	18/589
	GO:0019886	antigen processing and presentation of exogenous peptide antigen via MHC class II	-6.5852	4/14
	GO:0002684	positive regulation of immune system process	-6.4589	15/740
	GO:0071347	cellular response to interleukin-1	-5.0470	5/68
	GO:0048514	blood vessel morphogenesis	-4.9833	11/524
	GO:0035924	cellular response to vascular endothelial growth factor stimulus	-4.8954	4/35
	GO:0032480	negative regulation of type I interferon production	-4.4409	3/16
	GO:0045597	positive regulation of cell differentiation	-3.9210	13/937
	GO:0050707	regulation of cytokine secretion	-3.3559	5/154
	GO:0060548	negative regulation of cell death	-3.3500	12/934
	GO:0051336	regulation of hydrolase activity	-3.1791	11/839
	GO:0006874	cellular calcium ion homeostasis	-3.0533	7/373
	GO:0030029	actin filament-based process	-3.0206	9/613
	GO:0002683	negative regulation of immune system process	-2.9998	7/381
	GO:0002573	myeloid leukocyte differentiation	-2.9245	5/192
	GO:0032675	regulation of interleukin-6 production	-2.8424	4/118
	GO:2001234	negative regulation of apoptotic signaling pathway	-2.7804	5/207
	GO:0008360	regulation of cell shape	-2.6288	4/135
	GO:0007422	peripheral nervous system development	-2.6121	3/65
	GO:0061061	muscle structure development	-2.3933	8/620
Cluster 5	GO:0048524	positive regulation of viral process	-4.5455	6/77
	GO:0006897	endocytosis	-3.7769	13/510
	GO:0044712	single-organism catabolic process	-3.2380	14/657
	GO:0032103	positive regulation of response to external stimulus	-3.0952	8/254
	GO:0044255	cellular lipid metabolic process	-3.0304	16/853
	GO:0019915	lipid storage	-2.8517	4/63
	GO:0008203	cholesterol metabolic process	-2.7074	5/115
	GO:0042733	embryonic digit morphogenesis	-2.7055	4/69
	GO:0060976	coronary vasculature development	-2.6599	4/71
	GO:1900181	negative regulation of protein localization to nucleus	-2.6599	4/71

	GO:0031929	TOR signaling	-2.3954	4/84
	GO:0005975	carbohydrate metabolic process	-2.3940	12/640
	GO:0030163	protein catabolic process	-2.3254	13/738
	GO:0014074	response to purine-containing compound	-2.2551	4/92
	GO:0045596	negative regulation of cell differentiation	-2.2043	12/677
	GO:1903047	mitotic cell cycle process	-2.1994	12/678
	GO:0007040	lysosome organization	-2.0816	3/54
	GO:0098609	cell-cell adhesion	-2.0447	15/983
	GO:0007034	vacuolar transport	-1.9356	6/244
	GO:1902580	single-organism cellular localization	-1.8667	14/937
Cluster 6	GO:0009791	post-embryonic development	-2.8643	4/131
	GO:0007623	circadian rhythm	-2.3317	4/184
	GO:0006520	cellular amino acid metabolic process	-2.3070	4/187
	GO:0060401	cytosolic calcium ion transport	-1.9833	3/123
	GO:0060491	regulation of cell projection assembly	-1.8081	3/143
	GO:0032496	response to lipopolysaccharide	-1.5691	4/310
	GO:0009306	protein secretion	-1.4947	5/483
	GO:0030324	lung development	-1.3493	3/216
Cluster 7	GO:0048812	neuron projection morphogenesis	-6.8697	24/568
	GO:0006397	mRNA processing	-4.9575	17/407
	GO:0022904	respiratory electron transport chain	-4.1875	6/57
	GO:0060997	dendritic spine morphogenesis	-3.5930	5/47
	GO:0021795	cerebral cortex cell migration	-3.4250	5/51
	GO:0032204	regulation of telomere maintenance	-2.9088	5/66
	GO:0051129	negative regulation of cellular component organization	-2.7470	17/627
	GO:0060491	regulation of cell projection assembly	-2.7357	7/143
	GO:0022613	ribonucleoprotein complex biogenesis	-2.7128	12/369
	GO:0010501	RNA secondary structure unwinding	-2.6719	4/45
	GO:0008584	male gonad development	-2.6483	6/110
	GO:0051642	centrosome localization	-2.6409	3/22
	GO:0048668	collateral sprouting	-2.4289	3/26
	GO:0007416	synapse assembly	-2.4246	6/122
	GO:0048745	smooth muscle tissue development	-2.3816	3/27
	GO:0006336	DNA replication-independent nucleosome assembly	-2.3363	3/28
	GO:0051276	chromosome organization	-2.3238	22/989

	GO:0044708	single-organism behavior	-2.2925	13/470
	GO:0048255	mRNA stabilization	-2.0978	3/34
	GO:0000122	negative regulation of transcription from RNA polymerase II promoter	-2.0856	17/731
Cluster 8	GO:0070979	protein K11-linked ubiquitination	-3.0066	3/26
	GO:0003143	embryonic heart tube morphogenesis	-2.8436	4/64
	GO:0001508	action potential	-2.5701	5/125
	GO:0007204	positive regulation of cytosolic calcium ion concentration	-2.5302	7/248
	GO:0090184	positive regulation of kidney development	-2.3430	3/44
	GO:0051592	response to calcium ion	-2.2551	4/93
	GO:0051053	negative regulation of DNA metabolic process	-1.9886	4/111
	GO:0048545	response to steroid hormone	-1.9817	6/241
	GO:0048469	cell maturation	-1.9504	5/176
	GO:0032990	cell part morphogenesis	-1.9409	13/834
	GO:0010822	positive regulation of mitochondrion organization	-1.7047	4/135
	GO:0001649	osteoblast differentiation	-1.5751	5/220
	GO:0042158	lipoprotein biosynthetic process	-1.5423	3/87
	GO:0014706	striated muscle tissue development	-1.4941	7/396
	GO:0007219	Notch signaling pathway	-1.4357	4/164
	GO:0051047	positive regulation of secretion	-1.4015	7/415
Cluster 9	GO:2000191	regulation of fatty acid transport	-3.7116	3/27
	GO:0034723	DNA replication-dependent nucleosome organization	-3.5303	3/31
	GO:0045597	positive regulation of cell differentiation	-3.2578	12/937
	GO:0006900	membrane budding	-3.0781	3/44
	GO:0034637	cellular carbohydrate biosynthetic process	-2.7292	3/58
	GO:0071407	cellular response to organic cyclic compound	-2.7250	7/417
	GO:0034766	negative regulation of ion transmembrane transport	-2.5500	3/67
	GO:0042742	defense response to bacterium	-2.3042	5/262
	GO:0060048	cardiac muscle contraction	-1.9960	3/106
	GO:0009628	response to abiotic stimulus	-1.9405	9/878
	GO:0030162	regulation of proteolysis	-1.9057	7/593
	GO:0043085	positive regulation of catalytic activity	-1.8474	9/910
	GO:0007631	feeding behavior	-1.8040	3/125
	GO:0009612	response to mechanical stimulus	-1.7329	3/133

	GO:0055082	cellular chemical homeostasis	-1.6263	7/676
	GO:0008284	positive regulation of cell proliferation	-1.6122	8/837
	GO:0016042	lipid catabolic process	-1.5994	4/264
	GO:0006457	protein folding	-1.5533	3/156
	GO:0000122	negative regulation of transcription from RNA polymerase II promoter	-1.4672	7/731
	GO:0050792	regulation of viral process	-1.4521	4/294

Table 3.3. Pathway analysis. Significantly enriched KEGG pathways were identified by PaintOmics 3. The pathway name, number of genes in the pathway, and the p-value of the enriched pathway is displayed for each cluster.

	Pathway name	# of genes in pathway	p value
Cluster 1	Chronic myeloid leukemia	73	0.000338686
	FoxO signaling pathway	132	0.000787849
	Acute myeloid leukemia	57	0.001240835
	AGE-RAGE signaling pathway in diabetic complications	99	0.001358973
	Viral carcinogenesis	227	0.003864846
	Osteoclast differentiation	129	0.004585344
	Hepatitis B	144	0.006808734
	Notch signaling pathway	49	0.007625999
	One carbon pool by folate	19	0.010484035
	Proximal tubule bicarbonate reclamation	21	0.012737603
	cGMP-PKG signaling pathway	169	0.013022535
	Longevity regulating pathway - multiple species	64	0.015772463
	Chemokine signaling pathway	179	0.016325768
	Pancreatic cancer	66	0.017118778
	Prolactin signaling pathway	71	0.020757752
	B cell receptor signaling pathway	72	0.021532519
	Measles	133	0.024248336
	D-Glutamine and D-glutamate metabolism	3	0.024466109
	HTLV-I infection	280	0.028510832
	MicroRNAs in cancer	142	0.029879555
	Epstein-Barr virus infection	213	0.031572226
	Fc gamma R-mediated phagocytosis	86	0.034021457
	Non-alcoholic fatty liver disease (NAFLD)	151	0.036972563
	Aldosterone-regulated sodium reabsorption	39	0.040831368
	Cyanoamino acid metabolism	6	0.048337103
	Carbohydrate digestion and absorption	43	0.048715614

Cluster 2	Ribosome	142	1.96159E-72
	Lysosome	123	3.06624E-11
	Antigen processing and presentation	83	1.38481E-06
	Alzheimer's disease	171	7.79893E-06
	Phagosome	172	8.30585E-06
	Pertussis	71	0.000215411
	Graft-versus-host disease	57	0.000435438
	Complement and coagulation cascades	82	0.000557173
	Type I diabetes mellitus	63	0.000681039
	Tuberculosis	171	0.000723784
	Bile secretion	66	0.000872904
	Staphylococcus aureus infection	49	0.001534731
	Cardiac muscle contraction	73	0.001589831
	Huntington's disease	192	0.001729474
	Chagas disease (American trypanosomiasis)	102	0.001754501
	Oxidative phosphorylation	132	0.001955027
	Prion diseases	33	0.002244083
	Rheumatoid arthritis	80	0.002370084
	Herpes simplex infection	202	0.002414791
	Allograft rejection	56	0.002547832
	Parkinson's disease	141	0.002938146
	Other glycan degradation	18	0.003252371
	Glycolysis / Gluconeogenesis	62	0.004259306
	Glycosaminoglycan degradation	20	0.004431495
	Cell adhesion molecules (CAMs)	159	0.006023755
	Mineral absorption	44	0.006436557
	Autoimmune thyroid disease	70	0.006665082
	Gastric acid secretion	71	0.007072876
	Salivary secretion	76	0.00937542
	Viral myocarditis	77	0.009891034
	Endocrine and other factor-regulated calcium reabsorption	50	0.010090529
	Pentose phosphate pathway	29	0.012698676
	Hematopoietic cell lineage	81	0.012762553
	Inflammatory bowel disease (IBD)	57	0.015790116
	Folate biosynthesis	13	0.019716855

	Leishmaniasis	63	0.023181653
	Protein processing in endoplasmic reticulum	167	0.023909382
	Osteoclast differentiation	129	0.024222426
	Measles	133	0.025851804
	Glycosaminoglycan biosynthesis - keratan sulfate	15	0.025958871
	Renin secretion	66	0.026894996
	Glucagon signaling pathway	100	0.027615013
	Aldosterone-regulated sodium reabsorption	39	0.028072934
	Renal cell carcinoma	68	0.028207221
	Apoptosis	136	0.028429976
	HIF-1 signaling pathway	106	0.035496724
	PPAR signaling pathway	75	0.038449724
	Biosynthesis of amino acids	76	0.041718329
	Carbon metabolism	111	0.04189573
	Glycosaminoglycan biosynthesis - chondroitin sulfate / atan sulfate	20	0.044448465
	Non-alcoholic fatty liver disease (NAFLD)	151	0.045022657
	Thyroid hormone signaling pathway	116	0.047484995
	Proximal tubule bicarbonate reclamation	21	0.048589788
Cluster 3	Tight junction	132	0.000449328
	Platelet activation	120	0.001554302
	Regulation of actin cytoskeleton	211	0.001664998
	Fc gamma R-mediated phagocytosis	86	0.001981086
	Chemokine signaling pathway	179	0.002637014
	cAMP signaling pathway	196	0.004345735
	Adherens junction	73	0.006904076
	cGMP-PKG signaling pathway	169	0.008321814
	Transcriptional misregulation in cancer	171	0.009785672
	Axon guidance	128	0.010644426
	Notch signaling pathway	49	0.014116065
	Staphylococcus aureus infection	49	0.014905033
	MicroRNAs in cancer	142	0.016075698
	Pertussis	71	0.03850312
	B cell receptor signaling pathway	72	0.03850312
	Cytokine-cytokine receptor interaction	243	0.040790945

	Salmonella infection	76	0.04406318
	Bacterial invasion of epithelial cells	78	0.046985103
Cluster 4	Tuberculosis	171	1.85124E-07
	Phagosome	172	1.94492E-07
	Leishmaniasis	63	7.46613E-07
	Salmonella infection	76	2.07544E-06
	Rheumatoid arthritis	80	2.80769E-06
	Hematopoietic cell lineage	81	3.24575E-06
	Staphylococcus aureus infection	49	4.74381E-06
	Inflammatory bowel disease (IBD)	57	9.12161E-06
	AGE-RAGE signaling pathway in diabetic complications	99	9.70705E-06
	Legionellosis	57	9.94319E-06
	Influenza A	158	1.35429E-05
	Pertussis	71	2.87456E-05
	NF-kappa B signaling pathway	94	0.000103498
	Asthma	21	0.000146154
	Toxoplasmosis	107	0.000190548
	Graft-versus-host disease	57	0.000194419
	Cytokine-cytokine receptor interaction	243	0.000205507
	Type I diabetes mellitus	63	0.00026785
	HTLV-I infection	280	0.000483461
	Osteoclast differentiation	129	0.00048588
	Herpes simplex infection	202	0.000503979
	Antigen processing and presentation	83	0.000766244
	Intestinal immune network for IgA production	41	0.001090404
	Viral carcinogenesis	227	0.001261183
	Toll-like receptor signaling pathway	98	0.00142353
	MAPK signaling pathway	248	0.001459362
	Chagas disease (American trypanosomiasis)	102	0.001649676
	Transcriptional misregulation in cancer	171	0.001777287
	Allograft rejection	56	0.002687588
	Regulation of actin cytoskeleton	211	0.004060283
	Epstein-Barr virus infection	213	0.00414188
	Autoimmune thyroid disease	70	0.00504931
	Systemic lupus erythematosus	125	0.005979268

	Viral myocarditis	77	0.006581812
	Complement and coagulation cascades	82	0.008363187
	Pancreatic secretion	90	0.010401889
	Chemokine signaling pathway	179	0.012038559
	Amoebiasis	100	0.013773675
	HIF-1 signaling pathway	106	0.016061351
	Focal adhesion	197	0.016571097
	TNF signaling pathway	110	0.01728048
	Proteoglycans in cancer	201	0.017705098
	Rap1 signaling pathway	211	0.021069414
	PI3K-Akt signaling pathway	332	0.024842079
	Ras signaling pathway	225	0.02552088
	Measles	133	0.028309022
	Caffeine metabolism	6	0.029298773
	Apoptosis	136	0.029967003
	NOD-like receptor signaling pathway	58	0.033427937
	MicroRNAs in cancer	142	0.03343389
	Hepatitis B	144	0.034634035
	Pancreatic cancer	66	0.042293638
	Pathways in cancer	387	0.043085504
	RIG-I-like receptor signaling pathway	67	0.043457558
	Cell adhesion molecules (CAMs)	159	0.04502588
	Arrhythmogenic right ventricular cardiomyopathy (ARVC)	71	0.048230725
Cluster 5	Glycosphingolipid biosynthesis - ganglio series	15	0.000321529
	Glycosphingolipid biosynthesis - globo series	15	0.000321529
	Viral myocarditis	77	0.000722932
	Lysosome	123	0.000977412
	Phagosome	172	0.001126874
	Cell adhesion molecules (CAMs)	159	0.003690038
	Intestinal immune network for IgA production	41	0.006321519
	Amino sugar and nucleotide sugar metabolism	48	0.009787246
	Parkinson's disease	141	0.010172831
	Staphylococcus aureus infection	49	0.010943817
	Non-alcoholic fatty liver disease (NAFLD)	151	0.013355332
	Glycosaminoglycan degradation	20	0.0143502

	Oxytocin signaling pathway	155	0.014427422
	Allograft rejection	56	0.014870721
	Graft-versus-host disease	57	0.016334203
	Type I diabetes mellitus	63	0.020334892
	Leishmaniasis	63	0.02119389
	Autoimmune thyroid disease	70	0.026760576
	Citrate cycle (TCA cycle)	31	0.032882809
	Rheumatoid arthritis	80	0.03760084
	Aldosterone synthesis and secretion	86	0.047650242
	Regulation of autophagy	39	0.049968309
Cluster 6	Nicotinate and nicotinamide metabolism	31	0.009297065
	Valine, leucine and isoleucine biosynthesis	3	0.014030096
Cluster 7	Oxidative phosphorylation	132	0.005730666
	Parkinson's disease	141	0.00811303
	Homologous recombination	28	0.009977523
	Spliceosome	131	0.019876836
	Intestinal immune network for IgA production	41	0.027884342
	Cardiac muscle contraction	73	0.031210438
	Ether lipid metabolism	43	0.031539467
	Olfactory transduction	1043	0.032719034
	Arginine biosynthesis	18	0.033184638
	Arginine and proline metabolism	46	0.037468013
Cluster 8	ECM-receptor interaction	80	0.006858186
	Hypertrophic cardiomyopathy (HCM)	81	0.007162509
	Dilated cardiomyopathy	86	0.008817923
	Alcoholism	181	0.012256982
	Amphetamine addiction	66	0.024256306
	Arrhythmogenic right ventricular cardiomyopathy (ARVC)	71	0.029290025
	Arachidonic acid metabolism	79	0.038399514
	Rheumatoid arthritis	80	0.039628397
Clu 9	Alcoholism	181	9.41407E-05

	Systemic lupus erythematosus	125	0.000119965
	Influenza A	158	0.001463712
	Estrogen signaling pathway	97	0.001695261
	Protein processing in endoplasmic reticulum	167	0.001867186
	Type II diabetes mellitus	49	0.00215949
	Toxoplasmosis	107	0.002426251
	Legionellosis	57	0.0034956
	Dopaminergic synapse	126	0.004363112
	Longevity regulating pathway - multiple species	64	0.004614275
	Insulin signaling pathway	141	0.006480008
	Maturity onset diabetes of the young	26	0.008135072
	Viral carcinogenesis	227	0.008794291
	MAPK signaling pathway	248	0.009874044
	Aldosterone synthesis and secretion	86	0.011103854
	Melanogenesis	99	0.015642679
	Insulin resistance	110	0.020112568
	TNF signaling pathway	110	0.020112568
	Sphingolipid signaling pathway	120	0.025214494
	AMPK signaling pathway	125	0.028002707
	PI3K-Akt signaling pathway	332	0.030852427
	Osteoclast differentiation	129	0.031556514
	FoxO signaling pathway	132	0.032170781
	NOD-like receptor signaling pathway	58	0.037137078
	Adrenergic signaling in cardiomyocytes	146	0.041422616
	Thyroid hormone synthesis	68	0.049493423

Table 3.4. Genes found in each maSigPro cluster. Genes present in each cluster are listed (gene symbol). Clusters 1-2 (Column A), clusters 3-5 (Column B), clusters 6-7 (Column C), and clusters 8-9 (Column D).

Column A: Clusters 1-2	Column B: Cluster 3-5	Column C: Clusters 6-7	Column D: Clusters 8-9
Cluster 1: 251 Genes	**Cluster 3: 245 Genes**	**Cluster 6: 140 Genes**	**Cluster 8: 239 Genes**
Gm26888	Pcsk2	Llgl2	Gm43423
Mir99ahg	Mtmr3	Gm11791	Gm6096
Nfkbie	Crebbp	Mup7	Tbl1x
Gm3336	Bivm	Olfr494	Sppl2b
Ttpal	Snn	Epha10	Epn1
Vamp1	Gm3755	Olfr645	Amacr
Amz1	Iws1	Ccdc85b	Azin1
Gm26615	Tmem173	Gm42594	Fos
RP23-158G17.1	Pde3b	Gm9899	Fbn2
Gm15545	Fermt3	Gm37350	C3ar1
Gm38042	Olfr133	Zfp771	Atf4
Fam53c	Synj2bp	C230029F24Rik	Notch3
Pde1b	Olfr1218	Actrt1	Itga9
5430405H02Rik	Epb41l2	Tcstv1	9330136K24Rik
6820402A03Rik	Bmp2k	Alox8	Kprp
Nufip2	Setd1b	Gm6420	Coch
Son	Cthrc1	Gm3448	Colec10
Mroh1	P2ry13	Gm27199	Pla2g6
Gm28192	Gm26868	Gm5891	Hyls1
Srgap2	Ap5z1	Gm10860	Lrit1
Fosl2	Nhlrc3	Gm16381	Cluap1
Srcap	Marcks	4930401G09Rik	BC030336
Pcdhga9	Pld1	Gm29081	Gcc2
Prkg1	Abca9	4930515L19Rik	Myo19
Gls	Itga6	Gm10803	Sep15
Maml3	Hist2h3c2	Gm26945	Gm37504
Cyb561	Gm7075	Gm37134	Ryr2
Gm38162	Adgrg1	Gm5269	Afg3l1
Fbxl18	Vav1	Zfp446	Mmgt1
Gm38318	Gm26661	Trpc3	Rhox2f
Gm38071	Phf23	A830018L16Rik	Selenbp2
Gm37205	Gm12111	Zfp451	Paqr9
4930442H23Rik	Fer	Gm12718	Eef1d
1700008B11Rik	Zfpm1	Alb	Gm37985
4933403L11Rik	Gm4673	Gm10710	Ints9

Taf4b	Zfp36l2	1700021L23Rik	Plin3
Wdr13	Psg18	Fam186a	Fut4
Ccdc97	Gm8898	Gm43181	Stk32c
Hnrnph1	Sema4c	Smr2	Ctse
Srsf7	Bank1	Ctgf	Padi2
Sfpq	Mlip	Gm35584	Gm26751
Runx1	Gm42443	Col27a1	Gabrp
Kalrn	Qk	Hrasls	Gm12869
Gm28496	Zbtb7a	Gm9894	Atp5g2
Elmo1	Mef2a	Gm2762	Htr6
C130089K02Rik	Hes1	Dpysl3	Pcdh19
Fam71a	Sema4b	Fam109b	Gm42882
Pde4c	Vmn1r40	Ctrc	Mcrs1
Gm37233	Serping1	Zmynd8	Gm15764
Eif4a1	Anapc11	Psmc3ip	Clnk
Gm12940	Maf	4930589P08Rik	Ankrd33b
Gm37084	Sh3bp5	1700029M20Rik	Zfp397
Zswim4	Grap	Zmynd11	Gm43721
9330160F10Rik	Msl3l2	Gm29187	Ube2d2b
Pirb	Kdm4b	Tulp4	RP24-83C9
Neat1	Gm10552	Mc5r	Olfr390
Stat3	9530026F06Rik	Gm15941	Adgrg3
Zfhx3	Soga1	Gm6133	2310034O05Rik
Mzf1	Lysmd1	Gm5538	Rxfp3
Hpn	1110004F10Rik	Scgb2a2	5530400C23Rik
Kdm6bos	9930111J21Rik2	Hrc	Slitrk6
Efna2	Olfr1395	Gm5797	Gm37355
Gm29488	Rere	1700028E10Rik	Prtg
Nfat5	Ggta1	Ncl	Sult6b1
Mir22hg	BC049352	Olfr638	Rbms1
2010310C07Rik	Olfr539	Sf3b1	Dpy30
Mir17hg	D5Ertd577e	Prdm1	Comp
Tmem184b	Tmem119	Slc36a1	Trpc2
Gpr4	Csf1r	Peg10	Mob3b
Smcr8	Rgs7bp	RP23-354F7	Gm37824
Gsk3a	Me3	Ankdd1b	Smok3b
Macf1	Khdrbs1	Serpina1e	Pank2
Dst	Wdr26	Gm6594	Desi1
Whrn	Olfr1418	Gm43108	Gm12569
Rnf34	Hltf	Kcnj1	Kifc3
Nrm	Gna15	Swt1	Pkhd1l1
Snx29	Rpe	Vmn1r25	Gpr182
Gdap10	Sall1	Gm13837	C2cd3
Snrpa	Dtx4	Gm14617	Ednrb
Chd4	Gm37746	Hnrnpf	Desi2
Rin3	Olfr870	Gm38079	RP24-314D22
Gm42941	Gm43449	Gm9922	Gm15655
Trim72	Pdia4	Gm13442	Gm15972

RP24-144C5.1	Gm38349	Hlf	Coa3
Spred3	Gm7982	Dopey2	Gm2381
1810013L24Rik	Dock10	Gml	Hap1
Btg1	P2ry12	RP24-434O21	Zbtb44
4933423P22Rik	Olfr450	Ang2	Skap1
Nfe2l3	Bckdha	Ing1	Farsb
Morn1	Hmgxb4	Cic	Gm21987
Adra2b	Myh9	Cep104	Psmc6
Rsrp1	Gm37848	Socs7	Cenpt
Fbrs	Il16	Gm43777	Csrp1
Trpm2	Entpd1	Gm43280	Npas3
Gm15708	Bin2	1700034E13Rik	Serpinb13
Slc35g3	A430010J10Rik	9330104G04Rik	Gm29671
Gm43484	Gm43507	Olfr585	Gm29162
Map3k12	Dsel	Ankef1	Catsper3
Gm26981	Kif21b	Nt5c3	Gm42418
Dand5	RP23-477L5	Hs3st2	Cdc42se2
Pdap1	Tbc1d31	Pamr1	5730488B01Rik
Hpca	Gm829	Tspan18	Abhd8
Tmem109	Fbxl19	BC048507	Srcin1
Nav2	Gm4980	Gm37595	Itga11
Gm10513	Ivns1abp	Fkrp	Dnajc9
Bptf	Slco2b1	Nmnat1	Trim68
RP23-434H14.7	Mtus1	RP24-313L21	Tapbp
Gm3739	Mxd1	Catip	Gm42803
Gm37376	Pacsin2	Gm15755	Exoc1
RP23-292B24.1	Sla	Gm38246	Lclat1
Gm15533	Gm10830	Anapc15-ps	Abcb10
Polg2	Sf3b2	Gm10662	Xk
5031425E22Rik	Ptafr	Tars2	Dynlt3
Wdr6	Tgfb1i1	Pou4f1	Gm37324
Gm37728	Crybb1	Olfr774	Endod1
Unc13a	Sox4	Gm15735	Gm13212
Gm11753	Snx4	Gm38337	Rsph3a
Gm43677	Eng	Olfr1220	Tjp3
Ucp2	Olfr1055	Tcp10a	Slitrk2
Gm38157	Pvrl2	Prkg2	Zfp521
Stat5a	Olfr1392	C1qtnf5	2700089I24Rik
Gm43029	Gm34866	Olfr373	Arhgap40
Chd7	Clta	Zcwpw1	Gm6787
Atp1b2	Arid3c	Pycr1	Catsperg2
Gadd45gip1	Taok1	Heg1	Scn11a
Gm37558	Cyth4	Gm10433	Ppapdc1b
Trpm5	Lyn	Nckap1	Slc35e4
Cyb5d1	Gm12603	Gm20917	Vmn2r58
Hdlbp	Abcb4	Ppbp	Scimp
Gm38292	Cxxc5	Sds	Cep41
Gm16861	Gm15884	Gm21292	Cd82

Nmrk2	Ppp1r10	Olfr1391	Nrcam
Gm37420	Accs	Vmn1r128	Snhg18
Csmd3	Sfmbt1	Mrps30	Rsph10b
Gm38055	Vmn2r110	Rprl1	C79798
Bcl6	Golm1	Zfhx4	Bri3bp
Gm17705	Gm11646	Mup1	Olfr119
Fus	Lrba	Ccdc77	Prl7a1
Pik3r2	4930511M18Rik	Palm3	4930568D16Rik
Rad23a	1700030C14Rik	Nrg4	Sox11
Tldc1	Dock8	**Cluster 7: 445 Genes**	Gm26917
Gm43813	Sgce	Ubqlnl	Wfdc6a
Gtf2ird2	Ckb	Ubap2l	Gm14444
Kcnq1ot1	Tnfrsf1b	Cxxc4	Tcp10b
Mthfs	Zfp296	Mrps9	Slc35d2
Tanc2	Tob2	Ddx3x	Tctex1d1
Hdac1	Tcl1	1700007G11Rik	Tat
Gm37859	Gm8973	Ddx3y	Chchd6
Srrm2	Usp24	Gm15788	Bfsp1
Gm37613	Mef2c	Cftr	Ndfip1
Rnf19b	Lifr	Gm37811	Mgst3
RP23-337M7.12	Tnfrsf21	Helq	Zfp213
Atcayos	Cdk2ap2	Sema3a	Slc37a1
Pygm	Bcl10	Tox	Nudt16
Opa3	Klc2	Lrif1	Gm26965
Sec24a	Ckm	Gm26624	Gm12426
Plekhg2	Gpr165	Got1	A930018P22Rik
Chchd2	Hist1h2br	Cdc73	Ccdc158
Slc5a3	Tal1	Smg6	RP23-480I16
Vasp	Ddx47	Gm43518	Ccdc186
RP24-259P13.3	Gm3164	Lrrc7	Gm2396
Fyb	Exoc3	Vmn2r36	Gpx3
Ikbke	Stx16	Gm20821	Acat1
Sag	Ppp1r12a	Mxra8	Maml1
Eva1b	Gnai2	Olfr872	4930517L18Rik
Gm28720	Zfp90	Gm21092	Dapl1
Gpr3	Cd151	Fam49b	Il11
Sh3d21	Hcls1	Gm29303	Vmn1r206
G630030J09Rik	Abl1	Tma7	Erich6
Atg16l1	Nckap1l	Arpp21	Dchs2
Naa38	Snx13	Tax1bp1	Pdzd4
A530013C23Rik	Pnp	Gm42441	Lelp1
4921531C22Rik	Kdm3b	Sh3d19	Wfdc8
Gm16586	Olfr382	Rtl1	Cyp2j9
Gm37285	Ago1	RP23-32A8	Gm16235
Gm26672	4930522H14Rik	Igsf10	Gm14664
Gm37342	Chd9	Gm43009	H3f3b
Bcl2l11	Slc7a8	Pcdhb8	Rps26-ps1

Zc3h18	Selplg	Osbpl6	Fhl3
RP23-89M16.5	0610010K14Rik	Nr2f2	AW551984
Malat1	Ppp1r9b	RP24-100O13	Gm10283
Egr1	Prex1	Map4k5	Gm43753
Lysmd4	Irf4	RP23-411N5	Arpc2
Gm43256	Cmtm6	Vmn1r132	Zdhhc8
P4htm	Exosc2	Apc	Mblac2
Eif5	Gm42871	Hirip3	Ostn
5430420F09Rik	1700074H08Rik	Skil	Fosb
Nlrp1b	Ecscr	Eif4e2	Slc18a3
Sirt1	Rhoa	Pcdh1	Tbx2
Zfp526	Ifngr1	Unc5c	RP23-201L15
Taf13	Dock4	Phxr4	Ice2
Gm43162	Gm19744	Phf14	RP24-276E19
BC024978	Prr12	Sfi1	B4galnt2
Pttg1	9130213A22Rik	Atr	Asah2
Reep2	Dync1i2	D630029K05Rik	Pgls
Hnrnpa2b1	Rgmb	Gm43049	Foxd1
Gm15853	Mtss1	Sat1	Hsd17b7
Jund	Gm17657	Rabgap1	Gpr25
Gm38346	Gm15589	Gm38197	4930513D17Rik
D430018E03Rik	Siglech	Gm37708	Gm37366
E230013L22Rik	4930590L20Rik	Gm12735	A830019P07Rik
Gm37472	Nek7	Zfp729a	Gm5617
Dedd2	Arid1a	Slc22a14	C2cd2
Tmem88	Fam83e	Olfr1275	Adamts20
Col23a1	Mylip	Gm37589	Gm15482
Gm16310	Defb15	Foxp2	Cptp
Dock2	Basp1	Safb2	Klhdc7a
Ptms	Gm5773	Olfr1016	B4galt7
Gm38056	Kat6a	Gm13165	Dnajc6
Rab3a	Megf6	Gm37620	Cst3
Aff4	Mertk	Gm10721	Pgm5
Ldlrad4	Rdx	Arid4a	Cdc14b
5330406M23Rik	Hpgd	Gm11168	3110082I17Rik
A230103J11Rik	Gm12434	Map1b	Pced1b
Fam210a	Kpnb1	mt-Nd4	Zdhhc1
Gabpb2	Gm37497	Vmn1r148	Ube2d3
Mknk2	Apobr	Cdk14	Gm28306
Lincpint	Cx3cr1	1700049G17Rik	Gm43611
4930403P22Rik	Gpr34	Sept7	Rfx1
Myo18b	Trim8	Rbm12b2	Gm16105
Phykpl	Hmox2	Ppan	Vmn1r157
RP23-8I8.3	Akirin2	Gm36957	Apobec1
Hnrnpa3	Arid3a	Zfp280d	Cdc23
Rbpjl	Tubgcp5	Cd86	Glod4
Shmt1	Cmya5	S100a3	Gm15742
Tssc4	Tmem44	1700016F12Rik	Meis3

Chka	Mtdh	Plb1	Gata3
Tgfb1	Fv1	Gm43194	Ngef
Cpne9	Cfh	Crebl2	Kcnd2
Gm37352	Krtap4-8	2610203C22Rik	Rap1gap2
Dleu2	Frmd4a	Gm26804	Tgfb3
RP23-4F16.11	0610031O16Rik	Olfr655	Col9a2
Gm13293	Col26a1	Dhx36	Gm38272
Gm11175	Ddx17	Il20	Prlhr
Nasp	Gm27184	Pate2	Hoxd1
Pcdhgb4	Wnk1	Top3b	Gm27029
1700008J07Rik	Cap1	Trim5	Gm16031
Ifitm10	Rtn4rl1	2900037B21Rik	Tiam2
Rab10os	Tagap	Gm26573	Gm13734
Apobec3	Tppp	Sox2ot	**Cluster 9: 155 Genes**
RP24-333B11.5	Prkcd	Ppfia1	Slc9a5
Gm5475	Plcl2	Phip	Gm28587
Agmo	Scoc	Thrap3	Slc25a41
Zfp36	Itgb5	Crtc2	Mos
Orai2	Smok3a	Syt2	Bmp10
4930562C15Rik	**Cluster 4: 125 Genes**	Gm12707	Gm37388
Gm37474	Dhx40	Lpar6	Tmem150a
Gm9929	Rela	Zmym5	Gm38125
Gm37755	Gm13411	Ccdc54	Gm11973
RP24-174G2.2	6430511E19Rik	Gm43101	RP24-430K15
Fam196b	Csta1	Fbxo11	Slc7a5
Cluster 2: 336 Genes	Casp4	Dnm3	Nr4a1
Rpl13	Ccl3	mt-Nd6	Rhox2c
Cpd	Prss50	Apbb1ip	Gm40190
Mpv17l2	Hmga1-rs1	Rdh19	Flg
Brix1	RP23-172P1	Mt4	Mbd6
Il1rn	Gm14023	Zc3h7a	Vps37b
Csf1	Pnliprp1	Cwf19l2	Gm10575
Phf11b	Gm37602	Gm42669	Nek5
Baiap2l2	H2-Ab1	RP23-473K6	Prrc2a
Fabp5	Il3ra	Krt33a	Gm28839
Scand1	Gm7676	4933407L21Rik	5330439B14Rik
Itm2c	Eif3g	Gm21738	Eif4ebp3
AI607873	Ccdc96	Gm10801	Leap2
Nsa2	Rcan1	Grip1os1	Gm37820
Bsg	Cd14	Olfr1176	Tbc1d24
Gm43323	Nrp2	Cyp2g1	Trmt12
Apoe	Gm3460	Gm4181	Qrfp
Xylt1	Gm43305	Fras1	Mapk9
Gng12	Lmna	Gnl2	RP23-385F8
Cndp2	Cd74	Gm16116	P2rx7
Pgam1	Nwd1	mt-Nd5	Gm37874
Ifitm3	Tubb6	Scn9a	RP23-435E16

Ifi202b	Gm13393	Plxna4os2	Pllp
Itgax	Trabd	Las1l	Gm37624
Chst2	Gm26671	Gm13412	Cdh23
Rtcb	Egr3	Sec62	H2afx
Gas2l3	Sowahc	Dnajc7	Hamp
Rpl37a	Olfr669	Tchp	Hspa8
C1qa	Gm14097	Ppm1l	Gm16897
Smim3	Gm43430	Olfr867	Tgm2
Taldo1	Dot1l	Tox2	Anks1
Rps17	C5ar1	Pigb	Gm28157
Snora26	Cep85	Gm20806	Mc1r
Axl	Kdm6b	Olfr1087	Gm11309
Prdx6	Slc44a1	Gm10718	Gm10392
Lgals3bp	Irg1	Agps	Cyp2d12
Hspa12a	Cxcl16	Zfp827	Rilp
Pianp	Gm14636	Scgb1b27	Sidt1
Sh3bgrl3	C5ar2	Gm13839	Slc43a1
Ctsd	Gm28706	Gm28079	Hist1h4h
Rps13	Slc22a5	Gm15319	Plk3
Slfn5	Myof	Thsd7b	Sh3tc2
Cacna1a	Gas7	Cdc42bpa	Tmigd1
Spp1	Cxcl2	1700122D07Rik	RP23-449F12
Gba	Map2k3	Wdr49	Gm28352
Clint1	Stau2	Gm26907	BC002189
Sik1	Slc15a3	Bod1l	Gyg
Cirh1a	Olfr293	Gm3867	Vldlr
Ankrd45	Hat1	Adam32	Gm37270
Npc2	Ipmk	Srrm1	Gm15729
Haao	Itga5	Dixdc1	Pcdhga6
AI504432	Vegfa	C230088H06Rik	Junb
Cpvl	Aim1	Smarce1	Hist1h4c
Rps5	Klf2	Gm42970	Jup
Naalad2	Slc24a5	Olfr1426	Col6a3
Plbd2	Trmt6	Eif4a2	Cdk18
C1qc	Gm5092	Flg	Gm29324
Rpl12	Ndel1	Pde1c	Slc3a1
Il1b	Egr2	Rbm6	Gm21900
Fkbp2	Lilr4b	Zfp644	Iah1
Rftn1	1810009J06Rik	Clk1	Gm14862
Os9	Fxyd1	Gm28633	2810407A14Rik
Gm11639	Gnaq	Vmn2r42	Kank3
Cotl1	Dcun1d4	Gm29154	Gm26904
Ch25h	Gm15420	Txndc11	D430040D24Rik
Lgi2	Figf	4933427J07Rik	Gm43201
Rps11	Aldoart2	Atrx	Tctex1d4
Rpl22	Muc2	Gm37382	Marcksl1
Gaa	Usp50	Ptpn13	Sh2b2
Tyrobp	Cd83	mt-Co3	Sybu

Atp1a1	Arpc1b	Gm10800	Olfr1262
AU020206	Pigo	4930431F12Rik	Gm42592
Abca7	Cypt4	Cd59b	Gm26918
Nme2	Mctp2	Vmn1r160	Gm43292
Tlr2	Cd44	Taf3	Ahdc1
Eif4b	Phlda1	Gm3298	Dscc1
Atp1a3	Tank	Vmn1r55	Gm37469
Capn1	Gm38091	Gm37752	Neu1
Stat1	Rgs1	Ppara	Zfp574
Ifit2	H2-Eb1	Arsk	Gm38374
Snrpb2	Rnase11	Tmem243	Plin4
Dkk2	Nfkbiz	Zfand5	Npw
Ctsb	Aimp1	Rptn	Rarb
Sema6b	Gm6377	Zfp286	Ptprcap
Enpp2	Ehd1	Gm10717	Mrpl41
Gtf3a	Plaur	Atf3	Arl4d
Rps8	H2-Aa	Gm42806	Gm42944
Gm37439	Cybb	Papola	Zfp703
Rpl10a	Maff	Tpm3	Gm17334
Rps18	Tmsb4x	Gm13667	Gm11754
Mael	Xdh	Olfr635	Hist1h3g
Pak4	C3	Zfp867	4930518I15Rik
B2m	Gm11635	Atxn3	6430503K07Rik
Slc39a4	Gm21984	Olfr50	Wdr86
Gm11563	Nfkb2	Olfr1205	RP23-455C13
Chst11	Gm6890	9530003O04Rik	Foxa3
Gm43792	Trib1	Gm26853	RP23-292C5
Nrp1	RP24-127M20	Olfr44	Plcb3
Rpl26	Cd209g	Asun	Gatc
Ptchd1	Tmem132a	Jmjd1c	Gm10305
Meikin	Diap1	Rad54l	Naip5
Wfdc17	Snrpf	Atg4a-ps	Ppp2r5b
Sec13	RP23-356N23	Spen	Creb3l4
Supt4a	4930555O08Rik	Gas5	Gm37033
Gm12227	Plekho2	Chd2	Gm7876
Fcgr4	Rel	mt-Nd4l	9530036M11Rik
Cd81	Gm38387	Olfr145	Gm20816
Anxa2	Ube2f	Gm3618	Fam196a
Calm3	Dennd4a	Gm7120	Tssk3
Ctsz	Relb	Olfr167	Itpkc
Dynlrb2	Ckap2l	Auts2	Hspa1a
Rap2b	Gm37653	Srsf6	Pcdhga8
Rpl37	Rhbdf2	Zfp9	Socs1
C1qb	Gm3512	Ptcd3	4833413G10Rik
Esyt1	Sorbs3	Vmn1r100	Lman1l
St14	Mrps6	4930523C07Rik	Gm42790
Gcnt2	RP23-222G6	Usp17ld	Hesx1
Cadm1	Slc24a1	2610305D13Rik	Dnajb5

9430069I07Rik	Il1a	Cbfa2t2	A230083G16Rik
Ly9	Srxn1	Sry	Lalba
Rai14	**Cluster 5: 220 Genes**	RP23-207N5	Irs2
Lpl	Gns	4933438K21Rik	Recql5
Rassf3	Naga	Gm14461	Gm9752
Arnt2	Pcsk9	Gm10722	Csf3r
Tram2	Spg11	Ccdc141	Tubb4b
Atp5f1	A730071L15Rik	Gm17535	Olfr272
H2-M3	Actr1a	Gm15155	Ushbp1
Oas1g	Abhd4	Gm12130	Nkx2-2
Sod2	Agap2	Plagl1	Tmprss4
Mpeg1	Mybph	Sgk3	Shisa2
2700060E02Rik	Elac2	Gm10696	Gm20268
Ldlr	Zbtb16	Hjurp	Gm14327
Gnb2l1	B4galnt1	Gm7942	Kcnh2
Ly6e	Ndst1	Fam133b	Fam184b
Numbl	Lrp5	Rnasel	Papln
Ifi27l2a	9430037G07Rik	1700044K03Rik	Ksr1
Rab7b	Cabin1	Speer4d	Ankrd10
Hcar2	B230206L02Rik	Gm15859	Olfr455
Trim30a	Tmem115	4632433K11Rik	Gssos1
Gnptg	Tm9sf2	Zeb2	Dnajc22
Ctss	Gna12	Gm26802	Ocstamp
Rpl9	Cpox	Gm37606	Dnajb1
Cd63	Mmp19	Srsf4	Gm26720
Slfn2	Usp25	Gm43856	Exd1
Mpp1	Gm37305	Hmgn2	
Dna2	Ddb1	Smndc1	
Oas1a	RP23-436D14	Fbxo9	
Eif3k	Taf5	Slc7a9	
Rpn2	Cand2	Dlgap1	
Abhd14a	M6pr	E430024P14Rik	
Prickle1	Gm15579	Gm37465	
Akr1a1	Rab29	Epha5	
Fmn1	Fastkd3	Adgrb3	
Rpl32	Mgrn1	Gm26739	
Cox6a1	Camkk1	Spock1	
Oasl2	Vmn2r48	Dpep2	
Ppib	Rpl27-ps3	Dnajb4	
Gm9843	2410016O06Rik	Man1a2	
Etl4	Ppfia4	Olfr642	
Rpl23	Parp12	Gm26995	
Rpl11	Olfr1255	Lrrn1	
Gpnmb	Mrpl52	Gm4141	
Efr3b	Impad1	Gm37145	
Aprt	Slc17a1	Myo5b	
Rpl23a	Sh3bp1	Gm37533	

Ubxn1	Gzma	Gm8024
Trak1	Lzts2	BC050972
Lilrb4a	Pdia5	9430053O09Rik
St8sia6	Cyc1	Glt8d2
Rxrg	Med29	Dtd2
Cox4i1	Pcx	A530083M17Rik
Npnt	Ccdc86	Hnrnpu
Sult2a1	Gm5814	Gal3st2
Myo1e	Sptbn2	Adam12
Hexa	Herpud2	Pou2f1
Cd68	Fam168b	Zfp407
Gm28967	Cntf	Lppr1
Psme1	Fcgr1	B430010I23Rik
Rpsa	Gm3002	Nos1
Rplp2	Wwtr1	4930435C17Rik
Pea15a	Caskin1	Tmie
Fau	Larp1	RP23-361A18
Lrp10	Dnmt3bos	St6galnac3
Aplp2	Foxd2	Hypk
Cst7	Hck	Duxf3
Chst1	Alox5ap	Olfr1289
Gm20625	Gm26852	Dcbld2
Serpine2	Snw1	1500004A13Rik
Gusb	0610025J13Rik	Olfr73
Rps26	Zfp954	Gm15584
Ankar	Serpinb9	Cep57l1
F10	Gm28901	Gm26788
Uba52	Pld4	Pqlc3
Rps24	Cs	Sox6
Gm10256	Tjp2	Gm27200
H2-Q7	Cars2	Ppp1r9a
Fam20c	Oas1c	Heatr6
Cox6c	Cd99l2	Gm14209
Pyhin1	Efhd2	Adgrl2
Crlf2	Ormdl2	Gm37091
Csf2ra	6530402F18Rik	Calm1
App	Ttbk1	Gm38000
Gch1	Ptpra	Gm37954
Timp2	Micall1	Ptprz1
Lamp1	Ano8	Gm15731
Tex12	Abcc4	Col4a3
Ddi2	Trim30d	Golga4
H2-T23	Psap	Gm36942
Stk39	Naprt	Gm43666
Cd69	Tuba1b	Cyyr1
Mocs1	Calb2	BC048546
Tagln2	Tgfbr2	Gm37026
Sardhos	Gm26652	Cd2ap

Rps14	Aars2	Tardbp
Rplp0	Irf9	Gm43152
Rpl36	Slit1	Vmn1r139
Zfp773	Rsad1	Snrnp70
Nceh1	Fbxw15	Crygn
Mfsd12	Gm37759	Pafah1b1
Egln3	Trpm4	Gm20559
Gm26771	B430306N03Rik	E130311K13Rik
Rpl18a	Dpysl2	Ffar2
Srebf2	Megf8	Lsamp
Rpl30	Acvr1b	Defb11
Helz2	Gm28778	Gm26686
Rpl36a	Pkd1	L3mbtl2
Kcnj2	Gm15092	Gm11657
4633401B06Rik	Mbtps1	Gm37724
Treml2	Dhx58	Nrxn2
C4b	Cd80	Gm27201
Atp6v1d	Gm11772	9030612E09Rik
Rpl14	Cxcl14	Zbtb1
Aqp12	Vegfb	Dcaf6
Lgals3	Galnt12	Map4
Eef1b2	Pfn1	Xrcc2
Rpl7a	Gm43474	Rbm25
Pkm	Gm9745	Gm3015
Ildr2	Gm29202	Zfhx2
Vps13c	Slc38a1	Cpb1
Ramp1	Atg4d	Arhgap39
Naca	Tbc1d22a	Gm20522
Rps15	Ldoc1l	Gm43568
Odf4	Psmb10	Speer4f2
Bhlhe40	Tssk6	Fcf1
Rpl28	Icosl	Adnp
Rps23	Gm29500	Muc6
Plekhh2	Map3k11	Olfr125
Pdcd1	Gm15290	Cttnbp2nl
H2-D1	Rnf17	Ap4e1
Tnfsf8	Txndc5	Olfr149
Rps25	Gga1	C130026I21Rik
Gm28201	Cdh24	Olfr147
Atp10a	Zfp938	Gm26870
Gm42757	Mlst8	Mrgprb5
Rps3a1	Gm37062	Gm4201
Bst2	Oaz1	Crb1
Eif3m	Rttn	Olfr118
Gm37706	Actb	Gm42900
Ap2a1	Gm20511	Nbea
Myo1f	Rnh1	Slco1a6
Vdac1	Gm37817	Gm29205

Igf1	Klhl42	Gm13270
Rpl7	Clptm1	Gtpbp10
Rps15a	Slc25a5	Gm37596
Aldoa	Ubl3	Gm4175
Colgalt1	Peli2	RP23-296J10
Inf2	Cetn2	Sprr2a2
AF529169	Dpp9	Luc7l2
Sc5d	Zfp775	AW822073
Cd9	Zc3h7b	4930452N14Rik
Ccl6	Etaa1	mt-Nd2
Prkcsh	Eef2	Ccnl1
Uqcrq	Gm29336	Gm12316
1700124L16Rik	3110021N24Rik	Gm43687
Rpl10-ps3	Lemd2	Map2
Ccdc154	Gm37815	Ccl25
C130060K24Rik	Pi4k2a	Gm9874
Gpi1	Pde2a	Gm21816
Fxyd5	Zfp28	CH25-241D1
Ctsl	Neurl1b	Gm15299
Lag3	Gm20688	Nr5a2
Pld3	Bcl2l14	Gm13236
Sdc3	Trappc10	Cse1l
Spag1	Atrnl1	Defb21
2900055J20Rik	Tprn	Syt1
Cd5	Arhgap33	Gm42751
Arhgap24	Znfx1	Sdcbp
Eef1a1	Hsd17b4	Gm6260
Cxcr4	Klk8	Enoph1
Gnas	Churc1	Ank3
Rpl18	Fam110a	RP23-142H1
Daam1	Sept5	Rbbp6
Mnda	Rpl13a	Rmnd1
Plekhh1	Daglb	RP23-365E22
Colec12	Aplp1	Cacna2d4
Ttr	Ndufa11	Tnfrsf13c
Trem2	St8sia1	Gm10719
Fabp3	Lrrc3	Fbxo36
Sh3rf1	Fam159b	Ccdc24
Ergic3	Ctdsp2	Ipo4
Rplp1	Itpr3	Pcf11
Dock6	Tep1	Tmem209
Gm10874	Gm12523	Rcsd1
Rpl29	Mrs2	Gm12089
Gm2a	Htatip2	Olfr1427
Hif1a	Irf2bp1	Ngf
Il23a	BC106179	Olfr527
Ndufa1	Supt16	Gm15736
Rpl19	H2-Oa	Wsb1

Actr3b	Prkaa2	Gm37934
Mamdc2	Neo1	Slit2
Rnf213	Trappc9	Pnisr
Rpl8	Hexb	1700074A21Rik
Rps7	Npl	Samd7
Ank	Gm12223	Krtap16-3
Bag1	Gm5901	Zfp691
Rps12	Ubxn8	Uvssa
Ddost	Tmem86a	Gm42611
Fth1	Tmem2	Cntn4
Serpine1	Kif1c	Spin2e
Cspg4	Gm20403	Sult3a1
Adamts1	Espl1	1200014J11Rik
Rpl34	Itgb2	Usp3
Naglu	Abcg1	Gm42439
Prdm4	Mmp15	mt-Cytb
Atp5h	Gm10644	Gm13383
Gars	Arhgef25	Gm37496
Man2b1	H2-Q1	RP23-178C20
Myo9b	Smim22	Olfr122
Rps19	Rhobtb2	Golga3
Sdf4	Bora	Olfr1143
Lyz2	Gm3289	Gm10323
Gm10398	Sall3	Snhg14
Lox	Nudt4	Gm6337
Cfhr1	Cept1	Tshz3
Rps2	Fuk	
Rps27a	Pacs1	
	Tex11	
	BC023829	
	9930111J21Rik1	
	Prss36	

Reference List

Abe T, Hosur KB, Hajishengallis E, Reis ES, Ricklin D, Lambris JD, Hajishengallis G (2012) Local complement-targeted intervention in periodontitis: proof-of-concept using a C5a receptor (CD88) antagonist. J Immunol 189:5442-5448.

Ager RR, Fonseca MI, Chu SH, Sanderson SD, Taylor SM, Woodruff TM, Tenner AJ (2010) Microglial C5aR (CD88) expression correlates with amyloid-beta deposition in murine models of Alzheimer's disease. J Neurochem 113:389-401.

Alexander JJ, Anderson AJ, Barnum SR, Stevens B, Tenner AJ (2008) The complement cascade: Yin-Yang in neuroinflammation--neuro-protection and -degeneration. J Neurochem 107:1169-1187.

Alzheimer's A (2016) 2016 Alzheimer's disease facts and figures. Alzheimers Dement 12:459-509.

Arumugam TV, Magnus T, Woodruff TM, Proctor LM, Shiels IA, Taylor SM (2006) Complement mediators in ischemia-reperfusion injury. Clinica Chimica Acta 374:33-45.

Aubry C, Corr SC, Wienerroither S, Goulard C, Jones R, Jamieson AM, Decker T, O'Neill LAJ, Dussurget O, Cossart P (2012) Both TLR2 and TRIF Contribute to Interferon-beta Production during Listeria Infection. Plos One 7.

Balderas I, Rodriguez-Ortiz CJ, Salgado-Tonda P, Chavez-Hurtado J, McGaugh JL, Bermudez-Rattoni F (2008) The consolidation of object and context recognition memory involve different regions of the temporal lobe. LearnMem 15:618-624.

Bamberger ME, Landreth GE (2002) Inflammation, apoptosis, and Alzheimer's disease. Neuroscientist 8:276-283.

Benoit ME, Tenner AJ (2011) Complement protein C1q-mediated neuroprotection is correlated with regulation of neuronal gene and microRNA expression. J Neurosci 31:3459-3469.

Benoit ME, Hernandez MX, Dinh ML, Benavente F, Vasquez O, Tenner AJ (2013) C1q-induced LRP1B and GPR6 Proteins Expressed Early in Alzheimer Disease Mouse Models, Are Essential for the C1q-mediated Protection against Amyloid-beta Neurotoxicity. J BiolChem 288:654-665.

Bensa JC, Reboul A, Colomb MG (1983) Biosynthesis in vitro of complement subcomponents C1q, C1s and C1 inhibitor by resting and stimulated human monocytes. The Biochemical journal 216:385-392.

Bodea LG, Wang Y, Linnartz-Gerlach B, Kopatz J, Sinkkonen L, Musgrove R, Kaoma T, Muller A, Vallar L, Di Monte DA, Balling R, Neumann H (2014) Neurodegeneration by activation of the microglial complement-phagosome pathway. JNeurosci 34:8546-8556.

Bradt BM, Kolb WP, Cooper NR (1998) Complement-dependent proinflammatory properties of the Alzheimer's disease beta-peptide. J Exp Med 188:431-438.

Brennan FH, Gordon R, Lao HW, Biggins PJ, Taylor SM, Franklin RJ, Woodruff TM, Ruitenberg MJ (2015) The Complement Receptor C5aR Controls Acute Inflammation and Astrogliosis following Spinal Cord Injury. J Neurosci 35:6517-6531.

Cain SA, Monk PN (2002) The orphan receptor C5L2 has high affinity binding sites for complement fragments C5a and C5a des-Arg(74). The Journal of Biological Chemistry 277:7165-7169.

Calame DG, Mueller-Ortiz SL, Morales JE, Wetsel RA (2014) The C5a anaphylatoxin receptor (C5aR1) protects against Listeria monocytogenes infection by inhibiting type 1 IFN expression. Journal of Immunology 193:5099-5107.

Cheng IH, Palop JJ, Esposito LA, Bien-Ly N, Yan F, Mucke L (2004) Aggressive amyloidosis in mice expressing human amyloid peptides with the Arctic mutation. NatMed 10:1190-1192.

Cheng IH, Scearce-Levie K, Legleiter J, Palop JJ, Gerstein H, Bien-Ly N, Puolivali J, Lesne S, Ashe KH, Muchowski PJ, Mucke L (2007) Accelerating amyloid-beta fibrillization reduces oligomer levels and functional deficits in Alzheimer disease mouse models. The Journal of Biological Chemistry 282:23818-23828.

Cipriani G, Dolciotti C, Picchi L, Bonuccelli U (2011) Alzheimer and his disease: a brief history. Neurol Sci 32:275-279.

Clark CM, Xie S, Chittams J, Ewbank D, Peskind E, Galasko D, Morris JC, McKeel DW, Jr., Farlow M, Weitlauf SL, Quinn J, Kaye J, Knopman D, Arai H, Doody RS, DeCarli C, Leight S, Lee VM, Trojanowski JQ (2003) Cerebrospinal fluid tau and beta-amyloid: how well do these biomarkers reflect autopsy-confirmed dementia diagnoses? Archives in Neurology 60:1696-1702.

Cole TA (2013) Complement activation in Alzheimer's disease: contribution of C5a and its receptor CD88 (Doctoral dissertation). University of California, Irvine. Retrieved from ProQuest Dissertations Publishing (Accession No. 3556682).

Colton CA (2009) Heterogeneity of microglial activation in the innate immune response in the brain. J NeuroimmunePharmacol 4:399-418.

Colton CA, Wilcock DM (2010) Assessing activation states in microglia. CNSNeurolDisordDrug Targets 9:174-191.

Costello DA, Lyons A, Denieffe S, Browne TC, Cox FF, Lynch MA (2011) Long term potentiation is impaired in membrane glycoprotein CD200-deficient mice: a role for Toll-like receptor activation. The Journal of Biological Chemistry 286:34722-34732.

Cotman CW, Anderson AJ (1995) A potential role for apoptosis in neurodegeneration and Alzheimer's disease. Mol Neurobiol 10:19-45.

Crehan H, Hardy J, Pocock J (2013) Blockage of CR1 prevents activation of rodent microglia. NeurobiolDis 54:139-149.

Cribbs DH, Berchtold NC, Perreau V, Coleman PD, Rogers J, Tenner AJ, Cotman CW (2012) Extensive innate immune gene activation accompanies brain aging, increasing vulnerability to cognitive decline and neurodegeneration: a microarray study. JNeuroinflammation 9:179.

Davoust N, Jones J, Stahel PF, Ames RS, Barnum SR (1999) Receptor for the C3a anaphylatoxin is expressed by neurons and glial cells. Glia 26:201-211.

De Santa F, Totaro MG, Prosperini E, Notarbartolo S, Testa G, Natoli G (2007) The histone H3 lysine-27 demethylase Jmjd3 links inflammation to inhibition of polycomb-mediated gene silencing. Cell 130:1083-1094.

Dobin A, Davis CA, Schlesinger F, Drenkow J, Zaleski C, Jha S, Batut P, Chaisson M, Gingeras TR (2013) STAR: ultrafast universal RNA-seq aligner. Bioinformatics 29:15-21.

Doens D, Fernandez PL (2014) Microglia receptors and their implications in the response to amyloid beta for Alzheimer's disease pathogenesis. J Neuroinflammation 11:48.

Eikelenboom P, van EE, Veerhuis R, Rozemuller AJ, van Gool WA, Hoozemans JJ (2012) Innate immunity and the etiology of late-onset Alzheimer's disease. NeurodegenerDis 10:271-273.
El Khoury J, Luster AD (2008) Mechanisms of microglia accumulation in Alzheimer's disease: therapeutic implications. Trends in Pharmacological Sciences 29:626-632.
El Khoury J, Toft M, Hickman SE, Means TK, Terada K, Geula C, Luster AD (2007) Ccr2 deficiency impairs microglial accumulation and accelerates progression of Alzheimer-like disease. Nat Med 13:432-438.
Farlow MR, Miller ML, Pejovic V (2008) Treatment options in Alzheimer's disease: maximizing benefit, managing expectations. Dement Geriatr Cogn Disord 25:408-422.
Fitzgerald KA, Rowe DC, Barnes BJ, Caffrey DR, Visintin A, Latz E, Monks B, Pitha PM, Golenbock DT (2003) LPS-TLR4 signaling to IRF-3/7 and NF-kappaB involves the toll adapters TRAM and TRIF. J Exp Med 198:1043-1055.
Fonseca MI, Zhou J, Botto M, Tenner AJ (2004) Absence of C1q leads to less neuropathology in transgenic mouse models of Alzheimer's disease. J Neurosci 24:6457-6465.
Fonseca MI, Head E, Velazquez P, Cotman CW, Tenner AJ (1999) The presence of isoaspartic acid in beta-amyloid plaques indicates plaque age. Exp Neurol 157:277-288.
Fonseca MI, Chu SH, Berci AM, Benoit ME, Peters DG, Kimura Y, Tenner AJ (2011) Contribution of complement activation pathways to neuropathology differs among mouse models of Alzheimer's disease. J Neuroinflammation 8:4.
Fonseca MI, Ager RR, Chu SH, Yazan O, Sanderson SD, LaFerla FM, Taylor SM, Woodruff TM, Tenner AJ (2009) Treatment with a C5aR antagonist decreases pathology and enhances behavioral performance in murine models of Alzheimer's disease. Journal of Immunology 183:1375-1383.
Fonseca MI, Chu S, Pierce AL, Brubaker WD, Hauhart RE, Mastroeni D, Clarke EV, Rogers J, Atkinson JP, Tenner AJ (2016) Analysis of the Putative Role of CR1 in Alzheimer's Disease: Genetic Association, Expression and Function. PLoSONE 11:e0149792.
Fraser DA, Pisalyaput K, Tenner AJ (2010) C1q enhances microglial clearance of apoptotic neurons and neuronal blebs, and modulates subsequent inflammatory cytokine production. J Neurochem 112:733-743.
Fraser DA, Laust AK, Nelson EL, Tenner AJ (2009) C1q differentially modulates phagocytosis and cytokine responses during ingestion of apoptotic cells by human monocytes, macrophages, and dendritic cells. J Immunol 183:6175-6185.
Garcia-Alcalde F, Garcia-Lopez F, Dopazo J, Conesa A (2011) Paintomics: a web based tool for the joint visualization of transcriptomics and metabolomics data. Bioinformatics 27:137-139.
Giannakopoulos P, Herrmann FR, Bussiere T, Bouras C, Kovari E, Perl DP, Morrison JH, Gold G, Hof PR (2003) Tangle and neuron numbers, but not amyloid load, predict cognitive status in Alzheimer's disease. Neurology 60:1495-1500.
Ginhoux F, Lim S, Hoeffel G, Low D, Huber T (2013) Origin and differentiation of microglia. Front Cell Neurosci 7:45.
Ginhoux F, Greter M, Leboeuf M, Nandi S, See P, Gokhan S, Mehler MF, Conway SJ, Ng LG, Stanley ER, Samokhvalov IM, Merad M (2010) Fate mapping analysis reveals that adult microglia derive from primitive macrophages. Science 330:841-845.

Giunta B, Fernandez F, Nikolic WV, Obregon D, Rrapo E, Town T, Tan J (2008) Inflammaging as a prodrome to Alzheimer's disease. J Neuroinflammation 5:51.
Guerreiro R et al. (2013) TREM2 variants in Alzheimer's disease. New England Journal of Medicine 368:117-127.
Guo RF, Ward PA (2006) C5a, a therapeutic target in sepsis. Recent Pat AntiinfectDrug Discov 1:57-65.
Haettig J, Stefanko DP, Multani ML, Figueroa DX, McQuown SC, Wood MA (2011) HDAC inhibition modulates hippocampus-dependent long-term memory for object location in a CBP-dependent manner. LearnMem 18:71-79.
Hardy J, Selkoe DJ (2002) The amyloid hypothesis of Alzheimer's disease: progress and problems on the road to therapeutics. Science 297:353-356.
Heneka MT et al. (2015) Neuroinflammation in Alzheimer's disease. Lancet Neurol 14:388-405.
Henn A, Lund S, Hedtjarn M, Schrattenholz A, Porzgen P, Leist M (2009) The suitability of BV2 cells as alternative model system for primary microglia cultures or for animal experiments examining brain inflammation. ALTEX 26:83-94.
Hernandez MX, Namiranian P, Nguyen E, Fonseca MI, Tenner AJ (2017) C5a increases the injury to primary neurons elicited by fibrillar amyloid beta. ASNeuro.
Hickman SE, Allison EK, El KJ (2008) Microglial dysfunction and defective beta-amyloid clearance pathways in aging Alzheimer's disease mice. JNeurosci 28:8354-8360.
Holland MC, Morikis D, Lambris JD (2004) Synthetic small-molecule complement inhibitors. CurrOpinInvestigDrugs 5:1164-1173.
Hollmann TJ, Mueller-Ortiz SL, Braun MC, Wetsel RA (2008) Disruption of the C5a receptor gene increases resistance to acute Gram-negative bacteremia and endotoxic shock: Opposing roles of C3a and C5a. Molecular Immunology 45:1907-1915.
Hong S, Beja-Glasser VF, Nfonoyim BM, Frouin A, Li S, Ramakrishnan S, Merry KM, Shi Q, Rosenthal A, Barres BA, Lemere CA, Selkoe DJ, Stevens B (2016) Complement and microglia mediate early synapse loss in Alzheimer mouse models. Science:712-716.
Horvath RJ, Nutile-McMenemy N, Alkaitis MS, Deleo JA (2008) Differential migration, LPS-induced cytokine, chemokine, and NO expression in immortalized BV-2 and HAPI cell lines and primary microglial cultures. J Neurochem 107:557-569.
Jacobson AC, Weis JH (2008) Comparative functional evolution of human and mouse CR1 and CR2. J Immunol 181:2953-2959.
Jana M, Palencia CA, Pahan K (2008) Fibrillar amyloid-beta peptides activate microglia via TLR2: implications for Alzheimer's disease. J Immunol 181:7254-7262.
Jay TR, Hirsch AM, Broihier ML, Miller CM, Neilson LE, Ransohoff RM, Lamb BT, Landreth GE (2016) Disease progression-dependent effects of TREM2 deficiency in a mouse model of Alzheimer's disease. J Neurosci.
Jay TR, Miller CM, Cheng PJ, Graham LC, Bemiller S, Broihier ML, Xu G, Margevicius D, Karlo JC, Sousa GL, Cotleur AC, Butovsky O, Bekris L, Staugaitis SM, Leverenz JB, Pimplikar SW, Landreth GE, Howell GR, Ransohoff RM, Lamb BT (2015) TREM2 deficiency eliminates TREM2+ inflammatory macrophages and ameliorates pathology in Alzheimer's disease mouse models. JExpMed 212:287-295.
Ji K, Akgul G, Wollmuth LP, Tsirka SE (2013) Microglia actively regulate the number of functional synapses. PLoS One 8:e56293.

Jiang H, Burdick D, Glabe CG, Cotman CW, Tenner AJ (1994) beta-Amyloid activates complement by binding to a specific region of the collagen-like domain of the C1q A chain. J Immunol 152:5050-5059.
Jin JJ, Kim HD, Maxwell JA, Li L, Fukuchi K (2008) Toll-like receptor 4-dependent upregulation of cytokines in a transgenic mouse model of Alzheimer's disease. J Neuroinflammation 5:23.
Jones L et al. (2010) Genetic evidence implicates the immune system and cholesterol metabolism in the aetiology of Alzheimer's disease. PLoS One 5:e13950.
Jonsson T et al. (2013) Variant of TREM2 associated with the risk of Alzheimer's disease. New England Journal of Medicine 368:107-116.
Jung S, Aliberti J, Graemmel P, Sunshine MJ, Kreutzberg GW, Sher A, Littman DR (2000) Analysis of fractalkine receptor CX(3)CR1 function by targeted deletion and green fluorescent protein reporter gene insertion. MolCell Biol 20:4106-4114.
Karch CM, Goate AM (2015) Alzheimer's disease risk genes and mechanisms of disease pathogenesis. Biological Psychiatry 77:43-51.
Kastl SP, Speidl WS, Kaun C, Rega G, Assadian A, Weiss TW, Valent P, Hagmueller GW, Maurer G, Huber K, Wojta J (2006) The complement component C5a induces the expression of plasminogen activator inhibitor-1 in human macrophages via NF-kappaB activation. J Thromb Haemost 4:1790-1797.
Kawai T, Akira S (2007) Signaling to NF-kappaB by Toll-like receptors. Trends Mol Med 13:460-469.
Kettenmann H, Hanisch UK, Noda M, Verkhratsky A (2011) Physiology of microglia. Physiol Rev 91:461-553.
Kohl J (2006) Drug evaluation: the C5a receptor antagonist PMX-53. CurrOpinMolTher 8:529-538.
Konteatis ZD, Siciliano SJ, Van RG, Molineaux CJ, Pandya S, Fischer P, Rosen H, Mumford RA, Springer MS (1994) Development of C5a receptor antagonists. Differential loss of functional responses. Journal of Immunology 153:4200-4205.
Krabbe G, Halle A, Matyash V, Rinnenthal JL, Eom GD, Bernhardt U, Miller KR, Prokop S, Kettenmann H, Heppner FL (2013) Functional Impairment of Microglia Coincides with Beta-Amyloid Deposition in Mice with Alzheimer-Like Pathology. PLoS ONE 8.
Lambert JC et al. (2009) Genome-wide association study identifies variants at CLU and CR1 associated with Alzheimer's disease. Nat Genet 41:1094-1099.
Landlinger C, Oberleitner L, Gruber P, Noiges B, Yatsyk K, Santic R, Mandler M, Staffler G (2015) Active immunization against complement factor C5a: a new therapeutic approach for Alzheimer's disease. J Neuroinflammation 12:150.
Lee S, Varvel NH, Konerth ME, Xu G, Cardona AE, Ransohoff RM, Lamb BT (2010) CX3CR1 deficiency alters microglial activation and reduces beta-amyloid deposition in two Alzheimer's disease mouse models. AmJ Pathol 177:2549-2562.
Leroy K, Ando K, Laporte V, Dedecker R, Suain V, Authelet M, Heraud C, Pierrot N, Yilmaz Z, Octave JN, Brion JP (2012) Lack of tau proteins rescues neuronal cell death and decreases amyloidogenic processing of APP in APP/PS1 mice. Am J Pathol 181:1928-1940.
Li B, Dewey CN (2011) RSEM: accurate transcript quantification from RNA-Seq data with or without a reference genome. BMC Bioinformatics 12:323.

Li M, Pisalyaput K, Galvan M, Tenner AJ (2004) Macrophage colony stimulatory factor and interferon-gamma trigger distinct mechanisms for augmentation of beta-amyloid-induced microglia-mediated neurotoxicity. J Neurochem 91:623-633.
Liddelow SA et al. (2017) Neurotoxic reactive astrocytes are induced by activated microglia. Nature.
Liu S, Liu Y, Hao W, Wolf L, Kiliaan AJ, Penke B, Rube CE, Walter J, Heneka MT, Hartmann T, Menger MD, Fassbender K (2012) TLR2 is a primary receptor for Alzheimer's amyloid beta peptide to trigger neuroinflammatory activation. Journal of Immunology 188:1098-1107.
Liu Z, Condello C, Schain A, Harb R, Grutzendler J (2010) CX3CR1 in microglia regulates brain amyloid deposition through selective protofibrillar amyloid-beta phagocytosis. JNeurosci 30:17091-17101.
Lucin KM, Wyss-Coray T (2009) Immune activation in brain aging and neurodegeneration: too much or too little? Neuron 64:110-122.
Lui H et al. (2016) Progranulin Deficiency Promotes Circuit-Specific Synaptic Pruning by Microglia via Complement Activation. Cell 165:921-935.
Lynch MA, Mills KH (2012) Immunology meets neuroscience--opportunities for immune intervention in neurodegenerative diseases. Brain BehavImmun 26:1-10.
Maddalena A, Papassotiropoulos A, Muller-Tillmanns B, Jung HH, Hegi T, Nitsch RM, Hock C (2003) Biochemical diagnosis of Alzheimer disease by measuring the cerebrospinal fluid ratio of phosphorylated tau protein to beta-amyloid peptide42. Archives in Neurology 60:1202-1206.
Matcovitch-Natan O et al. (2016) Microglia development follows a stepwise program to regulate brain homeostasis. Science 353:aad8670.
Matsuoka Y, Picciano M, Malester B, LaFrancois J, Zehr C, Daeschner JM, Olschowka JA, Fonseca MI, O'Banion MK, Tenner AJ, Lemere CA, Duff K (2001) Inflammatory responses to amyloidosis in a transgenic mouse model of Alzheimer's disease. AmJ Pathol 158:1345-1354.
Mawuenyega KG, Sigurdson W, Ovod V, Munsell L, Kasten T, Morris JC, Yarasheski KE, Bateman RJ (2010) Decreased clearance of CNS beta-amyloid in Alzheimer's disease. Science 330:1774.
Meraz-Rios MA, Toral-Rios D, Franco-Bocanegra D, Villeda-Hernandez J, Campos-Pena V (2013) Inflammatory process in Alzheimer's Disease. Front IntegrNeurosci 7:59.
Meyer-Luehmann M, Spires-Jones TL, Prada C, Garcia-Alloza M, de CA, Rozkalne A, Koenigsknecht-Talboo J, Holtzman DM, Bacskai BJ, Hyman BT (2008) Rapid appearance and local toxicity of amyloid-beta plaques in a mouse model of Alzheimer's disease. Nature 451:720-724.
Miller AM, Stella N (2008) Microglial cell migration stimulated by ATP and C5a involve distinct molecular mechanisms: Quantification of migration by a novel near-infrared method. Glia.
Mizutani M, Pino PA, Saederup N, Charo IF, Ransohoff RM, Cardona AE (2012) The fractalkine receptor but not CCR2 is present on microglia from embryonic development throughout adulthood. Journal of Immunology 188:29-36.
Molina H, Kinoshita T, Inoue K, Carel JC, Holers VM (1990) A molecular and immunochemical characterization of mouse CR2. Evidence for a single gene model of mouse complement receptors 1 and 2. Journal of Immunology 145:2974-2983.

Monk PN, Scola AM, Madala P, Fairlie DP (2007) Function, structure and therapeutic potential of complement C5a receptors. British Journal of Pharmacology 152:429-448.
Morley BJ, Walport M (2000) The complement factsbook. San Diego, CA: Academic Press.
Mosher KI, Wyss-Coray T (2014) Microglial dysfunction in brain aging and Alzheimer's disease. Biochemical Pharmacology 88:594-604.
Mumby DG, Gaskin S, Glenn MJ, Schramek TE, Lehmann H (2002) Hippocampal damage and exploratory preferences in rats: memory for objects, places, and contexts. LearnMem 9:49-57.
Murphy K, Weaver C (2016) Janeway's immunobiology, 9th edition. Edition. New York, NY: Garland Science/Taylor & Francis Group, LLC.
Murray PJ et al. (2014) Macrophage activation and polarization: nomenclature and experimental guidelines. Immunity 41:14-20.
Nayak D, Zinselmeyer BH, Corps KN, McGavern DB (2012) In vivo dynamics of innate immune sentinels in the CNS. Intravital 1:95-106.
Nilsberth C, Westlind-Danielsson A, Eckman CB, Condron MM, Axelman K, Forsell C, Stenh C, Luthman J, Teplow DB, Younkin SG, Naslund J, Lannfelt L (2001) The 'Arctic' APP mutation (E693G) causes Alzheimer's disease by enhanced Abeta protofibril formation. NatNeurosci 4:887-893.
Njie EG, Boelen E, Stassen FR, Steinbusch HW, Borchelt DR, Streit WJ (2012) Ex vivo cultures of microglia from young and aged rodent brain reveal age-related changes in microglial function. NeurobiolAging 33:195-112.
Nueda MJ, Tarazona S, Conesa A (2014) Next maSigPro: updating maSigPro bioconductor package for RNA-seq time series. Bioinformatics 30:2598-2602.
O'Barr SA, Caguioa J, Gruol D, Perkins G, Ember JA, Hugli T, Cooper NR (2001) Neuronal expression of a functional receptor for the C5a complement activation fragment. J Immunol 166:4154-4162.
Oddo S, Caccamo A, Shepherd JD, Murphy MP, Golde TE, Kayed R, Metherate R, Mattson MP, Akbari Y, LaFerla FM (2003) Triple-transgenic model of Alzheimer's disease with plaques and tangles: intracellular Abeta and synaptic dysfunction. Neuron 39:409-421.
Okinaga S, Slattery D, Humbles A, Zsengeller Z, Morteau O, Kinrade MB, Brodbeck RM, Krause JE, Choe HR, Gerard NP, Gerard C (2003) C5L2, a nonsignaling C5A binding protein. Biochemistry 42:9406-9415.
Ong WY, Tanaka K, Dawe GS, Ittner LM, Farooqui AA (2013) Slow excitotoxicity in Alzheimer's disease. JAlzheimersDis 35:643-668.
Pan ZK (1998) Anaphylatoxins C5a and C3a induce nuclear factor kappaB activation in human peripheral blood monocytes. Biochim Biophys Acta 1443:90-98.
Parkhurst CN, Yang G, Ninan I, Savas JN, Yates JR, III, Lafaille JJ, Hempstead BL, Littman DR, Gan WB (2013) Microglia promote learning-dependent synapse formation through brain-derived neurotrophic factor. Cell 155:1596-1609.
Pavlovski D, Thundyil J, Monk PN, Wetsel RA, Taylor SM, Woodruff TM (2012) Generation of complement component C5a by ischemic neurons promotes neuronal apoptosis. FASEB J 26:3680-3690.
Persson T, Popescu BO, Cedazo-Minguez A (2014) Oxidative stress in Alzheimer's disease: why did antioxidant therapy fail? OxidMedCell Longev 2014:427318.

Pisalyaput K, Tenner AJ (2008) Complement component C1q inhibits beta-amyloid- and serum amyloid P-induced neurotoxicity via caspase- and calpain-independent mechanisms. JNeurochem 104:696-707.
Przanowski P, Dabrowski M, Ellert-Miklaszewska A, Kloss M, Mieczkowski J, Kaza B, Ronowicz A, Hu F, Piotrowski A, Kettenmann H, Komorowski J, Kaminska B (2014) The signal transducers Stat1 and Stat3 and their novel target Jmjd3 drive the expression of inflammatory genes in microglia. Journal of Molecular Medicine 92:239-254.
Ramadass M, Ghebrehiwet B, Kew RR (2015) Enhanced recognition of plasma proteins in a non-native state by complement C3b. A possible clearance mechanism for damaged proteins in blood. Mol Immunol 64:55-62.
Ramadori G, Rasokat H, Burger R, Meyer Zum Buschenfelde KH, Bitter-Suermann D (1984) Quantitative determination of complement components produced by purified hepatocytes. Clin Exp Immunol 55:189-196.
Ransohoff RM, El Khoury J (2015) Microglia in Health and Disease. Cold Spring Harb Perspect Biol 8:a020560.
Ricklin D, Lambris JD (2013) Complement in immune and inflammatory disorders: pathophysiological mechanisms. J Immunol 190:3831-3838.
Ricklin D, Hajishengallis G, Yang K, Lambris JD (2010) Complement: a key system for immune surveillance and homeostasis. Nat Immunol 11:785-797.
Ridge PG, Hoyt KB, Boehme K, Mukherjee S, Crane PK, Haines JL, Mayeux R, Farrer LA, Pericak-Vance MA, Schellenberg GD, Kauwe JS, Alzheimer's Disease Genetics C (2016) Assessment of the genetic variance of late-onset Alzheimer's disease. Neurobiol Aging 41:200 e213-220.
Rogers J, Li R, Mastroeni D, Grover A, Leonard B, Ahern G, Cao P, Kolody H, Vedders L, Kolb WP, Sabbagh M (2006) Peripheral clearance of amyloid beta peptide by complement C3-dependent adherence to erythrocytes. NeurobiolAging 27:1733-1739.
Rovelet-Lecrux A, Hannequin D, Raux G, Le Meur N, Laquerriere A, Vital A, Dumanchin C, Feuillette S, Brice A, Vercelletto M, Dubas F, Frebourg T, Campion D (2006) APP locus duplication causes autosomal dominant early-onset Alzheimer disease with cerebral amyloid angiopathy. Nat Genet 38:24-26.
Saederup N, Cardona AE, Croft K, Mizutani M, Cotleur AC, Tsou CL, Ransohoff RM, Charo IF (2010) Selective chemokine receptor usage by central nervous system myeloid cells in CCR2-red fluorescent protein knock-in mice. PLoSONE 5:e13693.
Sahin F, Ozkan MC, Mete NG, Yilmaz M, Oruc N, Gurgun A, Kayikcioglu M, Guler A, Gokcay F, Bilgir F, Ceylan C, Bilgir O, Sari IH, Saydam G (2015) Multidisciplinary clinical management of paroxysmal nocturnal hemoglobinuria. AmJBlood Res 5:1-9.
Saido T, Leissring MA (2012) Proteolytic degradation of amyloid beta-protein. Cold Spring Harb Perspect Med 2:a006379.
Sarma JV, Ward PA (2012) New developments in C5a receptor signaling. Cell Health Cytoskelet 4:73-82.
Saunders AM, Strittmatter WJ, Schmechel D, George-Hyslop PH, Pericak-Vance MA, Joo SH, Rosi BL, Gusella JF, Crapper-MacLachlan DR, Alberts MJ, et al. (1993) Association of apolipoprotein E allele epsilon 4 with late-onset familial and sporadic Alzheimer's disease. Neurology 43:1467-1472.

Scahill RI, Schott JM, Stevens JM, Rossor MN, Fox NC (2002) Mapping the evolution of regional atrophy in Alzheimer's disease: Unbiased analysis of fluid-registered serial MRI. Proceedings of the National Academy of Sciences of the United States of America 99:4703-4707.
Schafer DP, Lehrman EK, Kautzman AG, Koyama R, Mardinly AR, Yamasaki R, Ransohoff RM, Greenberg ME, Barres BA, Stevens B (2012) Microglia sculpt postnatal neural circuits in an activity and complement-dependent manner. Neuron 74:691-705.
Scheuner D et al. (1996) Secreted amyloid beta-protein similar to that in the senile plaques of Alzheimer's disease is increased in vivo by the presenilin 1 and 2 and APP mutations linked to familial Alzheimer's disease. Nat Med 2:864-870.
Scola AM, Johswich KO, Morgan BP, Klos A, Monk PN (2009) The human complement fragment receptor, C5L2, is a recycling decoy receptor. MolImmunol 46:1149-1162.
Sekar A, Bialas AR, de RH, Davis A, Hammond TR, Kamitaki N, Tooley K, Presumey J, Baum M, Van DV, Genovese G, Rose SA, Handsaker RE, Daly MJ, Carroll MC, Stevens B, McCarroll SA (2016) Schizophrenia risk from complex variation of complement component 4. Nature.
Selkoe DJ, Hardy J (2016) The amyloid hypothesis of Alzheimer's disease at 25 years. EMBO MolMed.
Sewell DL, Nacewicz B, Liu F, Macvilay S, Erdei A, Lambris JD, Sandor M, Fabry Z (2004) Complement C3 and C5 play critical roles in traumatic brain cryoinjury: blocking effects on neutrophil extravasation by C5a receptor antagonist. J Neuroimmunol 155:55-63.
Shalova IN, Kajiji T, Lim JY, Gomez-Pina V, Fernandez-Ruiz I, Arnalich F, Iau PT, Lopez-Collazo E, Wong SC, Biswas SK (2012) CD16 regulates TRIF-dependent TLR4 response in human monocytes and their subsets. Journal of Immunology 188:3584-3593.
Shi Q, Colodner KJ, Matousek SB, Merry K, Hong S, Kenison JE, Frost JL, Le KX, Li S, Dodart JC, Caldarone BJ, Stevens B, Lemere CA (2015) Complement C3-Deficient Mice Fail to Display Age-Related Hippocampal Decline. JNeurosci 35:13029-13042.
Shrivastava K, Gonzalez P, Acarin L (2012) The immune inhibitory complex CD200/CD200R is developmentally regulated in the mouse brain. J Comp Neurol 520:2657-2675.
Singhrao S, Neal JW, Morgan BP, Gasque P (1999) Increased complement biosynthesis by microglia and complement activation on neurons in Huntington's Disease. ExpNeurol 159:362-376.
Song WC (2012) Crosstalk between complement and toll-like receptors. ToxicolPathol 40:174-182.
Stefanko DP, Barrett RM, Ly AR, Reolon GK, Wood MA (2009) Modulation of long-term memory for object recognition via HDAC inhibition. ProcNatlAcadSciUSA 106:9447-9452.
Stephan AH, Madison DV, Mateos JM, Fraser DA, Lovelett EA, Coutellier L, Kim L, Tsai HH, Huang EJ, Rowitch DH, Berns DS, Tenner AJ, Shamloo M, Barres BA (2013) A Dramatic Increase of C1q Protein in the CNS during Normal Aging. J Neurosci 33:13460-13474.
Stevens B, Allen NJ, Vazquez LE, Howell GR, Christopherson KS, Nouri N, Micheva KD, Mehalow AK, Huberman AD, Stafford B, Sher A, Litke AM, Lambris JD, Smith SJ, John

SW, Barres BA (2007) The classical complement cascade mediates CNS synapse elimination. Cell 131:1164-1178.
Stewart CR, Stuart LM, Wilkinson K, van Gils JM, Deng J, Halle A, Rayner KJ, Boyer L, Zhong R, Frazier WA, Lacy-Hulbert A, El Khoury J, Golenbock DT, Moore KJ (2010) CD36 ligands promote sterile inflammation through assembly of a Toll-like receptor 4 and 6 heterodimer. Nat Immunol 11:155-161.
Stoka V, Turk V, Turk B (2016) Lysosomal cathepsins and their regulation in aging and neurodegeneration. Ageing Res Rev 32:22-37.
Su JH, Anderson AJ, Cummings BJ, Cotman CW (1994) Immunohistochemical evidence for apoptosis in Alzheimer's disease. NeuroReport 5:2529-2533.
Tahara K, Kim HD, Jin JJ, Maxwell JA, Li L, Fukuchi K (2006) Role of toll-like receptor signalling in Abeta uptake and clearance. Brain 129:3006-3019.
Tan J, Town T, Mori T, Wu Y, Saxe M, Crawford F, Mullan M (2000) CD45 opposes beta-amyloid peptide-induced microglial activation via inhibition of p44/42 mitogen-activated protein kinase. JNeurosci 20:7587-7594.
Tenner AJ, Pisalyaput K (2008) The Complement System in the CNS: Thinking again. In: C entral Nervous System Diseases and Inflammation (Lane TE, Carson MJ, Bergmann C, Wyss-Coray T, eds), pp 153-174. New York: Springer.
Tian L, Rauvala H, Gahmberg CG (2009) Neuronal regulation of immune responses in the central nervous system. Trends Immunol 30:91-99.
Toledo JB, Weiner MW, Wolk DA, Da X, Chen K, Arnold SE, Jagust W, Jack C, Reiman EM, Davatzikos C, Shaw LM, Trojanowski JQ (2014) Neuronal injury biomarkers and prognosis in ADNI subjects with normal cognition. Acta NeuropatholCommun 2:26.
Tripathi S et al. (2015) Meta- and Orthogonal Integration of Influenza "OMICs" Data Defines a Role for UBR4 in Virus Budding. Cell Host Microbe 18:723-735.
Udan ML, Ajit D, Crouse NR, Nichols MR (2008) Toll-like receptors 2 and 4 mediate Abeta(1-42) activation of the innate immune response in a human monocytic cell line. J Neurochem 104:524-533.
Vasek MJ et al. (2016) A complement-microglial axis drives synapse loss during virus-induced memory impairment. Nature 534:538-543.
Veerhuis R, Nielsen HM, Tenner AJ (2011) Complement in the brain. Mol Immunol 48:1592-1603.
Vergunst CE, Gerlag DM, Dinant H, Schulz L, Vinkenoog M, Smeets TJ, Sanders ME, Reedquist KA, Tak PP (2007) Blocking the receptor for C5a in patients with rheumatoid arthritis does not reduce synovial inflammation. Rheumatology(Oxford) 46:1773-1778.
Verkhusha VV, Kuznetsova IM, Stepanenko OV, Zaraisky AG, Shavlovsky MM, Turoverov KK, Uversky VN (2003) High stability of Discosoma DsRed as compared to Aequorea EGFP. Biochemistry 42:7879-7884.
Walker DG, Dalsing-Hernandez JE, Campbell NA, Lue LF (2009) Decreased expression of CD200 and CD200 receptor in Alzheimer's disease: a potential mechanism leading to chronic inflammation. ExpNeurol 215:5-19.
Wang Y, Cella M, Mallinson K, Ulrich JD, Young KL, Robinette ML, Gilfillan S, Krishnan GM, Sudhakar S, Zinselmeyer BH, Holtzman DM, Cirrito JR, Colonna M (2015) TREM2 lipid sensing sustains the microglial response in an Alzheimer's disease model. Cell 160:1061-1071.

Wang Y, Ulland TK, Ulrich JD, Song W, Tzaferis JA, Hole JT, Yuan P, Mahan TE, Shi Y, Gilfillan S, Cella M, Grutzendler J, DeMattos RB, Cirrito JR, Holtzman DM, Colonna M (2016) TREM2-mediated early microglial response limits diffusion and toxicity of amyloid plaques. J Exp Med 213:667-675.

Webster SD, Galvan MD, Ferran E, Garzon-Rodriguez W, Glabe CG, Tenner AJ (2001) Antibody-mediated phagocytosis of the amyloid beta-peptide in microglia is differentially modulated by C1q. Journal of Immunology 166:7496-7503.

Woodruff TM, Nandakumar KS, Tedesco F (2011) Inhibiting the C5-C5a receptor axis. Mol Immunol 48:1631-1642.

Woodruff TM, Ager RR, Tenner AJ, Noakes PG, Taylor SM (2010) The role of the complement system and the activation fragment C5a in the central nervous system. NeuromolecularMed 12:179-192.

Woodruff TM, Costantini KJ, Crane JW, Atkin JD, Monk PN, Taylor SM, Noakes PG (2008) The complement factor C5a contributes to pathology in a rat model of amyotrophic lateral sclerosis. J Immunol 181:8727-8734.

Woodruff TM, Crane JW, Proctor LM, Buller KM, Shek AB, de VK, Pollitt S, Williams HM, Shiels IA, Monk PN, Taylor SM (2006) Therapeutic activity of C5a receptor antagonists in a rat model of neurodegeneration. FASEB J 20:1407-1417.

Wyss-Coray T (2006) Inflammation in Alzheimer disease: driving force, bystander or beneficial response? NatMed 12:1005-1015.

Wyss-Coray T, Rogers J (2012) Inflammation in Alzheimer disease-a brief review of the basic science and clinical literature. Cold Spring HarbPerspectMed 2:a006346.

Yao J, Harvath L, Gilbert DL, Colton CA (1990) Chemotaxis by a CNS macrophage, the microglia. JNeurosciRes 27:36-42.

Zhang B et al. (2013) Integrated Systems Approach Identifies Genetic Nodes and Networks in Late-Onset Alzheimer's Disease. Cell 153:707-720.

Zhang X, Kimura Y, Fang C, Zhou L, Sfyroera G, Lambris JD, Wetsel RA, Miwa T, Song WC (2007) Regulation of Toll-like receptor-mediated inflammatory response by complement in vivo. Blood 110:228-236.

CHAPTER 4

Comparing Surface Expression of Proteins on Microglia *in vitro* vs *in vivo* and Microglial Changes in AD

Abstract

Alzheimer's disease (AD) is characterized by the presence of plaques containing aggregated β-amyloid (Aβ), neurofibrillary tangles (NTF) formed by hyperphosphorylated tau, and a loss of neurons resulting in brain atrophy and cognitive loss. Genome-wide association studies (GWAS) have identified variants of CR1 and TREM2 associated with increased risk for AD. Given the anti-inflammatory role of TREM2, the associated increased risk for AD may be attributed to loss of regulation of inflammation in the brain and/or a decrease in phagocytic potential by microglia. Here, we assessed the expression of TREM2 and CR1 as well as CD200R (another receptor with antiinflammatory properties) by flow cytometry on microglia isolated from aged 3xTg mice and age-matched controls. Microglia isolated from 3xTg mice had greater expression of TREM2 compared to controls. Although primary neonatal microglia expressed both CD200R and CR1, microglia isolated from adult mice (both 3xTg and controls) showed no expression of these two surface proteins. Consistent with what has been reported, CD45 was significantly increased in the 3xTg mice compared to controls. To further explore the molecular signature of microglia in AD mouse models, we studied the gene expression changes in yet another mouse model of AD with or without proinflammatory C5aR1. This model was chosen as we have previously demonstrated

that treatment with a C5a receptor antagonist, PMX205, rescued the behavior performance in a mouse model of AD and significantly reduced the amyloid plaque load and reactive glia found surrounding Aβ plaques in two murine models. Gene expression studies identified 25 differentially expressed genes from brains of Arctic compared to Arctic C5aR1KO mice. The genes point to a decrease of interferon-related genes in the Arctic C5aR1KO, with Stat1 being a prominent transcription factor found to be decreased with the loss of C5aR1. Chemokine signaling genes are also found to be differentially expressed, with Ccl5 and Ccl9 decreased and Ccl8 increased in the C5aR1-deficient brains in the AD model. Absence of differentially expressed neuron-related genes in the neurodegenerative panel suggest microglia are primarily altered in the Arctic C5aR1KO. Thus, studying microglial gene expression in AD models may elucidate the mechanism by which C5aR1 blockade improves cognitive deficits in the Arctic model.

Introduction

The immune response in the CNS is largely mediated through innate immune cells such as microglia, resident macrophages, and dendritic cells. While resident populations of macrophages and dendritic cells exist in the perivascular space, meninges and choroid plexus (Nayak et al., 2012), microglia are the dominant innate immune cell found in the brain parenchyma under normal conditions, where they play a role in immune surveillance and support tissue maintenance (Kettenmann et al., 2011). Unlike the specialized resident macrophages of the meninges, perivascular space, and choroid plexus, microglia derive from precursor cells from the embryonic yolk sac that populate the CNS early during development (Ginhoux et al., 2010). During development and during learning, microglia play a role in synaptic pruning and facilitate the protection and remodeling of synapses (Ji et al., 2013; Parkhurst et al., 2013).

Microglia activation results in a wide range of phenotypes. In the periphery, macrophage activation leads to what has been described as classic, proinflammatory phenotype (M1) or non-inflammatory phenotype (M2). M1 macrophages secrete proinflammatory cytokines such as IL-1, IL-6, and TNF-alpha, potent inducers of inflammation. Unlike the single proinflammatory phenotype, macrophages with anti-inflammatory capabilities have been categorized in three different states; M2a, M2b, and M2c, with M2b having both pro and anti-inflammatory functions (reviewed in (Colton and Wilcock, 2010)). These M1 and M2 activation states represent extreme phenotypes of macrophages that can be induced with specific cytokines. Although useful to study *in vitro* functional outcomes, this categorization is oversimplified and a growing body of literature suggests macrophages can exhibit many phenotypes across the spectrum of M1 and M2

activation states (Murray et al., 2014). Like macrophages, microglia are likely to take on many activation states under chronic inflammation to correspond to their many functional duties in the CNS.

Alzheimer's disease (AD) is the most common form of dementia among the elderly. Characteristic neuropathological changes seen in AD brain include synaptic and neuronal loss, neurofibrillary tangles (NFTs), extracellular senile plaques composed of amyloid (Aβ) protein deposits and evidence of inflammatory events. The relative contributions of these pathological markers to the cognitive dysfunction in AD remains controversial, but clinical and transgenic animal studies are increasingly suggesting that Aβ alone is not sufficient for the neuronal loss and subsequent cognitive decline observed in AD ((Aizenstein et al., 2008;Blurton-Jones et al., 2009;Fonseca et al., 2009) and reviewed in (Selkoe and Hardy, 2016)). The role of neuroinflammation in neurodegenerative diseases, particularly relating to Alzheimer's disease, is an active area of research (reviewed in (Wilcock et al., 2011;Wyss-Coray and Rogers, 2012)), and immune activation in the brain has been identified by many groups as a potential therapeutic target ((Bachstetter et al., 2012) and reviewed in (Heneka et al., 2015)).

Recent clinical and genetic work involving genome-wide association studies (GWAS) have linked the pathology in AD with neuroinflammation, suggesting a more prominent role in the pathogenesis of the disease (Zhang et al., 2013; Karch and Goate, 2015; Ridge et al., 2016). Innate immunity and the complement cascade have been specifically implicated as disease risk factors (Jones et al., 2010). TREM2 and CR1 are involved with Aβ clearance and in GWAS studies were found to be associated with increased risk for AD. Unlike other single nucleotide polymorphisms (SNPs) associated with AD, the TREM2 SNP conferred a risk of

Alzheimer's disease similar to the risk of one ApoE ε4 allele, although the frequency of the variant occurs less than the frequency of ApoE ε4 allele (Saunders et al., 1993; Guerreiro et al., 2013; Jonsson et al., 2013). TREM2 has been shown to be involved with detection of lipids known to be associated with fibrillar Aβ and a loss of TREM2 in the 5xFAD mouse model of AD lead to an increase in Aβ accumulation (Wang et al., 2015), though more recent work has implicated TREM2 in keeping the plaque compact rather than affecting amyloid burden (Wang et al., 2016) . CR1 is also associated with AD risk (Lambert et al., 2009), although to a lesser extent than TREM2. Recent data suggests CR1 likely has a primary role on clearance of Aß outside of the CNS (Fonseca et al., 2016).

The complement system is a well-known powerful effector mechanism of the immune system that normally contributes to protection from infection and resolution of injury (Ricklin and Lambris, 2013). Complement activation generates activation fragments C3a and C5a that interact with cellular receptors to recruit and/or activate phagocytes (including microglia) (Davoust et al., 1999; Monk et al., 2007). Fibrill*ar* Aß can activate the classical complement pathway (in the absence of antibody) or the alternative complement pathway (Jiang et al., 1994; Bradt et al., 1998) and complement components are associated with plaques in human AD and mouse models of AD (Afagh et al., 1996; Matsuoka et al., 2001; Fonseca et al., 2011). We have previously demonstrated that treatment with a C5a receptor antagonist, PMX205, rescued the behavior performance in a mouse model of AD and significantly reduced the amyloid plaque load and reactive glia found surrounding Aβ plaques in two murine models (Fonseca et al., 2009).

Here, we investigated microglia cell surface expression of CR1, TREM2, and CD200R in the 3xTg mouse model. We found CR1 and CD200R were not expressed by adult microglia,

nor were they upregulated in the 3xTg, although they were expressed in primary microglia and the BV2 cell line and upregulated by cytokine stimulation in those cultured cells. Importantly, at 4 months, before plaque pathology, there was no difference in TREM2 expression between 3xTG and control mice. However, TREM2 was significantly increased in microglia isolated from aged (19mo) 3xTG but not in age matched controls. Finally, using Arctic model of AD which develops accelerated plaque deposition (2-6 months) and behavior deficits as early as 10 months, we investigated the expression of immunology-related genes and neurodegenerative-related genes using two separate panels from Nanostring technologies between wild type and Arctic, but importantly also in C5aR1-deficient Arctic mice. We identified 27 differentially expressed genes from brains of Arctic compared to Arctic with C5aR1 deleted in (23 in the immunology panel and an additional 4 genes in the neurodegenerative panel). The genes point to a decrease of interferon (IFN) -related genes in the Arctic C5aR1KO, with Stat1 being a prominent transcription factor found to be decreased with the loss of C5aR1. Chemokine signaling genes are also found to be differentially expressed, with Ccl5 and Ccl9 decreased and Ccl8 increased in the C5aR1-deficient brains. Absence of differentially expressed neuron-related genes in the neurodegenerative panel may suggest microglia are primarily altered in the Arctic C5aR1KO. However, studies at earlier ages need to be conducted to determine if neuronal changes occur at earlier ages and more comprehensive investigation of neuronal genes is required. Thus, further study of microglial gene expression in AD models may elucidate the mechanism by which C5aR1 blockade improves cognitive deficits in the Arctic model.

Materials & Methods

Reagents

Hanks' balanced salt solution (HBSS), was obtained from ThermoFisher. Dulbecco's modified eagle medium (DMEM) with high glucose, glutamine and pyruvate was obtained from Hyclone. HL-1 chemically defined serum-free media was obtained from Lonza. Fetal bovine serum (FBS) was obtained from Gibco. Cellstripper was from Corning. Anti mouse CR1 monoclonal antibody (7G6), CD45 (30-F11), and mouse Fc block was obtained from BD Pharmingen. CD200R monoclonal antibody (OX-110) was from AbD Serotec. TREM2 monoclonal antibody (237920) was from R&D Systems. CD11b antibody (M1/70), IFN-γ (mouse recombinant), and IL-4 (mouse recombinant) was obtained from eBioscience. Nanostring "Immunology" and custom "Neurodegeneration" panel were purchased from Nanostring Technologies. All buffers are made with Millipore-purified water with additional filters to eliminate LPS and are periodically tested for endotoxin using the *Limulus* amebocyte lysate clot assay (all solutions added to cells were < 0.1 EU/mL; 1 EU is equivalent to 0.1 ng/mL LPS).

Animals

All animal experimental procedures were reviewed and approved by the Institutional Animal Care and Use Committee of University of California at Irvine, and performed in accordance with the NIH Guide for the Care and Use of Laboratory Animals. For adult microglia isolations, 3xTg mice harboring the APP Swedish mutation, a human four-repeat (tau P301L) mutation and a knock-in mutation of presenilin 1 (PS1M146V) (Oddo et al., 2003) and wildtype controls were used. For Nanostring analysis, C57BL/6J (WT) were purchased from Jackson Laboratory and bred to Arctic. The AD mouse model used was the

Arctic48 (Arctic), which carry the human APP transgene with the Indiana (V717F), Swedish (K670N + M671L), and Arctic (E22G) mutations (under the control of the platelet-derived growth factor-ß promoter), that produce Aß protofibrils and fibrils as early as 2-4 months old (Cheng et al., 2004), graciously provided by Dr. Lennart Mucke (Gladstone Institute, San Francisco, CA, USA). Arctic mice were maintained as heterozygous for the Arctic transgene by crossing to C57BL/6J mice. In addition, Arctic mice were crossed to mice with a homozygous deficiency of C5aR1 (C5aR1KO), also on a C57BL/6J background (Hollmann et al., 2008). The F1 Arctic mice were crossed to C5aR1KO to generate Arctic C5aR1KO mice which were subsequently bred to C5aR1KO to derive littermates of C5aR1KO mice with and without the Arctic APP transgene. Mice did not exhibit any gross abnormalities and bred normally.

Tissue collection for RNA and IHC

Mice were anesthetized with Isoflurane gas (4%) for about 60 seconds. A small portion of their tails was obtained for genotyping verification. They were then perfused with phosphate buffered saline (PBS). The brain was dissected at 4^{o} C with half of the tissue (minus olfactory bulbs and cerebellum) immediately frozen on dry ice, for later RNA extraction, and the other half drop-fixed overnight in 4% paraformaldehyde-PBS at 4˚C for immunohistochemical studies. After 24 hours, the fixed tissue was placed in PBS/0.02% sodium azide at 4˚C until use.

Microglia isolation

Adapted from (Njie et al., 2012), mice from WT, C5aR1KO, Arctic and Arctic C5aR1KO genotypes were perfused with PBS at 2, 5, 7 and 10 months, and the brains (without olfactory bulbs or cerebellum) collected for microglia isolation. Brains were treated with Dispase II (Roche) at 37˚C for 1 hr and passed through a 70 μM nylon cell mesh strainer (BD Biosciences) to obtain a single cell suspension. The cell suspension was washed in cold HBSS; and spun at 1000 x *g* for 10 min at 4˚C. The cell pellet was resuspended in 70% Percoll (Sigma; diluted in HBSS), and 35% Percoll (diluted in HBSS) was carefully layered over to create a discontinuous Percoll gradient. After centrifugation at 800 x g for 45 min at 4˚C, the cells at the interphase were quickly collected, washed with ice-cold HBSS.

Cell culture

To generate primary microglia, cortical tissue was obtained from neonatal mice (P1-P3), dissociated by trituration and exposure to 0.25% tissue culture trypsin for 10 min, pelleted by centrifugation at 540 × *g* for 7 min, resuspended in DMEM supplemented with 10% FBS, and added to poly l-lysine-coated flasks. After 24 h, 75% of the supernatant was replaced with fresh medium. Every 3 days, a third of the media was replaced with fresh media. Microglia were obtained for experimental procedures following culture intervals of 7–14 days by shaking flasks using a rotary shaker (New Brunswick, Edison, NJ, USA) at 140 r.p.m. and 37°C for 90 min, centrifugation at 540 × *g* for 7 min, washing and resuspending in HL-1 media. Cells were plated in 6-well plates in 2.5 mL of HL-1 at a concentration of 250,000 per mL and allowed to grow for 24 hours prior to stimulation with Il-4 (20ng/mL) or IFN-γ (100U/mL). 24 hours after stimulation, the cells were harvested

with Cellstripper and pelleted by centrifugation and resuspended in FACS buffer (HBSS supplemented with 2% BSA and 0.02% NaN_3).

BV2 cells were similarly grown in HL-1 media overnight prior to stimulation with either Il-4 or IFN-γ in poly l-lysine-coated flasks. BV2 cells were collected using warmed 0.05% trypsin and washed with ice-cold HBSS prior to staining for flow cytometry.

Flow cytometry

Microglia cells (BV2, neonatal primary, and adult isolated) were stained in FACS buffer with CD11b-PE-Cy7 (0.2 μg), CD45-APC (0.2 μg), CR1-FITC (0.5 μg), CD200R-PE (0.25 μg), and TREM2-PE (0.25 μg). Isotype controls were used for gating and the median fluorescent intensity was calculated for each fluorophore. The samples were run on a 4-color FACSCalibur using CellQuestPro (v5.1) and analyzed using FlowJo (v8.8.7).

Nanostring gene expression analysis

10 mg of pulverized brain tissue per sample was used to extract RNA using the PureLink RNA Mini Kit (Life Technologies) following manufacturer's instructions. RNA concentration and quality was determined using a spectrophotometer (Beckman Du 530). 100 ng of RNA per sample was sent to the University of California at Irvine Genomics High Throughput Facility (GHTF) where the "Immunology" and the custom made "Neurodegeneration" panels were run (**Table 4.5**). Quality control of the raw counts was done using the nSolver Analysis Software. The GHTF at UCI analyzed the Nanostring data to identify differentially expressed (DE) genes from the following ratios (WT vs C5aR1KO, WT vs Arctic, and Arctic vs Arctic C5aR1KO). Tables of DE genes were made from each

comparison and the Log2 fold change (Log2FC) was used for further pathway analysis. Ingenuity Pathway Analysis (IPA) software was used for pathway and functional enrichment analysis.

Results

Differential upregulation of CR1, CD200R, and TREM2 on microglia from BV2 cell line and primary mouse microglia upon cytokine treatment

Studies comparing primary rat microglia from BV2 cells have shown that they have all the classical microglia markers observed in primary microglia and respond to LPS by releasing nitric oxide (NO), although lesser amounts (Horvath et al., 2008), and over 90% of the genes induced by LPS in primary microglia are induced by LPS in BV2 cells, again although again to a lesser extent (Henn et al., 2009). Little was reported on the expression of CR1, CD200R, and TREM2 and some data was conflicting. In order to characterize the expression of the surface receptors and how that expression was modulated by the local cytokine environment, here we investigated the cell surface expression of CR1, CD200R, and TREM2 on microglia, BV2 and primary neonatal, and investigated the effects of M1 and M2a cytokines on the expression these 3 cell surface proteins. We evaluated the basal expression of these proteins on BV2 cells. There was no basal CR1 expression as the histogram overlaps with the isotype control (**Figure 4.1A**), however, upon IFN-gamma stimulation for 24hrs, the expression as measured by MFI is doubled (**Figure 4.1A**). IL-4 has no effect on the expression of CR1 (**Figure 4.1A,**). Unlike CR1, CD200R and TREM2 are highly expressed on BV2 cells. IFN-gamma and IL-4 increases CD200R expression (**Figure 4.1B**). TREM2 on BV2 cells is increased about 6-fold with IFN-gamma but like CR1, IL-4 has no effect on the

expression of TREM2 (**Figure 4.1C**). The expression of these proteins in neonatal primary microglia differed. Basal expression of CR1 was found, although low and IFN-gamma increased CR1 expression (**Figure 4.1D**) much like in BV2 cells**.** CD200R was not expressed as highly by primary cells, and in contrast to BV2 cells, IFN-gamma slightly decreased the expression while IL-4 increased the expression of CD200R (**Figure 4.1E**). TREM2 was similarly basally expressed and IFN-gamma increased TREM2 while IL-4 had no effect on expression (**Figure 4.1F**) as similarly seen with BV2 cells.

Surface expression of CR1, CD200R, and TREM2 on microglia isolated from adult control and 3xTg mice

Although cell lines and neonatal cultures of microglia recapitulate most of the LPS-induced gene expression, studies have shown that neither is similar to microglia from adult mice (Butovsky et al., 2014). Whereas low levels of CR1 expression was detected in primary microglia, CR1 was not detected above isotype levels in young, 4 months (**Figure 4.2A**), or old, 19 months (**Figure 4.2B**), wildtype (WT) or 3xTg mice. In contrast to high levels on neonatal microglia, CD200R was similarly absent from microglia isolated from adult mice, both young and old, in WT and 3xTg (**Figure 4.2C-D**). Like other groups have reported, we found that TREM2 was expressed by microglia in the adult mouse (**Figure 4.2E-F**). At 19mo, more than 85% of CD11b-positive, $CD45^{low}$ microglia were positive for TREM2 (**Figure 4.2F**). When we compared the expression levels of TREM2 and CD45 in the 3xTg with WT, we found that aged 3xTg mice had a 30% increase in TREM2 and CD45 expression level compared to age-matched WT controls (**Figure 4.2H**). Importantly, the increase in TREM2 was only observed in aged 3xTg mice and not in young 3xTg mice. At 4 months, an age when

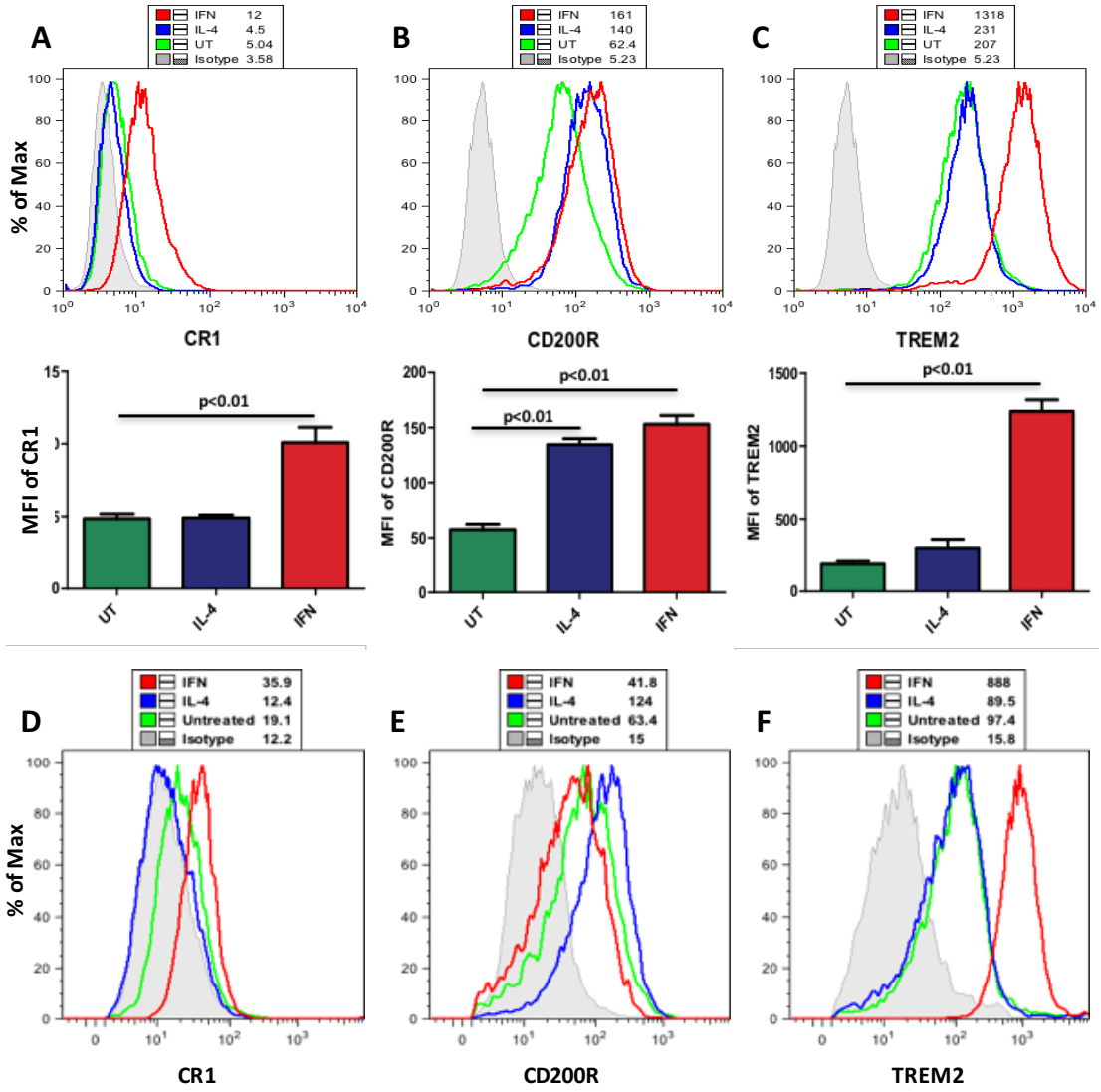

Figure 4.1. CR1, CD200R, and TREM2 cell surface expression in M0, M1, and M2a-polarized BV2 and primary neonatal microglia. CR1 (**A**), CD200R (**B**) and TREM2 (**C**) cell surface expression in untreated (UT, green), interferon-γ (IFN, red) or interleukin 4 (IL-4, blue)- treated BV2 cells. Representative flow cytometry histograms of fluorescence intensity of N=2. (top) and median fluorescence intensity quantified +/- SEM (bottom). P values from two-tailed student's t-test. CR1 (**D**), CD200R (**E**) and TREM2 (**F**) cell surface expression in untreated (UT, green), interferon-γ (IFN, red) or interleukin 4 (IL-4, blue)- treated primary neonatal cells, N=1.

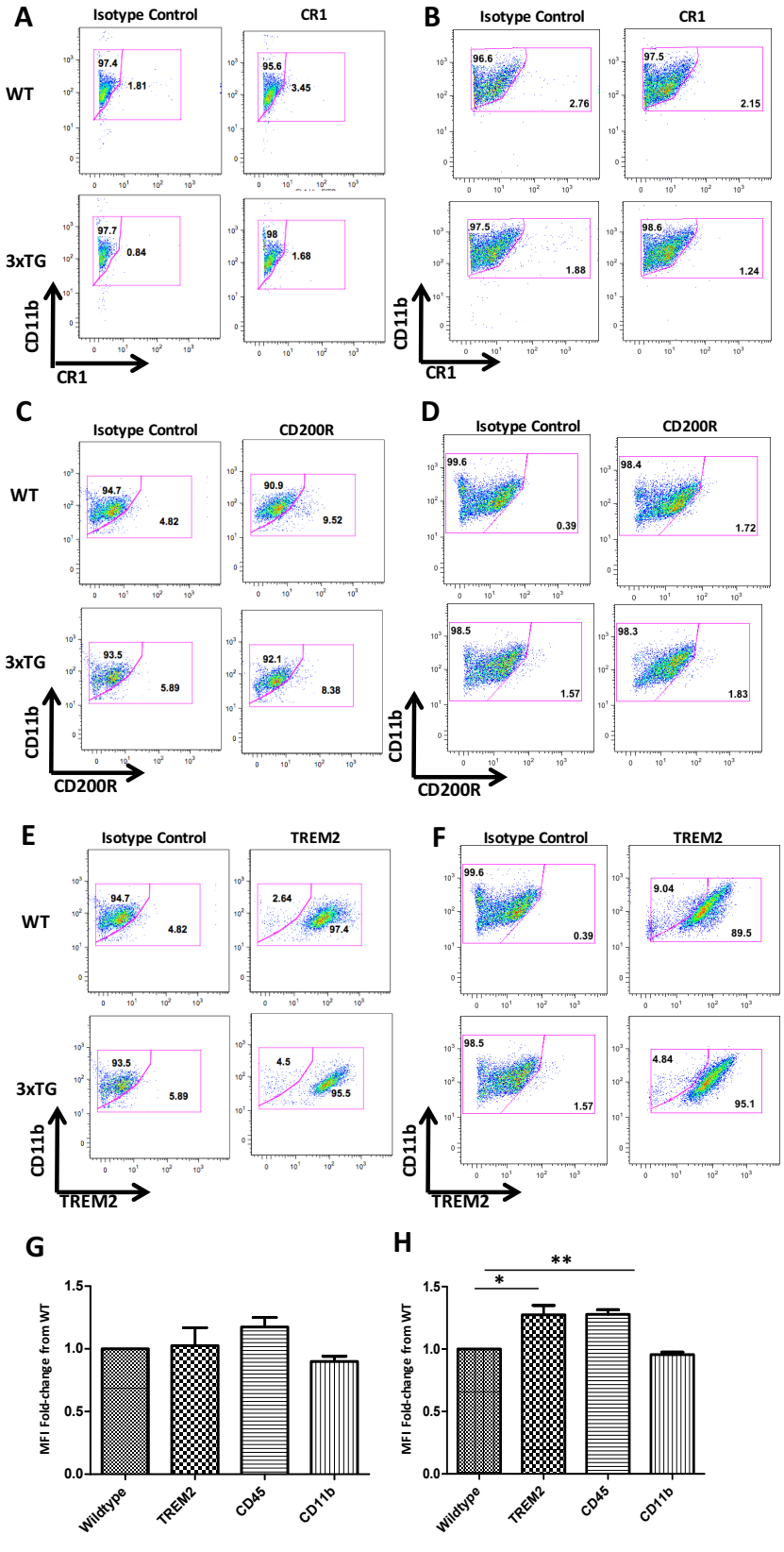
A
Isotype Control
CR1
WT
3xTG
97.4
1.81
95.6
3.45
97.7
0.84
98
1.68
CD11b
CR1
B
Isotype Control
CR1
96.6
2.76
97.5
2.15
97.5
1.88
98.6
1.24
CD11b
CR1
C
Isotype Control
CD200R
WT
3xTG
94.7
4.82
90.9
9.52
93.5
5.89
92.1
8.38
CD11b
CD200R
D
Isotype Control
CD200R
99.6
0.39
98.4
1.72
98.5
1.57
98.3
1.83
CD11b
CD200R
E
Isotype Control
TREM2
WT
3xTG
94.7
4.82
2.64
97.4
93.5
5.89
4.5
95.5
CD11b
TREM2
F
Isotype Control
TREM2
99.6
0.39
9.04
89.5
98.5
1.57
4.84
95.1
CD11b
TREM2
G
MFI Fold-change from WT
1.5
1.0
0.5
0.0
Wildtype
TREM2
CD45
CD11b
H
**
*
MFI Fold-change from WT
1.5
1.0
0.5
0.0
Wildtype
TREM2
CD45
CD11b

Figure 4.2. Surface expression of CR1, CD200R, and TREM2 on microglia isolated from adult mice. CR1 surface expression on microglia from (**A**)4 month and (**B**)19 month old mice. CD2OOR surface expression on microglia from (**C**) 4 month and (**D**)19 month old mice. TREM2 surface expression on microglia from (**E**) 4 month and (**F**)19 month old mice. MFI fold change from WT of TREM, CD45 and CD11b on microglia from (G) 4 month and (H) 19 month old mice.+/- SEM. * $p < 0.05$, ** $p < 0.01$, two-tailed student's t-test. N=4 at each age for each genotype.

there is an absence of pathology, TREM2, as well as CD45 and CD11b is expressed in the 3xTg at similar levels to WT (**Figure 4.2G**).

Differential gene expression of immunology-related genes in Arctic AD mice deficient for C5aR1 indicate decrease in inflammation

Since previous work (discussed in chapter 3, **Figure 3.1**) showed behavior deficits at 10 months in the Arctic AD mouse model that was absent when C5aR1 is genetically ablated, we investigated gene expression of half brains (minus cerebellum) from 24 mice from the behavior study (n = 4-8 mice per genotype). Given that in the CNS, microglia largely mediate the immune response, we assessed the gene expression of 539 immunology-related genes using the "Immunology" Nanostring panel. This panel is a pre-fabricated panel which includes 547 genes of interest and 14 housekeeping genes. We analyzed the dataset using the following 8 housekeeping genes: g6pdx, hprt, polr1b, polr2a, ppia, rpl19, sdha, and tbp. Additionally, 8 genes (cfh, csf1r, ikbkb, il1r2, stat2, trem2, ccl12, ikbke) were removed from the analysis due to changes in the primer sequence between the Immunology panel and the custom-made "Neurodegeneration" Nanostring panel (**Table 4.5**). (Although TREM2 was eliminated from our analysis, it was not differentially expressed in any of the four genotypes in either panel in these 10 month samples (data not shown)). Initial quality control examination of the 24 samples analyzed showed the samples had similar levels of counts across all genes, demonstrating gene expression was largely similar for all genotypes (**Figure 4.3A**). Hierarchical clustering showed that the samples cluster based on whether

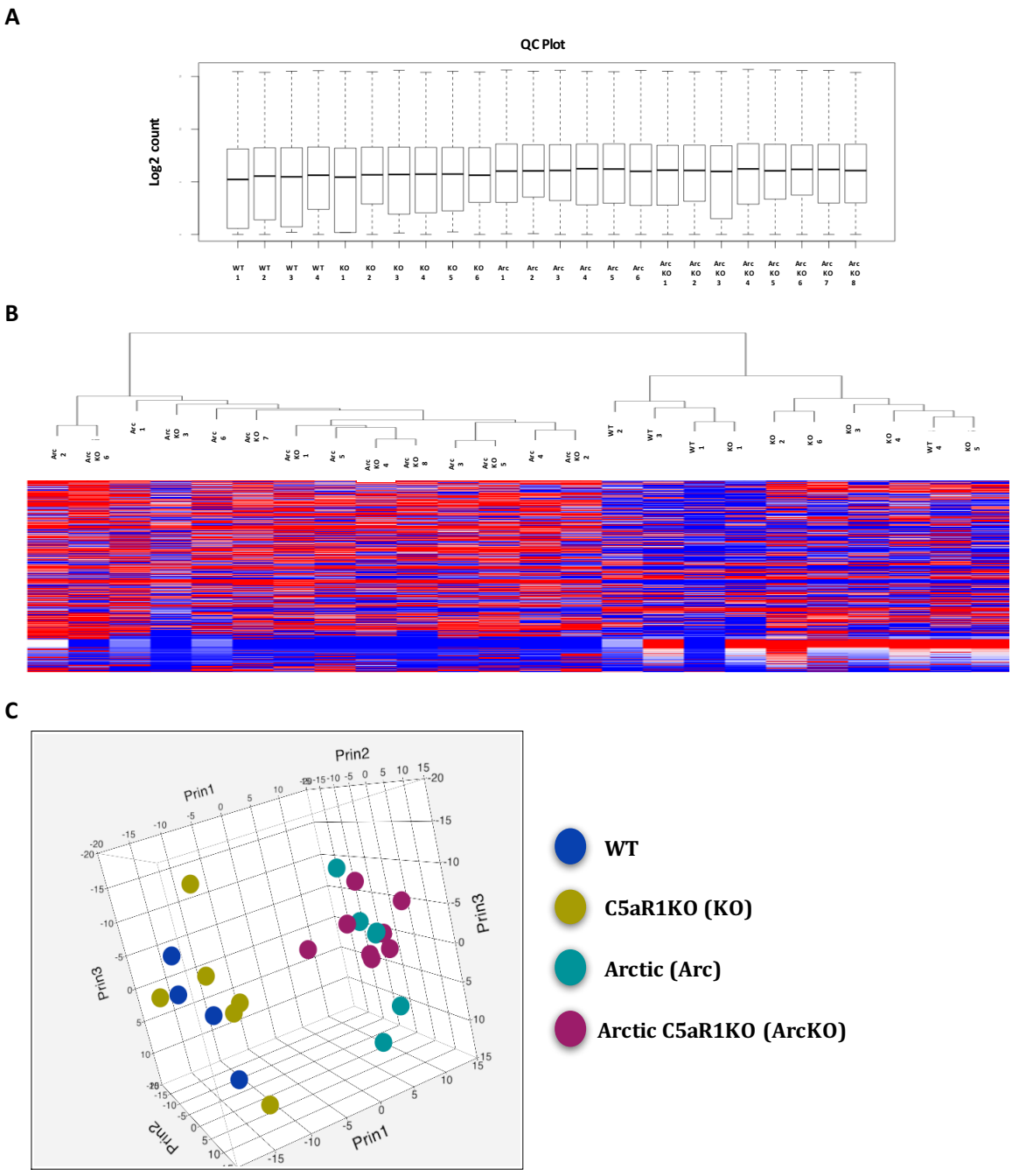

Figure 4.3. Quality control of 24 samples assayed. (**A**) Mean log2 counts of all genes in immunology panel per sample. (**B**) Hierarchical clustering of gene expression of 24 samples used in immunology panel. (**C**) Principal component analysis (3D) of 24 samples. N = 4 (WT), N = 6 (C5aR1KO), N= 6 (Arctic), N= 8 (Arctic C5aR1KO).

they are Arctic or not, suggesting the Arctic phenotype is the dominant force driving the gene expression (**Figure 4.3B**). The principal component analysis (PCA) also highlights the separation of the samples based on the Arctic phenotype. On the left in blue and yellow (WT and C5aR1KO respectively) are the samples that lack the APP transgene and on the right in green and red (Arctic and Arctic C5aR1KO respectively) are the samples that possess the APP transgene (**Figure 4.3C**).

Out of the 539 immunology-related genes assayed, 199 were differentially expressed (DE) between the four genotypes. The majority of the DE genes were in the WT vs Arctic comparison, where 168 genes were differentially expressed (**Figure 4.4A,** blue circle), the majority increased in the Arctic relative to WT (data not shown). Between the C5aR1KO and WT there were 48 DE genes (**Figure 4.4A,** yellow circle). In the Arctic and Arctic C5aR1KO comparison there were 21 DE genes (**Figure 4.4A-B**) In contrast to the largely increased gene expression seen in the Arctic relative to the WT, in the Arctic C5aR1KO, most genes were decreased relative to Arctic (**Figure 4.4B**). Ccl5 and Ccl9 were differentially expressed in all three comparisons (**Figure 4.4A**). Both genes were upregulated in the Arctic mice (relative to WT) and downregulated in the Arctic C5aR1KO (relative to Arctic), although not to WT levels. Interestingly, Ccl5 was increased and Ccl9 was decreased in the C5aR1KO relative to WT (data not shown).

Of the 21 DE genes in the Arctic C5aR1KO relative to Arctic, 12 were shared between the WT and Arctic comparison (**Figure 4.4C**). Eight were upregulated in the Arctic (relative to WT) and downregulated in the Arctic C5aR1KO (relative to Arctic), including: Ddx58, Fcgr1 (CD64), Fcgr4 (CD16-2), Ifi204, Ifi35, Irgm1, Stat1, Tap1; these genes are all

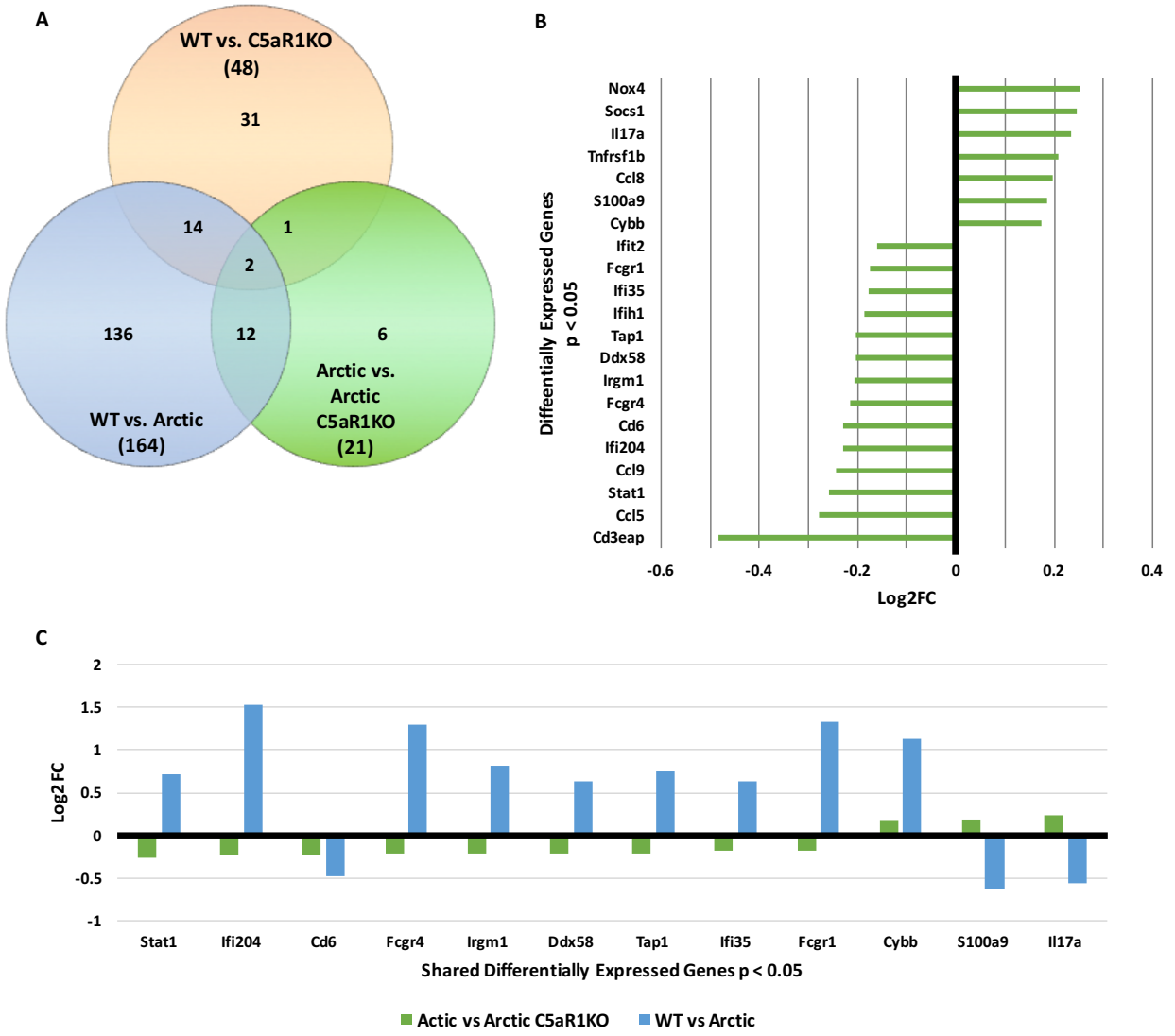

Figure 4.4. Differentially expressed genes identified in the immunology panel. (**A**) Venn diagram of 3 gene expression comparisons identified differentially expressed genes in WT vs Arctic (blue), WT vs C5aR1KO (yellow) and Artic vs Arctic C5aR1KO (green). (**B**) 21 DE genes from Arctic vs Arctic C5aR1KO comparison. Bars represent individual genes showing Log2 fold change (FC). (**C**) 12 shared DE genes from the WT vs Arctic comparison (blue bars) and Arctic vs Arctic C5aR1KO comparison (green bars). All DE genes $p < 0.05$. N = 4 (WT), N = 6 (C5aR1KO), N= 6 (Arctic), N= 8 (Arctic C5aR1KO).

involved in interferon signaling pathways, either induced by, upstream of, or activators of interferon α,β, or γ (**Figure 4.5**). Two genes, s100a9 and IL-17a, were downregulated in the Arctic (relative to WT) and upregulated in the Arctic C5aR1KO (relative to Arctic). Six additional genes were only differentially expressed in the Arctic C5aR1KO vs Arctic with small fold changes, including: Ifih1 and Ifit2, decreasing in the Arctic C5aR1KO (interferon pathway) and CCL8, Tnfrsf1b, Socs1, and Nox4 increasing, although all changes were slight being in the 10-20% range (**Figure 4.4B**).

Pathway analysis using Ingenuity Pathway Analysis (IPA) identified the following inflammation related signaling pathways as activated: pattern recognition receptor (PPRs) signaling, TREM1 signaling, NFAT regulation of the immune response, OX-40/CD134 signaling, and leukocyte extravasation signaling, among other pathways (see **Table 4.1**) in the Arctic relative to the WT. The only pathway that was downregulated in the Arctic relative to the WT was GNRH (gonadotropin-releasing hormone) signaling. The functional categories that were largely found to be increased in the Arctic relative to WT were: phagocytosis-related functions, chemotaxis, and development/differentiation of blood cells (see **Table 4.2** for full list).

Pathway analysis of the 21 DE genes found in the Arctic C5aR1KO relative to Arctic identified 3 pathways that were inhibited in the Arctic C5aR1KO brain, Interferon signaling, PPR signaling, and activation of IRF by cytosolic PPRs (**Table 4.3, Figure 4.5**). Diseases and functions predicted to be altered in the Arctic C5aR1KO include: proliferation of leukocytes and lymphocytes (decreased) and proliferation of endothelial cells, viral replication, and injury to CNS (increased). See **Table 4.4** for full list of diseases and functions as well as the number of DE genes that fit into each function.

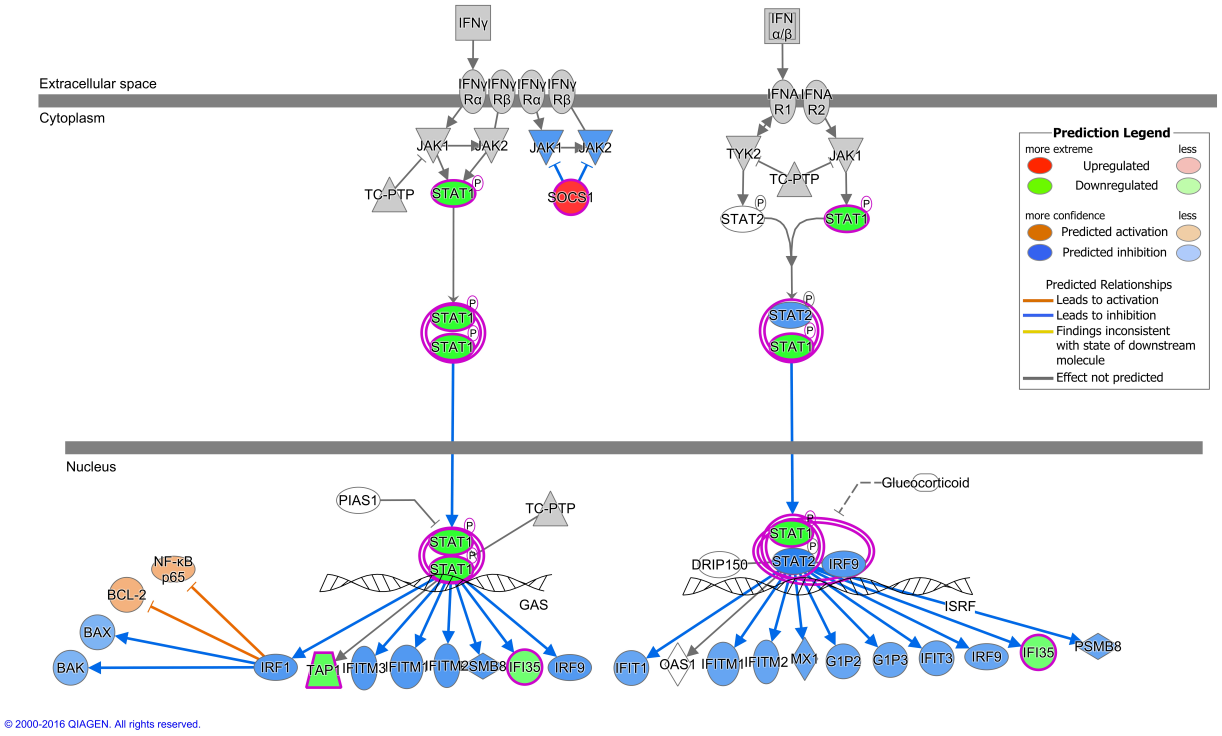

Figure 4.5. Interferon signaling pathway. IPA software predicted interferon signaling to be inhibited/decreased in Arctic C5aR1KO relative to Arctic. Red shaded genes are upregulated and green shaded genes are downregulated in Arctic C5aR1KO relative to Arctic. Blue shaded genes are predicted to be decreased and orange shaded genes are predicted to be increased.

Neurodegeneration panel shows increase in inflammation and decrease in neuronal survival signaling in Arctic relative to WT

The neurodegeneration panel that included autophagy and neuronal genes found 88 DE genes between all three comparisons (15 in WT vs C5aR1KO, 80 in WT vs Arctic, and 7 in Arctic vs Arctic C5aR1KO) (**Figure 4.6A**). Five of the seven DE genes (C5aR1, as expected, as well as Bdnf, Stat1, Ccl5 and Ide) in the Arctic C5aR1KO were decreased relative to Arctic. The remaining two, Ctsb and MAP1LC3A were upregulated in the Arctic C5aR1KO relative to Arctic (**Figure 4.6B**). Of note, only two of the seven genes mentioned above, Ccl5 and Stat1, were shared between the WT and Arctic comparison and the Arctic and Arctic C5aR1KO comparison, both of which were increased in the Arctic (relative to WT) and decreased significantly, though not substantially, in the Arctic C5aR1KO (relative to Arctic) (**Figure 4.6C**).

The pathways that were activated in the Arctic samples relative to WT were the following: complement system, TLR signaling, and TREM1 signaling. Pathways inhibited between Arctic and WT were primarily neuronal survival/growth related pathways such as: CREB signaling in neurons, CDK5 signaling, Neurotrophin/TRK signaling, NGF signaling and Synaptic LTP. Other pathways inhibited were GNRH signaling, calcium signaling, thrombin signaling and PPARα/RXRα activation (**Table 4.6**). Key functions that were downregulated in the Arctic (relative to WT) were neuronal and included: long-term potentiation (LTP), learning, and memory. Many of the functions upregulated were related to chemotaxis and differentiation/development of leukocytes (**Table 4.7**). Due to the limited number of genes found to be DE between the Arctic and Arctic C5aR1KO (**Figure 4.6B**), no pathways or functions were identified to be significantly affected.

Nanostring results are reproducible from panel to panel

Given that we had two panels of genes, of which 63 genes were shared, we had the opportunity to compare the reproducibility of Nanostring from one panel to the other. Of the 63 shared genes, a total of 33 genes were differentially expressed (29 in WT vs Arctic, 2 in WT vs C5aR1KO, and 2 in Arctic vs Arctic C5aR1KO) as shown in **Figure 4.7**. Of the 30 remaining genes, some were DE in the Immunology panel, but not in the Neurodegeneration panel. Interestingly, the immunology panel had far lower p values than the neurodegeneration panel, though the reason is not clear. All shared genes that were found to be DE at the $p < 0.05$ level had log2 fold changes in the same direction in both panels in each comparison, although the magnitudes differed somewhat (**Figure 4.7B, C**), thus validating the reproducibility of Nanostring.

Table 4.1. Canonical pathways predicted to be activated or inhibited in the Arctic brain relative to WT from immunology panel. Pathway analysis by IPA (p value < 0.05). All pathways with a magnitude greater than 2 (negative or positive) were considered to be significant.

	Pathways
Positive Z-Score: Predicted activated	Dendritic Cell Maturation
	Role of PRRs in Recognition of Bacteria and Virus
	TREM1 Signaling
	Role of NFAT in Regulation of the Immune Response
	OX40 Signaling Pathway
	Leukocyte Extravasation Signaling
	MIF-mediated Glucocorticoid Regulation
Negative Z-Score: Predicted inhibited	GNRH Signaling

Table 4.2. Diseases and functions enriched in the Arctic brain relative to WT from immunology panel. Diseases and functions with an activation score greater than +2 were considered activated whereas a z-score lower than -2 was considered to decrease activation or inhibit the function.

Diseases or Functions Annotation	p-Value	Predicted Activation State	Activation z-score	# of Molecules
migration of dendritic cells	6.72E-18	Increased	2.006	18
innate immune response	9.99E-19	Increased	2.008	23
advanced malignant solid tumor	4.17E-17	Increased	2.01	37
homeostasis of leukocytes	6.23E-57	Increased	2.015	72
cell movement of granulocytes	9.23E-44	Increased	2.025	52
immune response of antigen presenting cells	6.22E-31	Increased	2.032	32
cell death of leukemia cell lines	2.25E-19	Increased	2.039	29
differentiation of T lymphocytes	3.01E-43	Increased	2.042	52
cell movement of myeloid cells	6.73E-50	Increased	2.045	65
accumulation of myeloid cells	9.92E-35	Increased	2.048	34
cell movement of phagocytes	3.13E-53	Increased	2.05	68
homing of cells	3.06E-46	Increased	2.06	63
phosphorylation of protein	3.27E-25	Increased	2.082	48
cell movement of dendritic cells	6.57E-28	Increased	2.095	28
differentiation of lymphatic system cells	1.85E-60	Increased	2.128	75
cytolysis	3.78E-37	Increased	2.132	41
tyrosine phosphorylation of protein	4.29E-27	Increased	2.133	29
cell death of malignant tumor	7.95E-17	Increased	2.135	29
cell viability of mononuclear leukocytes	1.48E-18	Increased	2.136	23
extravasation of cells	1.76E-18	Increased	2.154	16
immune response of phagocytes	2.24E-36	Increased	2.167	37
response of phagocytes	3.89E-39	Increased	2.182	40
apoptosis of liver cells	2.38E-17	Increased	2.188	20
development of lymphocytes	6.09E-63	Increased	2.19	77
development of blood cells	1.52E-64	Increased	2.201	84

cell death of tumor	5.99E-20	Increased	2.201	35
necrosis of tumor	4.61E-19	Increased	2.201	34
cell death of tumor cells	1.71E-17	Increased	2.201	32
internalization of cells	3.10E-20	Increased	2.202	23
development of lymphatic system cells	4.52E-71	Increased	2.206	85
response of antigen presenting cells	1.74E-35	Increased	2.211	36
cell viability of blood cells	4.95E-34	Increased	2.212	40
cell death of liver cells	2.25E-17	Increased	2.225	22
differentiation of lymphocytes	2.78E-51	Increased	2.226	64
development of mononuclear leukocytes	1.05E-66	Increased	2.226	80
cell movement of epithelial cell lines	2.91E-17	Increased	2.227	18
immune response of neutrophils	8.16E-21	Increased	2.232	18
differentiation of leukocytes	9.08E-65	Increased	2.241	82
cell movement of connective tissue cells	2.11E-19	Increased	2.246	25
apoptosis of epithelial cells	8.87E-19	Increased	2.281	27
chemotaxis of antigen presenting cells	1.68E-21	Increased	2.289	23
differentiation of mononuclear leukocytes	9.71E-58	Increased	2.313	71
differentiation of macrophages	7.81E-24	Increased	2.33	24
chemotaxis of cells	1.37E-43	Increased	2.363	59
damage of genitourinary system	7.05E-21	Increased	2.386	22
adhesion of blood cells	4.49E-59	Increased	2.401	63
occlusion of artery	1.77E-19	Increased	2.402	35
recruitment of antigen presenting cells	1.28E-18	Increased	2.411	19
cell viability of lymphatic system cells	3.51E-18	Increased	2.437	23
accumulation of phagocytes	4.46E-35	Increased	2.481	32
activation of connective tissue cells	9.65E-22	Increased	2.485	23
cell death	3.15E-62	Increased	2.487	143
binding of cells	6.18E-38	Increased	2.488	52
extravasation	2.72E-19	Increased	2.494	18
injury of kidney	1.72E-17	Increased	2.502	16
engulfment of antigen presenting cells	4.60E-21	Increased	2.502	22
migration of antigen presenting cells	1.01E-22	Increased	2.503	25
chemotaxis	5.02E-44	Increased	2.515	60

phagocytosis of phagocytes	2.31E-23	Increased	2.523	24
phagocytosis of myeloid cells	1.26E-24	Increased	2.609	25
damage of kidney	1.18E-20	Increased	2.616	21
adhesion of tumor cell lines	2.25E-20	Increased	2.635	29
phagocytosis of cells	4.45E-33	Increased	2.702	39
engulfment of myeloid cells	2.34E-25	Increased	2.736	26
phagocytosis of blood cells	1.19E-24	Increased	2.737	26
atherosclerosis	4.38E-19	Increased	2.737	34
phagocytosis	3.56E-35	Increased	2.87	42
differentiation of cells	1.47E-40	Increased	2.88	103
cell survival	1.03E-30	Increased	2.893	73
engulfment of phagocytes	8.91E-25	Increased	2.925	26
cell viability	3.23E-28	Increased	2.95	68
migration of phagocytes	9.85E-35	Increased	3.014	40
engulfment of leukocytes	1.60E-26	Increased	3.163	28
engulfment of blood cells	4.29E-27	Increased	3.228	29
engulfment of cells	3.10E-30	Increased	3.366	43
systemic inflammatory response syndrome and/or sepsis	4.98E-26	Decreased	-2.688	27
sepsis	3.41E-22	Decreased	-2.331	24
cell death of lymphatic system cells	6.30E-34	Decreased	-2.1	46

Table 4.3. Canonical pathways predicted to be activated or inhibited in the Arctic C5aR1KO brain relative to Arctic from immunology panel. Pathway analysis by IPA (p value < 0.05). All pathways with a magnitude greater than 2 (negative or positive) were considered to be significant.

	Pathways
Negative Z-Score: Predicted inhibited	Interferon Signaling
	Role of PRRs in Recognition of Bacteria and Virus
	Activation of IRF by Cytosolic PPRs

Table 4.4. Diseases and functions enriched in the Arctic C5aR1KO relative to Arctic from immunology panel. Diseases and functions with an activation score greater than +2 were considered activated whereas a z-score lower than -2 was considered to decrease activation or inhibit the function.

Diseases or Functions Annotation	p-Value	Predicted Activation State	Activation z-score	# of Molecules
differentiation of myoblasts	1.15E-05	Increased	2	4
injury of central nervous system	1.60E-05	Increased	2	4
proliferation of endothelial cells	6.17E-04	Increased	2	4
Viral Infection	4.98E-08	Increased	2.431	13
replication of RNA virus	1.76E-07	Increased	2.709	8
cell proliferation of T lymphocytes	8.52E-07	Decreased	-2.288	8
proliferation of mononuclear leukocytes	3.87E-07	Decreased	-2.206	9
antiviral response	8.73E-10	Decreased	-2.184	8
T cell development	6.92E-05	Decreased	-2.155	6
immune response of cells	3.67E-08	Decreased	-2.035	9

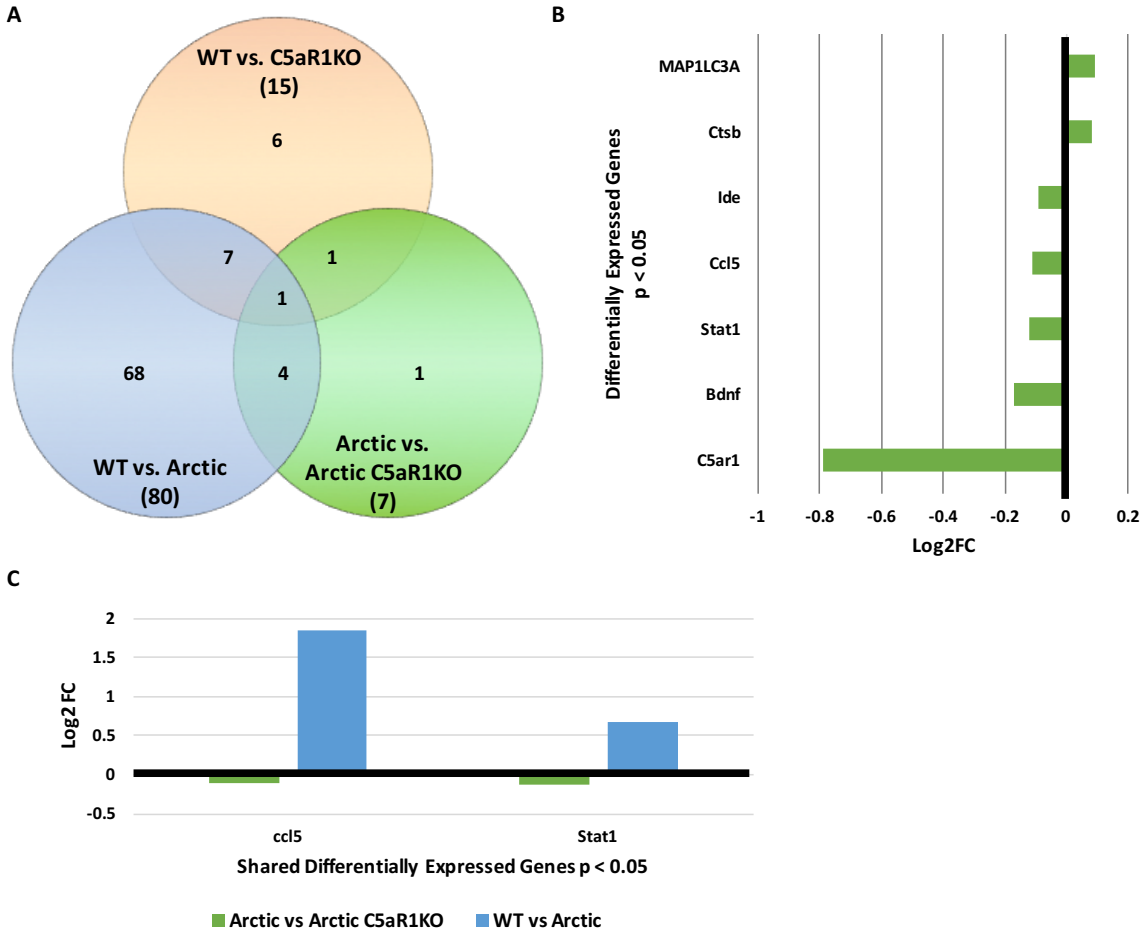

Figure 4.6. Differentially expressed genes identified in the custom neurodegeneration panel. (**A**) Venn diagram of 3 gene expression comparisons identified differentially expressed genes in WT vs Arctic (blue), WT vs C5aR1KO (yellow) and Artic vs Arctic C5aR1KO (green). (**B**) 7 DE genes from Arctic vs Arctic C5aR1KO comparison. Bars represent individual genes showing Log2 fold change (FC). (**C**) 2 shared DE genes from the WT vs Arctic comparison (blue bars) and Arctic vs Arctic C5aR1KO comparison (green bars). All DE genes $p < 0.05$. N = 4 (WT), N = 6 (C5aR1KO), N= 6 (Arctic), N= 8 (Arctic C5aR1KO).

Table 4.5 Genes in Neurodegeneration Nanostring panel. List of 171 genes in the custom-made Neurodegeneration Nanostring panel.

Genes in Neurodegeneration Panel						
Abca1	C2	Chil3	Grin1	Mmp2	Ptk2	Tlr2
Ache	C3	Chrm1	Grin2b	Mmp7	Pvalb	Tlr3
Adam10	C4a	Chrm5	Gsk3b	Mmp9	Pycard	Tlr4
Adam9	C5ar1	Chrna7	Hc	Mrc1	Rela	Tlr7
Anxa5	C7	Cltc	Hdac1	Mtor	Relb	Tnf
Aph1	Calb1	Clu	Hdac6	Myd88	S100b	Tollip
Apoe	Camk2a	Creb1	Hsf1	Ncstn	Siglech	Tom1
App	Capn1	Crh	Icam-1	Nfkb1	Sirt1	Vcam-1
Arc	Capn2	Crhr1	Ide	Ngf	Sirt6	Vegfa
Arg1	Casp3	Csf1	Ifi204	Ngfr	Smad3	ccl5
Atf2	Ccl2	Ctsb	Il10	Nos2	Socs1	fcgr4
Atg10	Ccl3	Ctsc	Il12a	Nr1h2	Socs3	il17f
Atg12	Ccr2	Ctsd	Il1b	Ntrk1	Sod1	nlrp3
Atg4a	Cd2ap	Cxcl10	Il1r1	Ntrk2	Sod2	G6pdx
Atg5	Cd40	Dync1h1	Il6	Olfml3	Sorl1	Hprt
Atg7	Cd40lg	Egr1	Il6ra	P2rx7	Sort1	Polr1b
Atg9a	Cd55	Fgf2	Itgb2	Panx1	Sphk1	Polr2a
Bace1	Cdk1	Fgfr1	Jun	Pdcd1	Stat1	Ppia
Bace2	Cdk2	Fos	Junb	Pen2	Stat3	Rpl19
Bdnf	Cdk5	GFAP	Kif3a	Picalm	Synpo	Sdha
Becn1	Cdk6	GPR6	Lamp1	Pik3c3	Tacr1	Tbp
Bin1	Cdkn1a	Gabbr1	Lrp1	Pparg	Tbxa2r	
Bub1b	Cdkn1c	Gabra1	Lrp1b	Ppp2ca	Tgfb1	
C1qa	Cdkn2a	Gdnf	MAP1LC3A	Psen1	Tgfbr1	
C1s	Cfb	Gfra1	Mapt	Psen2	Tgfbr2	

Table 4.6. Canonical pathways predicted to be activated or inhibited in the Arctic brain relative to WT from neurodegeneration panel. Pathway analysis by IPA (p value < 0.05). All pathways with a magnitude greater than 2 (negative or positive) were considered to be significant.

	Pathways
Positive Z-Score: Predicted activated	Complement System
	TLR Signaling
	TREM1 Signaling
Negative Z-Score: Predicted inhibited	CREB Signaling in Neurons
	CDK5 Signaling
	GNRH Signaling
	Neurotrophin/TRK Signaling
	Calcium Signaling
	Neuropathic Pain Signaling in Dorsal Horn Neurons
	Thrombin Signaling
	NGF Signaling
	Synaptic LTP
	PPARα/RXRα Activation

Table 4.7. Diseases and functions enriched in the Arctic relative to WT from neurodegeneration panel. Diseases and functions with an activation score greater than +2 were considered activated whereas a z-score lower than -2 was considered to decrease activation or inhibit the function.

Diseases or Functions Annotation	p-Value	Predicted Activation State	Activation z-score	# of Molecules
development of lymphatic system cells	1.53E-16	Increased	3.135	25
damage of genitourinary system	8.67E-17	Increased	2.911	15
development of blood cells	2.94E-18	Increased	2.907	28
development of mononuclear leukocytes	4.16E-15	Increased	2.797	23
damage of kidney	5.39E-16	Increased	2.755	14
cell death of leukemia cell lines	2.34E-11	Increased	2.712	15
development of lymphatic system	6.17E-18	Increased	2.684	28
recruitment of leukocytes	1.72E-25	Increased	2.672	26
development of leukocytes	2.07E-17	Increased	2.649	26
recruitment of inflammatory leukocytes	6.37E-12	Increased	2.646	7
recruitment of cells	1.16E-28	Increased	2.627	29
differentiation of lymphatic system cells	3.06E-11	Increased	2.577	19
apoptosis of leukemia cell lines	4.20E-11	Increased	2.535	14
recruitment of blood cells	9.93E-27	Increased	2.503	27
homeostasis of leukocytes	1.70E-16	Increased	2.496	24
T cell homeostasis	5.66E-15	Increased	2.496	22
T cell development	4.21E-14	Increased	2.496	21
development of lymphocytes	3.61E-14	Increased	2.464	22
leukocyte migration	5.52E-34	Increased	2.456	44
adhesion of blood cells	7.00E-18	Increased	2.443	22
chemotaxis of antigen presenting cells	3.40E-11	Increased	2.435	11
differentiation of Th17 cells	6.21E-11	Increased	2.419	9
emotional behavior	1.33E-15	Increased	2.371	17

cell death of tumor cell lines	1.95E-21	Increased	2.315	42
recruitment of phagocytes	2.41E-21	Increased	2.298	21
differentiation of leukocytes	7.39E-15	Increased	2.275	24
apoptosis of tumor cell lines	3.56E-22	Increased	2.257	39
synthesis of reactive oxygen species	3.06E-15	Increased	2.245	23
differentiation of mononuclear leukocytes	7.47E-13	Increased	2.206	20
chemotaxis of connective tissue cells	1.69E-11	Increased	2.204	8
mobilization of cells	2.37E-11	Increased	2.114	9
recruitment of neutrophils	2.92E-18	Increased	2.108	17
apoptosis	5.45E-30	Increased	2.101	60
attraction of cells	2.45E-11	Increased	2.095	10
cellular infiltration	3.41E-25	Increased	2.07	29
differentiation of blood cells	1.39E-14	Increased	2.028	26
replication of RNA virus	8.52E-15	Decreased	-2.04	21
assembly of cells	3.82E-15	Decreased	-2.057	19
quantity of neurons	1.15E-17	Decreased	-2.073	22
inflammation of intestine	1.09E-18	Decreased	-2.077	20
colitis	3.93E-17	Decreased	-2.105	18
replication of virus	4.84E-17	Decreased	-2.206	24
long-term potentiation	7.95E-18	Decreased	-2.245	19
inflammation of large intestine	2.53E-18	Decreased	-2.267	19
infection of mammalia	4.10E-15	Decreased	-2.334	18
quantity of cellular protrusions	2.85E-15	Decreased	-2.399	14
learning	2.66E-22	Decreased	-2.444	26
memory	7.66E-25	Decreased	-2.486	24
Viral Infection	1.17E-23	Decreased	-2.646	44

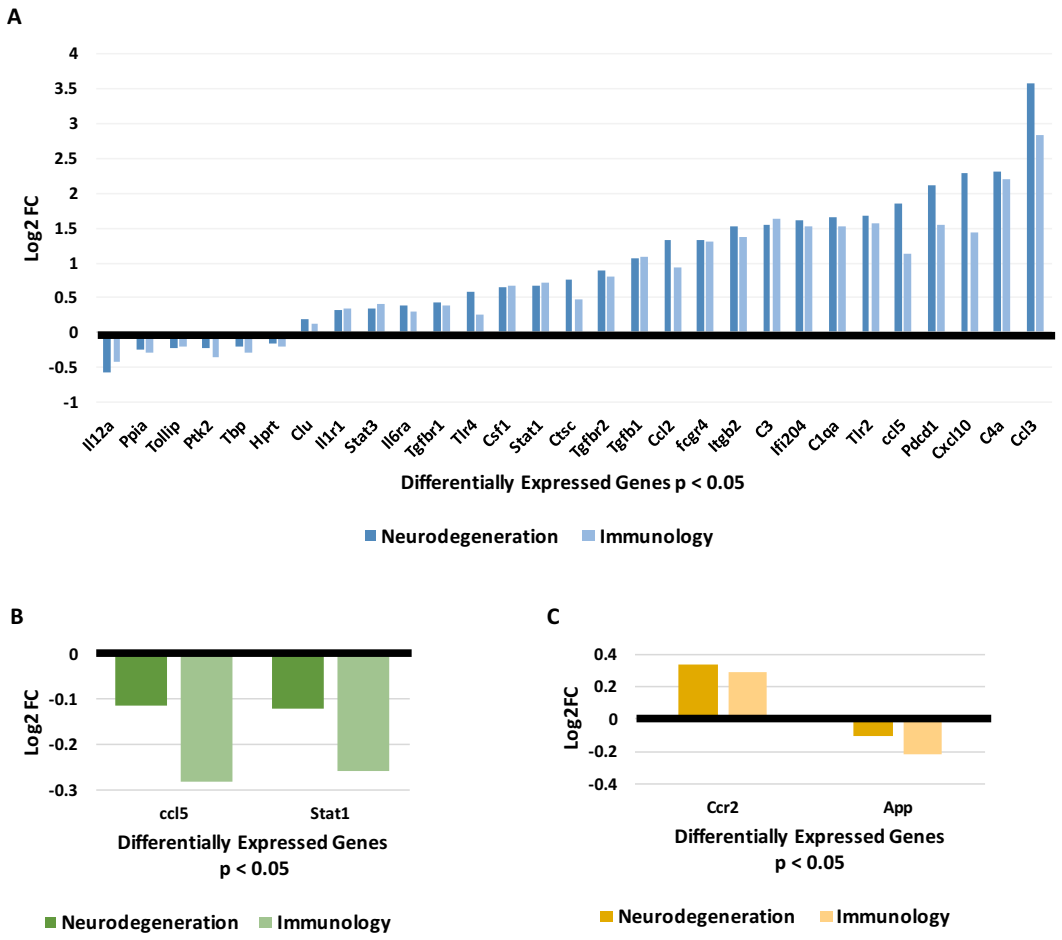

Figure 4.7. Differentially expressed genes shared between immunology and neurodegeneration Nanostring panels. (**A**) 29 DE genes from WT vs Arctic comparison that were present in both the neurodegeneration panel (dark blue) and the immunology panel (light blue). (**B**) 2 DE genes from the Arctic vs Arctic C5aR1KO comparison that were present in both the neurodegeneration panel (dark green) and the immunology panel (light green). (**C**) 2 DE genes from the WT vs C5aR1KO comparison that were present in both the neurodegeneration panel (dark yellow) and the immunology panel (light yellow). All DE genes $p < 0.05$. N = 4 (WT), N = 6 (C5aR1KO), N= 6 (Arctic), N= 8 (Arctic C5aR1KO).

Discussion

Comparing CR1, CD200R, and TREM2 surface expression in the murine BV2 microglia cell line to primary neonatal microglia showed similar expression patterns in unstimulated and cytokine-stimulated microglia. Strikingly, adult isolated microglia lacked CR1 and CD200R cell surface expression and the proteins were not induced in the 3xTg AD mouse model. In contrast, high TREM2 expression was found in adult microglia and was increased in aged 3xTg mice. Gene expression analysis in the Arctic AD model revealed inflammatory related genes were increased in the Arctic mice, many involved in interferon signaling pathways (α, β, and γ). Most the interferon-related genes (type1 and type2) were reduced with genetic deletion of C5aR1 in the Arctic mice relative to C5aR1-sufficient Arctic mice

A genome-wide association study showed an association of some variants of CR1 and CLU with late-onset AD risk (Lambert et al., 2009), suggesting a central role for complement in the pathogenesis of the disease. The expression and distribution of CR1 differs in the mouse from humans since CR1 is encoded by a separate gene in humans, whereas in mice CR1 is encoded by the CR2 gene, which encodes both CR1 and CR2 that is alternatively spliced (Molina et al., 1990). Although Crehan et al., showed activated microglia have increased expression of CR1 (Crehan et al., 2013), it's been reported that only B cells and follicular dendritic cells express CR1 in the mouse (reviewed in (Jacobson and Weis, 2008)). Our finding demonstrating very little CR1 expression in cultured microglia and an absence of CR1 staining in adult microglia suggests CR1 staining observed in culture may be an artifact of *in vitro* systems. A study using multiple antibodies against CR1 in the brain of AD patients found no CR1 staining on microglia, or anywhere in the parenchyma aside from some astrocyte staining and the staining found in red blood cells (Fonseca et al., 2016). More

likely, the protective effects of CR1 are due to the clearance of peripheral Aβ by erythrocytes expressing CR1, as first described by Rogers et al. (Rogers et al., 2006a). The data presented here are important as they show that cell lines and cell populations (neonatal vs adult) are not interchangeable as a subsequent and more extensive gene expression study has validated (Matcovitch-Natan et al., 2016)

Modulation of the immune response is critical and increasingly considered to be central to the pathogenesis of neurodegenerative diseases (reviewed in (Lynch and Mills, 2012; Heneka et al., 2015)). Microglia, as the primary immune cells of the brain, express several cell surface receptors enabling them to respond to their environment and take on functional states to carry out multiple functions (reviewed in (Colton and Wilcock, 2010). Neurons and astrocytes are reported to express CD200, the ligand for CD200R exclusively expressed on cells of myeloid origin. Importantly, it's been reported that in AD there is a dysregulation of microglia response (reviewed in (Mosher and Wyss-Coray, 2014)), and specifically CD200 and CD200R has been found to be decreased in AD (Walker et al., 2009). It has also been reported that disruption of the CD200/CD200R axis alters the microglia inflammatory response. Microglia generated from $CD200^{-/-}$ mice had a greater inflammatory response to LPS (Costello et al., 2011) . Although there is abundant literature on the role of CD200 and CD200R in keeping myeloid cells in a more quiescent state, most of the literature on microglia has been done on murine primary neonatal cells. Shrivastava and colleagues characterized the expression of CD200/CD200R in C57B6 mice brains across developmental stages from embryonic to adult and found CD200R colocalized with IBA+ microglia up to P5 in the parenchyma whereas meningeal, perivascular, and choroid plexus macrophages remained CD200R+ through adulthood, though less in number (Shrivastava et al., 2012).

Taken together, our neonatal primary work supports the developmental expression pattern of CD200R observed by Shrivastava et al. although it remains to be determined why the function of CD200R appears to be unnecessary in adult mice.

Heterozygous rare variants of TREM2 have also been associated with a high risk of Alzheimer's disease, particularly the rs75932628 SNP encoding R47H (Guerreiro et al., 2013). There has been some controversy in the field as to whether TREM2 is detrimental or beneficial in AD due to conflicting results on TREM2 deficient AD mouse models showing differing Aβ plaque burden as well as differing source of myeloid cells (monocyte-derived or resident microglia) expressing TREM2 in the CNS of AD mice (Jay et al., 2015; Wang et al., 2016). Jay and colleagues have recently shown that in the same APP/PS1 model they previously studied, that showed TREM2 was absent in microglia-associated plaques and deletion of TREM2 was beneficial, when studied at later ages, TREM2 deficiency exacerbates amyloid pathology and point to a decrease in microglia associated with plaques (Jay et al., 2016), corroborating the finding by Wang et al. that TREM2 is important in containment of Aβ plaques. Similarly, our studies in the 3xTg showed microglia associated with plaques have increase CD45 expression and here we show TREM2 and CD45 is increased in microglia isolated from 3xTg, likely representing the microglia surrounding plaques.

Pursuing other known factors influencing the process of phagocytosis and inflammation, our lab has demonstrated that treatment of mouse models of AD with a specific C5aR1 antagonist, PMX205, decreased fibrillar plaque accumulation and microglial CD45 expression and enhanced behavioral performance (Fonseca et al., 2009). We also studied behavior deficits and changes in pathology in the Arctic AD mouse model and the influence of C5aR1 on microglia, described in Chapter 3. Here, we extracted RNA from brains

of the same 10 month old mice used for behavior and pathology experiments (Chapter 3, **Figure 3.1-2**). We hypothesized we would see a decrease in inflammation in Arctic mice lacking C5aR1 since it has been found that toll-like receptors (TLRs) synergize with C5aR1 and lead to greater proinflammatory cytokine release in models of inflammatory disease in the periphery (reviewed in (Song, 2012)). Since fibrillar Aß is a ligand for TLR2 and TLR4 (Jana et al., 2008; Jin et al., 2008; Udan et al., 2008) and these receptors have been shown to contribute to the detrimental effects of Aß, C5a may synergistically enhance microglia-mediated inflammation in response to Aß interactions with such receptors on the C5a-stimulated plaque associated glia cells (Tahara et al., 2006).

While the focus of this study was to assess the changes in gene expression due to the absence of C5aR in the AD mouse model, most differentially expressed genes in the two panels were due to the Arctic APP transgene in 10 month mice (Arctic vs WT comparison). In the Immunology panel, these genes included: Itgax (alpha chain of CR4, 6.5x), Ccl3 (6x), Lilrb4 (5.3x), C4a (3.5x) and Tyrobp (3.3x). In addition, two other complement genes were upregulated more than 1.5 fold as well (C1q, C3). This expression pattern is consistent with data from Zhang and colleagues (Zhang et al., 2013) showing complement, TLRs and Tyrobp as being key networks and nodes in late onset Alzheimer's disease (LOAD). In the absence of C5aR1, the Arctic brain had decreased gene expression of inflammatory mediators, many involved in IFN signaling. In the periphery, C5aR1 is critical for normal host immune response against the intracellular pathogen L. monocytogenes, due to its role in inhibition of type 1 IFN expression (Calame et al., 2014). Here, C5aR1 deletion lead to a decrease in IFN-related (type 1 and 2) genes. This apparent discrepancy may be due to differing mechanism of action in Listeria infections in the periphery vs. amyloid burden in the brain. Indeed, in the

periphery, TLR2 and TLR4 have been shown to induce type 1 interferon via TIR domain–containing adaptor-inducing IFN-β (TRIF, also known as TICAM-1) (Aubry et al., 2012; Shalova et al., 2012). It seems likely that the increase in inflammatory components we observed in this study is due to crosstalk between TLRs and C5aR1, as mentioned above, since in the absence of C5aR1 the expression of several inflammatory genes is limited, even though amyloid plaques, a TLR ligand, is unchanged.

In summary, CR1 and CD200R are not found on microglia in adult mice, though they are present in neonatal microglia. Microglial TREM2 surface expression is increased in the 3xTg, likely representing the plaque-associated TREM2-expressing microglia, supporting more recent results reported with other models that TREM2 is important for microglial association with plaques. Gene expression from Arctic brains at 10 months showed an increase in inflammatory mediators, particularly IFN-related genes. Genetic ablation of C5aR1 decreased the expression of the IFN-related inflammatory genes. The findings are consistent with neuroinflammation being central to AD pathogenesis and supports C5a/C5aR1 axis as a therapeutic target in AD.

Reference List

Aubry C, Corr SC, Wienerroither S, Goulard C, Jones R, Jamieson AM, Decker T, O'Neill LAJ, Dussurget O, Cossart P (2012) Both TLR2 and TRIF Contribute to Interferon-beta Production during Listeria Infection. Plos One 7.

Bradt BM, Kolb WP, Cooper NR (1998) Complement-dependent proinflammatory properties of the Alzheimer's disease beta-peptide. J Exp Med 188:431-438.

Calame DG, Mueller-Ortiz SL, Morales JE, Wetsel RA (2014) The C5a anaphylatoxin receptor (C5aR1) protects against Listeria monocytogenes infection by inhibiting type 1 IFN expression. Journal of Immunology 193:5099-5107.

Cheng IH, Palop JJ, Esposito LA, Bien-Ly N, Yan F, Mucke L (2004) Aggressive amyloidosis in mice expressing human amyloid peptides with the Arctic mutation. NatMed 10:1190-1192.

Colton CA, Wilcock DM (2010) Assessing activation states in microglia. CNSNeurolDisordDrug Targets 9:174-191.

Costello DA, Lyons A, Denieffe S, Browne TC, Cox FF, Lynch MA (2011) Long term potentiation is impaired in membrane glycoprotein CD200-deficient mice: a role for Toll-like receptor activation. The Journal of Biological Chemistry 286:34722-34732.

Crehan H, Hardy J, Pocock J (2013) Blockage of CR1 prevents activation of rodent microglia. NeurobiolDis 54:139-149.

Davoust N, Jones J, Stahel PF, Ames RS, Barnum SR (1999) Receptor for the C3a anaphylatoxin is expressed by neurons and glial cells. Glia 26:201-211.

Fonseca MI, Chu SH, Berci AM, Benoit ME, Peters DG, Kimura Y, Tenner AJ (2011) Contribution of complement activation pathways to neuropathology differs among mouse models of Alzheimer's disease. J Neuroinflammation 8:4.

Fonseca MI, Ager RR, Chu SH, Yazan O, Sanderson SD, LaFerla FM, Taylor SM, Woodruff TM, Tenner AJ (2009) Treatment with a C5aR antagonist decreases pathology and enhances behavioral performance in murine models of Alzheimer's disease. Journal of Immunology 183:1375-1383.

Fonseca MI, Chu S, Pierce AL, Brubaker WD, Hauhart RE, Mastroeni D, Clarke EV, Rogers J, Atkinson JP, Tenner AJ (2016) Analysis of the Putative Role of CR1 in Alzheimer's Disease: Genetic Association, Expression and Function. PLoSONE 11:e0149792.

Ginhoux F, Greter M, Leboeuf M, Nandi S, See P, Gokhan S, Mehler MF, Conway SJ, Ng LG, Stanley ER, Samokhvalov IM, Merad M (2010) Fate mapping analysis reveals that adult microglia derive from primitive macrophages. Science 330:841-845.

Guerreiro R et al. (2013) TREM2 variants in Alzheimer's disease. New England Journal of Medicine 368:117-127.

Heneka MT et al. (2015) Neuroinflammation in Alzheimer's disease. Lancet Neurol 14:388-405.

Henn A, Lund S, Hedtjarn M, Schrattenholz A, Porzgen P, Leist M (2009) The suitability of BV2 cells as alternative model system for primary microglia cultures or for animal experiments examining brain inflammation. ALTEX 26:83-94.

Hollmann TJ, Mueller-Ortiz SL, Braun MC, Wetsel RA (2008) Disruption of the C5a receptor gene increases resistance to acute Gram-negative bacteremia and endotoxic shock: Opposing roles of C3a and C5a. Molecular Immunology 45:1907-1915.

Horvath RJ, Nutile-McMenemy N, Alkaitis MS, Deleo JA (2008) Differential migration, LPS-induced cytokine, chemokine, and NO expression in immortalized BV-2 and HAPI cell lines and primary microglial cultures. J Neurochem 107:557-569.
Jacobson AC, Weis JH (2008) Comparative functional evolution of human and mouse CR1 and CR2. J Immunol 181:2953-2959.
Jana M, Palencia CA, Pahan K (2008) Fibrillar amyloid-beta peptides activate microglia via TLR2: implications for Alzheimer's disease. J Immunol 181:7254-7262.
Jay TR, Hirsch AM, Broihier ML, Miller CM, Neilson LE, Ransohoff RM, Lamb BT, Landreth GE (2016) Disease progression-dependent effects of TREM2 deficiency in a mouse model of Alzheimer's disease. J Neurosci.
Jay TR, Miller CM, Cheng PJ, Graham LC, Bemiller S, Broihier ML, Xu G, Margevicius D, Karlo JC, Sousa GL, Cotleur AC, Butovsky O, Bekris L, Staugaitis SM, Leverenz JB, Pimplikar SW, Landreth GE, Howell GR, Ransohoff RM, Lamb BT (2015) TREM2 deficiency eliminates TREM2+ inflammatory macrophages and ameliorates pathology in Alzheimer's disease mouse models. JExpMed 212:287-295.
Ji K, Akgul G, Wollmuth LP, Tsirka SE (2013) Microglia actively regulate the number of functional synapses. PLoS One 8:e56293.
Jiang H, Burdick D, Glabe CG, Cotman CW, Tenner AJ (1994) beta-Amyloid activates complement by binding to a specific region of the collagen-like domain of the C1q A chain. J Immunol 152:5050-5059.
Jin JJ, Kim HD, Maxwell JA, Li L, Fukuchi K (2008) Toll-like receptor 4-dependent upregulation of cytokines in a transgenic mouse model of Alzheimer's disease. J Neuroinflammation 5:23.
Jones L et al. (2010) Genetic evidence implicates the immune system and cholesterol metabolism in the aetiology of Alzheimer's disease. PLoS One 5:e13950.
Jonsson T et al. (2013) Variant of TREM2 associated with the risk of Alzheimer's disease. New England Journal of Medicine 368:107-116.
Karch CM, Goate AM (2015) Alzheimer's disease risk genes and mechanisms of disease pathogenesis. Biological Psychiatry 77:43-51.
Kettenmann H, Hanisch UK, Noda M, Verkhratsky A (2011) Physiology of microglia. Physiol Rev 91:461-553.
Lambert JC et al. (2009) Genome-wide association study identifies variants at CLU and CR1 associated with Alzheimer's disease. Nat Genet 41:1094-1099.
Lynch MA, Mills KH (2012) Immunology meets neuroscience--opportunities for immune intervention in neurodegenerative diseases. Brain BehavImmun 26:1-10.
Matcovitch-Natan O et al. (2016) Microglia development follows a stepwise program to regulate brain homeostasis. Science 353:aad8670.
Matsuoka Y, Picciano M, Malester B, LaFrancois J, Zehr C, Daeschner JM, Olschowka JA, Fonseca MI, O'Banion MK, Tenner AJ, Lemere CA, Duff K (2001) Inflammatory responses to amyloidosis in a transgenic mouse model of Alzheimer's disease. AmJ Pathol 158:1345-1354.
Molina H, Kinoshita T, Inoue K, Carel JC, Holers VM (1990) A molecular and immunochemical characterization of mouse CR2. Evidence for a single gene model of mouse complement receptors 1 and 2. Journal of Immunology 145:2974-2983.

Monk PN, Scola AM, Madala P, Fairlie DP (2007) Function, structure and therapeutic potential of complement C5a receptors. British Journal of Pharmacology 152:429-448.
Mosher KI, Wyss-Coray T (2014) Microglial dysfunction in brain aging and Alzheimer's disease. Biochemical Pharmacology 88:594-604.
Murray PJ et al. (2014) Macrophage activation and polarization: nomenclature and experimental guidelines. Immunity 41:14-20.
Nayak D, Zinselmeyer BH, Corps KN, McGavern DB (2012) In vivo dynamics of innate immune sentinels in the CNS. Intravital 1:95-106.
Njie EG, Boelen E, Stassen FR, Steinbusch HW, Borchelt DR, Streit WJ (2012) Ex vivo cultures of microglia from young and aged rodent brain reveal age-related changes in microglial function. NeurobiolAging 33:195-112.
Oddo S, Caccamo A, Shepherd JD, Murphy MP, Golde TE, Kayed R, Metherate R, Mattson MP, Akbari Y, LaFerla FM (2003) Triple-transgenic model of Alzheimer's disease with plaques and tangles: intracellular Abeta and synaptic dysfunction. Neuron 39:409-421.
Parkhurst CN, Yang G, Ninan I, Savas JN, Yates JR, III, Lafaille JJ, Hempstead BL, Littman DR, Gan WB (2013) Microglia promote learning-dependent synapse formation through brain-derived neurotrophic factor. Cell 155:1596-1609.
Ricklin D, Lambris JD (2013) Complement in immune and inflammatory disorders: pathophysiological mechanisms. J Immunol 190:3831-3838.
Ridge PG, Hoyt KB, Boehme K, Mukherjee S, Crane PK, Haines JL, Mayeux R, Farrer LA, Pericak-Vance MA, Schellenberg GD, Kauwe JS, Alzheimer's Disease Genetics C (2016) Assessment of the genetic variance of late-onset Alzheimer's disease. Neurobiol Aging 41:200 e213-220.
Rogers J, Li R, Mastroeni D, Grover A, Leonard B, Ahern G, Cao P, Kolody H, Vedders L, Kolb WP, Sabbagh M (2006) Peripheral clearance of amyloid beta peptide by complement C3-dependent adherence to erythrocytes. NeurobiolAging 27:1733-1739.
Saunders AM, Strittmatter WJ, Schmechel D, George-Hyslop PH, Pericak-Vance MA, Joo SH, Rosi BL, Gusella JF, Crapper-MacLachlan DR, Alberts MJ, et al. (1993) Association of apolipoprotein E allele epsilon 4 with late-onset familial and sporadic Alzheimer's disease. Neurology 43:1467-1472.
Shalova IN, Kajiji T, Lim JY, Gomez-Pina V, Fernandez-Ruiz I, Arnalich F, Iau PT, Lopez-Collazo E, Wong SC, Biswas SK (2012) CD16 regulates TRIF-dependent TLR4 response in human monocytes and their subsets. Journal of Immunology 188:3584-3593.
Shrivastava K, Gonzalez P, Acarin L (2012) The immune inhibitory complex CD200/CD200R is developmentally regulated in the mouse brain. J Comp Neurol 520:2657-2675.
Song WC (2012) Crosstalk between complement and toll-like receptors. ToxicolPathol 40:174-182.
Tahara K, Kim HD, Jin JJ, Maxwell JA, Li L, Fukuchi K (2006) Role of toll-like receptor signalling in Abeta uptake and clearance. Brain 129:3006-3019.
Udan ML, Ajit D, Crouse NR, Nichols MR (2008) Toll-like receptors 2 and 4 mediate Abeta(1-42) activation of the innate immune response in a human monocytic cell line. J Neurochem 104:524-533.

Walker DG, Dalsing-Hernandez JE, Campbell NA, Lue LF (2009) Decreased expression of CD200 and CD200 receptor in Alzheimer's disease: a potential mechanism leading to chronic inflammation. ExpNeurol 215:5-19.
Wang Y, Cella M, Mallinson K, Ulrich JD, Young KL, Robinette ML, Gilfillan S, Krishnan GM, Sudhakar S, Zinselmeyer BH, Holtzman DM, Cirrito JR, Colonna M (2015) TREM2 lipid sensing sustains the microglial response in an Alzheimer's disease model. Cell 160:1061-1071.
Wang Y, Ulland TK, Ulrich JD, Song W, Tzaferis JA, Hole JT, Yuan P, Mahan TE, Shi Y, Gilfillan S, Cella M, Grutzendler J, DeMattos RB, Cirrito JR, Holtzman DM, Colonna M (2016) TREM2-mediated early microglial response limits diffusion and toxicity of amyloid plaques. J Exp Med 213:667-675.
Zhang B et al. (2013) Integrated Systems Approach Identifies Genetic Nodes and Networks in Late-Onset Alzheimer's Disease. Cell 153:707-720.

CHAPTER 5

Summary and Future Directions

This chapter will highlight the results of the studies performed in this dissertation and discuss the findings in the context of what has been previously published. The limitations and remaining questions of each study will be considered and future studies will be proposed that would elucidate the unresolved questions.

In the second chapter, the effect C5a has on fAβ-injured neurons was investigated by measuring neuronal injury, via MAP-2 staining, to model what occurs in the AD brain.

Neurons, and the complex network of synapses they make, can be injured in the aging and AD brain in a variety of ways. Evidence of apoptosis in AD has been reported for over 20 years (Su et al., 1994; Cotman and Anderson, 1995). Moreover, excitotoxicity (Ong et al., 2013) and oxidative damage due to mitochondrial dysfunction (Persson et al., 2014) have also been implicated in neuronal dysfunction and apoptosis in AD. Recent studies have shown that C5aR1 signaling is detrimental in various neurodegenerative disease mouse models (Woodruff et al., 2006; Woodruff et al., 2008; Fonseca et al., 2009; Brennan et al., 2015). The effects of C5a on neurons *in vitro* have been studied, although the results have varied greatly. Some studies have shown C5a can directly act on C5aR1 and cause apoptosis (Farkas et al., 1998;Pavlovski et al., 2012). Here, we showed that C5a injures mouse primary neurons in a concentration-dependent manner, corroborating the previous findings. Importantly, we provide both pharmacological and genetic evidence that the injury was mediated by C5aR1, since a C5aR1 antagonist blocked the injury to untreated levels and

primary neurons generated from C5aR1KO mice did not differ from untreated neurons after C5a treatment (**Figure 2.4**). Although we did not examine the mechanism by which C5aR1 lead to neuronal injury, Pavlovski and colleagues demonstrated the proapoptotic signaling protein Bax and cleaved caspase 3 was significantly increased in primary neurons stimulated with recombinant mouse C5a (Pavlovski et al., 2012).

Since others have shown that addition of C5a can protect terminally differentiated neuroblastoma cells from Aβ toxicity (O'Barr et al., 2001), we sought to determine the effect of C5a on Aβ treated primary neurons. We found C5a, through C5aR1 signaling, additively enhanced the neuronal injury elicited by fAβ (**Figure 2.5**). O'Barr and colleagues not only found a protective effect with Aβ but also found C5a alone did not injure the RA-differentiated neuroblastoma cells. The disparity between our findings in Aβ-treated neurons may be explained by the difference in biology when comparing cell lines used in that report to primary cultures used here or to the effect of RA-induced differentiation

An interesting finding by Pavlovski and colleagues was that C5a was minimally generated by primary neurons and was upregulated in response to glucose deprivation and oxygen-glucose deprivation (cell models of ischemic stress) (Pavlovski et al., 2012). Although we did not measure C5a in our study, our blocking experiments with PMX53 in fAβ-treated neurons showed PMX53 had no effect on the fAβ-induced injury to neurons (**Figure 5.1**), suggesting fAβ did not upregulate C5a generation (at least not to levels where an additive effect would be detected) and suggests that C5a and fAβ employ distinct mechanisms by which they injure neurons. However, it is likely that the mechanism by which C5a caused apoptosis in the cell model of ischemic stress mentioned above is the same that

was observed in our study since addition blocking C5a with PMX53 prevented the cell death elicited by glucose deprivation (Pavlovski et al., 2012).

That study left unanswered the contribution of other C5aR1-expressing cells in the CNS. Given that microglia also express C5aR1, and the protein has been shown to be upregulated on microglia in mouse models of AD (Ager et al., 2010), a future study should investigate the effect C5a has on fAβ-treated microglia. Co-culture studies, to model the microglia and neurons in the brain, could determine if microglia, activated by C5a and/or fAβ, can add to the C5a/fAβ injury of neurons by releasing cytotoxic mediators. Adult-derived microglia or neonatal microglia induced with TGFβ (Butovsky et al., 2014) would be necessary since my attempts to show elevated proinflammatory cytokines or nitric oxide were unsuccessful using neonatal microglia (data not shown). It's also possible that microglia may rescue neurons from some of the C5a-elicted damage to neurons by sequestering C5a via C5aR2, a receptor that is found on microglia, since it has been postulated that C5aR2 may serve as a decoy receptor in the periphery (Scola et al., 2009).

Our lab has previously demonstrated that treatment with the C5aR1 antagonist, PMX205, rescued the behavior performance in the TG2576 mouse model of AD and significantly reduced the amyloid plaque load and reactive glia found surrounding Aβ plaques in the same AD mouse model as well as in the 3xTg (Fonseca et al., 2009). Chapter 3 presents investigations to elucidate the mechanism by which PMX205 was protective by assessing the effect of C5aR1 gene ablation on behavior, pathology and microglial gene expression in the Arctic AD mouse model.

The origin of the myeloid cells surrounding amyloid plaques in Alzheimer's disease is still controversial in the field (blood-borne myeloid vs resident microglia). Up until recently,

the origin of progenitor cells that give rise to microglia during development was also not well understood. Elegant studies by Ginhoux and colleagues demonstrated, more definitively, that microglial progenitors derive from the yolk sac macrophages that seed the brain during early fetal development((Ginhoux et al., 2010) and reviewed in (Ginhoux et al., 2013)). It has been difficult to distinguish resident microglia from infiltrating monocytes due to the lack of markers known to definitively differentiate them from each other. CX3CR1^{GFP} and CCR2^{RFP} reporter mice have been used to differentiate microglia from infiltrating CCR2-positive monocytes in the experimental autoimmune encephalomyelitis mouse model of multiple sclerosis (Mizutani et al., 2012). Here, an exhaustive search for RFP+ myeloid cells in the brain of Arctic mice found RFP+ cells only in the meninges, although 2-6% of CX3CR1+ cells were also RFP+ by FACS (**Figure 3.5**). Our data suggests the CX3CR1+ cells around the plaques are resident microglia and not infiltrating myeloid cells. Our finding supports the more recent finding in the 5XFAD and APP/PS1 mouse models, where parabiosis experiments found plaque-associated myeloid cells were derived from resident microglia and not peripheral monocytes (Wang et al., 2016).

In this study, we also validated that the antagonist effect observed in our previous study was specifically via C5aR1 inhibition since genetically eliminating the receptor rescued, or delayed, the cognitive impairment observed at 10 months in the Arctic mice (**Figure 3.2**). In contrast to what we observed in the PMX205 studies in the Tg2576 and 3xTg AD mouse models, gene ablation of C5aR1 in the Arctic mice did not affect plaque burden or CD45 microglial expression (**Figure 3.3**). Although all three models carry the human APP transgene, each with its own set of familial mutations, the "Arctic" mutation leads to rapid fibril formation, *in vitro,* with very little non-fibrillar detected (Cheng et al., 2004) and

accelerated thioflavine-positive plaque deposition, *in vivo* (Cheng et al., 2007) However, the prevention of cognitive loss even in the presence of massive plaque accumulation, supports the idea that the fibrillar plaque itself is not the sole contributor to cognitive loss, but rather it is the microglial inflammatory response to the plaque that leads to neurotoxicity (Wyss-Coray and Rogers, 2012).

RNA-seq from microglia isolated from adult Arctic mouse brain revealed an increase in gene expression of inflammatory genes transcriptionally regulated by NF-κB or upstream activators of NF-κB. Importantly, knocking out C5aR1KO reduced these inflammatory genes in the Arctic mice (**Figure 3.8**). It's been demonstrated that C5a stimulation in monocytes leads to activation of NF-κB (Pan, 1998). What's more, fibrillar Aβ is a ligand for TLR2 and TLR4 (Jana et al., 2008; Jin et al., 2008; Udan et al., 2008) and these receptors have been shown to contribute to the detrimental effects of Aβ by activating microglia to a proinflammatory phenotype, in part by activation of NF-κB via MyD88-dependent and TRIF-dependent pathways ((Fitzgerald et al., 2003) and reviewed in (Kawai and Akira, 2007)) . Toll-like receptors (TLRs) have been found to synergize with C5aR1 and lead to greater proinflammatory cytokine release in models of inflammatory disease in the periphery (reviewed in (Song, 2012)). Thus, the decrease in inflammatory gene expression in the Arctic/C5aR1KO mice is likely due to a loss of synergy between TLRs and C5aR1, which is supported by the relative decreased expression of several inflammatory genes in the absence of C5aR1, even though amyloid plaques, a TLR ligand, is unchanged.

At the same age that we first observed changes in inflammation, phagosome/lysosome genes are also upregulated in microglia isolated from Arctic mice and further increased in the C5aR1-deficient Arctic mice (**Figure 3.9**). A recent study linked

microglial activation in mice via LPS, a ligand for TLR4, to neurodegeneration via complement and activation of the phagosome pathway. Repeated LPS challenges increased microglial expression of chemokines, cathepsins, Fc-gamma receptors, and MHCI genes (Bodea et al., 2014). Interestingly, in this model of repeated systemic injection of LPS, knocking out C3 attenuated the loss of the dopaminergic neurons, suggesting a decrease in the phagosome pathways. The receptor for C3 cleavage products, CR3 (also known as MAC1), is classically known to mediate phagocytosis of aggregated/misfolded protein or pathogens covalently bound to C3b ((Ramadass et al., 2015) and reviewed in (Merle et al., 2015)) and it has also been shown to be essential for synaptic pruning during development (Stevens et al., 2007). With aging and in neurodegenerative disorders such as Alzheimer disease, dysregulation of synaptic pruning has been shown to lead to aberrant and increased synapse elimination; deletion of C3 in mice rescues age-related and AD-related cognitive hippocampal impairments (Shi et al., 2015; Hong et al., 2016). In contrast, knocking out C5aR1 in our study increased the phagosome pathway.

It's important to note that suppression of C5aR1 would not affect the upstream complement components, such as C3, therefore, we would still expect the phagocytosis-promoting complement components to be present. Taken together, we propose that phagocytosis-promoting components of complement such as C1q, C4b, C3b, and iC3b (the latter 3 covalently bound via a thioester bond to plaques) could enhance clearance of Aβ fibrils. Subsequent generation of C5a at the onset of greater plaque load can bind to C5aR1 and synergize with TLRs, polarizing the microglia to a more inflammatory state, suppressing sufficient induction of degradation pathways (**Figure 3.10**).

Although we found an increase in gene expression of genes in the phagosome and lysosome pathway in the Arctic/C5aR1KO mice, we did not test whether the microglia in the Arctic/C5aR1KO mice had greater phagocytic and/or degradative potential. A future study investigating whether genetic deletion of C5aR1 enhances the phagocytic capacity of microglia, particularly the ability to successfully ingest and degrade amyloid, would be crucial to linking the beneficial effect on cognition observed. In addition, since we did not observe a gross difference in amyloid plaque burden, characterization of amyloid species as well as an analysis on plaque size and number of microglia associated with plaques in C5aR1 sufficient Arctic mice compared to C5aR1KO would help elucidate the functional outcome of increased phagosome/lysosome pathways.

Studies of isolated microglia are crucial to understand the biology of those cells in the context of AD. However, studying only a single cell population misses the interactions of those cells with other cells in the CNS, such as neurons and astrocytes. A caveat of our study is the absence of gene expression studies on the other cells of the brain. Neurons have been shown to modulate the activation of microglia (reviewed in (Tian et al., 2009)). Understanding how activated microglia alter neuronal health by investigating neurons has led to greater understating of the intricate crosstalk between the cells of the CNS in aging and disease. Recent research from the Barres lab and colleagues showed that LPS-activated microglia can induce astrocytes to a neurotoxic phenotype (Liddelow et al., 2017), illustrating the importance of studying the interaction of activated microglia with other cells. Future RNA-seq studies from dissected hippocampi from the same cohort investigated in chapter 3 could reveal associations with the microglia gene expression findings with neuronal and astrocytic gene expression profiles.

In chapter 4, microglial expression of immune-modulating proteins was investigated in the 3xTg mouse model of AD (which displays both plaque and tau pathology and thus is claimed to be a better model of human AD). Further, immune-related genes and those linked with neurodegeneration in brains from Arctic mice with and without the C5aR1 deletion corroborated the RNA-seq data in Chapter 3.

CR1 and CD200R were found to be expressed and upregulated in IFNγ-activated BV2 and neonatal primary microglia. However, microglia isolated from young, aging and/or 3xTg mice showed no expression or upregulation of CR1 or CD200R, a relatively surprising observation at the time, highlighting the caveat of equating different populations of microglia (and transformed cell lines). In contrast, TREM2 was highly expressed on BV2 and neonatal primary microglia and significantly increased by IFNγ. Similarly, TREM2 was highly expressed in microglia isolated from adult mice and significantly increased in the 3xTg relative to aged-matched controls. Of note, TREM2 was only upregulated in old (19 month) 3xTg and not young (4 month) 3xTg (**Figure 4.1-2**). Our findings are consistent with the findings of more recent studies in the 5XFAD and APP/PS1 mice, where TREM2 was found to be upregulated by microglia in AD mouse models. It's now been reported that TREM2 is important for containment of Aβ plaques by microglia and crucial for the association of microglia to plaques. (Jay et al., 2016; Wang et al., 2016). Additionally, since CD45 is upregulated on microglia associated with plaques in the 3xTg and CD45 was found to be significantly increased in microglia isolated from aged 3xTg (**Figure 4.2**), it's likely that the increase in TREM2 in our studies is due to TREM2 upregulation by plaque-associated microglia.

Gene expression analysis from half brains (minus cerebellum and olfactory bulbs) showed an increase in inflammatory genes in the Arctic mice that was attenuated in the Arctic/C5aR1KO mice (**Figure 4.4**). Many of the differentially expressed (DE) genes are involved in interferon signaling pathways, either induced by, upstream of, or activators of interferon α,β, or γ, with Stat1 being a central transcription factor (**Figure 4.5**). Stat1 is known to drive inflammation in LPS-stimulated microglia via the transcription factor Jmjd3 (Przanowski et al., 2014) that is regulated by NF-κB (De Santa et al., 2007). Some of the same classes of genes found to be DE in chapter 4 were also found to be DE in chapter 3 on microglia isolated from Arctic/C5aR1KO mice. For example, chemokines Ccl5, Ccl8, and Ccl9 were increased in the Arctic (relative to WT) and decreased in the Arctic/C5aR1KO (relative to Arctic) (**Figure 4.4**) in the Immunology panel. In contrast, chemokines Ccl3 and Ccl4 were unchanged in Arctic relative to WT but decreased in the Arctic/C5aR1KO (relative to Arctic) (**Figure 3.8**) as found in the RNA-seq analysis at 10 months. These chemokines are reported to influence chemotaxis by monocytes (Murphy and Weaver, 2016) and presumably would function similarly on microglia. In addition, Cathepsin B was increased in the Arctic (relative to WT) in isolated microglia (**Figure 3.9**) and similarly increased in Arctic mice and further increased in the Arctic/C5aR1KO in brain (**Figure 4.6**). The overlap of some of the families of genes found in both chapters further validates our data and suggests the expression was high enough on microglia so as to not be washed out in the whole-brain analysis.

Since gene expression was from whole-brain samples (Chapter 4), neuronal and astrocytic gene expression was investigated in the "neurodegeneration" panel that included genes related to autophagy and neurons. The pathways that were activated in the Arctic samples relative to WT were likely microglia-related and included: complement system, TLR

signaling, and TREM1 signaling. Pathways inhibited were primarily neuronal survival/growth related pathways such as: CREB signaling in neurons, CDK5 signaling, Neurotrophin/TRK signaling, NGF signaling and Synaptic LTP (**Table 4.6**). Key functions that were downregulated in the Arctic (relative to WT) were neuronal and included: long-term potentiation (LTP), learning, and memory, while key functions upregulated were likely microglial (**Table 4.7**). The small number of DE genes between the Arctic and Arctic/C5aR1KO in the "neurodegeneration" panel illustrates that the microglial response is likely key to the neuronal dysfunction (cognitive loss) seen in Arctic mice that are C5aR1 sufficient. Additionally, since in chapter 3, the differences in gene expression between the Arctic and Arctic/C5aR1KO were substantially larger at 5 months compared to 10 months (**Figure 3.8C, 3.9C**) it is likely that we would have observed greater differences had we investigated earlier ages rather than at 10 months as done after behavior testing.

In summary, this thesis investigated the role of C5aR1 in Alzheimer's disease. Chapter 2 showed that C5a can directly injure neurons alone and add to the damage caused by fAβ. Chapter 3 demonstrated that in the Arctic mouse model of AD, C5aR1 signaling on microglia polarized the cells to a more inflammatory state and inhibited the phagosome and lysosome pathways. Deletion of C5aR1 in Arctic mice delayed cognitive deficits observed at 10 months, shifted the microglia to a less inflammatory state and enhanced the induction of clearance pathways. Chapter 4 validated our findings in chapter 3 and identified interferon signaling as being suppressed in the Arctic/C5aR1KO relative to Arctic. Despite the alarming statistics concerning AD in the US, to this day there is no disease-modifying drug available. This thesis provides additional compelling rationale to pursue C5aR1 as a candidate therapeutic target

to slow the progression of AD in humans and is consistent with the increasingly proposed role of inflammation in neurodegenerative disorders.

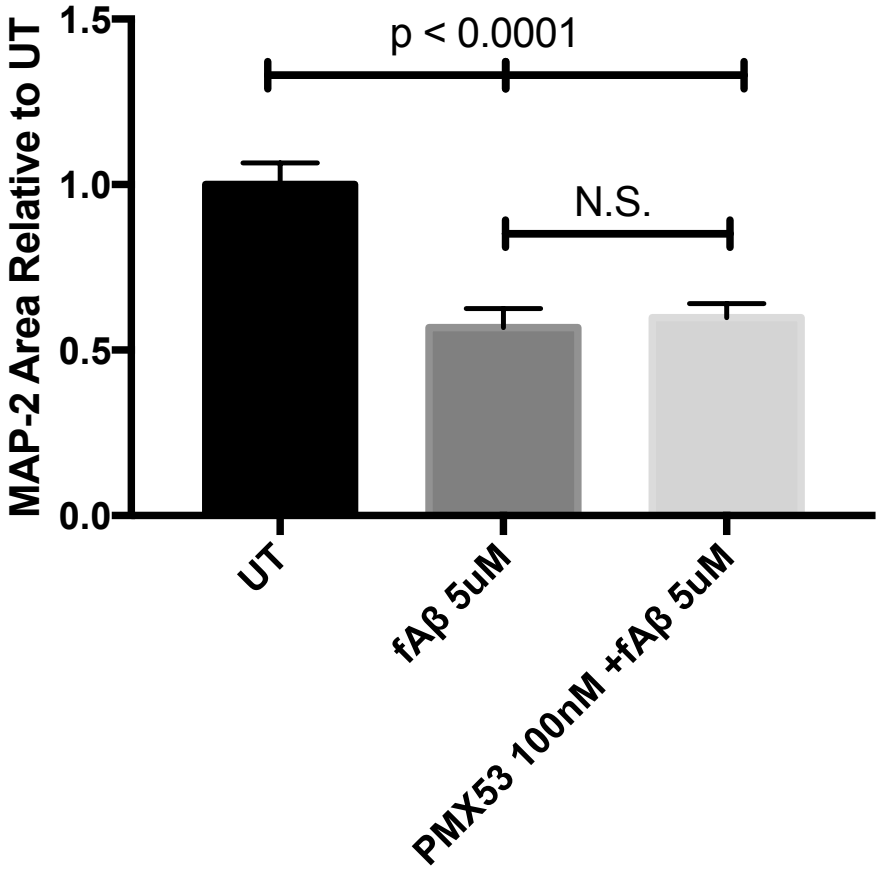

Figure 5.1. PMX53 does not rescue fAβ-induced MAP-2 loss. Primary neurons from WT mice were generated using E15-E16 pups and cultured for 7-10 days. The cells were then stimulated or not with 5 μM fAβ and/or 100nM PMX53 for 24 hours. MAP-2 was visualized by immunocytochemistry (20x magnification) and quantified using ImageJ software. Data are presented as MAP-2 area relative to untreated (UT) +/- SEM. N = 3 independent experiments, each with 3 coverslips per treatment, 5 images per coverslip. P values are calculated using unpaired 2-tailed t-test. Values of $p < 0.05$ were considered statistically significant.

Reference List

Abe T, Hosur KB, Hajishengallis E, Reis ES, Ricklin D, Lambris JD, Hajishengallis G (2012) Local complement-targeted intervention in periodontitis: proof-of-concept using a C5a receptor (CD88) antagonist. J Immunol 189:5442-5448.

Afagh A, Cummings BJ, Cribbs DH, Cotman CW, Tenner AJ (1996) Localization and cell association of C1q in Alzheimer's disease brain. ExpNeurol 138:22-32.

Ager RR, Fonseca MI, Chu SH, Sanderson SD, Taylor SM, Woodruff TM, Tenner AJ (2010) Microglial C5aR (CD88) expression correlates with amyloid-beta deposition in murine models of Alzheimer's disease. J Neurochem 113:389-401.

Alexander JJ, Anderson AJ, Barnum SR, Stevens B, Tenner AJ (2008) The complement cascade: Yin-Yang in neuroinflammation--neuro-protection and -degeneration. J Neurochem 107:1169-1187.

Alzheimer's A (2016) 2016 Alzheimer's disease facts and figures. Alzheimers Dement 12:459-509.

Arumugam TV, Magnus T, Woodruff TM, Proctor LM, Shiels IA, Taylor SM (2006) Complement mediators in ischemia-reperfusion injury. Clinica Chimica Acta 374:33-45.

Aubry C, Corr SC, Wienerroither S, Goulard C, Jones R, Jamieson AM, Decker T, O'Neill LAJ, Dussurget O, Cossart P (2012) Both TLR2 and TRIF Contribute to Interferon-beta Production during Listeria Infection. Plos One 7.

Balderas I, Rodriguez-Ortiz CJ, Salgado-Tonda P, Chavez-Hurtado J, McGaugh JL, Bermudez-Rattoni F (2008) The consolidation of object and context recognition memory involve different regions of the temporal lobe. LearnMem 15:618-624.

Bamberger ME, Landreth GE (2002) Inflammation, apoptosis, and Alzheimer's disease. Neuroscientist 8:276-283.

Benoit ME, Tenner AJ (2011) Complement protein C1q-mediated neuroprotection is correlated with regulation of neuronal gene and microRNA expression. J Neurosci 31:3459-3469.

Benoit ME, Hernandez MX, Dinh ML, Benavente F, Vasquez O, Tenner AJ (2013) C1q-induced LRP1B and GPR6 Proteins Expressed Early in Alzheimer Disease Mouse Models, Are Essential for the C1q-mediated Protection against Amyloid-beta Neurotoxicity. J BiolChem 288:654-665.

Bensa JC, Reboul A, Colomb MG (1983) Biosynthesis in vitro of complement subcomponents C1q, C1s and C1 inhibitor by resting and stimulated human monocytes. The Biochemical journal 216:385-392.

Bodea LG, Wang Y, Linnartz-Gerlach B, Kopatz J, Sinkkonen L, Musgrove R, Kaoma T, Muller A, Vallar L, Di Monte DA, Balling R, Neumann H (2014) Neurodegeneration by activation of the microglial complement-phagosome pathway. JNeurosci 34:8546-8556.

Bradt BM, Kolb WP, Cooper NR (1998) Complement-dependent proinflammatory properties of the Alzheimer's disease beta-peptide. J Exp Med 188:431-438.

Brennan FH, Gordon R, Lao HW, Biggins PJ, Taylor SM, Franklin RJ, Woodruff TM, Ruitenberg MJ (2015) The Complement Receptor C5aR Controls Acute Inflammation and Astrogliosis following Spinal Cord Injury. J Neurosci 35:6517-6531.

Butovsky O, Jedrychowski MP, Moore CS, Cialic R, Lanser AJ, Gabriely G, Koeglsperger T, Dake B, Wu PM, Doykan CE, Fanek Z, Liu L, Chen Z, Rothstein JD, Ransohoff RM, Gygi SP, Antel JP, Weiner HL (2014) Identification of a unique TGF-beta-dependent molecular and functional signature in microglia. NatNeurosci 17:131-143.

Cain SA, Monk PN (2002) The orphan receptor C5L2 has high affinity binding sites for complement fragments C5a and C5a des-Arg(74). The Journal of Biological Chemistry 277:7165-7169.

Calame DG, Mueller-Ortiz SL, Morales JE, Wetsel RA (2014) The C5a anaphylatoxin receptor (C5aR1) protects against Listeria monocytogenes infection by inhibiting type 1 IFN expression. Journal of Immunology 193:5099-5107.

Cheng IH, Palop JJ, Esposito LA, Bien-Ly N, Yan F, Mucke L (2004) Aggressive amyloidosis in mice expressing human amyloid peptides with the Arctic mutation. NatMed 10:1190-1192.

Cheng IH, Scearce-Levie K, Legleiter J, Palop JJ, Gerstein H, Bien-Ly N, Puolivali J, Lesne S, Ashe KH, Muchowski PJ, Mucke L (2007) Accelerating amyloid-beta fibrillization reduces oligomer levels and functional deficits in Alzheimer disease mouse models. The Journal of Biological Chemistry 282:23818-23828.

Cipriani G, Dolciotti C, Picchi L, Bonuccelli U (2011) Alzheimer and his disease: a brief history. Neurol Sci 32:275-279.

Clark CM, Xie S, Chittams J, Ewbank D, Peskind E, Galasko D, Morris JC, McKeel DW, Jr., Farlow M, Weitlauf SL, Quinn J, Kaye J, Knopman D, Arai H, Doody RS, DeCarli C, Leight S, Lee VM, Trojanowski JQ (2003) Cerebrospinal fluid tau and beta-amyloid: how well do these biomarkers reflect autopsy-confirmed dementia diagnoses? Archives in Neurology 60:1696-1702.

Cole TA (2013) Complement activation in Alzheimer's disease contribution of C5a and its receptor CD88. In, p 1 online resource (189 p.). Irvine, Calif.: University of California, Irvine,.

Colton CA (2009) Heterogeneity of microglial activation in the innate immune response in the brain. J NeuroimmunePharmacol 4:399-418.

Colton CA, Wilcock DM (2010) Assessing activation states in microglia. CNSNeurolDisordDrug Targets 9:174-191.

Costello DA, Lyons A, Denieffe S, Browne TC, Cox FF, Lynch MA (2011) Long term potentiation is impaired in membrane glycoprotein CD200-deficient mice: a role for Toll-like receptor activation. The Journal of Biological Chemistry 286:34722-34732.

Cotman CW, Anderson AJ (1995) A potential role for apoptosis in neurodegeneration and Alzheimer's disease. Mol Neurobiol 10:19-45.

Crehan H, Hardy J, Pocock J (2013) Blockage of CR1 prevents activation of rodent microglia. NeurobiolDis 54:139-149.

Cribbs DH, Berchtold NC, Perreau V, Coleman PD, Rogers J, Tenner AJ, Cotman CW (2012) Extensive innate immune gene activation accompanies brain aging, increasing vulnerability to cognitive decline and neurodegeneration: a microarray study. JNeuroinflammation 9:179.

Davoust N, Jones J, Stahel PF, Ames RS, Barnum SR (1999) Receptor for the C3a anaphylatoxin is expressed by neurons and glial cells. Glia 26:201-211.

De Santa F, Totaro MG, Prosperini E, Notarbartolo S, Testa G, Natoli G (2007) The histone H3 lysine-27 demethylase Jmjd3 links inflammation to inhibition of polycomb-mediated gene silencing. Cell 130:1083-1094.
Dobin A, Davis CA, Schlesinger F, Drenkow J, Zaleski C, Jha S, Batut P, Chaisson M, Gingeras TR (2013) STAR: ultrafast universal RNA-seq aligner. Bioinformatics 29:15-21.
Doens D, Fernandez PL (2014) Microglia receptors and their implications in the response to amyloid beta for Alzheimer's disease pathogenesis. J Neuroinflammation 11:48.
Eikelenboom P, van EE, Veerhuis R, Rozemuller AJ, van Gool WA, Hoozemans JJ (2012) Innate immunity and the etiology of late-onset Alzheimer's disease. NeurodegenerDis 10:271-273.
El Khoury J, Luster AD (2008) Mechanisms of microglia accumulation in Alzheimer's disease: therapeutic implications. Trends in Pharmacological Sciences 29:626-632.
El Khoury J, Toft M, Hickman SE, Means TK, Terada K, Geula C, Luster AD (2007) Ccr2 deficiency impairs microglial accumulation and accelerates progression of Alzheimer-like disease. Nat Med 13:432-438.
Farlow MR, Miller ML, Pejovic V (2008) Treatment options in Alzheimer's disease: maximizing benefit, managing expectations. Dement Geriatr Cogn Disord 25:408-422.
Fitzgerald KA, Rowe DC, Barnes BJ, Caffrey DR, Visintin A, Latz E, Monks B, Pitha PM, Golenbock DT (2003) LPS-TLR4 signaling to IRF-3/7 and NF-kappaB involves the toll adapters TRAM and TRIF. J Exp Med 198:1043-1055.
Fonseca MI, Zhou J, Botto M, Tenner AJ (2004) Absence of C1q leads to less neuropathology in transgenic mouse models of Alzheimer's disease. J Neurosci 24:6457-6465.
Fonseca MI, Head E, Velazquez P, Cotman CW, Tenner AJ (1999) The presence of isoaspartic acid in beta-amyloid plaques indicates plaque age. Exp Neurol 157:277-288.
Fonseca MI, Chu SH, Berci AM, Benoit ME, Peters DG, Kimura Y, Tenner AJ (2011) Contribution of complement activation pathways to neuropathology differs among mouse models of Alzheimer's disease. J Neuroinflammation 8:4.
Fonseca MI, Ager RR, Chu SH, Yazan O, Sanderson SD, LaFerla FM, Taylor SM, Woodruff TM, Tenner AJ (2009) Treatment with a C5aR antagonist decreases pathology and enhances behavioral performance in murine models of Alzheimer's disease. Journal of Immunology 183:1375-1383.
Fonseca MI, Chu S, Pierce AL, Brubaker WD, Hauhart RE, Mastroeni D, Clarke EV, Rogers J, Atkinson JP, Tenner AJ (2016) Analysis of the Putative Role of CR1 in Alzheimer's Disease: Genetic Association, Expression and Function. PLoSONE 11:e0149792.
Fraser DA, Pisalyaput K, Tenner AJ (2010) C1q enhances microglial clearance of apoptotic neurons and neuronal blebs, and modulates subsequent inflammatory cytokine production. J Neurochem 112:733-743.
Fraser DA, Laust AK, Nelson EL, Tenner AJ (2009) C1q differentially modulates phagocytosis and cytokine responses during ingestion of apoptotic cells by human monocytes, macrophages, and dendritic cells. J Immunol 183:6175-6185.
Garcia-Alcalde F, Garcia-Lopez F, Dopazo J, Conesa A (2011) Paintomics: a web based tool for the joint visualization of transcriptomics and metabolomics data. Bioinformatics 27:137-139.

Giannakopoulos P, Herrmann FR, Bussiere T, Bouras C, Kovari E, Perl DP, Morrison JH, Gold G, Hof PR (2003) Tangle and neuron numbers, but not amyloid load, predict cognitive status in Alzheimer's disease. Neurology 60:1495-1500.
Ginhoux F, Lim S, Hoeffel G, Low D, Huber T (2013) Origin and differentiation of microglia. Front Cell Neurosci 7:45.
Ginhoux F, Greter M, Leboeuf M, Nandi S, See P, Gokhan S, Mehler MF, Conway SJ, Ng LG, Stanley ER, Samokhvalov IM, Merad M (2010) Fate mapping analysis reveals that adult microglia derive from primitive macrophages. Science 330:841-845.
Giunta B, Fernandez F, Nikolic WV, Obregon D, Rrapo E, Town T, Tan J (2008) Inflammaging as a prodrome to Alzheimer's disease. J Neuroinflammation 5:51.
Guerreiro R et al. (2013) TREM2 variants in Alzheimer's disease. New England Journal of Medicine 368:117-127.
Guo RF, Ward PA (2006) C5a, a therapeutic target in sepsis. Recent Pat AntiinfectDrug Discov 1:57-65.
Haettig J, Stefanko DP, Multani ML, Figueroa DX, McQuown SC, Wood MA (2011) HDAC inhibition modulates hippocampus-dependent long-term memory for object location in a CBP-dependent manner. LearnMem 18:71-79.
Hardy J, Selkoe DJ (2002) The amyloid hypothesis of Alzheimer's disease: progress and problems on the road to therapeutics. Science 297:353-356.
Heneka MT et al. (2015) Neuroinflammation in Alzheimer's disease. Lancet Neurol 14:388-405.
Henn A, Lund S, Hedtjarn M, Schrattenholz A, Porzgen P, Leist M (2009) The suitability of BV2 cells as alternative model system for primary microglia cultures or for animal experiments examining brain inflammation. ALTEX 26:83-94.
Hernandez MX, Namiranian P, Nguyen E, Fonseca MI, Tenner AJ (2017) C5a Increases the Injury to Primary Neurons Elicited by Fibrillar Amyloid Beta. ASN Neuro 9:1759091416687871.
Hickman SE, Allison EK, El KJ (2008) Microglial dysfunction and defective beta-amyloid clearance pathways in aging Alzheimer's disease mice. JNeurosci 28:8354-8360.
Holland MC, Morikis D, Lambris JD (2004) Synthetic small-molecule complement inhibitors. CurrOpinInvestigDrugs 5:1164-1173.
Hollmann TJ, Mueller-Ortiz SL, Braun MC, Wetsel RA (2008) Disruption of the C5a receptor gene increases resistance to acute Gram-negative bacteremia and endotoxic shock: Opposing roles of C3a and C5a. Molecular Immunology 45:1907-1915.
Hong S, Beja-Glasser VF, Nfonoyim BM, Frouin A, Li S, Ramakrishnan S, Merry KM, Shi Q, Rosenthal A, Barres BA, Lemere CA, Selkoe DJ, Stevens B (2016) Complement and microglia mediate early synapse loss in Alzheimer mouse models. Science:712-716.
Horvath RJ, Nutile-McMenemy N, Alkaitis MS, Deleo JA (2008) Differential migration, LPS-induced cytokine, chemokine, and NO expression in immortalized BV-2 and HAPI cell lines and primary microglial cultures. J Neurochem 107:557-569.
Jacobson AC, Weis JH (2008) Comparative functional evolution of human and mouse CR1 and CR2. J Immunol 181:2953-2959.
Jana M, Palencia CA, Pahan K (2008) Fibrillar amyloid-beta peptides activate microglia via TLR2: implications for Alzheimer's disease. J Immunol 181:7254-7262.

Jay TR, Hirsch AM, Broihier ML, Miller CM, Neilson LE, Ransohoff RM, Lamb BT, Landreth GE (2016) Disease progression-dependent effects of TREM2 deficiency in a mouse model of Alzheimer's disease. J Neurosci.

Jay TR, Miller CM, Cheng PJ, Graham LC, Bemiller S, Broihier ML, Xu G, Margevicius D, Karlo JC, Sousa GL, Cotleur AC, Butovsky O, Bekris L, Staugaitis SM, Leverenz JB, Pimplikar SW, Landreth GE, Howell GR, Ransohoff RM, Lamb BT (2015) TREM2 deficiency eliminates TREM2+ inflammatory macrophages and ameliorates pathology in Alzheimer's disease mouse models. JExpMed 212:287-295.

Ji K, Akgul G, Wollmuth LP, Tsirka SE (2013) Microglia actively regulate the number of functional synapses. PLoS One 8:e56293.

Jiang H, Burdick D, Glabe CG, Cotman CW, Tenner AJ (1994) beta-Amyloid activates complement by binding to a specific region of the collagen-like domain of the C1q A chain. J Immunol 152:5050-5059.

Jin JJ, Kim HD, Maxwell JA, Li L, Fukuchi K (2008) Toll-like receptor 4-dependent upregulation of cytokines in a transgenic mouse model of Alzheimer's disease. J Neuroinflammation 5:23.

Jones L et al. (2010) Genetic evidence implicates the immune system and cholesterol metabolism in the aetiology of Alzheimer's disease. PLoS One 5:e13950.

Jonsson T et al. (2013) Variant of TREM2 associated with the risk of Alzheimer's disease. New England Journal of Medicine 368:107-116.

Jung S, Aliberti J, Graemmel P, Sunshine MJ, Kreutzberg GW, Sher A, Littman DR (2000) Analysis of fractalkine receptor CX(3)CR1 function by targeted deletion and green fluorescent protein reporter gene insertion. MolCell Biol 20:4106-4114.

Karch CM, Goate AM (2015) Alzheimer's disease risk genes and mechanisms of disease pathogenesis. Biological Psychiatry 77:43-51.

Kastl SP, Speidl WS, Kaun C, Rega G, Assadian A, Weiss TW, Valent P, Hagmueller GW, Maurer G, Huber K, Wojta J (2006) The complement component C5a induces the expression of plasminogen activator inhibitor-1 in human macrophages via NF-kappaB activation. J Thromb Haemost 4:1790-1797.

Kawai T, Akira S (2007) Signaling to NF-kappaB by Toll-like receptors. Trends Mol Med 13:460-469.

Kettenmann H, Hanisch UK, Noda M, Verkhratsky A (2011) Physiology of microglia. Physiol Rev 91:461-553.

Kohl J (2006) Drug evaluation: the C5a receptor antagonist PMX-53. CurrOpinMolTher 8:529-538.

Konteatis ZD, Siciliano SJ, Van RG, Molineaux CJ, Pandya S, Fischer P, Rosen H, Mumford RA, Springer MS (1994) Development of C5a receptor antagonists. Differential loss of functional responses. Journal of Immunology 153:4200-4205.

Krabbe G, Halle A, Matyash V, Rinnenthal JL, Eom GD, Bernhardt U, Miller KR, Prokop S, Kettenmann H, Heppner FL (2013) Functional Impairment of Microglia Coincides with Beta-Amyloid Deposition in Mice with Alzheimer-Like Pathology. PLoS ONE 8.

Lambert JC et al. (2009) Genome-wide association study identifies variants at CLU and CR1 associated with Alzheimer's disease. Nat Genet 41:1094-1099.

Landlinger C, Oberleitner L, Gruber P, Noiges B, Yatsyk K, Santic R, Mandler M, Staffler G (2015) Active immunization against complement factor C5a: a new therapeutic approach for Alzheimer's disease. J Neuroinflammation 12:150.

Lee S, Varvel NH, Konerth ME, Xu G, Cardona AE, Ransohoff RM, Lamb BT (2010) CX3CR1 deficiency alters microglial activation and reduces beta-amyloid deposition in two Alzheimer's disease mouse models. AmJ Pathol 177:2549-2562.
Leroy K, Ando K, Laporte V, Dedecker R, Suain V, Authelet M, Heraud C, Pierrot N, Yilmaz Z, Octave JN, Brion JP (2012) Lack of tau proteins rescues neuronal cell death and decreases amyloidogenic processing of APP in APP/PS1 mice. Am J Pathol 181:1928-1940.
Li B, Dewey CN (2011) RSEM: accurate transcript quantification from RNA-Seq data with or without a reference genome. BMC Bioinformatics 12:323.
Li M, Pisalyaput K, Galvan M, Tenner AJ (2004) Macrophage colony stimulatory factor and interferon-gamma trigger distinct mechanisms for augmentation of beta-amyloid-induced microglia-mediated neurotoxicity. J Neurochem 91:623-633.
Liddelow SA et al. (2017) Neurotoxic reactive astrocytes are induced by activated microglia. Nature.
Liu S, Liu Y, Hao W, Wolf L, Kiliaan AJ, Penke B, Rube CE, Walter J, Heneka MT, Hartmann T, Menger MD, Fassbender K (2012) TLR2 is a primary receptor for Alzheimer's amyloid beta peptide to trigger neuroinflammatory activation. Journal of Immunology 188:1098-1107.
Liu Z, Condello C, Schain A, Harb R, Grutzendler J (2010) CX3CR1 in microglia regulates brain amyloid deposition through selective protofibrillar amyloid-beta phagocytosis. JNeurosci 30:17091-17101.
Lucin KM, Wyss-Coray T (2009) Immune activation in brain aging and neurodegeneration: too much or too little? Neuron 64:110-122.
Lui H et al. (2016) Progranulin Deficiency Promotes Circuit-Specific Synaptic Pruning by Microglia via Complement Activation. Cell 165:921-935.
Lynch MA, Mills KH (2012) Immunology meets neuroscience--opportunities for immune intervention in neurodegenerative diseases. Brain BehavImmun 26:1-10.
Maddalena A, Papassotiropoulos A, Muller-Tillmanns B, Jung HH, Hegi T, Nitsch RM, Hock C (2003) Biochemical diagnosis of Alzheimer disease by measuring the cerebrospinal fluid ratio of phosphorylated tau protein to beta-amyloid peptide42. Archives in Neurology 60:1202-1206.
Matcovitch-Natan O et al. (2016) Microglia development follows a stepwise program to regulate brain homeostasis. Science 353:aad8670.
Matsuoka Y, Picciano M, Malester B, LaFrancois J, Zehr C, Daeschner JM, Olschowka JA, Fonseca MI, O'Banion MK, Tenner AJ, Lemere CA, Duff K (2001) Inflammatory responses to amyloidosis in a transgenic mouse model of Alzheimer's disease. AmJ Pathol 158:1345-1354.
Mawuenyega KG, Sigurdson W, Ovod V, Munsell L, Kasten T, Morris JC, Yarasheski KE, Bateman RJ (2010) Decreased clearance of CNS beta-amyloid in Alzheimer's disease. Science 330:1774.
Meraz-Rios MA, Toral-Rios D, Franco-Bocanegra D, Villeda-Hernandez J, Campos-Pena V (2013) Inflammatory process in Alzheimer's Disease. Front IntegrNeurosci 7:59.
Merle NS, Noe R, Halbwachs-Mecarelli L, Fremeaux-Bacchi V, Roumenina LT (2015) Complement System Part II: Role in Immunity. Front Immunol 6:257.
Meyer-Luehmann M, Spires-Jones TL, Prada C, Garcia-Alloza M, de CA, Rozkalne A, Koenigsknecht-Talboo J, Holtzman DM, Bacskai BJ, Hyman BT (2008) Rapid

appearance and local toxicity of amyloid-beta plaques in a mouse model of Alzheimer's disease. Nature 451:720-724.
Miller AM, Stella N (2008) Microglial cell migration stimulated by ATP and C5a involve distinct molecular mechanisms: Quantification of migration by a novel near-infrared method. Glia.
Mizutani M, Pino PA, Saederup N, Charo IF, Ransohoff RM, Cardona AE (2012) The fractalkine receptor but not CCR2 is present on microglia from embryonic development throughout adulthood. Journal of Immunology 188:29-36.
Molina H, Kinoshita T, Inoue K, Carel JC, Holers VM (1990) A molecular and immunochemical characterization of mouse CR2. Evidence for a single gene model of mouse complement receptors 1 and 2. Journal of Immunology 145:2974-2983.
Monk PN, Scola AM, Madala P, Fairlie DP (2007) Function, structure and therapeutic potential of complement C5a receptors. British Journal of Pharmacology 152:429-448.
Morley BJ, Walport M (2000) The complement factsbook. San Diego, CA: Academic Press.
Mosher KI, Wyss-Coray T (2014) Microglial dysfunction in brain aging and Alzheimer's disease. Biochemical Pharmacology 88:594-604.
Mumby DG, Gaskin S, Glenn MJ, Schramek TE, Lehmann H (2002) Hippocampal damage and exploratory preferences in rats: memory for objects, places, and contexts. LearnMem 9:49-57.
Murphy K, Weaver C (2016) Janeway's immunobiology, 9th edition. Edition. New York, NY: Garland Science/Taylor & Francis Group, LLC.
Murray PJ et al. (2014) Macrophage activation and polarization: nomenclature and experimental guidelines. Immunity 41:14-20.
Nayak D, Zinselmeyer BH, Corps KN, McGavern DB (2012) In vivo dynamics of innate immune sentinels in the CNS. Intravital 1:95-106.
Nilsberth C, Westlind-Danielsson A, Eckman CB, Condron MM, Axelman K, Forsell C, Stenh C, Luthman J, Teplow DB, Younkin SG, Naslund J, Lannfelt L (2001) The 'Arctic' APP mutation (E693G) causes Alzheimer's disease by enhanced Abeta protofibril formation. NatNeurosci 4:887-893.
Njie EG, Boelen E, Stassen FR, Steinbusch HW, Borchelt DR, Streit WJ (2012) Ex vivo cultures of microglia from young and aged rodent brain reveal age-related changes in microglial function. NeurobiolAging 33:195-112.
Nueda MJ, Tarazona S, Conesa A (2014) Next maSigPro: updating maSigPro bioconductor package for RNA-seq time series. Bioinformatics 30:2598-2602.
O'Barr SA, Caguioa J, Gruol D, Perkins G, Ember JA, Hugli T, Cooper NR (2001) Neuronal expression of a functional receptor for the C5a complement activation fragment. J Immunol 166:4154-4162.
Oddo S, Caccamo A, Shepherd JD, Murphy MP, Golde TE, Kayed R, Metherate R, Mattson MP, Akbari Y, LaFerla FM (2003) Triple-transgenic model of Alzheimer's disease with plaques and tangles: intracellular Abeta and synaptic dysfunction. Neuron 39:409-421.
Okinaga S, Slattery D, Humbles A, Zsengeller Z, Morteau O, Kinrade MB, Brodbeck RM, Krause JE, Choe HR, Gerard NP, Gerard C (2003) C5L2, a nonsignaling C5A binding protein. Biochemistry 42:9406-9415.

Ong WY, Tanaka K, Dawe GS, Ittner LM, Farooqui AA (2013) Slow excitotoxicity in Alzheimer's disease. JAlzheimersDis 35:643-668.
Pan ZK (1998) Anaphylatoxins C5a and C3a induce nuclear factor kappaB activation in human peripheral blood monocytes. Biochim Biophys Acta 1443:90-98.
Parkhurst CN, Yang G, Ninan I, Savas JN, Yates JR, III, Lafaille JJ, Hempstead BL, Littman DR, Gan WB (2013) Microglia promote learning-dependent synapse formation through brain-derived neurotrophic factor. Cell 155:1596-1609.
Pavlovski D, Thundyil J, Monk PN, Wetsel RA, Taylor SM, Woodruff TM (2012) Generation of complement component C5a by ischemic neurons promotes neuronal apoptosis. FASEB J 26:3680-3690.
Persson T, Popescu BO, Cedazo-Minguez A (2014) Oxidative stress in Alzheimer's disease: why did antioxidant therapy fail? OxidMedCell Longev 2014:427318.
Pisalyaput K, Tenner AJ (2008) Complement component C1q inhibits beta-amyloid- and serum amyloid P-induced neurotoxicity via caspase- and calpain-independent mechanisms. Journal of Neurochemistry 104:696-707.
Przanowski P, Dabrowski M, Ellert-Miklaszewska A, Kloss M, Mieczkowski J, Kaza B, Ronowicz A, Hu F, Piotrowski A, Kettenmann H, Komorowski J, Kaminska B (2014) The signal transducers Stat1 and Stat3 and their novel target Jmjd3 drive the expression of inflammatory genes in microglia. Journal of Molecular Medicine 92:239-254.
Ramadass M, Ghebrehiwet B, Kew RR (2015) Enhanced recognition of plasma proteins in a non-native state by complement C3b. A possible clearance mechanism for damaged proteins in blood. Mol Immunol 64:55-62.
Ramadori G, Rasokat H, Burger R, Meyer Zum Buschenfelde KH, Bitter-Suermann D (1984) Quantitative determination of complement components produced by purified hepatocytes. Clin Exp Immunol 55:189-196.
Ransohoff RM, El Khoury J (2015) Microglia in Health and Disease. Cold Spring Harb Perspect Biol 8:a020560.
Ricklin D, Lambris JD (2013) Complement in immune and inflammatory disorders: pathophysiological mechanisms. J Immunol 190:3831-3838.
Ricklin D, Hajishengallis G, Yang K, Lambris JD (2010) Complement: a key system for immune surveillance and homeostasis. Nat Immunol 11:785-797.
Ridge PG, Hoyt KB, Boehme K, Mukherjee S, Crane PK, Haines JL, Mayeux R, Farrer LA, Pericak-Vance MA, Schellenberg GD, Kauwe JS, Alzheimer's Disease Genetics C (2016) Assessment of the genetic variance of late-onset Alzheimer's disease. Neurobiol Aging 41:200 e213-220.
Rogers J, Li R, Mastroeni D, Grover A, Leonard B, Ahern G, Cao P, Kolody H, Vedders L, Kolb WP, Sabbagh M (2006) Peripheral clearance of amyloid beta peptide by complement C3-dependent adherence to erythrocytes. NeurobiolAging 27:1733-1739.
Rovelet-Lecrux A, Hannequin D, Raux G, Le Meur N, Laquerriere A, Vital A, Dumanchin C, Feuillette S, Brice A, Vercelletto M, Dubas F, Frebourg T, Campion D (2006) APP locus duplication causes autosomal dominant early-onset Alzheimer disease with cerebral amyloid angiopathy. Nat Genet 38:24-26.
Saederup N, Cardona AE, Croft K, Mizutani M, Cotleur AC, Tsou CL, Ransohoff RM, Charo IF (2010) Selective chemokine receptor usage by central nervous system myeloid cells in CCR2-red fluorescent protein knock-in mice. PLoSONE 5:e13693.

Sahin F, Ozkan MC, Mete NG, Yilmaz M, Oruc N, Gurgun A, Kayikcioglu M, Guler A, Gokcay F, Bilgir F, Ceylan C, Bilgir O, Sari IH, Saydam G (2015) Multidisciplinary clinical management of paroxysmal nocturnal hemoglobinuria. AmJBlood Res 5:1-9.
Saido T, Leissring MA (2012) Proteolytic degradation of amyloid beta-protein. Cold Spring Harb Perspect Med 2:a006379.
Sarma JV, Ward PA (2012) New developments in C5a receptor signaling. Cell Health Cytoskelet 4:73-82.
Saunders AM, Strittmatter WJ, Schmechel D, George-Hyslop PH, Pericak-Vance MA, Joo SH, Rosi BL, Gusella JF, Crapper-MacLachlan DR, Alberts MJ, et al. (1993) Association of apolipoprotein E allele epsilon 4 with late-onset familial and sporadic Alzheimer's disease. Neurology 43:1467-1472.
Scahill RI, Schott JM, Stevens JM, Rossor MN, Fox NC (2002) Mapping the evolution of regional atrophy in Alzheimer's disease: Unbiased analysis of fluid-registered serial MRI. Proceedings of the National Academy of Sciences of the United States of America 99:4703-4707.
Schafer DP, Lehrman EK, Kautzman AG, Koyama R, Mardinly AR, Yamasaki R, Ransohoff RM, Greenberg ME, Barres BA, Stevens B (2012) Microglia sculpt postnatal neural circuits in an activity and complement-dependent manner. Neuron 74:691-705.
Scheuner D et al. (1996) Secreted amyloid beta-protein similar to that in the senile plaques of Alzheimer's disease is increased in vivo by the presenilin 1 and 2 and APP mutations linked to familial Alzheimer's disease. Nat Med 2:864-870.
Scola AM, Johswich KO, Morgan BP, Klos A, Monk PN (2009) The human complement fragment receptor, C5L2, is a recycling decoy receptor. MolImmunol 46:1149-1162.
Sekar A, Bialas AR, de RH, Davis A, Hammond TR, Kamitaki N, Tooley K, Presumey J, Baum M, Van DV, Genovese G, Rose SA, Handsaker RE, Daly MJ, Carroll MC, Stevens B, McCarroll SA (2016) Schizophrenia risk from complex variation of complement component 4. Nature.
Selkoe DJ, Hardy J (2016) The amyloid hypothesis of Alzheimer's disease at 25 years. EMBO MolMed.
Sewell DL, Nacewicz B, Liu F, Macvilay S, Erdei A, Lambris JD, Sandor M, Fabry Z (2004) Complement C3 and C5 play critical roles in traumatic brain cryoinjury: blocking effects on neutrophil extravasation by C5a receptor antagonist. J Neuroimmunol 155:55-63.
Shalova IN, Kajiji T, Lim JY, Gomez-Pina V, Fernandez-Ruiz I, Arnalich F, Iau PT, Lopez-Collazo E, Wong SC, Biswas SK (2012) CD16 regulates TRIF-dependent TLR4 response in human monocytes and their subsets. Journal of Immunology 188:3584-3593.
Shi Q, Colodner KJ, Matousek SB, Merry K, Hong S, Kenison JE, Frost JL, Le KX, Li S, Dodart JC, Caldarone BJ, Stevens B, Lemere CA (2015) Complement C3-Deficient Mice Fail to Display Age-Related Hippocampal Decline. JNeurosci 35:13029-13042.
Shrivastava K, Gonzalez P, Acarin L (2012) The immune inhibitory complex CD200/CD200R is developmentally regulated in the mouse brain. J Comp Neurol 520:2657-2675.
Singhrao S, Neal JW, Morgan BP, Gasque P (1999) Increased complement biosynthesis by microglia and complement activation on neurons in Huntington's Disease. ExpNeurol 159:362-376.

Song WC (2012) Crosstalk between complement and toll-like receptors. ToxicolPathol 40:174-182.
Stefanko DP, Barrett RM, Ly AR, Reolon GK, Wood MA (2009) Modulation of long-term memory for object recognition via HDAC inhibition. ProcNatlAcadSciUSA 106:9447-9452.
Stephan AH, Madison DV, Mateos JM, Fraser DA, Lovelett EA, Coutellier L, Kim L, Tsai HH, Huang EJ, Rowitch DH, Berns DS, Tenner AJ, Shamloo M, Barres BA (2013) A Dramatic Increase of C1q Protein in the CNS during Normal Aging. J Neurosci 33:13460-13474.
Stevens B, Allen NJ, Vazquez LE, Howell GR, Christopherson KS, Nouri N, Micheva KD, Mehalow AK, Huberman AD, Stafford B, Sher A, Litke AM, Lambris JD, Smith SJ, John SW, Barres BA (2007) The classical complement cascade mediates CNS synapse elimination. Cell 131:1164-1178.
Stewart CR, Stuart LM, Wilkinson K, van Gils JM, Deng J, Halle A, Rayner KJ, Boyer L, Zhong R, Frazier WA, Lacy-Hulbert A, El Khoury J, Golenbock DT, Moore KJ (2010) CD36 ligands promote sterile inflammation through assembly of a Toll-like receptor 4 and 6 heterodimer. Nat Immunol 11:155-161.
Stoka V, Turk V, Turk B (2016) Lysosomal cathepsins and their regulation in aging and neurodegeneration. Ageing Res Rev 32:22-37.
Su JH, Anderson AJ, Cummings BJ, Cotman CW (1994) Immunohistochemical evidence for apoptosis in Alzheimer's disease. NeuroReport 5:2529-2533.
Tahara K, Kim HD, Jin JJ, Maxwell JA, Li L, Fukuchi K (2006) Role of toll-like receptor signalling in Abeta uptake and clearance. Brain 129:3006-3019.
Tan J, Town T, Mori T, Wu Y, Saxe M, Crawford F, Mullan M (2000) CD45 opposes beta-amyloid peptide-induced microglial activation via inhibition of p44/42 mitogen-activated protein kinase. JNeurosci 20:7587-7594.
Tenner AJ, Pisalyaput K (2008) The Complement System in the CNS: Thinking again. In: C entral Nervous System Diseases and Inflammation (Lane TE, Carson MJ, Bergmann C, Wyss-Coray T, eds), pp 153-174. New York: Springer.
Tian L, Rauvala H, Gahmberg CG (2009) Neuronal regulation of immune responses in the central nervous system. Trends Immunol 30:91-99.
Toledo JB, Weiner MW, Wolk DA, Da X, Chen K, Arnold SE, Jagust W, Jack C, Reiman EM, Davatzikos C, Shaw LM, Trojanowski JQ (2014) Neuronal injury biomarkers and prognosis in ADNI subjects with normal cognition. Acta NeuropatholCommun 2:26.
Tripathi S et al. (2015) Meta- and Orthogonal Integration of Influenza "OMICs" Data Defines a Role for UBR4 in Virus Budding. Cell Host Microbe 18:723-735.
Udan ML, Ajit D, Crouse NR, Nichols MR (2008) Toll-like receptors 2 and 4 mediate Abeta(1-42) activation of the innate immune response in a human monocytic cell line. J Neurochem 104:524-533.
Vasek MJ et al. (2016) A complement-microglial axis drives synapse loss during virus-induced memory impairment. Nature 534:538-543.
Veerhuis R, Nielsen HM, Tenner AJ (2011) Complement in the brain. Mol Immunol 48:1592-1603.
Vergunst CE, Gerlag DM, Dinant H, Schulz L, Vinkenoog M, Smeets TJ, Sanders ME, Reedquist KA, Tak PP (2007) Blocking the receptor for C5a in patients with

rheumatoid arthritis does not reduce synovial inflammation. Rheumatology(Oxford) 46:1773-1778.
Verkhusha VV, Kuznetsova IM, Stepanenko OV, Zaraisky AG, Shavlovsky MM, Turoverov KK, Uversky VN (2003) High stability of Discosoma DsRed as compared to Aequorea EGFP. Biochemistry 42:7879-7884.
Walker DG, Dalsing-Hernandez JE, Campbell NA, Lue LF (2009) Decreased expression of CD200 and CD200 receptor in Alzheimer's disease: a potential mechanism leading to chronic inflammation. ExpNeurol 215:5-19.
Wang Y, Cella M, Mallinson K, Ulrich JD, Young KL, Robinette ML, Gilfillan S, Krishnan GM, Sudhakar S, Zinselmeyer BH, Holtzman DM, Cirrito JR, Colonna M (2015) TREM2 lipid sensing sustains the microglial response in an Alzheimer's disease model. Cell 160:1061-1071.
Wang Y, Ulland TK, Ulrich JD, Song W, Tzaferis JA, Hole JT, Yuan P, Mahan TE, Shi Y, Gilfillan S, Cella M, Grutzendler J, DeMattos RB, Cirrito JR, Holtzman DM, Colonna M (2016) TREM2-mediated early microglial response limits diffusion and toxicity of amyloid plaques. J Exp Med 213:667-675.
Webster SD, Galvan MD, Ferran E, Garzon-Rodriguez W, Glabe CG, Tenner AJ (2001) Antibody-mediated phagocytosis of the amyloid beta-peptide in microglia is differentially modulated by C1q. Journal of Immunology 166:7496-7503.
Woodruff TM, Nandakumar KS, Tedesco F (2011) Inhibiting the C5-C5a receptor axis. Mol Immunol 48:1631-1642.
Woodruff TM, Ager RR, Tenner AJ, Noakes PG, Taylor SM (2010) The role of the complement system and the activation fragment C5a in the central nervous system. NeuromolecularMed 12:179-192.
Woodruff TM, Costantini KJ, Crane JW, Atkin JD, Monk PN, Taylor SM, Noakes PG (2008) The complement factor C5a contributes to pathology in a rat model of amyotrophic lateral sclerosis. J Immunol 181:8727-8734.
Woodruff TM, Crane JW, Proctor LM, Buller KM, Shek AB, de VK, Pollitt S, Williams HM, Shiels IA, Monk PN, Taylor SM (2006) Therapeutic activity of C5a receptor antagonists in a rat model of neurodegeneration. FASEB J 20:1407-1417.
Wyss-Coray T (2006) Inflammation in Alzheimer disease: driving force, bystander or beneficial response? NatMed 12:1005-1015.
Wyss-Coray T, Rogers J (2012) Inflammation in Alzheimer disease-a brief review of the basic science and clinical literature. Cold Spring HarbPerspectMed 2:a006346.
Yao J, Harvath L, Gilbert DL, Colton CA (1990) Chemotaxis by a CNS macrophage, the microglia. JNeurosciRes 27:36-42.
Zhang B et al. (2013) Integrated Systems Approach Identifies Genetic Nodes and Networks in Late-Onset Alzheimer's Disease. Cell 153:707-720.
Zhang X, Kimura Y, Fang C, Zhou L, Sfyroera G, Lambris JD, Wetsel RA, Miwa T, Song WC (2007) Regulation of Toll-like receptor-mediated inflammatory response by complement in vivo. Blood 110:228-236.